IL
NUOVO CIMENTO
ORGANO DELLA SOCIETÀ ITALIANA DI FISICA
SOTTO GLI AUSPICI DEL CONSIGLIO NAZIONALE DELLE RICERCHE

VOL. V, N. 4 *Serie decima* 1° Aprile 1957

Relazioni cristallografico-strutturali tra il difenile ed una serie di suoi nuovi derivati (*).

M. FENOGLIO

Istituto di Mineralogia e Petrografia dell'Università - Torino
Centro di studio per la Mineralogia e Petrografia delle Alpi Occidentali del C.N.R. - Torino

(ricevuto il 26 Settembre 1956)

Riassunto. — Sono esposti i risultati più notevoli sinora ottenuti nello studio cristallografico-strutturale di un gruppo di nuovi derivati del difenile, in parte nitroderivati ed in parte cloroaminoderivati. I reperti relativi sia alle proprietà morfologiche che a quelle ottiche hanno consentito innanzi tutto di istituire interessanti raffronti con le corrispondenti del composto capostipite: il difenile. Per quanto concerne le proprietà ottiche è stato messo in particolare evidenza il ruolo notevolmente importante ad esse attribuito nel determinare la forma, l'orientazione delle molecole nel reticolo cristallino. I risultati poi dell'indagine röntgenografica hanno permesso non solo di controllare la simmetria e le costanti cristallografiche, determinate per via goniometrica, dei nuovi derivati del difenile, ma hanno altresì fornito gli elementi indispensabili per la determinazione della struttura degli stessi, messa in relazione con la struttura del difenile. Corollario infine importantissimo delle ricerche strutturali è stato che su quattro dei nuovi derivati difenilici studiati di ben due fu possibile definire in modo univoco natura e formula, che, precedentemente determinate per via chimica, risultarono erronee.

Oggetto della presente comunicazione è di mettere in evidenza i risultati più notevoli sinora ottenuti nello studio cristallografico-strutturale di un gruppo di nuovi derivati del difenile e trarne quelle deduzioni che sono compatibili con lo stato attuale delle ricerche in corso. Le sostanze organiche in parola fanno parte di un'importante e ricca serie di nuovi derivati difenilici, pre-

(*) Presentato al Congresso di Torino, 11-16 Settembre 1956.

parati dal MASCARELLI e dai suoi allievi [1], serie che, da alcuni anni, è oggetto di ricerche cristallografico-röntgenografico-strutturali in questo Istituto da parte dello scrivente e collaboratori.

E precisamente, i nuovi composti studiati sono in parte nitroderivati e in parte cloroaminoderivati difenilici [2]; si tratta rispettivamente:

a) del 2.3′-dimetil-2′-nitro-difenile $CH_3 \cdot H_4C_6 \cdot C_6H_3 \cdot CH_3NO_2$ [3] e del 2.4.6′-trimetil-2′-nitro-difenile $(CH_3)_2H_3C_6 \cdot C_6H_3 \cdot CH_3NO_2$ [4,5];

b) del 2.3′-dimetil-2′-amino-5′-cloro-difenile $CH_3 \cdot H_4C_6 \cdot C_6H_2 \cdot CH_3ClNH_2$ [6] e del 2.3′.5-trimetil-2′-amino-5′-cloro-difenile $(CH_3)_2H_3C_6 \cdot C_6H_2 \cdot CH_3ClNH_2$ [7].

Dal punto di vista morfologico tanto i primi quanto i secondi risultarono appartenere — come del resto appartiene anche il difenile — al sistema monoclino, classe prismatica.

A differenza dei cristalli monoclino-prismatici del difenile, che sono tabulari secondo il pinacoide base {001}, quelli dei nostri derivati — pur essendo anch'essi monoclino-prismatici — presentano abito completamente differente da quello osservato nei primi. Infatti i due nitroderivati sono allungati nella direzione normale alla digira corrispondente all'asse *z*, con abito prismatico, mentre nei due aminocloroderivati si ha un tipo di sviluppo piuttosto raro nei cristalli appartenenti al sistema monoclino, essendo essi allungati secondo la digira, con abito di tipo schiettamente epidotico.

Il 2.3′-dimetil-2′-nitro-difenile si rivelò dimorfo: ambedue le fasi, α e β, risultarono monoclino-prismatiche.

Nella tabella I sono riportati i valori relativi alle costanti cristallografiche, determinate per via goniometrica, dei vari derivati difenilici studiati.

TABELLA I.

Derivati del difenile	Costanti cristallografiche
2.3′-dimetil-2′-nitro-difenile α	$a : b : c = 1.57063 : 1 : 1.02892$ $\beta = 116°31'$
2.3′-dimetil-2′-nitro-difenile β	$a : b : c = 0.69661 : 1 : 0.69617$ $\beta = 110°21'$
2.4.6′-trimetil-2′-nitro-difenile	$a : b : c = 1.3797 : 1 : 0.5213$ $\beta = 99°47'$
2.3′-dimetil-2′-amino-5′-cloro-difenile	$a : b : c = 2.2000 : 1 : 1.4422$ $\beta = 119° 4'$
2.3′.5-trimetil-2′-amino-5′-cloro-difenile	$a : b : c = 7.2956 : 1 : 2.6494$ $\beta = 104°16'$

(1) L. MASCARELLI e B. LONGO: *Gazz. Chim. Ital.*, **71**, 389 (1941); B. LONGO e M. PIRONA: *Gazz. Chim. Ital.*, **77**, 117, 127 (1947).

(2) M. FENOGLIO: *Rend. Soc. Min. Ital.*, **5**, 55 (1948).

(3) E. SANERO: *Atti Acc. Sc. di Torino*, **85**, 67 (1951).

(4) M. FENOGLIO: *Atti Acc. Sc. di Torino*, **84**, 208 (1950).

(5) M. FENOGLIO: *Atti Acc. Sc. di Torino*, **85**, 53 (1951).

(6) G. MAGNANO: *Rend. Soc. Min. Ital.*, **8**, 57 (1952); *Periodico di Mineralogia*, **22**, 35 (1953).

(7) G. MAGNANO: *Atti Acc. Sc. di Torino*, **85**, 83 (1951).

Anche le proprietà ottiche dei nuovi derivati del difenile poterono essere indagate a fondo, tranne quelle della modificazione β del 2.3′-dimetil-2′-nitro-difenile; nella tabella II ne sono schematicamente riassunti i valori.

Non mi pare inopportuno far rilevare che vi è tendenza ad attribuire alle proprietà ottiche delle sostanze cristalline un ruolo notevolmente importante nel determinare forma e orientazione dei loro leptoni. E segnatamente si ritiene che nelle sostanze organiche birifrangenti una forma piana della molecola porti con sè, quando le molecole siano disposte parallelamente, un'elevata birifrangenza negativa, con l'indice di rifrazione minore diretto secondo la normale al piano delle molecole stesse.

Tabella II.

Derivati del difenile	Segno ottico	Piano assi ottici	Bisettrice acuta	Indici di rifrazione			$2V$
				α	β	γ	
2.3′-dimetil-2′-nitro-difenile α	+	$\parallel\{010\}$	γ	1.5717	1.5903	1.7229	44° 42′
2.3′-dimetil-2′-nitro-difenile β		$\parallel\{010\}$	—	—	—	—	—
2.4.6′-trimetil-2′-nitro-difenile	—	$\parallel\{010\}$	α	1.5720	1.6529	1.6898	65° 52′
2.3′-dimetil-2′-amino-5′-cloro-difenile	—	$\perp\{010\}$	α	1.6404	1.6875	1.6940	39° 37′
2.3′.5-trimetil-2′-amino-5′-cloro-difenile	+	$\perp\{010\}$	γ	1.6517	1.6734	1.7410	61° 18′

Due dei composti da noi studiati rientrano appunto in questo caso: il 2.4.6′-trimetil-2′-nitro-difenile e il 2.3′-dimetil-2′-amino-5′-cloro-difenile. Per il primo il piano delle molecole (*) sarebbe, conforme a quanto sopra si è detto, approssimativamente perpendicolare a (010), e la normale a detto piano formerebbe un angolo di circa 68° con l'asse cristallografico delle z (vedi M. Fenoglio [5], p. 56). L'orientazione sarebbe dunque non dissimile da quella accertata da Dhar nel difenile [10]. Nel secondo dei due composti sopra citati invece il piano molecolare parrebbe praticamente coincidere con la (001); una siffatta disposizione delle molecole consente di ipotizzare una facile sfaldatura secondo questo piano: in effetti la sostanza presenta sfaldatura facile e perfettissima secondo {001}.

Negli altri due composti studiati, il 2.3′-dimetil-2′-nitro-difenile α e il 2.3′.5-trimetil-2′-amino-5′-cloro-difenile, l'elevata birifrangenza positiva farebbe

(*) È probabile che, in analogia con i risultati delle dettagliate ricerche su derivati difenilici effettuate da Smare [8], Fowweather e Hargreaves [9], i due nuclei benzenici non siano nei composti da noi studiati esattamente complanari, come si verifica invece nel difenile; intendiamo qui pertanto parlare di un piano « medio » della molecola.

([8]) D. L. Smare: *Acta cryst.*, **1**, 150 (1948).

([9]) F. Fowweather e A. Hargreaves: *Acta cryst.*, **3**, 81 (1950).

([10]) J. Dhar: *Ind. Journ. of Phys.*, **7**, 43 (1932).

TABELLA III.

Difenile e derivati	Costanti reticolari				Reticolo di traslazione	Gruppo spaziale	Z
Difenile	$a_0 = 8.38$ Å	$b_0 = 5.82$ Å	$c_0 = 9.47$ Å	$\beta = 95° 18'$	Γ_m	C_{2h}^5	2
2.3'-dimetil-2'-nitro-difenile α	$a_0 = 11.81$ Å	$b_0 = 7.46$ Å	$c_0 = 7.66$ Å	$\beta = 116° 31'$	Γ_m	C_{2h}^2	2
2.3'-dimetil-2'-nitro-difenile β	$a_0 = 7.65$ Å	$b_0 = 21.86$ Å	$c_0 = 7.64$ Å	$\beta = 110° 21'$	Γ_m	C_{2h}^1	4
2.4.6'-trimetil-2'-nitro-difenile	$a_0 = 21.28$ Å	$b_0 = 15.46$ Å	$c_0 = 8.09$ Å	$\beta = 99° 50'$	Γ_m	C_{2h}^1	8
2.3'-dimetil-2'-amino-5'-cloro-difenile	$a_0 = 16.75$ Å	$b_0 = 7.62$ Å	$c_0 = 10.96$ Å	$\beta = 118° 58'$	Γ_m	C_{2h}^5	4
2.3'.5-trimetil-2'-amino-5'-cloro-difenile	$a_0 = 37.63$ Å	$b_0 = 5.16$ Å	$c_0 = 13.66$ Å	$\beta = 104° 16'$	I'_m	C_{2h}^6	8

invece prevedere un allineamento degli assi molecolari (*) secondo la direzione dell'indice di rifrazione maggiore. Infatti la teoria sopra accennata stabilisce che quando le molecole di una sostanza presentano uno sviluppo preminente secondo una certa direzione, e sono per di più disposte parallelamente le une alle altre, allora l'indice di rifrazione è massimo lungo la direzione anzidetta.

I risultati dell'analisi röntgenografica hanno consentito di controllare la simmetria e le costanti cristallografiche dei nuovi derivati del difenile, oggetto di studio, ed hanno altresì contribuito a fornire gli elementi indispensabili per la determinazione della struttura degli stessi.

Nella tabella III sono riportati, a scopo di confronto, i valori delle costanti reticolari del difenile e quelli delle relative costanti reticolari dei suoi derivati studiati, nonchè i corrispondenti reticoli di traslazione della cella elementare ed i gruppi spaziali, ed infine il numero di molecole Z contenuto nella cella elementare.

Com'è noto, il valore di Z si ricava dalla relazione:

$$Z = \frac{V_0 \varrho N}{M},$$

in cui normalmente sono determinati per via sperimentale le costanti reticolari, che consentono di calcolare V_0, il peso specifico ϱ ed il peso molecolare M; N, come si sa, è il numero di Avogadro.

(*) Per asse molecolare si intende qui la direzione lungo la quale sono disposti gli atomi C_4, C_1, C'_1, C'_4.

Ora, è evidente che, note quattro delle cinque grandezze che figurano nella relazione sopra scritta, si può calcolare il valore della quinta. E quindi emerge chiaramente che l'espressione suddetta può consentire altresì di verificare il valore di N, costante di Avogadro, quando tale espressione venga applicata ad un numero cospicuo di casi, in cui le determinazioni di V_0, ϱ, M siano state eseguite con tecniche particolari, con molta cura e precisione.

Aggiungeremo infine che l'importanza della relazione testè considerata è veramente grande quando si abbia da determinare la struttura di sostanze imprecisamente note dal punto di vista chimico per la loro complessità di composizione, ciò che può accadere sia nei composti inorganici sia, più frequentemente, in quelli organici. Essa relazione infatti impone a Z dei valori interi, e ciò comporta limitazioni talvolta molto significative per i valori del peso molecolare, e, di conseguenza, per la formula esatta da attribuire alla sostanza studiata.

Appunto per tale via fu possibile, ad esempio, stabilire con certezza nel campo della chimica inorganica la formula esatta dell'idromagnesite $4MgCO_3 \cdot Mg(OH)_2 \cdot 4H_2O$ [11] e quella di minerali rari, come, ad esempio, la berzeelite $(Ca, Na)_3(Mg, Mn)_2[AsO_4]_3$, la schafarzikite $FeSb_2O_4$ e la trippkeite $CuAs_2O_4$ tra loro isomorfe [12], non che la formula del manganimolibdato ammonico $3(NH_4)_2O \cdot MnO_2 \cdot 9MoO_3 \cdot 6H_2O$ [13].

Per quanto concerne i composti organici, diremo subito che, su quattro derivati difenilici da noi studiati, di ben due fu possibile definire in modo univoco natura e formula. Essi sono il 2.3′-dimetil-2′-amino-5′-cloro-difenile $CH_3 \cdot H_4C_6 \cdot C_6H_2 \cdot CH_3ClNH_2$ [6] e il 2.3′.5-trimetil-2′-amino-5′-cloro-difenile $(CH_3)_2H_3C_6 \cdot C_6H_2 \cdot CH_3ClNH_2$ [7], ritenuti prima delle nostre indagini röntgenografico-strutturali rispettivamente il 2.3′-dimetil-2′-cloro-difenile $CH_3 \cdot H_4C_6 \cdot C_6H_3 \cdot CH_3Cl$ [14] e il 2.3′.5-trimetil-2′-cloro-difenile $(CH_3)_2H_3C_6 \cdot C_6H_3 \cdot CH_3Cl$ [15].

Ritornando alla tabella III, faremo ancora notare come dall'esame comparativo dei risultati dell'analisi röntgenografica in essa riportati emerge chiaramente che le modificazioni, che si verificano nel reticolo cristallino del difenile in seguito alla sostituzione nella sua molecola di atomi di H con CH_3 e NO_2 nei nitroderivati e con CH_3, NH_2 e Cl nei cloroaminoderivati, pur essendo rilevanti, non sono di entità tale da cagionare deformazioni profonde nel reticolo cristallino stesso, di guisa che si ha la sensazione di trovarci di fronte ad effetti morfotropici, che appariranno anche più evidenti dal confronto dei parametri

---

[11] M. Fenoglio: *Periodico di Mineralogia*, **7**, 257 (1936); *Rend. Acc. Naz. Lincei*, **6**, 24, 219 (1936).

[12] F. Machatschki: *Rend. Soc. Min. Ital.*, **8**, 131 (1952).

[13] V. Caglioti e A. M. Liquori: *Rend. Acc. Naz. Lincei*, **8**, 8, 443 (1950).

[14] B. Longo e M. Pirona: *Gazz. Chim. Ital.*, **77**, 117 (1947).

[15] B. Longo e M. Pirona: *Gazz. Chim. Ital.*, **77**, 127 (1947).

topici: χ, ψ, ω, calcolati in base ai valori delle costanti cristallografiche dedotte dai valori delle costanti reticolari.

Infatti, dal raffronto dei valori calcolati per i parametri topici, riportati nella tabella IV, appare chiaramente che esistono relazioni di morfotropia

Tabella IV.

Difenile e derivati	χ	ψ	ω
Difenile	5.5407	3.8482	6.2614
2.3′-dimetil-2′-nitro-difenile α	7.9580	5.0268	5.1615
2.3′-dimetil-2′-nitro-difenile β	4.0725	11.6325	4.0687
2.4.6′-trimetil-2′-nitro-difenile	9.0055	6.5423	3.4236
2.3′-dimetil-2′-amino-5′-cloro-difenile	8.9193	4.0575	5.8360
2.3′.5-trimetil-2′-amino-5′-cloro-difenile	15.9009	2.1804	5.7722

tra il difenile e la nostra serie di derivati difenilici; e precisamente, il passaggio dal primo ai secondi può immaginarsi avvenire attraverso sostituzioni che provocano variazioni notevoli, e non sempre regolari, nei parametri del composto capostipite; queste irregolarità si attenuano attraverso la comparazione dei derivati nitrodifenilici da una parte e dei derivati cloroaminodifenilici dall'altra.

Infatti si rileva (*) immediatamente che le varie sostituzioni degli atomi di H nella molecola del difenile con CH_3 e NO_2 nei nitroderivati e con CH_3, NH_2 e Cl nei cloroaminoderivati lasciano, nella maggior parte dei casi, quasi sempre pressochè invariato il valore del parametro ω; per il parametro χ invece si ha che i suoi valori per tutti i nostri derivati difenilici sono nettamente maggiori di quelli del difenile. Si potrebbe ancora rilevare che i valori di χ nei derivati difenilici sono i maggiori fra i valori dei parametri topici, mentre nel difenile il parametro maggiore è ω.

(*) Nelle considerazioni che stiamo per fare non sarà tenuto conto della fase β del 2.3′-dimetil-2′-nitro-difenile, poichè sono già state fatte dal Sanero (3), che la studiò, riserve, come si rileva dalle sue conclusioni provvisorie: « È particolarmente interessante notare che se raffrontiamo i valori delle costanti reticolari, testè riportati, delle due fasi α e β del 2.3′-dimetil-2′-nitrodifenile, colpisce immediatamente il fatto della singolare coincidenza di valori per le due modificazioni del periodo d'identità c_0, non che l'inversione dei valori di b_0 di α con a_0 di β, e infine il valore di b_0 di β quasi raddoppiato rispetto a quello di a_0 di α. Mi limito, per ora, a rilevare la singolarità di queste analogie, su cui conterei di ritornare in un prossimo futuro, poichè la spiegazione potrà forse essere data da considerazioni relative alla dinamica reticolare e alla disposizione spaziale delle molecole nell'edificio cristallino ».

Per i derivati nitrodifenilici si nota poi che i valori di χ e ψ vanno gradatamente crescendo rispetto a quelli del difenile con l'aumentare del numero degli atomi di H sostituiti dai gruppi CH_3 nella molecola difenilica, mentre quello di ω va invece simultaneamente decrescendo.

Per i derivati cloroaminodifenilici emerge infine chiaramente che il 2.3′.5-trimetil-2′-amino-5′-cloro-difenile, pur differendo solamente per la sostituzione di un atomo di H in più con un gruppo CH_3 dal 2.3′-dimetil-2′-amino-5′-cloro-difenile, manifesta tuttavia un notevole incremento del valore di χ, ed un altrettanto notevole decremento di quello di ψ relativamente ai corrispondenti valori degli stessi nell'omologo inferiore.

Per quanto riguarda la struttura dei nitroderivati e cloroaminoderivati difenilici da noi studiati, qualsiasi deduzione, anche provvisoria, si voglia trarre, è indispensabile rifarsi alle conoscenze acquisite sulla struttura del difenile. Esse, com'è noto, son dovute ad una schiera di studiosi, tra cui basterà appena ricordare i Bragg ([16]), Hengstenberg e Mark ([17]), Clark e Pickett ([18]), Dhar ([10]). Quest'ultimo Autore, utilizzando anche i risultati dei suoi predecessori in argomento, non che i risultati di altri studiosi che avevano indagato le proprietà fisiche (ottiche, magnetiche, elettriche) del difenile, è riuscito a concretare un tipo di struttura molecolare universalmente accettato.

E precisamente, Dhar arriva alla conclusione che i due nuclei benzenici del difenile sono complanari; la lunghezza del legame C—C tra i due nuclei è di 1.48 Å, intermedia quindi tra le distanze che sono caratteristiche tra gli atomi di carbonio nel nucleo benzenico (1.39 Å) e le distanze tra gli atomi di carbonio nei composti alifatici (1.54 Å).

Evidentemente i risultati röntgenografici, di cui attualmente disponiamo, non consentono ancora una previsione sicura del tipo di struttura attribuibile ai nostri derivati, ed è perciò impossibile istituire ora un confronto tra la struttura proposta per il difenile e quella dei derivati in parola, come abbiamo fatto invece per la parte morfologica, ottica e morfotropica. Tuttavia è indubitato che i nostri reperti potranno fornire una solida base all'interpretazione strutturistica vera e propria, che ci siamo proposti di effettuare in un prossimo futuro.

([16]) W. H. Bragg e W. L. Bragg: *X-Rays and Crystal Structure* (London, 1925).
([17]) J. Hengstenberg e H. Mark: *Zeits. f. Krist.*, **70**, 283 (1929).
([18]) G. L. Clark e L. W. Pickett: *Proc. Nat. Acad. Sci. U.S.A.*, **16**, 20 (1930).

SUMMARY

I explain here the most important results obtained so far on the crystallographic and structuristic study of a group of new diphenyl derivates, partly nitroderivates and partly chloroaminoderivates. The morphological and optical properties of these derivates are related to those of diphenyl. The optical properties of these organic crystals are valuable indications of their molecular arrangement, because they show the orientation of the molecules in the structure. The results of X-ray diffraction of these derivates enabled us to control the symmetry and the crystallographic constants, which had been previously determined by goniometric measurements. The structural data are related to those of diphenyl. From structural researches, it has been possible to determine the chemical formula of two derivates, previously erroneously established.

A New Method for the Determination of the Acoustic Absorption Coefficient in Liquids.

A. Carrelli and F. S. Gaeta

Istituto di Fisica dell'Università - Napoli

(ricevuto il 31 Ottobre 1956)

Summary. — A new way to obtain the acoustic absorption coefficient in liquids by an optical method, making use of standing ultrasonic waves. Some results are given, in good agreement with the experimental results of other authors who worked with different methods at the same frequency and temperature. A noteworthy exception is the case of Benzol, for which we obtained a value much lower (about a sixth) than the generally accepted experimental value. We wish to point out here that Benzol exhibited the strongest anomalies of the experimental absorption coefficient compared with the theoretical values. Our result approximates better the ideal value.

1. – Introduction.

It is well known that the existing theories on the acoustic absorption of liquids do not agree with the experimental results.

The theory worked out by Stokes [1] and Kirchhoff [2] takes into account the losses of energy by an acoustic wave travelling in a fluid, due to the combined effects of viscosity and thermal conductivity of the medium.

The coefficient α is given by the following expression:

$$\alpha = \alpha_v + \alpha_c = \frac{2\pi^2\nu^2}{\mu V^2}\left[\frac{4}{3}\eta + \frac{KTV^2a^2}{JC_p^2}\right], \tag{1}$$

where K is the thermal conductivity; T the Kelvin temperature; J the mechanical equivalent of heat, C_p the thermal capacity at constant pressure and η the internal friction coefficient of the fluid.

(1) G. G. Stokes: *Cambr. Trans. Phil. Soc.*, **8**, 287 (1845).
(2) G. Kirchhoff: *Pogg. Ann. Phys.*, **134**, 177 (1868).

The experimental results disagree, in the case of liquid mediums, with equation (1), both because the measured values of α are much higher than predicted, and because the ratio α/ν^2 is not independent from frequency as it would appear from (1). Moreover, α/ν^2 which should always become lesser with increasing temperature, on the contrary increases with increasing temperature.

The different experimental methods give often contrasting results. It is therefore of the utmost importance to develop a method capable of yielding the value of α in a completely new way. We present a new method to measure α employing standing waves.

2. – Theory of the Method.

Let a liquid be subjected to standing acoustic waves generated and maintained in it by a piezo-electric crystal excited on its fundamental frequency or an odd multiple of this frequency. The waves be plane and the liquid vibrating column be l cm long, where l is an integer multiple of the half wave length. On one end the liquid column is bounded by the quartz crystal, and on the other by a plane metallic reflector, parallel to the crystal.

Let us imagine what will happen in these conditions if we stop the oscillations of the crystal:

The intensity of the elastic oscillations will decrease (namely their amplitude will become lesser), as a consequence both of the transmission of acoustic energy in the limiting solid medium, and of the transformation in heat in which absorption consists.

If one determines quantitatively the law according to which the intensity of acoustic waves decreases with time, then one is able to determine a certain damping coefficient b made up of two parts, one, say b', representing the losses of energy due to the transmission to the surrounding media, and the other, b'', representing the energy lost in the absorption processes. This last coefficient b'' has, as we will see, a direct relation with the coefficient given by (1). To obtain the quantitative determination of b we proceeded as follows:

It is well known that a transparent medium perturbated by ultrasonic waves gives origin to optical diffraction phenomena, the intensity of the diffracted orders depending on the intensity of the acoustic waves.

The theory of these spectra, developed by RAMAN and NATH ([3-7]) in good

([3]) C. V. RAMAN and N. S. NAGENDRA NATH: *Proc. Ind. Acad. Sci.*, **2**, 406 (1935).
([4]) C. V. RAMAN and N. S. NAGENDRA NATH: *Proc. Ind. Acad. Sci.*, **2**, 413 (1935).
([5]) C. V. RAMAN and N. S. NAGENDRA NATH: *Proc. Ind. Acad. Sci.*, **3**, 75 (1936).
([6]) C. V. RAMAN and N. S. NAGENDRA NATH: *Proc. Ind. Acad. Sci.*, **3**, 119 (1936).
([7]) C. V. RAMAN and N. S. NAGENDRA NATH: *Proc. Ind. Acad. Sci.*, **3**, 495 (1936).

accord with experience, says that the ratio of the luminous intensities I_m and I_n of the m-th and n-th order in the diffraction pattern, is the same as the ratio $J_m^2(r)$ and $J_n^2(r)$ where $J_m(r)$ and $J_n(r)$ are the first kind Bessel functions of order m and n of the parameter r with

$$r = \frac{2n(\Delta n)_{\max} \cdot L}{\Lambda} \,. \tag{2}$$

In this expression $(\Delta n)_{\max}$ is the maximum variation of refractive index generated in the medium by the acoustic pressure $(\Delta p)_{\max}$ in the nodal planes of the perturbation. L is the diameter of the acoustic beam and Λ is the wave length of the monochromatic light employed.

The variation of refractive index which appears in (2) depends an $(\Delta p)_{\max}$ and, making use of the Lorentz-Lorenz law, one finds that:

$$(\Delta n)_{\max} = \frac{1}{\varepsilon} \frac{(n^2+2)(n^2-1)}{6n} (\Delta p)_{\max} \,, \tag{3}$$

where ε is the compressibility coefficient of the liquid.

Hubbard [8] obtained a relation between Δp and the velocity $\dot{a}$ of the particles of the medium in the acoustic field, for the case of stationary waves, in analogous conditions as ours. Hubbard's relation is similar to the well known $(\Delta p)_x = V\mu\dot{a}_x$, with the difference that in stationary conditions the velocity $\dot{a}_x$ at a distance x from the source (and $(1-x)$ from the reflector) results from the combination of the direct and reflected waves which together form the stationary system. As from the direction of the source come the direct waves, the waves reflected once on the reflector and once on the source itself etc., and from the direction of the reflector come the waves reflected just once on the reflector, the waves reflected a first time on the reflector, then on the source and finally a second time on the reflector etc., the expression will have to contain all these different contributions, so that, designating with $\dot{a}(+)$ and $\dot{a}(-)$ the total forward and the total backward velocity, Hubbard's relation will read:

$$(\Delta p)_x = V(\mu\dot{a}_x(+) - V\mu\dot{a}_x(-) \,, \tag{4}$$

where x means that (4) is written for the particles which are at a distance x from the source and $1-x$ from the reflector.

---

[8] J. C. Hubbard: *Phys. Rev.*, **38**, 1011 (1931).

In explicit form equation (4) becomes:

$$(5)\qquad (\Delta p) = V\mu\dot{a}_{\max}\frac{\exp[2\pi i\nu t]\left\{\exp\left[-\left(\alpha+\frac{2\pi i\nu}{V}\right)x\right]-\gamma\exp\left[-\left(\alpha+\frac{2\pi i\nu}{V}\right)(2l-x)\right]\right\}}{1-\gamma\exp\left[-\left(\alpha+\frac{2\pi i\nu}{V}\right)2l\right]}$$

where α is the acoustic absorption coefficient of the medium and γ is the reflecting power of the interface liquid-reflector.

The maximum amplitude of the pressure-wave, $(\Delta p)_{\max}$ will be obtained from equation (5) putting $\exp[2\pi i\nu t] = 1$ and $x = n(\lambda/2)$; with these positions eq. (5) becomes:

$$(6)\qquad (\Delta p)_{\max} = V\mu\dot{a}_{\max}\frac{\exp\left[-\left(\alpha+\frac{2\pi i\nu}{V}\right)n\frac{\lambda}{2}\right]-\gamma\exp\left[-\left(\alpha+\frac{2\pi i\nu}{V}\right)\left(2l-n\frac{\lambda}{2}\right)\right]}{1-\gamma\exp\left[-\left(\alpha+\frac{2\pi i\nu}{V}\right)2l\right.}$$

and confronting with (3) one obtains:

$$(7)\qquad (\Delta n)_{\max} = \frac{1}{\varepsilon}\frac{(n^2+2)(n^2-1)}{6n}\cdot$$

$$\cdot V\mu\dot{a}_{\max}\frac{\exp\left[-\left(\alpha+\frac{2\pi i\nu}{V}\right)n\frac{\lambda}{2}\right]-\gamma\exp\left[-\left(\alpha+\frac{2\pi i\nu}{V}\right)\left(2l-n\frac{\lambda}{2}\right)\right]}{1-\gamma\exp\left[-\left(\alpha+\frac{2\pi i\nu}{V}\right)2l\right.},$$

but it is well known that:

$$(8)\qquad E = \frac{1}{2}\frac{(\Delta p)^2_{\max}}{\mu V}$$

and therefore:

$$(9)\qquad E = \frac{1}{2}V\mu\dot{a}^2_{\max}\cdot\left[\frac{\exp\left[-\left(\alpha+\frac{2\pi i\nu}{V}\right)n\frac{\lambda}{2}\right]-\gamma\exp\left[-\left(\alpha+\frac{2\pi i\nu}{V}\right)\left(2l-n\frac{\lambda}{2}\right)\right]}{1-\gamma\exp\left[-\left(\alpha+\frac{2\pi i\nu}{V}\right)2l\right]}\right]^2$$

and from (2), (3) and (8) it follows that:

$$(10)\qquad E = \frac{9A^2\varepsilon^2}{2\pi^2\mu VL^2}\cdot\frac{n^2}{(n^2+2)^2(n^2-1)^2}\cdot r^2\,.$$

Equation (10) gives us the relation between the intensity E of the acoustic

stationary waves and r which in turn is connected with the luminous intensity distribution among the various orders of the observed diffraction pattern.

For a given liquid, a given exciting crystal, and a certain monochromatic light, the coefficient of r^2 in eq. (10) is constant and therefore one can write:

$$E = Cr^2 , \tag{11}$$

with C a constant.

If the intensity of the acoustic field decreases in time according to a certain law, then accordingly must change the observed distribution of the luminous intensity among the diffracted orders, and from Raman's theory we shall obtain $r(t)$ and therefore from eq. (10)$E(t)$.

Since the experimental results give an exponential law for $E = E(t)$, as we shall see, and as is to be expected however, we may write for two values E_1 and E_2 of E, corresponding to the light intensity distribution at the instants t_1 and t_2:

$$E_2 = E_1 \exp [- b(t_2 - t_1)]$$

and solving for b:

$$b = \frac{1}{t_2 - t_1} \lg_e \frac{E_1}{E_2} .$$

This equation gives us the global damping coefficient b which results from the added effects of both the losses of energy due to transmission to adjoining media and the losses due to real absorption.

If one assumes the transmission losses to be small compared with the absorption losses, then one may evaluate the absorption coefficient α from b obtaining in this way an excess value.

The problem is therefore to connect b with α. This can be effected as follows:

If one divides ideally the vibrating liquid into parallel layers, each $\lambda/2$ thick, normal to the direction of propagation of the acoustic waves, and calls dE/E the fraction of incident energy which each layer converts into heat during a compression and the subsequent expansion, the fraction of incident energy substracted from the acoustic waves by a layer one cm thick, is $(2/\lambda)(dE/E)$ because $2/\lambda$ are the layers contained in a column one centimeter long, and therefore $(\lambda/2)(dE/E) = \alpha$.

On the other hand each layer performs in a second ν complete cycles, each one consisting of a compression and an expansion.

Therefore it will convert into heat the fraction $\nu(dE/E)$ of the initial energy E. We called this fraction b''.

It follows that $dE/E = b''/\nu = (\lambda/2)\alpha$ that is:

$$b'' = \frac{\nu\lambda}{2} \alpha = \frac{V}{2} \alpha .$$

This is the relation between α and b'' which we wanted.

Now it would be necessary to evaluate b', but on the basis of the above mentioned assumption as to the relative magnitudes of b' and b'' we can substitute in eq. (12) b for b'' and obtain in this way an excess value for α. This is what we did, obtaining the results which we will present in the following pages.

3. – Experimental Method.

The experimental device we used is that schematically drawn in Fig. 1. The power station P feeds the transmitter T which consists of a Hartley-type circuit, and by means of a series of interchangeable panels allows to drive a piezoelectric crystal Q at frequencies between 200 kHz and 10 MHz. The alternated r.f. potential is fed to one face of the quartz Q, while the other face is connected to the ground together with the metallic trough VV'. This trough is filled with the liquid under examination, and in front of the quartz face and parallel to it, at some distance l away, a brass reflector R is placed, and by means of micrometric screws it is possible to change the orientation of R and its distance from Q, so that l can be made equal to $K(\lambda/2)$ with K being an integer. Two plane glass windows A and B allow a light beam normal to the ultrasonic beam to pass through the trough. The monochromatic light beam is produced by a sodium arc L placed in front of the slit F of a collimator C. The parallel beam emerging from B is focused by the objective O_b on the photographic plate P, where a clear image of F is to be seen.

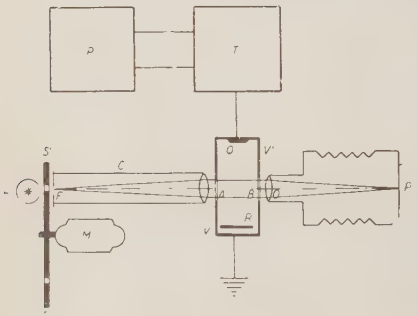

Fig. 1.

Let us point out here that the smallest of the following four openings: 1) the orifice of the collimator; 2) the window A; 3) the window B; and 4) the support of the objective O_b of the camera will act as the iris of the system, while none of them plays the part of field screen. We will shortly make use of this circumstance.

If we adjust the transmitter on one of the resonant frequencies of the quartz, and set the quartz into forces vibration, we observe on plate P, no more one, but many parallel images of slit F, each couple of images on either side of the central image having an intensity depending on the intensity of

the ultrasonic oscillations. From the aspect of this diffraction pattern one can easily decide, with a little practice, if the quartz is in resonance, and if the ultrasonic waves are stationary or not. A picture of the diffraction pattern taken in these conditions has the aspect of Fig. 2*a*.

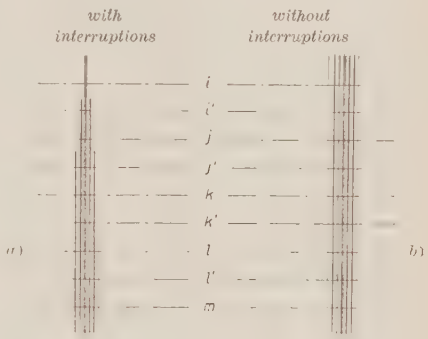

Fig. 2 *a*), *b*).

Now we place between the sodium arc L and the collimator C a stroboscopic disc SS' rotated by a motor M, and having a series of equidistant slits which as the disc turns pass in front of F, each normally to F. If one of the stroboscopic slits occupies a certain position in front of F, then only part of F is illuminated, and only a slice of the pattern, such as that comprised between i and i' in Fig. 2*a*, is to be seen in P. As the disc revolves, the illuminated slice sweeps over the entire picture in the same time as the slit of the disc passes before F. On the stroboscope itself, at even spaces between the slits, there are a series of contacts NN' which act on a relais causing the interruption of the r.f. Things are so arranged that while the transmitter is in function the light from L cannot reach P, and as soon as the light passes through a slit the transmitter is stopped. In such conditions the pattern impressed on plate P corresponds to the gradually disappearing ultrasonic grating, after the interruption of the vibrations of the crystal, and, the different levels on the photographic plate being illuminated in consecutive instants, on each of these levels will be pictured the diffraction pattern corresponding to the residual ultrasonic intensity propagating in the liquid at the same instant. The photographs obtained with the revolving disc have indeed the aspect of Fig. 2*b*. Once known the speed of transit of the slits of the disc before slit F, it is possible to estimate the time that the light beam takes to sweep from level ii' to levels jj', kk' etc. Then, determining by a microphotometric method the intensity of the light pattern on each level, one is able to evaluate, by means of Sander's [9] experimental curves, the parameter r in function of the time t and therefore, by means of equation (11), E at each of the corresponding instants. Plotting the values of $\log E$ against time, one expects to find a straight line the slope of which is b, as it is to be seen on Figs. 3, 4, 5 the experimental points falling well enough on a straight line.

[9] F. H. Sanders: *Can. Journ. Res.*, **14**(A), 158 (1936).

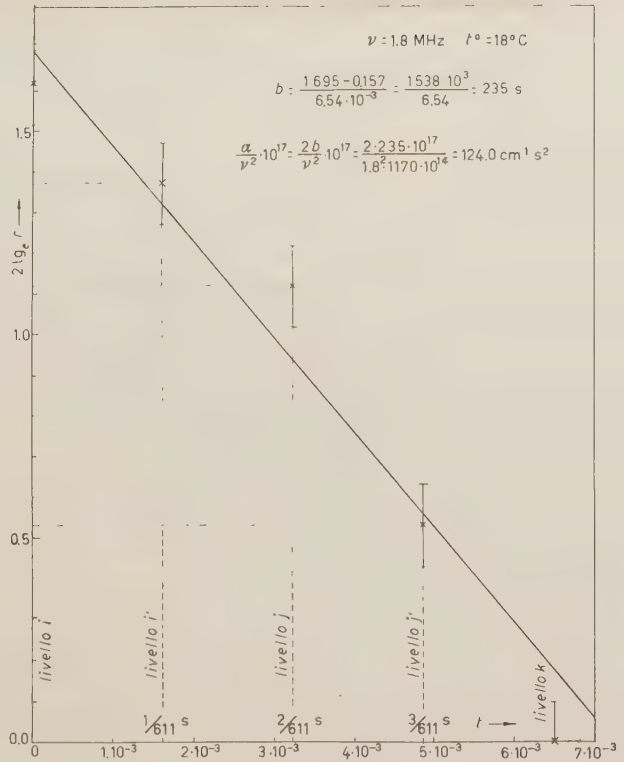

Fig. 3. – Ethyl-alcohol.

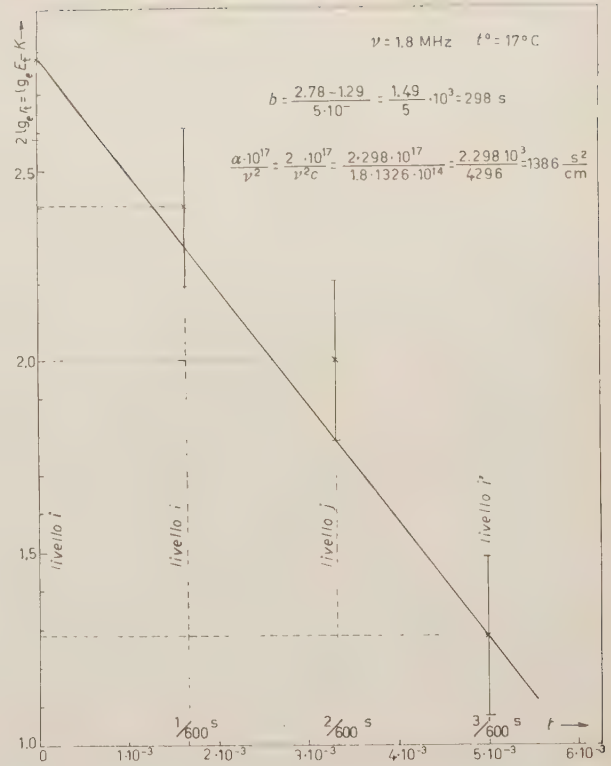

Fig. 4. – Benzol.

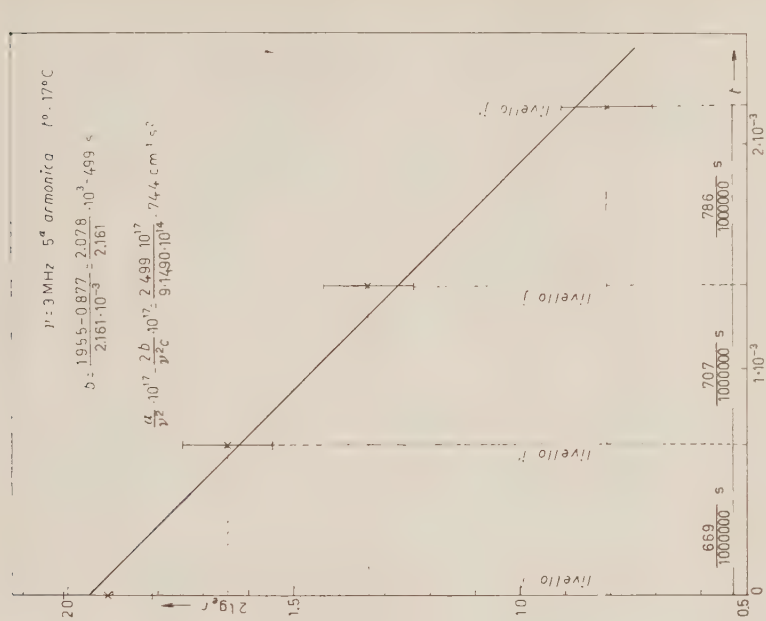

Fig. 6. – H_2O (distilled).

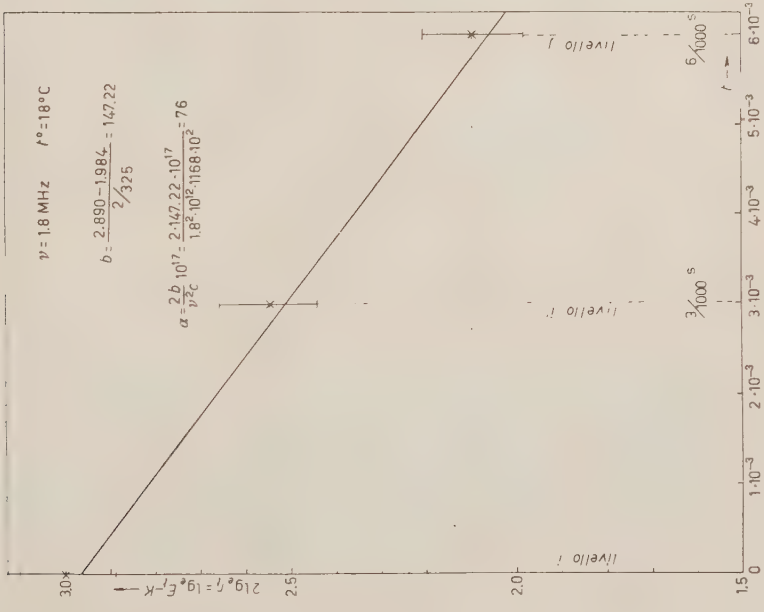

Fig. 5. – Isopropil-alcohol.

TABLE I.

Substance	Theoretical values for $\alpha/\nu^2 \cdot 10^{17}$ cm^{-1} s^2	Measured values of b and $\alpha/\nu^2 \cdot 10^{17}$ obtained with our method		Measured values of $\alpha/\nu^2 \cdot 10^{17}$ obtained by other authors with different methods at the same frequency
		b (s^{-1})	$\alpha/\nu^2 \cdot 10^{17}$ cm^{-1} s^2	
Iso-Propyl-Alcohol 1.8 MHz	33	235	124	150 Optical (PARTAHSARATY)
Benzol 1.8 MHz . . .	8.66	298	138	900 Many methods
Ethyl-Alcohol 1.8 MHz	22	147,2	76	86.5 Optical (PARTHASARATY)
Water (distilled) 1.8 MHz	8.5	157	78	70 Many methods
Water (distilled) 3 MHz	8.5	499	74	67 RÜFER; 50 Mechanic meth. BUSS
	8.5			

In Figs. 3, 4, 5 the experimental values of E are plotted against t for ethylic alcohol, benzol and iso-propyl-alcohol.

In the following table (Table I) we give the values obtained for b and α (with $\alpha = 2b/V$) together with the theoretical values of α and some of the best experimental results obtained by other authors who have worked with different methods at the same frequency. Our frequency was 1.8 MHz and the measurements were made at 17 °C in benzol and at 18 °C in the alcohols.

In the case of water we made two determinations, both at the temperature of 17 °C, but at two different frequencies 1,8 MHz and 3 MHz, that is on the 3-rd and 5-th armonic of our quartz.

We give in Fig. 6 the experimental points obtained for water at 3 MHz.

4. – Objections to the Method and Discussion of the Results.

Having discussed the method with other researchers we have met with one principal objection: that there could be the possibility that the quartz would not interrupt its oscillations at the same instant as the emission of the transmitter is ceasing. Such a possibility would have resulted in an alteration of the pattern of energy against time and given an erroneous value for b and α. That this is not the case can already be inferred from Figs. 3, 4, 5 and 6, which show a good alignment of the experimental points, but the fundamental character of such an objection caused us to make sure in a direct way of the instantaneous arrest of the oscillations of the crystal.

We therefore silvered the surface of our quartz dividing it in two sections, a large and a small one, insulated from each other. We connected in the normal way the large portion to the transmitter antenna, while the small portion was contacted to a separated electrode and connected to the deflecting vertical plates of a cathode-rays oscillograph. From inspection of the pattern appearing on the oscillograph we could control that the stop of the vibrations of the crystal took place in less than 10^{-4} s when the crystal was vibrating in air. For our purpose this means that the contribution of the inertia of the crystal to the permanence of the vibrations of the liquid column is practically zero, and that, as soon as the emission of the H.F. potential is stopped, the quartz ceases to act as a source of elastic waves, and acts only as a solid reflector.

After having cleared our path of this objection concerning the method, let us now examine critically our experimental results listed in Table I. As one can see our results agree in a general way with the results obtained by other authors; furthermore the ratio of coefficient b to the square of the frequency ν of the ultrasonic waves is constant as it appears from the coherent results for water at 1.8 MHz and at 3 MHz.

The only serious discrepancy is the one concerning Benzol for which we have found a value of 138 while that found by other authors is about 900. We repeated the measurements for benzol with great care and we found the same result (in Table I and in Fig. 4 we give this second more accurate determination).

Considering that benzol exhibits the greatest anomalies in the values of z, we think our result to be particularly interesting, as our method is the only one employing standing acoustic waves.

Unfortunately our experimental procedure is very long and cumbersome, especially the microphotometric measurements involved, we are therefore revising the method, trying to increase the accuracy of the results and to simplify very much the procedure and the calculations involved.

RIASSUNTO (*)

Si espone un nuovo procedimento per ottenere il coefficiente di assorbimento acustico con un metodo ottico che sfrutta le onde ultrasonore permanenti. Si danno alcuni risultati in buon accordo coi valori sperimentali di altri autori che hanno lavorato con altri metodi alla stessa frequenza e temperatura. Una notevole eccezione è data dal benzolo per il quale abbiamo ottenuto un valore molto minore (circa $\frac{1}{6}$) del dato sperimentale accettato. Desideriamo qui rilevare che il benzolo ha mostrato le più forti anomalie del coefficiente d'assorbimento sperimentale rispetto ai valori teorici. Il nostro risultato si approssima meglio al valore ideale.

(*) *Traduzione a cura della Redazione.*

IL NUOVO CIMENTO Vol. V, N. 4 1° Aprile 1957

Relativistic Kinematics of a Classical Point Particle in Spinor Form.

F. GÜRSEY

Theoretical Physics Department, University of Istanbul

(ricevuto il 6 Novembre 1956)

Summary. – A proper Frenet tetrad is associated with each point of the world-line of a classical point particle. It is shown that this is equivalent to the introduction of a unimodular 2×2 matrix (or, correspondingly, a suitably normed 4-spinor) as a function of the proper time. this « proper 4-spinor » being determined by the Lorentz transformation which transforms a fixed set of Cartesian axes into the proper tetrad at the point considered. The rate of change of the proper 4-spinor as the particle moves along the world-line is given by a spinor equation which involves the three curvatures and is entirely equivalent to the Frenet formulae. The proper 4-spinor is determined for simple types of world-lines. In particular, it is shown that in the case of 4-dimensional helices for which the third curvature vanishes and the other two curvatures remain constant, one obtains the world-line of a free spinning particle as described by WEYSSENHOFF while the proper 4-spinor attached to such a particle satisfies the classical analogue of Dirac's equation recently postulated by PROCA.

1. – Introduction.

The formulations of the equation of motion of a point electron in classical or wave mechanics differ in several respects. The classical Lorentz equation of motion expresses the rate of change of the velocity 4-vector in an electromagnetic field, so that a fluid of electrons can be described by a velocity field U_ν ($\nu = 0, 1, 2, 3$) which is required to satisfy a certain partial differential equation. On the other hand, the Dirac equation is concerned with the variation from point to point of a 4-spinor ψ associated with the electron. The current-

density 4-vector which corresponds to the 4-velocity field of the classical fluid is a quadratic expression in terms of the components of ψ. Thus, unlike the current and other tensorial densities, the wave function ψ which appears in the unquantized Dirac theory has no classical analogue. Accordingly, if one could introduce in classical mechanics a 4-spinor $\varphi(s)$, function of the proper time for a point particle, and a 4-spinor $q(x_\mu)$, function of position in space-time for a relativistic fluid, this would greatly facilitate the comparison between classical and quantum theories and maybe shed a new light on the process of first quantization. Thus, a new and direct way of going over from classical to quantum mechanics (such as the Feynman method) might be of value in case the Hamiltonian formalism happens to fail.

Attempts have been made [1-6] to devise classical fluid models which would exhibit some properties of the Dirac electron, the comparison being always limited to tensorial quantities in both theories. Recently, however, BOHM *et al.* [7,8] have introduced a spinor in classical (non relativistic) hydrodynamics in view of obtaining a causal model for the Pauli equation. Since it is known [9] that two complex numbers, namely the Cayley-Klein parameters, hence the corresponding spinor, can be used to describe the spatial rotation of a rigid body, their method consists in associating a spinor with the rotation of an element of the fluid. Unfortunately this method breaks down in point mechanics. Another disadvantage is the difficulty encountered in the relativistic generalization of the model. Another line of thought is due to PROCA [10,11] who arbitrarily attaches a 4-spinor to a point particle without, however, justifying this procedure by any geometrical interpretation of the associated 4-spinor. He then proceeds to find the equation of motion for the 4-spinor which would lead to the correct equation for the velocity 4-vector and the spin antisymmetrical tensor. Similar work had already been done by WEISS [12] who associated a partially determined quaternion with the motion of a relativistic particle.

[1] J. WEYSSENHOFF: *Acta Phys. Pol.*, **9**, 1, 46 (1947).

[2] P. A. M. DIRAC: *Proc. Roy. Soc.*, A **212**, 336 (1952).

[3] O. BUNEMAN: *Proc. Roy. Soc.*, A **215**, 346 (1952).

[4] T. TAKABAYASI: *Prog. Theor. Phys.*, **8**, 143 (1952); **13**, 222 (1955).

[5] M. SCHÖNBERG: *Nuovo Cimento*, **12**, 103 (1954); **1**, 543 (1955).

[6] J.-P. VIGIER: *Structure des micro-objets dans l'interprétation causale de la théorie des quanta*, Ch. I (Paris, 1956).

[7] D. BOHM, R. SCHILLER and J. TIOMNO: *Suppl. Nuovo Cimento*, **1**, 48 (1955).

[8] D. BOHM, R. SCHILLER and J. TIOMNO: *Suppl. Nuovo Cimento*, **1**, 67 (1955).

[9] See, for example, H. GOLDSTEIN: *Classical Mechanics*, Ch. IV (Cambridge Mass., 1950).

[10] A. PROCA: *Journ. de Phys. et Rad.*, **15**, 65 (1954).

[11] A. PROCA: *Nuovo Cimento*, **2**, 962 (1955).

[12] P. WEISS: *Proc. Roy. Irish. Acad.*, A **46**, 129 (1941).

Earlier and independently of BOHM and PROCA, the author ([13,14]) had developed a spinor formulation of relativistic kinematics readily applicable to a point particle, by introducing, in classical theory, a 4-spinor with a precise geometrical meaning and showing its relation to the wave function of a Dirac particle. The purpose of this paper is to give an account of the theory of the proper 4-spinor associated with the relativistic motion of a point particle with applications to the geometrical analysis of some simple but physically important world-lines.

The main idea behind the present investigation is the following. The relativistic motion of a point particle is described by a world-line at each point of which we can define an orthogonal tetrad consisting of the time-like velocity 4-vector and three suitably defined space-like unit vectors. This « proper tetrad » which was first considered by SYNGE ([15]) in connection with relativistic hydrodynamics is just the proper Frenet frame of reference generalized to space-time. Now, as we move from one point of the world-line to another, the proper tetrad undergoes a 4-dimensional rotation, i.e. a Lorentz transformation, which can be specified by the four complex components (the generalized Cayley-Klein parameters) of a unimodular 2×2 matrix depending on six real parameters ([16]). With this matrix of the second rank we can associate a 4-spinor normalized in such a way that the corresponding matrix is unimodular ([17-19]). In short, at each point of the world-line we have defined a 4-spinor $q(s)$ (the « proper 4-spinor ») which specifies the proper frame of reference. The equation of motion of the particle determines the world-line. The law of variation of $q(s)$ will be called the equation of motion for the proper 4-spinor. It can be used just as well to determine the world-line, hence, the motion of the particle.

In the case of a classical point electron the proper 4-spinor defined above is just the classical analogue of the Dirac wave function we have been looking for. This is corroborated by a detailed comparison of the properties of $q(s)$ with those of the wave function. For a classical fluid of point particles the comparison is more striking, since in that case we can define a 4-spinor at each point of space-time as the proper 4-spinor of the particle whose world-

([13]) F. GÜRSEY- *Classical and Wave Mechanics of Spinning Particles,* Habilitation Thesis, Univ. of Istanbul, March 1953 (unpublished).

([14]) F. GÜRSEY: *Phys. Rev.*, **97**, 1712 (1955).

([15]) J. L. SYNGE: *Proc. London Math. Soc.*, **43**, 376 (1937).

([16]) See, for example, F. D. MURNAGHAN: *The Theory of Group Representations*, Ch. XII (Baltimore, 1938 .

([17]) F. GÜRSEY: *Nuovo Cimento*, **3**, 988 (1956).

([18]) F. GÜRSEY: *Rev. Fac. Sc. Istanbul*, A **20**, 149 (1955).

([19]) F. GÜRSEY: *Rev. Fac. Sc. Istanbul*, A **21**, 33 (1956).

line passes through that point. The fluid may then be described by a 4-spinor field instead of a velocity field.

Here follows a sketch of the paper. Sect. 2 contains the Frenet formulae for a world-line and the definition of the basis vectors of the proper tetrad, namely the normal, the binormal and the trinormal. The antisymmetrical rotation tensor, which is the relativistic counterpart of the Darboux vector, is defined in Sect. 3 and expressed in terms of the derivatives of the velocity 4-vector. The proper matrix (hence the associated proper 4-spinor) is introduced in Sect. 4 and its equation of motion is derived. The following section deals with some special world-lines, namely helices with constant curvatures while Sect. 6 is devoted to a special study of helices for which the third curvature vanishes. In the latter case a 4-vector Π is defined which is not collinear to the velocity 4-vector and which has properties similar to the energy-momentum 4-vector in the Dirac theory. Such world-lines are physically important as they happen to represent the motion of free spinning particles (Weyssenhoff's theory) and, at the same time, correspond to stream-lines associated with plane wave solutions of Dirac's equation. Helices with constant curvatures may be visualized as arising in the motion of a point charge in a constant electromagnetic field. This special electromagnetic problem is solved in Sect. 7. Sect. 8 deals with the correspondence with Weyssenhoff's theory. Finally, in Sect. 9, the equation of motion of the proper 4-spinor, in the case of helices with vanishing third curvature, is shown to be the classical analogue, in Proca's sense, of the field free Dirac equation and the main results are summarized in 4-spinor form.

The theory of a spinning classical point charge in an arbitrary electromagnetic field and the correspondence, in this case, between the classical theory of the proper 4-spinor and Dirac's relativistic wave mechanics will be treated in subsequent papers.

In the non-relativistic case, the Cayley-Klein parameters (a 2-spinor) or a unitary 2×2 matrix can be used to describe the spatial rotation of the ordinary Frenet frame attached to the motion of a particle. This motion is then described by the rate of change of the proper 2-spinor. The resulting non-relativistic equation which would be the classical analogue of the Pauli equation will not be discussed here.

2. – The Proper Tetrad of a Moving Point.

Let the position 4-vectors of a moving point particle be denoted by

$$X(s) = [x^0(s), x^1(s), x^2(s), x^3(s)] , \tag{2.1}$$

where $x^0 = ct$ and $s = c\lambda$, λ being the proper time. We have

$$ds^2 = \gamma_{\mu\nu}\, dx^\mu\, dx^\nu \qquad (\mu, \nu = 0, 1, 2, 3), \tag{2.2}$$

$\gamma_{\mu\nu}$ standing for the metric tensor of special relativity. The components of the velocity 4-vector U are given by

$$U^\mu = \frac{\mathrm{d}x^\mu}{\mathrm{d}s}, \tag{2.3}$$

so that

$$\dot{X} = \frac{\mathrm{d}X}{\mathrm{d}s} = U\,. \tag{2.3'}$$

U is a time like unit vector, with the property

$$U_\mu U^\mu = 1\,, \tag{2.4}$$

the indices being raised and lowered by means of the metric tensor. We now put

$$U^{(0)}_\mu = U_\mu$$

and define the principal normal with components $U^{(1)}_\mu$ by means of the formula

$$\dot{U} = \varrho^{-1} U^{(1)}\,.$$

ϱ^{-1} is the first curvature and $U^{(1)}$ is a space-like unit vector orthogonal to the velocity vector U. It represents the unit acceleration vector.

The space-like unit vectors $U^{(2)}$ and $U^{(3)}$ called respectively the binormal and the trinormal, are defined by the Frenet formulae

$$\frac{\mathrm{d}U^{(0)}}{\mathrm{d}s} = \frac{1}{\varrho} U^{(1)}\,, \tag{2.5}$$

$$\frac{\mathrm{d}U^{(1)}}{\mathrm{d}s} = \frac{1}{\varrho} U^{(0)} + \frac{1}{\sigma} U^{(2)}\,, \tag{2.6}$$

$$\frac{\mathrm{d}U^{(2)}}{\mathrm{d}s} = -\frac{1}{\sigma} U^{(1)} + \frac{1}{\tau} U^{(3)}\,, \tag{2.7}$$

$$\frac{\mathrm{d}U^{(3)}}{\mathrm{d}s} = -\frac{1}{\tau} U^{2}\,, \tag{2.8}$$

where σ^{-1} and τ^{-1} denote the second and third curvature respectively.

The proper tetrad attached to the world-line

$$X = X(s) \tag{2.9}$$

consists of the velocity vector $U^{(0)}$ and the three space-like vectors $U^{(m)}$

($m = 1, 2, 3$) which satisfy the orthogonality conditions

$$U_{\alpha}^{(\mu)} U^{(\nu)\alpha} = \gamma^{\mu\nu} = \gamma_{\mu\nu} . \tag{2.10}$$

In terms of U we can write

$$U^{(0)} = U$$

$$U^{(1)} = \varrho \dot{U} \tag{2.11}$$

$$U^{(2)} = \sigma(\varrho \ddot{U} + \dot{\varrho} \dot{U} - \varrho^{-1} U) , \tag{2.12}$$

the first and second curvatures being given by

$$\varrho^{-2} = - \dot{U}_{\mu} \dot{U}^{\mu} \tag{2.13}$$

$$\sigma^{-2} = - \varrho^{2} \ddot{U}_{\mu} \ddot{U}^{\mu} + \varrho^{2}(1 - \dot{\varrho}^{2}) , \tag{2.14}$$

on account of the identities

$$\dot{U}_{\mu} U^{\mu} = 0 \tag{2.15}$$

$$\ddot{U}_{\mu} U^{\mu} = - \dot{U}_{\mu} \dot{U}^{\mu} = \varrho^{-2} \tag{2.16}$$

$$\ddot{U}_{\mu} \dot{U}^{\mu} = \dot{\varrho} \varrho^{-3} , \tag{2.17}$$

which can be derived from (2.4) and (2.13).

In the foregoing we have assumed that the world-line is not a null-path and that ϱ and σ do not vanish.

3. – The Antisymmetrical Rotation Tensor.

It is well-known that the introduction of the Darboux vector

$$\boldsymbol{\delta} = \beta \mathbf{v}^{(1)} + \alpha \mathbf{v}^{(3)} - \mathbf{v}^{(2)} \wedge \frac{\mathrm{d}\mathbf{v}^{(2)}}{\mathrm{d}s} , \tag{3.1}$$

where α is the curvature and β the torsion, allows the 3-dimensional Frenet formulae to be written in the more symmetrical form

$$\frac{\mathrm{d}\mathbf{v}^{(l)}}{\mathrm{d}s} = \boldsymbol{\delta} \wedge \mathbf{v}^{(l)} \qquad (l = 1, 2, 3), \tag{3.2}$$

$\mathbf{v}^{(1)}$, $\mathbf{v}^{(2)}$ and $\mathbf{v}^{(3)}$ denoting respectively the tangent, the normal and the binormal.

The parameter s is the length of the curve and $\boldsymbol{\delta}$ represents the rotation vector of the proper frame as it moves along the curve. If ω_{mn} is the antisymmetrical tensor which corresponds to $\boldsymbol{\delta}$, the equations (3.2) are equivalent to the tensor equation

$$\frac{\mathrm{d}V_m^{(l)}}{\mathrm{d}s} = \omega_{mn} V_n^{(l)}, \tag{3.3}$$

summation being implied over n.

Our immediate aim is to generalize (3.3) and find the antisymmetrical rotation tensor $\Omega_{\mu\nu}$ which describes the rotation of the proper frame attached to a world-line. It is found easily that $\Omega_{\mu\nu}$ is given by

$$\Omega_{\mu\nu} = \frac{1}{2}\left(\frac{\mathrm{d}U_{(\lambda)\mu}}{\mathrm{d}s} U_\nu^{(\lambda)} - \frac{\mathrm{d}U_{(\lambda)\nu}}{\mathrm{d}s} U_\mu^{(\lambda)}\right). \tag{3.4}$$

Indeed we have

$$\Omega_{\mu\nu} U^{(\varkappa)\nu} = \frac{\mathrm{d}U_\mu^{(\varkappa)}}{\mathrm{d}s} \tag{3.5}$$

on account of (2.10). Replacing the derivatives in (3.4) by the Frenet formulae (2.5-8) we find

$$\Omega_{\mu\nu} = \varrho^{-1}(U_\mu^{(1)} U_\nu^{(0)} - U_\nu^{(1)} U_\mu^{(0)}) + \sigma^{-1}(U_\mu^{(1)} U_\nu^{(2)} - U_\nu^{(1)} U_\mu^{(2)}) + \\ + \tau^{-1}(U_\mu^{(2)} U_\nu^{(3)} - U_\nu^{(2)} U_\mu^{(3)}), \tag{3.6}$$

i.e., an expression which generalizes (3.1).

We now proceed to give a 2×2 matrix expression of the rotation tensor. Introducing the matrices

$$I_0 = \begin{pmatrix} 1 & 0 \\ 0 & 1 \end{pmatrix}, \quad I_1 = \begin{pmatrix} 0 & 1 \\ 1 & 0 \end{pmatrix}, \quad I_2 = \begin{pmatrix} 0 & -i \\ i & 0 \end{pmatrix}, \quad I_3 = \begin{pmatrix} 1 & 0 \\ 0 & -1 \end{pmatrix}, \tag{3.7}$$

where I_0 is the unit matrix and I_1, I_2, I_3 the Pauli matrices, we can represent a 4-vector A_μ by the hermitian matrix

$$A = A_\mu I^\mu \tag{3.8}$$

and the antisymmetrical tensor $B_{\mu\nu}$ by the traceless matrix (*)

$$\boldsymbol{B} = \tfrac{1}{2} B_{\mu\nu} I^\mu \bar{I}^\nu, \tag{3.9}$$

(*) Traceless matrices are denoted by bold face type as they represent purely vectorial quaternions.

the bar denoting the operation of taking the adjoint matrix [see Ref. (17) def. (2.8)]. We have

$$\bar{I}_0 = I_0 \qquad \text{and} \qquad \bar{I}_m = -I_m \qquad (m = 1, 2, 3). \tag{3.10}$$

According to this scheme we introduce the matrices

$$U^{(\lambda)} = U^{(\lambda)}_{\mu} I^{\mu} \tag{3.11}$$

$$\boldsymbol{\Omega} = \tfrac{1}{2}\Omega_{\mu\nu} I^{\mu}\bar{I}^{\nu}\,. \tag{3.12}$$

The matrix equivalent of Eq. (3.5) is therefore

$$\frac{\mathrm{d}U^{(\lambda)}}{\mathrm{d}s} = \mathscr{H}(\boldsymbol{\Omega}U^{(\lambda)}) = \frac{1}{2}(\boldsymbol{\Omega}U^{(\lambda)} + U^{(\lambda)}\boldsymbol{\Omega}^{\dagger})\,, \tag{3.13}$$

where the dagger denotes the hermitian conjugate and the symbol $\mathscr{H}$ means the hermitian part of the matrix between brackets. Eq. (3.6) in matrix form reads

$$\boldsymbol{\Omega} = \varrho^{-1}U^{(1)}\bar{U}^{(0)} + \sigma^{-1}U^{(1)}\bar{U}^{(2)} + \tau^{-1}U^{(2)}\bar{U}^{(3)}\,. \tag{3.14}$$

The orthogonality conditions (2.10) are converted into the matrix relations

$$\mathrm{Tr}\,(U^{(\mu)}\bar{U}^{(\nu)}) = U^{(\mu)}\bar{U}^{(\nu)} + U^{(\nu)}\bar{U}^{(\mu)} = 2\gamma^{\mu\nu}\,. \tag{3.15}$$

On the other hand, from the properties of the Pauli matrices expressed by

$$I_1 I_2 = iI_3\,, \qquad \text{etc.} \tag{3.16}$$

we deduce

$$iU^{(0)}\bar{U}^{(1)} = U^{(2)}\bar{U}^{(3)} \tag{3.17}$$

and similar relations obtained by cyclic permutation of 1, 2, 3. Thus $\boldsymbol{\Omega}$, may as well be written as

$$\boldsymbol{\Omega} = \left(\frac{1}{\varrho} - \frac{i}{\tau}\right)U^{(1)}\bar{U}^{(0)} + \frac{1}{\sigma}U^{(3)}\bar{U}^{(2)}\,. \tag{3.18}$$

In this expression $U^{(3)}$ does not occur. Using the Frenet formulae we can also express $\boldsymbol{\Omega}$ in terms of U and its derivatives, thus obtaining

$$\boldsymbol{\Omega} = \frac{\varrho^2}{2}(\dot{U}\ddot{\bar{U}} - \ddot{U}\dot{\bar{U}}) - i\frac{\varrho}{\tau}\dot{U}\bar{U}\,. \tag{3.19}$$

Since multiplication of a matrix of the form (3.9) by the imaginary unit i gives the matrix formed by means of the dual of the antisymmetrical tensor $B_{\mu\nu}$ ([20]) it follows that we can write (3.19) in the tensor form

$$\Omega_{\mu\nu} = \varrho^2(\dot{U}_\mu \ddot{U}_\nu - \dot{U}_\nu \ddot{U}_\mu) - \varrho\tau^{-1}(\dot{U}_\mu U_\nu - \dot{U}_\nu U_\mu)^{\sim}, \tag{3.20}$$

where the tilde indicates the dual of the tensor in the second term.

4. – The Proper 4-Spinor and its Equation of Motion.

To any set of mutually orthogonal unit vectors in space-time we can always attach a unimodular matrix of the second rank Φ corresponding to the Lorentz transformation which transforms them into the unit vectors along the cartesian t, x, y and z axes. Thus we put

$$U^{(\mu)} = \Phi I^\mu \Phi^\dagger, \tag{4.1}$$

where the left hand side stands for the matrix defined by (3.11), the units I^μ denote the Pauli matrices (3.7) and Φ satisfies the condition

$$\mathrm{Det}\ (\Phi) = \Phi\bar{\Phi} = 1\,. \tag{4.2}$$

Φ is then uniquely determined, and, as shown elsewhere [Ref. ([18]), Sect. 8] is expressed by

$$\Phi = kU_{(\nu)}\bar{I}^\nu\,, \tag{4.3}$$

where k is a normalizing factor given by

$$k = [2\ \mathrm{Tr}\ (U_{(\nu)}\bar{I}^\nu)]^{-\frac{1}{2}}\,. \tag{4.4}$$

The unimodular matrix (4.3) will be called the proper matrix attached to the particle.

To find the equation of motion of Φ we put

$$2\,\frac{\mathrm{d}\Phi}{\mathrm{d}s}\,\bar{\Phi} = \boldsymbol{\Omega}'\,. \tag{4.5}$$

We first show that $\boldsymbol{\Omega}'$ is traceless. Indeed we have [see Ref. ([18]), (4.18)]

$$\mathrm{Tr}\ \boldsymbol{\Omega}' = \boldsymbol{\Omega}' + \bar{\boldsymbol{\Omega}}' = 2\left(\frac{\mathrm{d}\Phi}{\mathrm{d}s}\,\bar{\Phi} + \Phi\,\frac{\mathrm{d}\bar{\Phi}}{\mathrm{d}s}\right) = 0$$

([20]) F. GÜRSEY: *Rev. Fac. Sci. Univ. Istanbul*, A **19**, 154 (1954).

on account of (4.2). Now, differentiating (4.1) and using (4.5) we obtain

$$\frac{\mathrm{d}U^{(\mu)}}{\mathrm{d}s} = \frac{1}{2}(\boldsymbol{\Omega}' U^{(\mu)} + U^{(\mu)}\boldsymbol{\Omega}') \tag{4.6}$$

with the help of the equation

$$\boldsymbol{\Omega}'^{\dagger} = 2(\Phi)^{\dagger}\frac{\mathrm{d}\Phi^{\dagger}}{\mathrm{d}s}$$

which is associated with the hermitian conjugate of (4.5).

Comparing with (3.13) we obtain

$$(\boldsymbol{\Omega} - \boldsymbol{\Omega}')U^{(\mu)} + U^{(\mu)}(\boldsymbol{\Omega} - \boldsymbol{\Omega}')^{\dagger} = 0\,.$$

Multiplying this last relation to the right by $U_{(\mu)}$ and summing we have

$$\boldsymbol{\Omega} - \boldsymbol{\Omega}' = 0 \tag{4.7}$$

in view of the identities

$$U^{(\mu)}\overline{U}_{(\mu)} = 4 \tag{4.8}$$

and

$$U^{(\mu)}\boldsymbol{B}\,\overline{U}_{(\mu)} = 0 \tag{4.9}$$

valid for any traceless matrix B.

It follows from (4.7) and (4.5) that the equation of motion of the proper matrix is

$$\frac{\mathrm{d}\Phi}{\mathrm{d}s} = \frac{1}{2}\boldsymbol{\Omega}\Phi\,, \tag{4.10}$$

where $\boldsymbol{\Omega}$, given by (3.18) is just the traceless matrix which represents the antisymmetrical tensor of the proper frame.

Using (4.1) and (4.2) we can also write

$$U^{(1)}\overline{U}^{(0)} = \Phi I_1\Phi^{\dagger}\overline{\Phi}^{\dagger}\overline{\Phi} = \Phi I_1\overline{\Phi} \tag{4.11}$$

and

$$U^{(1)}\overline{U}^{(2)} = \Phi I_1\Phi^{\dagger}\overline{\Phi}^{\dagger}\overline{I}_2\overline{\Phi} = -\Phi I_1 I_2\overline{\Phi} = -i\Phi I_3\overline{\Phi} \tag{4.12}$$

on account of (3.16).

Thus a new matrix form of $\boldsymbol{\Omega}$ is obtained by substituting the expression

(4.11-12) into (3.18), namely

$$\mathbf{\Omega} = \Phi \boldsymbol{\omega} \overline{\Phi} \tag{4.13}$$

where

$$\boldsymbol{\omega} = \left(\frac{1}{\varrho} - \frac{i}{\tau}\right) I_1 - \frac{i}{\sigma} I_3 \,. \tag{4.14}$$

Accordingly, the equation of motion (4.10) may be written in the alternative form

$$\frac{\mathrm{d}\Phi}{\mathrm{d}s} = \frac{1}{2} \Phi \boldsymbol{\omega} \,, \tag{4.15}$$

where $\boldsymbol{\omega}$ is the traceless matrix (4.14), that is,

$$\boldsymbol{\omega} = \begin{pmatrix} -i\sigma^{-1} & \varrho^{-1} - i\tau^{-1} \\ \varrho^{-1} - i\tau^{-1} & i\sigma^{-1} \end{pmatrix} . \tag{4.14'}$$

The determinant of the rotation matrix is given by

$$\omega^2 = \mathrm{Det}\, \mathbf{\Omega} = \mathbf{\Omega}\mathbf{\Omega} = -\boldsymbol{\omega}\boldsymbol{\omega} = \sigma^{-2} - \varrho^{-2} - \tau^{-2} + 2i(\varrho\tau)^{-1} \,. \tag{4.16}$$

We have thus proved that the matrix equation (4.15) is entirely equivalent to the Frenet formulae (2.5-8) for a world-line.

It remains to find the 4-spinor form of (4.15). To this end we associate with the matrix Φ the Dirac 4-spinor φ with complex components φ_1, φ_2, φ_3, φ_4, by means of the formula

$$\Phi = \begin{pmatrix} \varphi_1 + \varphi_3 & -\varphi_2^* + \varphi_4^* \\ \varphi_2 + \varphi_4 & \varphi_1^* - \varphi_3^* \end{pmatrix} \tag{4.17}$$

where the star denotes complex conjugation. In a Lorentz transformation defined by the unimodular matrix L the vectors $U^{(\mu)}$ transform according to the law

$$U'^{(\mu)} = L U^{(\mu)} L^{+} \,, \tag{4.18}$$

so that the transformation law for Φ is

$$\Phi' = L\Phi \,. \tag{4.19}$$

This induces a transformation of the complex components of φ which can be represented by the 4×4 matrix Λ, i.e.

$$\varphi' = \Lambda\varphi \,, \tag{4.20}$$

where φ is written as a column matrix. It has been shown elsewhere [19] that (4.20) just expresses the correct transformation law for a 4-spinor, so that q defined by (4.17) is indeed a 4-spinor.

To each operation an the matrix Φ there corresponds an operation on the 4-spinor φ expressed by the Dirac matrices. Such correspondences have been worked out in detail in Ref. [19]. For our purpose we need the correspondences

$$\Phi i I_3 \to i\varphi \tag{4.21}$$

$$\Phi I_1 \to -i\alpha_2\beta\varphi^* \tag{4.22}$$

$$i\Phi \to \alpha_1\alpha_2\alpha_3\varphi = \gamma_5\varphi\,. \tag{4.23}$$

Here α_1, α_2, α_3, β are the familiar Dirac matrices while γ_5 is the matrix introduced by Pauli. If we note that

$$\varphi' = -i\alpha_2\beta\varphi^* \tag{4.24}$$

is the charge conjugate 4-spinor, instead of (4.15) we may write

$$\frac{\mathrm{d}q}{\mathrm{d}s} = (\varrho^{-1} - \gamma_5\tau^{-1})\varphi' - i\sigma^{-1}\varphi\,. \tag{4.25}$$

This is the 4-spinor equation equivalent to the Frenet formulae.

Introducing the relativistic matrices

$$\gamma_0 = \beta\,, \qquad \gamma_n = \beta\alpha_n \qquad (n = 1, 2, 3) \tag{4.26}$$

and the adjoint 4-spinor

$$\overline{\varphi} = \beta\varphi^* \tag{4.27}$$

we can derive the relations between q and the fundamental vectors of the proper frame. In Ref. [19] it is shown that

$$U_\mu^{(0)} = \overline{\varphi}\gamma_\mu\varphi \tag{4.28}$$

$$U_\mu^{(3)} = \overline{\varphi}\gamma_5\gamma_\mu\varphi \tag{4.29}$$

$$U_\mu^{(1)} + iU_\mu^{(2)} = \overline{\varphi}\gamma_\mu\varphi'\,, \tag{4.30}$$

where φ' is given by (4.24). These equations are equivalent to the matrix equations (4.1) and show that the velocity vector and the trinormal correspond respectively to the current density and spin density vectors in Dirac's

theory while the complex combination of the principal normal and the binormal corresponds to a complex vector involving the charge conjugate and first introduced by DE BROGLIE ([21]).

5. Special Helices for which the Three Curvatures are Constant.

Let us consider a class of simple world-lines, namely space-time helices defined by the property

$$\dot{\mathbf{\Omega}} = \mu(s)\mathbf{\Omega} \tag{5.1}$$

which is a generalization of the condition

$$\frac{\mathrm{d}\boldsymbol{\delta}}{\mathrm{d}s} = \mu(s)\boldsymbol{\delta} ,$$

obeyed by the Darboux vector for 3-dimensional helices. The scalar function μ can be eliminated by noting that (5.1) leads to

$$\mathbf{\Omega}\dot{\mathbf{\Omega}} - \dot{\mathbf{\Omega}}\mathbf{\Omega} = 0 , \tag{5.2}$$

in analogy with the condition

$$\boldsymbol{\delta} \times \frac{\mathrm{d}\boldsymbol{\delta}}{\mathrm{d}s} = 0$$

in the 3-dimensional case.

A simple calculation yields

$$\mathbf{\Omega}\dot{\mathbf{\Omega}} - \dot{\mathbf{\Omega}}\mathbf{\Omega} = \frac{2}{\sigma^2}\left\{\frac{\mathrm{d}}{\mathrm{d}s}\left(\frac{\sigma}{\varrho} - i\frac{\sigma}{\tau}\right)\right\} U\bar{U}^{(c)} ,$$

so that, for space-time helices, the ratios σ/ϱ, σ/τ and hence τ/ϱ must all be constant. Accordingly, their proper matrix satisfies the equation

$$\frac{\mathrm{d}\Phi}{\mathrm{d}s} = \frac{1}{2}\omega(s)\Phi\boldsymbol{a} , \tag{5.3}$$

where ω^2 is the determinant of $\mathbf{\Omega}$ defined by (4.17) and the matrix $\boldsymbol{a}$ is constant and unimodular.

In particular, we consider helices for which all the three curvatures are constant and different from zero. Then, $\mathbf{\Omega}$ and its determinant ω^2 are also

([21]) L. DE BROGLIE: *Une Nouvelle Théorie de la Lumière*, vol. I (Paris, 1940).

constant. From (3.12) and (3.14) we obtain

$$\mathbf{\Omega} U^{(1)} = (\varrho^{-1} - i\tau^{-1}) U + \sigma^{-1} U^{(2)} .$$

Taking the antihermitian parts of the matrices in both sides and using the first Frenet formula (2.5) we obtain the equation

$$\frac{1}{2}\left(\mathbf{\Omega}\frac{\mathrm{d}U}{\mathrm{d}s} - \frac{\mathrm{d}U}{\mathrm{d}s}\mathbf{\Omega}^{\dagger}\right) = -\frac{i}{\varrho\tau} U , \tag{5.4}$$

which can be integrated immediately, giving

$$X - X_0 = \frac{i}{2}\varrho\tau\,(\mathbf{\Omega} U - U\mathbf{\Omega}^{\dagger}) = i\varrho\tau\mathscr{A}(\mathbf{\Omega} U) , \tag{5.5}$$

where X_0 is the matrix which corresponds to a constant vector and the symbol $\mathscr{A}$ stands for « antihermitian part ». The constant coefficient on the right hand side may also be expressed in terms of $\mathbf{\Omega}$ by noting that (4.16) leads to

$$i\varrho\tau/2 = 2(\omega^{*2} - \omega^2)^{-1} . \tag{5.6}$$

It now remains to determine the function $U(s)$; Eq. (4.10) gives

$$\Phi(s) = \exp\left[\tfrac{1}{2}\mathbf{\Omega} s\right]\Phi(0) , \tag{5.7}$$

so that we have

$$U(s) = \Phi\Phi^{\dagger} = \exp\left[\tfrac{1}{2}\mathbf{\Omega} s\right] U(0) \exp\left[\tfrac{1}{2}\mathbf{\Omega}^{\dagger} s\right] , \tag{5.8}$$

where $U(0)$ is the initial velocity. Accordingly the world-line is given by

$$X(s) - X_0 = i\varrho\tau \exp\left[\tfrac{1}{2}\mathbf{\Omega} s\right]\left\{\mathscr{A}[\mathbf{\Omega} U(0)]\right\}\exp\left[\tfrac{1}{2}\mathbf{\Omega}^{\dagger} s\right] . \tag{5.9}$$

6. - Special Helices for which the Third Curvature Vanishes. The Constant 4-Vector Π.

If the third curvature τ^{-1} of a space-time helix vanishes the method of integration of the preceding section is no longer valid. In this Section we study such world-lines which, according to the Frenet formula (2.8) are characterized by a constant trinormal. In this case the trinormal is defined not by (2.7), but as a 4-vector orthogonal to U, $U^{(1)}$ and $U^{(2)}$. The vanishing of τ^{-1} is important by itself as it can be shown that it is a conformal invariant condition.

For a helix with zero third curvature the equation of motion of the proper matrix is given by (5.3) where

$$\omega = (\sigma^{-2} - \varrho^{-2})^{\frac{1}{2}} \tag{6.1}$$

and

$$\boldsymbol{a} = \omega^{-1}\boldsymbol{\omega} = (1 - \sigma^2\varrho^{-2})^{-\frac{1}{2}}(\sigma\varrho^{-1}I_1 - iI_3)\,. \tag{6.2}$$

In the following we shall concern ourselves with helices for which ω is real. In this case the radius of second curvature is less than the radius of first curvature and we may put

$$\sigma/\varrho = \operatorname{tgh}\alpha\,, \tag{6.3}$$

α being a constant positive real scalar. We have then

$$\sigma^{-1} = \omega\cosh\alpha\,, \qquad \varrho^{-1} = \omega\sinh\alpha\,. \tag{6.4}$$

It is useful to introduce the antihermitian matrices $\boldsymbol{e}_n$ (quaternion units) defined by

$$\boldsymbol{e}_n = -iI_n \qquad (n = 1, 2, 3). \tag{6.5}$$

The matrix $\boldsymbol{a}$ can now be put in the form

$$\boldsymbol{a} = I_1\sinh\alpha - iI_3\cosh\alpha = \exp[i\boldsymbol{e}_2\alpha]\boldsymbol{e}_3\,. \tag{6.6}$$

If we define a new matrix Ψ by

$$\Psi = \Phi\exp[i\boldsymbol{e}_2\alpha/2]\,, \tag{6.7}$$

then, Eq. (5.7) takes the simple form

$$\frac{\mathrm{d}\Psi}{\mathrm{d}s} = \frac{1}{2}\omega(s)\Psi\boldsymbol{e}_3\,. \tag{6.8}$$

Denoting by ψ the 4-spinor associated with Ψ we obtain the equivalent spinor equation

$$i\frac{\mathrm{d}\psi}{\mathrm{d}s} = \frac{1}{2}\omega(s)\psi\,. \tag{6.9}$$

We now introduce an important 4-vector Π orthogonal to both $U^{(1)}$ and $U^{(3)}$

which, like $U^{(3)}$ remains constant during the motion. We define

$$\Pi = U + \sigma\varrho^{-1}U^{(2)} = \Phi(1 + I_2 \operatorname{tgh} \alpha)\Phi^\dagger \tag{6.10}$$

or

$$\Pi = (\cosh \alpha)^{-1}\Phi \exp[i\boldsymbol{e}_2\alpha]\Phi^\dagger = (\cos h\alpha)^{-1}\Psi\Psi^\dagger . \tag{6.11}$$

In terms of $\boldsymbol{\Omega}$ it can also be expressed by

$$\Pi = i\sigma\boldsymbol{\Omega}U^{(3)} = (\cos h\alpha)^{-1}i\boldsymbol{a}U^{(3)} \tag{6.12}$$

on account of

$$\boldsymbol{\Omega} = \omega\Psi\boldsymbol{e}_3\Psi \tag{6.13}$$

and

$$U^{(3)} = \Phi I_3\Phi^\dagger = i\Psi\boldsymbol{e}_3\Psi^\dagger . \tag{6.14}$$

It is seen from (6.12) that Π remains constant, since α, $\boldsymbol{a}$ and the trinormal are constant.

The equation of motion (4.10) may now be given a new form by using the 4-vector Π. From (6.12) we get

$$\boldsymbol{\Omega} = i\sigma^{-1}\Pi\bar{U}^{(3)} ,$$

so that, remembering the definition (4.1) of $U^{(3)}$, we can write

$$\frac{\mathrm{d}\Phi}{\mathrm{d}s} = \frac{1}{2}\sigma^{-1}\Pi\bar{\Phi}^\dagger\boldsymbol{e}_3 . \tag{6.15}$$

To translate this equation into 4-spinor language we need the correspondences [Ref. (19), Sect. 3]

$$\Phi^\dagger \to \beta\varphi , \tag{6.16}$$

$$I_n\Phi \to \alpha_n\varphi , \tag{6.17}$$

where φ is the 4-spinor associated with the matrix Φ. Using the matrices γ_ν (1.26) and denoting the components of Π by Π^ν we derive the correspondence

$$\Pi\bar{\Phi}^\dagger = \Pi^\nu I_\nu\bar{\Phi}^\dagger \to \Pi^\nu\gamma_\nu\varphi . \tag{6.18}$$

From (4.21) we obtain finally the 4-spinor equation

$$2i\sigma\frac{\mathrm{d}\varphi}{\mathrm{d}s} = \Pi^\nu\gamma_\nu\varphi , \tag{6.19}$$

where σ is the radius of second curvature and Π a constant 4-vector. Unlike the equation obtained by putting $\tau^{-1} = 0$ in (4.25), the equation of motion for the proper 4-spinor in the form (6.19) does not involve the charge conjugate function and is more readily comparable with the relativistic wave equation in quantum mechanics. It is seen to have the same form as the field free equation postulated by PROCA ([10]) who had arbitrarily attached a 4-spinor to a moving point. In our notations Proca's equation reads

$$i\hbar \frac{\mathrm{d}\varphi}{\mathrm{d}s} = p^\nu \gamma_\nu \varphi \,, \tag{6.20}$$

where p^ν represents the energy momentum 4-vector of the particle.

We now proceed to determine the world-line when $\boldsymbol{\omega}$ is constant. In this case both ϱ and σ are constant. First we note that from (4.18)

$$\boldsymbol{\Omega} U = \varrho^{-1} U^{(1)} - i\sigma^{-1} U^{(2)} \,. \tag{6.21}$$

Hence, the hermitian part of both sides gives

$$\mathscr{H}(\boldsymbol{\Omega} U) = \tfrac{1}{2}(\boldsymbol{\Omega} U + U\boldsymbol{\Omega}^\dagger) = \varrho^{-1} U^{(1)} \,, \tag{6.22}$$

which is just one of the equations (3.13), while the antihermitian part gives

$$\mathscr{A}(\boldsymbol{\Omega} U) = \tfrac{1}{2}(\boldsymbol{\Omega} U - U^\dagger \boldsymbol{\Omega}) = -i\sigma^{-1} U^{(2)} \,, \tag{6.23}$$

so that from (6.12) we obtain

$$\Pi = ic\boldsymbol{\Omega} U^{(2)} = -\sigma^2 \boldsymbol{\Omega} \mathscr{A}(\boldsymbol{\Omega} U) \,. \tag{6.24}$$

Now, combining Eq. (6.10) with the Frenet formula (2.6) we have

$$\Pi = (1 - \sigma^2 \varrho^{-2}) U + \sigma^2 \varrho^{-1} \frac{\mathrm{d}U^{(1)}}{\mathrm{d}s} = (\cosh \alpha)^{-2} \left(U + \omega^{-1} \sinh \alpha \frac{\mathrm{d}U^{(1)}}{\mathrm{d}s} \right) , \tag{6.25}$$

which can be integrated immediately, giving

$$X - X_0 = (\Pi \cosh^2 \alpha) s - \omega^{-1} \sinh \alpha \; U^{(1)}(s) \,, \tag{6.26}$$

where X_0 is a constant 4-vector. To compare thise quation with the solution (5.5) in the previous case, we substitute in (6.26) for Π and $U^{(1)}$ which are given respectively by (6.24) and (6.22). Thus we obtain

$$X(s) - X_0 = \omega^{-2} \{ [\boldsymbol{\Omega} \mathscr{A}(\boldsymbol{\Omega} U)] s - \mathscr{H}(\boldsymbol{\Omega} U) \} \,. \tag{6.27}$$

To determine $U(s)$ we use again (5.8) where $\mathbf{\Omega}$ is now given by (6.13) or

$$\mathbf{\Omega} = \omega \Psi(0) \boldsymbol{e}_3 \Psi(0) ,$$

since, in this case, Eq. (6.8) yields

$$\Psi(s) = \Psi(0) \exp[\tfrac{1}{2} \boldsymbol{e}_3 \omega s] = \exp[\tfrac{1}{2} \mathbf{\Omega} s] \Psi(0) . \tag{6.28}$$

Hence, the world-line has the equation

$$X(s) - X_0 = \omega^{-2} \{ \mathbf{\Omega} \mathscr{R}_e \mathbf{\Omega} I^{\cdot}(0) \} \} s \quad \omega^{-2} \exp[\tfrac{1}{2} \mathbf{\Omega} s] \{ \mathscr{R}[\mathbf{\Omega} I^{\cdot}(0)] \} \exp[\tfrac{1}{2} \mathbf{\Omega}^{\dagger} s] . \tag{6.29}$$

It may be noted that from (6.26) and (6.28) we obtain the following expression for the average velocity 4-vector

$$\langle U(s) \rangle_{\text{Av.}} = \Pi \cosh^2 \alpha \tag{6.30}$$

which is thus seen to be proportional to the constant 4-vector Π.

In the rest system of Π we have

$$\begin{aligned} X'(s) - X'_0 &= \bar{\Psi}(0)(X - X_0) \bar{\Psi}^{\dagger}(0) \\ &= (\cosh \alpha) s - \omega^{-1} \sinh \alpha \exp[\tfrac{1}{2} \boldsymbol{e}_3 \omega s] \boldsymbol{i} \boldsymbol{e}_1 \exp[-\tfrac{1}{2} \boldsymbol{e}_3 \omega s] , \end{aligned} \tag{6.31}$$

so that, in this system the particle revolves with constant angular velocity ω on a circle of radius

$$r_0 = \omega^{-1} \sinh \alpha = \omega^{-2} \varrho^{-1} = \tfrac{1}{2} \sigma \sinh 2\alpha \tag{6.32}$$

in the Ox, Oy plane.

7. – Motion of a Point Charge in a Constant Electromagnetic Field.

The Lorentz equation for a charged particle moving in the electromagnetic field $F_{\mu\nu}$ reads

$$\frac{\mathrm{d} U^{\mu}}{\mathrm{d} s} = k F^{\mu}{}_{\nu} U^{\nu} , \tag{7.1}$$

where U is the velocity 4-vector and k the ratio of the charge of the particle to its rest mass. If the traceless 2×2 matrix corresponding to $F_{\mu\nu}$ is denoted by

$$\boldsymbol{F} = \tfrac{1}{2} F_{\mu\nu} I^{\mu} \bar{I}^{\nu} , \tag{7.2}$$

Eq. (7.1) takes the matrix form

$$\frac{\mathrm{d}U}{\mathrm{d}s} = k\mathcal{H}(\boldsymbol{F}U) = \frac{1}{2}k(\boldsymbol{F}U + U\boldsymbol{F}^{\dagger}) , \tag{7.3}$$

which is similar to the first Frenet formula (3.13) with $k\boldsymbol{F}$ replacing the rotation matrix $\boldsymbol{\Omega}$.

In case the field is constant, Eq. (7.3) can be integrated easily as already shown by TAUB ([22]). In this section we show that the corresponding world-lines are special helices of the type considered in Sect. **5**.

Since Eq. (7.3) is satisfied by a world-line the rotation matrix of which is

$$\boldsymbol{\Omega} = k\boldsymbol{F} , \tag{7.4}$$

the proper matrix Φ of that world-line may be chosen as to satisfy the equation

$$\frac{\mathrm{d}\Phi}{\mathrm{d}s} = \frac{1}{2}k\boldsymbol{F}\Phi , \tag{7.5}$$

which was first proposed by TAUB in a 4-spinor form. Hence the world-line with equation (5.9) is a solution of (7.1). On the other hand we have

$$\mathrm{Det}\,\boldsymbol{F} = \boldsymbol{F}\overline{\boldsymbol{F}} = -\boldsymbol{F}^2 = g + ih , \tag{7.6}$$

where

$$g = F_{\mu\nu}F^{\mu\nu} \qquad \text{and} \qquad h = F_{\mu\nu}\tilde{F}^{\mu\nu} . \tag{7.6'}$$

Accordingly the world-line of the point charge is given by

$$X(s) - X_0 = i(kh)^{-1}\exp\left[\tfrac{1}{2}k\boldsymbol{F}s\right]\left\{\mathcal{H}[\boldsymbol{F}U(0)]\right\}\exp\left[\tfrac{1}{2}k\boldsymbol{F}^{\dagger}s\right] . \tag{7.7}$$

In case

$$h = 0 \qquad \text{and} \qquad g > 0 , \tag{7.8}$$

the solution (7.7) is no longer valid and the world-line becomes a helix with constant first and second curvatures but zero third curvature, as described in the preceding section. We have from (6.29)

$$X(s) - X_0 = g^{-1}\left\{\boldsymbol{F}\mathcal{H}[\boldsymbol{F}U(0)]\right\}s + \\ + (kg)^{-1}\exp\left[\tfrac{1}{2}k\boldsymbol{F}s\right]\left\{\mathcal{H}[\boldsymbol{F}U(0)]\right\}\exp\left[\tfrac{1}{2}k\boldsymbol{F}^{\dagger}s\right] . \tag{7.9}$$

([22]) A. H. TAUB: *Rev. Mod. Phys.*, **21**, 388 (1949).

Therefore, helices with constant and non vanishing curvatures can be physically realized by the world-lines of point charges in a constant electromagnetic field for which the invariants (7.6′) are both different from zero, while helices with vanishing third curvature correspond to the motion of point charges in an electromagnetic field in which the electric and magnetic vectors are perpendicular and the latter larger in magnitude than the former.

8. – Motion of a Free Spinning Particle.

We now propose to give another physical illustration of the helices with constant first and second curvature and vanishing third curvature considered in Sect. **6**. It will presently be shown that such helices are the world-lines of free spinning point particles fully studied by WEYSSENHOFF [1] following FRENKEL [23], THOMAS [24] and others.

WEYSSENHOFF has shown that for a free spinning particle the energy-momentum 4-vector P remains constant while the velocity 4-vector $U(s)$ varies periodically along the world-line. This is the fundamental difference with spinless particles for which P is proportional to U.

Let the spin of the particle be represented by the antisymmetrical tensor $S_{\alpha\beta}$. We have the condition

$$S_{\alpha\beta}U^{\beta} = 0 \tag{8.1}$$

expressing that the components S_{01}, S_{02}, S_{03} vanish in the rest system. Further, the following relations hold

$$U_{\alpha}P^{\alpha} = m_0 \tag{8.2}$$

$$U_{\alpha}P_{\beta} - U_{\beta}P_{\alpha} = -\dot{S}_{\alpha\beta}\,, \tag{8.3}$$

where the dot denotes differentiation with respect to the proper time s, and m_0 is the rest mass of the particle. The total angular momentum $M_{\alpha\beta}$ which is the sum of the orbital angular momentum $L_{\alpha\beta}$ and the spin angular momentum $S_{\alpha\beta}$ is a constant of the motion, i.e.

$$M_{\alpha\beta} = L_{\alpha\beta} + S_{\alpha\beta} = X_{\alpha}P_{\beta} - X_{\beta}P_{\alpha} + S_{\alpha\beta} = \text{const}\,. \tag{8.4}$$

The differentiation of this last equation leads immediately to (8.3). Integrating (8.2) with a suitable initial condition we obtain

$$P^{\alpha}X_{\alpha} = m_0 s\,. \tag{8.5}$$

(23) J. FRENKEL: *Zeits. f. Phys.*, **37**, 273 (1926).
(24) L. H. THOMAS: *Phil. Mag.*, **3**, 1 (1927).

Let X, U and P be the hermitian 2×2 matrices respectively associated with X_α, U_α and P_α. Define further the traceless matrix $\boldsymbol{S}$ by

$$\boldsymbol{S} = \tfrac{1}{2}S_{\alpha\beta}I^\alpha\bar{I}^\beta \tag{8.6}$$

and $\boldsymbol{M}$ and $\boldsymbol{L}$ in a similar manner. Then we have the equivalent matrix relations

$$\tilde{\mathscr{C}}(\boldsymbol{S}U) = \tfrac{1}{2}(\boldsymbol{S}U + U\boldsymbol{S}^\dagger) = 0 \tag{8.7}$$

$$\boldsymbol{M} = \tfrac{1}{2}(X\bar{P} - P\bar{X}) + \boldsymbol{S} = \text{const} \tag{8.8}$$

and

$$\tfrac{1}{2}\,\mathrm{Tr}\,(X\bar{P}) = m_0 s\,. \tag{8.9}$$

Returning now to the special helices of Sect. **6** we have

$$(X - X_0)\dot{\bar{\Pi}} = s - \omega^{-1}\sinh\alpha\; U^{(1)}(s)\bar{\Pi}\,. \tag{8.10}$$

Taking the trace of both sides we find

$$\tfrac{1}{2}\,\mathrm{Tr}\,(X\bar{\Pi}) = s + \text{const} \tag{8.11}$$

and subtracting (8.11) from (8.10) we get

$$\tfrac{1}{2}(X\dot{\bar{\Pi}} - \Pi\dot{\bar{X}}) + \tfrac{1}{2}\omega^{-1}\sinh\alpha(U^{(1)}\bar{\Pi} - \Pi\bar{U}^{(1)}) = \text{const}\,. \tag{8.12}$$

Define the traceless matrix $\boldsymbol{\Lambda}$ by

$$\boldsymbol{\Lambda} = \tfrac{1}{2}(X\bar{\Pi} - \Pi\bar{X})\,. \tag{8.13}$$

Using (6.11) and the expression

$$U^{(1)} = \Phi i\boldsymbol{e}_1\Phi^\dagger = \Psi i\boldsymbol{e}_1\Psi^\dagger \tag{8.14}$$

for $U^{(1)}$, we obtain from (8.12)

$$\boldsymbol{\Lambda} = -\,\omega^{-1}(\mathrm{tgh}\,\alpha)\Psi i\boldsymbol{e}_1\bar{\Psi} + \text{const}\,. \tag{8.15}$$

We now use the relation

$$\Psi\boldsymbol{e}_3\bar{\Psi} = (\cosh\alpha)^{-1}\Phi\boldsymbol{e}_3\bar{\Phi} - (\mathrm{tgh}\,\alpha)\Psi i\boldsymbol{e}_1\bar{\Psi}\,, \tag{8.16}$$

which is obtained by multiplying the identity

$$\exp[i\boldsymbol{e}_2\alpha]\boldsymbol{e}_3 = (\cosh\alpha)^{-1}\boldsymbol{e}_3 - (\operatorname{tgh}\alpha)\exp[i\boldsymbol{e}_2\alpha]i\boldsymbol{e}_1\,,$$

to the left by Φ, to the right by $\overline{\Phi}$ and taking (6.7) into account. Introducing the matrix

$$\boldsymbol{\Sigma} = (\omega\cosh\alpha)^{-1}\Phi\boldsymbol{e}_3\overline{\Phi} = -i\sigma U^{(3)}\overline{U} \tag{8.17}$$

and employing (6.13) and (8.15), we may write (8.16) in the form

$$\text{const} + \omega^{-2}\boldsymbol{\Omega} = \boldsymbol{\Lambda} + \boldsymbol{\Sigma}\,. \tag{8.18}$$

On the other hand, we have

$$\mathscr{H}(\boldsymbol{\Sigma}U) = \tfrac{1}{2}(\boldsymbol{\Sigma}U + U\boldsymbol{\Sigma}) = 0 \tag{8.19}$$

directly from the definition (8.17). We also have

$$\tfrac{1}{2}\operatorname{Tr}(X\overline{\Pi}) = s + \text{const}\,. \tag{8.20}$$

We can always choose the origin as to make X_0 vanish in (6.26-27). In that case the constants which occur in (8.18) and (8.20) vanish too, so that the pairs of equations (8.7-8.19), (8.8-8.18) and (8.9-8.20) become identical if we put

$$P = m_0\Pi\,, \tag{8.21}$$

$$\boldsymbol{S} = m_0\boldsymbol{\Sigma}\,, \tag{8.22}$$

$$\boldsymbol{L} = m_0\boldsymbol{\Lambda}\,, \tag{8.23}$$

$$\boldsymbol{M} = m_0\omega^{-2}\boldsymbol{\Omega} = -m_0\boldsymbol{\Omega}^{-1}\,. \tag{8.24}$$

The fact that Π and $\boldsymbol{\Omega}$ are constant along the helix expresses that the energy-momentum 4-vector and the total angular momentum tensor are constants of the motion. The velocity $U(s)$, the spin $m_0\boldsymbol{\Sigma}(s)$ and the orbital angular momentum $m_0\boldsymbol{\Lambda}(s)$ are not constant. The spin is expressed by the rotation of the proper Frenet frame of the particle in such a way that the trinormal remains constant. The spin pseudovector is defined by

$$K_\mu = \tilde{S}_{\mu\nu}U^\nu\,,$$

which may be written in matrix form as

$$iK = \mathscr{R}(\boldsymbol{S}U) = \boldsymbol{S}U = m_0\sigma\boldsymbol{\Sigma}U\,,$$

so that we have

$$K = m_0 \sigma U^{(3)} . \tag{8.25}$$

Therefore the spin pseudovector is proportional to the trinormal and is also a constant of motion.

We also obtain easily the relation

$$m_0 U \overline{\Pi} = - m_c \mathbf{\Sigma\Omega} , \tag{8.26}$$

from which we derive

$$\tfrac{1}{2} \operatorname{Tr} (U\overline{P}) = - \tfrac{1}{2} \operatorname{Tr} (\boldsymbol{S\Omega}) = m_0 \tag{8.27}$$

and

$$\tfrac{1}{2}(U\overline{P} - P\overline{U}) = \tfrac{1}{2}(\mathbf{\Omega}\boldsymbol{S} - \boldsymbol{S\Omega}) = - \dot{\boldsymbol{S}} . \tag{8.28}$$

Another relation between P and U is obtained by multiplying (8.28) to the right by U, namely

$$\tfrac{1}{2} U\overline{P}U - \tfrac{1}{2} P = - \dot{\boldsymbol{S}} U . \tag{8.29}$$

On the other hand we have

$$U\overline{P}U = 2(U \cdot \overline{P})U - P = 2m_0 U - P ,$$

so that (8.29) gives

$$P = (m_0 + \dot{\boldsymbol{S}})U . \tag{8.30}$$

Taking the reciprocals of both sides we have

$$P^{-1} = \overline{U}(m_0 + \dot{\boldsymbol{S}})^{-1}$$

from which we derive

$$U = (\overline{P})^{-1}(m_0 - \dot{\boldsymbol{S}}) = M_0^{-2} P(m_0 - \dot{\boldsymbol{S}}) , \tag{8.31}$$

where

$$M_0 = (P\overline{P})^{\frac{1}{2}} = m_0 (\cosh \alpha)^{-1} \tag{8.32}$$

is the rest mass energy defined as the magnitude of the energy-momentum 4-vector and is different from m_0 as in Weyssenhoff's theory.

These relations which all have their analogues in relativistic quantum mechanics are characteristic of a classical spinning particle and can be found in tensor form in Weyssenhoff's paper, except the last relation (8.31) which is the classical analogue of Gordon's decomposition of the Dirac current.

9. – Classical Analogue of the Field Free Dirac Equation and Summary of the Main Results.

Our next object is to find the relation between the rest energy, the magnitude of the spin and the frequency of the 4-spinor associated with the particle. The solution given by (6.28) and (6.7) shows that the angular frequency of the 4-spinor attached to the Frenet frame is

$$a = \tfrac{1}{2}\omega$$

since the argument of the exponential in the expression of q is $(i\omega s/2)$. On the other hand, the magnitude of the spin can be obtained from (8.22) and (8.17). We have

$$\text{spin} = m_0\sigma = m_0(\omega \cosh \alpha)^{-1} .$$

The rest energy (8.32) may therefore be written as

$$M_0 = m_0\sigma(\sigma \cosh \alpha)^{-1} = m_0\sigma \times \omega = 2 \times \text{spin} \times a . \tag{9.1}$$

This shows that the rest energy is given by the product of twice the spin magnitude with the angular frequency of the proper 4-spinor. In particular, if the spin has the value $\hbar/2$ as in the case of the electron, then we obtain

$$M_0 = \hbar a = h\nu_0 ,$$

where ν_0 is the rest frequency of φ. This is just the correct quantum mechanical relation which shows that ν_0 is the rest frequency of the proper 4-spinor associated with the particle and not the frequency of its velocity 4-vector.

The equation of motion of the proper 4-spinor φ, namely (6.19) may also be written as

$$2im_0\sigma \frac{\mathrm{d}\varphi}{\mathrm{d}s} = p^\nu \gamma_\nu \varphi , \tag{9.2}$$

on multiplication of both sides by m_0. Here, on account of (8.21) the constants p^ν are now the components of the energy-momentum 4-vector. Again, if $\hbar/2$ denotes the spin magnitude $m_0\sigma$, then (8.34) takes the form

$$i\hbar \frac{\mathrm{d}\varphi}{\mathrm{d}s} = p^\nu \gamma_\nu \varphi , \tag{9.2'}$$

which is the same as the Proca equation (6.20).

Corresponding to the condition (4.2) we have the normalization conditions

$$\bar{\varphi}\varphi = 1 \qquad \text{and} \qquad \bar{\varphi}\gamma_5\varphi = 0\,. \tag{9.3}$$

Another form of the equation of motion for φ which may be obtained from (4.2) with the help of (3.12) and the correspondences (6.16-17) is

$$\frac{\mathrm{d}\varphi}{\mathrm{d}s} = \frac{1}{8}(\gamma_\mu\gamma_\nu - \gamma_\nu\gamma_\mu)\Omega_{\mu\nu}\varphi\,, \tag{9.4}$$

where $\Omega_{\mu\nu}$ represents the antisymmetrical rotation tensor

$$\Omega_{\mu\nu} = \varrho^2(\dot{U}_\mu\ddot{U}_\nu - \dot{U}_\nu\ddot{U}_\mu) \tag{9.4}$$

obtained from (3.20) in the case of zero third curvature.

Another equation equivalent to (9.2) and (9.4), and involving the charge conjugate 4-spinor is

$$\frac{\mathrm{d}\varphi}{\mathrm{d}s} = \varrho^{-1}\varphi' - i\sigma^{-1}\varphi \tag{9.6}$$

which is the same as (4.25) if we put $\tau^{-1} = 0$.

The transformation of the above equations into the simpler form (6.9), i.e.

$$i\frac{\mathrm{d}\psi}{\mathrm{d}s} = \frac{1}{2}\omega\psi$$

is carried out by means of the transformation formula (6.7) which is equivalent to the 4-spinor relation

$$\psi = \left((\cosh\frac{\alpha}{2}\right)\varphi + i\left(\sinh\frac{\alpha}{2}\right)\varphi' \tag{9.7}$$

on account of (4.21-22) and (4.24).

The essential fact in the present paper is that the Proca equation (9.2′) is purely classical, since φ is the classical 4-spinor attached to the proper frame of the world-line, P with components p_ν denotes the classical energy-momentum 4-vector and $\hbar$ stands for twice the spin magnitude of the proper frame. On the other hand this equation completely characterizes the world-line of a Weyssenhoff particle and may be used instead of the tensorial equations in Weyssenhoff's theory. It bears a very close resemblance to the Dirac theory, of which it is the classical analogue for a point particle.

The foregoing considerations show clearly that some of the features of the wave theory of the electron which were thought to be intrinsically quantum mechanical in character already make their appearance in classical theory and can be understood within its framework.

RIASSUNTO (*)

Una appropriata tetrade di Frenet è associata ad ogni punto della linea d'universo per l'introduzione di una matrice 2×2 unimodulare (o, corrispondentemente, un 4-spinore opportunamente normato) come funzione del tempo proprio, essendo tale « 4-spinore proprio » determinato dalla trasformazione di Lorentz che trasforma una terna fissa di assi cartesiani nella tetrade propria nel punto considerato. La misura della variazione del 4-spinore proprio quando la particella percorre la linea d'universo è data da un'equazione spinoriale che comprende le tre curvature ed è del tutto equivalente alle formule di Frenet. Si determina il 4-spinore proprio per alcuni tipi semplici di linee d'universo. Si mostra in particolare che nel caso di eliche quadridimensionali, per le quali la terza curvatura si annulla e le altre due restano costanti, si ottiene la linea d'universo di una particella liberamente rotante come descritta da Weissenhoff mentre il 4-spinore proprio unito a una simile particella corrisponde all'analogo classico dell'equazione di Dirac recentemente postulato da Proca.

(*) *Traduzione a cura della Redazione.*

IL NUOVO CIMENTO Vol. V, N. 4 1° Aprile 1957

Quantum Statistics of Fields and Multiple Production of Mesons.

H. Ezawa, Y. Tomozawa and H. Umezawa

Department of Physics, University of Tokyo, Japan

(ricevuto il 20 Novembre 1956)

Summary. — Thermodynamical relations in quantum field theory will be discussed. This gives a possibility to decide whether or not the interactions are renormalizable, i.e., of the first or the second kind. The renormalization procedure is elucidated by formulating the perturbational calculation. The possibility for proceeding to the non-perturbational method is also pointed out. These general considerations are applied to find out the interaction effects in the multiple production phenomena, which have been disregarded in Fermi-Landau's statistical theory.

1. – Introduction.

It was Fermi who firstly applied the quantum statistics to the multiple production phenomena [1] in nuclear collision. In his theory it was assumed that the interactions among the π-mesons and nucleons are strong enough to distribute uniformly the collision energy of incident particles in a small portion of space. Then the whole system of the particles will quickly arrive at the state of the thermal equilibrium. The mesons are assumed to come out from this state, and, therefore, their energy spectrum can be calculated by means of the theory of quantum statistics.

Although the theoretical prediction for the number of the mesons produced (multiplicity) seems to show rather nice agreement with the experimental results, the theory can hardly explain the fact that the mesons are produced in narrow cones [2]. Furthermore, it seems unreasonable to assume that

[1] E. Fermi: *Progr. Theor. Phys.*, **5**, 570 (1950); *Phys. Rev.*, **81**, 683 (1951).
[2] Nishimura: Private communication.

the mesons are produced straightly from the state of thermal equilibrium in a small space, because the mesons, crowded in such a small portion of space, interact strongly on each other and, thus, the particle picture is not suitable for them. This was pointed out by LANDAU ([3]). In his theory, when the thermal equilibrium state is achieved, the whole system of mesons starts to expand. The expansion process goes on untill the average distance among the mesons increases over the range of the interactions and then the mesons are observed as free particles. LANDAU applied the hydrodynamics of the relativistic ideal fluid to describe the expansion process. There, the stress tensor is given by

$$T_{\mu\nu}(x) = (\bar{p} + \bar{\varepsilon})u_\mu u_\nu + \bar{p}\delta_{\mu\nu} . \tag{1.1}$$

The quantities $\bar{p}$ and ε are pressure and energy density respectively. Since the equation

$$\partial_\nu T_{\mu\nu}(x) = 0 \tag{1.2}$$

leads to the conservation of the total entropy, which is assumed to be proportional to the total number of mesons, under the expansion process, we see that the theoretical prediction for the multiplicity of the mesons may be determined by the thermal equilibrium state. However, the angular distribution of mesons depends essentially on the expansion phenomena.

Since the space of the thermal equilibrium state is contracted in the direction of the incoming particles, say the x_1-axis, the uncertainty $\Delta \boldsymbol{k}$ of the momentum $\boldsymbol{k}$ is extremely large in the x_1-direction. Thus the system expands mainly in the x_1-direction to give a reasonable angular distribution. LANDAU solved the equation (1.2) to estimate the angular distribution of the mesons. Throughout his theory, he made use of the relation $\bar{p} = \frac{1}{3}\bar{\varepsilon}$, which leads to the multiplicity $N \propto E'^{\frac{1}{4}}$ (E': energy of two nucleons in the laboratory system).

Now, we have three questions about Fermi-Landau's theory. The first is to ask how the system could attain the thermal equilibrium state. The second is under what condition his hydrodynamical treatment is justified. How is this theory related to the field theory or S-matrix theory? We don't touch these problems in this paper; we only give a brief comment on Landau's assumption (1.1). One of our aims is to discuss the third question. This is to find out how Landau's result should be modified considering the various interactions which play the essential role in field theory. To see this we introduce the pressure and the energy density operators in a ge-

([3]) L. D. LANDAU: *Izv. Akad. Nauk SSSR, Ser. Fiz.*, **17**, 51 (1953).

neral form, because their relations are intimately connected with the multiplicity and the angular distribution of mesons in Fermi-Landau's theory. In this way, we investigate the relation between the interactions and the multiplicity of mesons in nuclear collision.

Quite generally, we can show that the difference between two sorts of interactions, the interactions of the first kind and of the second kind, may reflect on the state equation of the mesons. So it may be possible to decide whether or not the interactions in the high energy region are renormalizable, as far as we can obtain the precise experimental results on the multiple production of mesons.

It is our second aim to develop the perturbational treatment of quantum statistics. This problem has been once discussed by MATSUBARA [4]. Refining his results, we give a method which is especially useful for performing the renormalization procedure. We apply this method to the system of π-mesons with the λq^4 interaction. The results seem not to agree well with the general argument, which may probably show the inadequacy of the perturbation approximation.

The possibility of the non-perturbational calculation is also pointed out.

2. – Pressure and Energy Density.

We first derive some general formulae for quantized fields in a thermal equilibrium state. The density matrix ϱ of a canonical ensemble [5] is known to be written in terms of the hamiltonian H as

$$\varrho = \exp[-\beta H] \tag{2.1}$$

with

$$\beta = \frac{1}{kT} .$$

The expectation value $\overline{X}$ of any observable X is given by

$$\overline{X} = \langle X \rangle = \mathrm{Tr}(\varrho X)/\mathrm{Tr}\,(\varrho) . \tag{2.2}$$

The Helmholtz free energy F can be written in terms of ϱ as

$$F = -\frac{1}{\beta}\log \mathrm{Tr}\,(\varrho) . \tag{2.3}$$

(4) T. MATSUBARA: *Prog. Theor. Phys.*, **14**, 351 (1955).
(5) A. E. SCHEIDEGGER and C. D. MCKAY: *Phys. Rev.*, **83**, 125 (1951).

Suppose that the system is in the box, whose edges have the length L_1, L_2 and L_3, respectively. By changing L_1 into aL_1 with $a = 1+\mathrm{d}a$ ($\mathrm{d}a$: an infinitesimal quantity), the pressure $\bar{p}_1$ existing on the surface perpendicular to the x_1-axis can be expressed by

$$\bar{p}_1 = -\left(\frac{\partial F}{\partial V}\right)_1 = -\frac{1}{V}\frac{\partial F}{\partial a}, \tag{2.4}$$

where $V = L_1 L_2 L_3$. This, with (2.3), leads to

$$\bar{p}_1 = \langle p_1$$

with

$$p_1 = -\frac{1}{V}\frac{\partial}{\partial a} H . \tag{2.5}$$

We shall call p_1 the pressure operator. (2.5) shows that the expansion of the box induces the energy change by the pressure, which is expressed by the change of hamiltonian.

We shall now prove the relation

$$\bar{p}_1 = \left\langle \frac{1}{V}\int T_{11}(x)\,\mathrm{d}^3x \right\rangle , \tag{2.6}$$

where $T_{11}(x)$ is the (1, 1)-component of the canonical energy-momentum tensor, i.e. the flow in the x_1-direction of the x_1-component of the field momenta.

If the system is invariant under space rotation, the pressure does not depend on the direction and it proves to be

$$\bar{p} = \bar{p}_1 = \bar{p}_2 = \bar{p}_3 = \left\langle \frac{1}{3V}\sum_{i=1}^{3}\int T_{ii}(x)\,\mathrm{d}^3x \right\rangle \tag{2.7}$$

on account of (2.6).

To derive the relation (2.6), we calculate the change in the field variables and then in the hamiltonian under the expansion transformation $L_1 \to (1+\mathrm{d}a)L_1$.

Now the field variables before the expansion of the box have satisfied the following commutation relations:

$$[\varphi^{(\alpha)}(\boldsymbol{x}, t), \pi^{(\beta)}(\boldsymbol{x}', t)] = i\delta_{\alpha\beta}\delta(\boldsymbol{x}-\boldsymbol{x}') , \tag{2.8a}$$

where

$$0 \leqslant x_i \leqslant L_i . \tag{2.8b}$$

Let the field variables in the expanded box be $\varphi^{(\alpha)'}(z)$, $\pi^{(\alpha)'}(z)$:

$$\varphi^{(\alpha)}(x) \to \varphi^{(\alpha)'}(z) \equiv \frac{1}{\sqrt{1+\mathrm{d}a}}\varphi^{(\alpha)a}(x)\,, \tag{2.9a}$$

$$\pi^{(\alpha)}(x) \to \pi^{(\alpha)'}(z) \equiv \frac{1}{\sqrt{1+\mathrm{d}a}}\pi^{(\alpha)a}(x)\,,$$

where

$$z_1 = (1+\mathrm{d}a)x_1\,, \qquad z_2 = z_2\,, \qquad z_3 = x_3 \tag{2.9b}$$

$$0 \leqslant z_1 \leqslant (1+\mathrm{d}a)L_1\,, \qquad 0 \leqslant z_2 \leqslant L_2\,, \qquad 0 \leqslant z_3 \leqslant L_3 \tag{2.9c}$$

and new variables $\varphi^{(\alpha)a}(x)$ and $\pi^{(\alpha)a}(x)$ are defined in the right hand sides. The factor $1/\sqrt{1+\mathrm{d}a}$ is responsible for the change in normalization volume. The variables $\varphi^{(\alpha)a}(x)$ and $\pi^{(\alpha)a}(x)$ so defined satisfy the same commutation relations as those (2.8a) of the field variables before the expansion of the box, since

$$[\varphi^{(\alpha)a}(\boldsymbol{x},t),\pi^{(\beta)a}(\boldsymbol{x}',t)] = (1+\mathrm{d}a)[\varphi^{(\alpha)'}(\boldsymbol{z},t),\pi^{(\beta)'}(\boldsymbol{z}',t) = \tag{2.10}$$

$$= (1+\mathrm{d}a)\,i\delta_{\alpha\beta}\,\delta(\boldsymbol{z}-\boldsymbol{z}') = i\delta_{\alpha\beta}\,\delta(\boldsymbol{x}-\boldsymbol{x}')\,.$$

Use is made here of the commutation relations for the fields in the expanded box,

$$[\varphi^{(\alpha)'}(\boldsymbol{z},t),\pi^{(\beta)'}(\boldsymbol{z}',t)] = i\delta_{\alpha\beta}\delta(\boldsymbol{z}-\boldsymbol{z}')$$

and the identidy $\delta(cx) = (1/c)\delta(x)$.

Therefore, $(\varphi^{(\alpha)a}(x),\pi^{(\alpha)a}(x))$ and $(\varphi^{(\alpha)}(x),\pi^{(\alpha)}(x))$ can be connected by a canonical transformation. Since the expansion of the box is infinitesimal, the canonical transformation may also be an infinitesimal one:

$$\varphi^{(\alpha)a}(x) = (1+R\,\mathrm{d}a)\varphi^{(\alpha)}(x)(1-R\,\mathrm{d}a)\,, \quad \text{etc.} \tag{2.11}$$

Then, let us consider the change in the hamiltonian caused by the expansion of the box. The hamiltonian density after the expansion is (*)

$$\begin{aligned}\mathcal{H}'(z) &= i\pi^{(\alpha)}(z)q_4^{(\alpha)'}(z) - \mathcal{L}(q^{(\alpha)'}(z),\,q_\mu^{(\alpha)'}(z)) \\ &= (1+R\,\mathrm{d}a)\Big\{\frac{1}{1+\mathrm{d}a}\,i\pi^{(\alpha)}(x)q_4^{(\alpha)}(x) - \\ &- \mathcal{L}\Big[\frac{1}{\sqrt{1+\mathrm{d}a}}q^{(\alpha)}(x),\ \frac{1}{(1+\mathrm{d}a)^{\frac{3}{2}}}q_1^{(\alpha)}(x)\,,\ \frac{1}{\sqrt{1+\mathrm{d}a}}q_2^{(\alpha)}(x),\ \ldots\Big]\Big\}(1-R\,\mathrm{d}a) \\ &= (1+R\,\mathrm{d}a)\big\{(1-\mathrm{d}a)(i\pi^{(\alpha)}\varphi_4^{(\alpha)} - \mathcal{L}) - A\,\mathrm{d}a\big\}(1-R\,\mathrm{d}a)\,,\end{aligned}$$

(*) Here we should like to give a brief comment on the change of $\varphi_4^{(\alpha)}(x)$ for the expansion transformation. Though $\varphi_4^{(\alpha)'}(z)$ in the expanded box is not connected with the

where

$$A = \mathcal{L} - \frac{1}{2}\frac{\partial \mathcal{L}}{\partial q^{(\alpha)}} q^{(\alpha)} - \frac{\partial \mathcal{L}}{\partial q_1^{(\alpha)}} q_1^{(\alpha)} - \frac{1}{2}\frac{\partial \mathcal{L}}{\partial q_\mu^{(\alpha)}} q_\mu^{(\alpha)} . \tag{2.12}$$

Without affecting first or lower order terms, we can rewrite

$$\mathcal{H}'(z) = (1 - \mathrm{d}a)\{(1 + R\,\mathrm{d}a)(i\pi^{(\alpha)}\varphi_4^{(\alpha)} - \mathcal{L})(1 - R\,\mathrm{d}a) - A\,\mathrm{d}a\} .$$

Thus, the hamiltonian in the box after the expansion is

$$H' = \int \mathcal{H}'(z)\,\mathrm{d}^3 z , \tag{2.13}$$

where the domain of integration is given by (2.9*c*). Changing the variables according to (2.9*b*), the domain of integration is reduced into (2.8*b*), and (2.13) becomes

$$\begin{aligned} H' &= \int \{(1 + R\,\mathrm{d}a)(i\pi^{(\alpha)}\dot{q}_4^{(\alpha)} - \mathcal{L})(1 - R\,\mathrm{d}a) - A\,\mathrm{d}a\}\,\mathrm{d}^3 x \\ &= \int \{(1 + R\,\mathrm{d}a)\,\mathcal{H}(1 - R\,\mathrm{d}a) - A\,\mathrm{d}a\}\,\mathrm{d}^3 x \\ &= H - \mathrm{d}a\left(\int A\,\mathrm{d}^3 x - [R, H]\right) . \end{aligned} \tag{2.14}$$

Thus, we have obtained the change in the hamiltonian. By the definition (2.5), the pressure operator becomes

$$p_1 = \frac{1}{V}\left\{\int A\,\mathrm{d}^3 x - [R, H]\right\} . \tag{2.15}$$

original $\varphi_4^{(\alpha)}(x)$'s by the same relation as $(\varphi^{(\alpha)'}(z), \pi^{(\alpha)'}(z))$ with $(\varphi^{(\alpha)}(x), \pi^{(\alpha)}(x))$, we can regard it as if it were so only when we are concerned with the change in the hamiltonian. To see this, define $\delta\varphi_4^{(\alpha)}(x)$, as follows to be infinitesimal,

$$\varphi_4^{(\alpha)'}(z) = \frac{1}{\sqrt{1 + \mathrm{d}a}}\,\varphi_4^{(\alpha)a}(x) + \delta\varphi_4^{(\alpha)}(x) ,$$

where

$$\varphi_4^{(\alpha)a}(x) \equiv (1 + R\,\mathrm{d}a)\,\varphi_4^{(\alpha)}(x)(1 - R\,\mathrm{d}a) .$$

In the text we have neglected $\delta\varphi_4^{(\alpha)}(x)$. To justify this we show that the change in the hamiltonian caused by $\delta\varphi_4^{(\alpha)}(x)$ cancels out in the following way:

$$i\,\pi^{(\alpha)'}(z)\delta\varphi_4^{(\alpha)}(x) - \frac{\partial \mathcal{L}'}{\partial \varphi_4^{(\alpha)'}(z)}\,\delta\varphi_4^{(\alpha)}(x) = \left(i\pi^{(\alpha)} - \frac{\partial \mathcal{L}}{\partial \varphi_4^{(\alpha)}}\right)\delta\varphi_4^{(\alpha)}(x) = 0 .$$

To rewrite (2.15) into the form (2.6) is easy. Firstly, the second term in (2.15) is averaged to be zero in the trace calculation (2.2), since

$$\mathrm{Tr}\,\{[R, H]\exp[-\beta H]\} = \mathrm{Tr}\,\{[H, \exp[-\beta H]]R\} = 0$$

Secondly, we rewrite A making use of the fact that no divergence term has any contribution to the calculation of the trace (*), e.g., (2.2). Adding to (2.12) a divergence term $\partial_\mu((\partial\mathcal{L}/\partial\varphi_\mu^{(\alpha)})\varphi^{(\alpha)})$, we have

$$A = \mathcal{L} - \frac{\partial\mathcal{L}}{\partial\varphi_1^{(\alpha)}}\varphi_1^{(\alpha)} - \frac{1}{2}\left(\frac{\partial\mathcal{L}}{\partial\varphi^{(\alpha)}} - \partial_\mu\frac{\partial\mathcal{L}}{\partial\varphi_\mu^{(\alpha)}}\varphi^{(\alpha)}\right)$$

$$= \mathcal{L} - \frac{\partial\mathcal{L}}{\partial\varphi_1^{(\alpha)}}\varphi_1^{(\alpha)} = T_{11}\,. \tag{2.16}$$

Use is made here of the field equations. This expression with (2.15) leads to (2.6).

We shall now find out the relation between the energy density and the pressure. The former is given by

$$\bar{\varepsilon} = \varepsilon \tag{2.17}$$

with the energy density operator

$$\varepsilon = \frac{1}{V}\int\mathcal{H}(x)\,\mathrm{d}^3x = -\frac{1}{V}\int T_{44}(x)\,\mathrm{d}^3x\,. \tag{2.18}$$

Thus, (2.7) leads to the relation

$$3\bar{p} - \bar{\varepsilon} = \left\langle\frac{1}{V}\int T_{\mu\mu}(x)\,\mathrm{d}^3x\right\rangle. \tag{2.19}$$

Now we write the coupling constants of the interaction terms $\mathcal{L}^{i}$ ($i=1, 2, \ldots$) in the lagrangian and their dimensions by g_i and $[L]^{n_i}$, respectively. The n_i

(*) We are here concerned with the trace of the space integration of $\partial B_\mu/\partial x_\mu$:

$$\mathrm{Tr}\left(\varrho\int\frac{\partial B_\mu}{\partial x_\mu}\,\mathrm{d}^3x\right) = \mathrm{Tr}\left(\varrho\left\{\int\frac{\partial B_0}{\partial t}\,\mathrm{d}^3x + \int\sum_{k=1}^{3}\frac{\partial B_k}{\partial x_k}\,\mathrm{d}^3x\right\}\right),$$

the second term reduces to the surface integration and vanishes. The first term vanishes on account of the identity

$$\mathrm{Tr}\left(\varrho\frac{\partial C}{\partial t}\right) = i\,\mathrm{Tr}\,(\varrho[H, C]) = i\,\mathrm{Tr}\,([\varrho, H]C) = 0\,.$$

is known to be given by [6]

$$\eta_l = A_l + S_l + C_l - 4 \,. \tag{2.20}$$

Here, A_l means the number of the derivative operators (∂_μ) appearing in $\mathcal{L}^l$, C_l the number of field operators in $\mathcal{L}^l$ and S_l the sum of the spins $s^{(\alpha)}$ of all the field operators in $\mathcal{L}^l$ except that $s^{(\alpha)} = 0$ for the Bose fields with *zero masses* and $s^{(\alpha)} = \frac{1}{2}$ for the Fermi fields with *zero masses*. In other words, each field operator contributes to η_l by $(s^{(\alpha)}+1)$ and each derivative operator ∂_μ does by 1. Thus we have

$$\sum_l \eta_l \mathcal{L}^l = \sum_l \left[\sum_\alpha \left\{ (s^{(\alpha)} + 2) \frac{\partial \mathcal{L}^l}{\partial q_\mu^{(\alpha)}} q_\mu^{(\alpha)} - (s^{(\alpha)} + 1) \frac{\partial \mathcal{L}^l}{\partial q^{(\alpha)}} q^{(\alpha)} \right\} - 4\mathcal{L}^l \right] . \tag{2.21}$$

For the free lagrangian density $\mathcal{L}_0$, we have

$$\sum_\alpha \left\{ (s^{(\alpha)} + 2) \frac{\partial \mathcal{L}_0}{\partial q_\mu^{(\alpha)}} q_\mu^{(\alpha)} + (s^{(\alpha)} + 1) \frac{\partial \mathcal{L}_0}{\partial q^{(\alpha)}} q^{(\alpha)} \right\} - 4\mathcal{L}_0 = \sum_\alpha \eta_0^{(\alpha)} \mathcal{L}_0^{(\alpha)}(m) \,. \tag{2.22}$$

Here $\mathcal{L}_0^{(\alpha)}(m)$ means the mass term in the free lagrangian density $\mathcal{L}_0^{(\alpha)}$ and $[L]\eta_0^{(\alpha)}$ is the dimension of the constant appearing in $\mathcal{L}_0^{(\alpha)}(m)$, e.g. $\eta_0 = -2$ and -1 for the scalar field and the spin $\frac{1}{2}$ field respectively. Then we have $\eta_0 \mathcal{L}_0(m) = m^2 q^2$ for the scalar field, $m\bar{\psi}\psi$ for the spin $\frac{1}{2}$ field. Now, equations (2.21) and (2.22) lead to

$$\sum_l \eta_l \mathcal{L}^l - \sum_\alpha \left\{ (s^{(\alpha)} + 2) \frac{\partial \mathcal{L}}{\partial q_\mu^{(\alpha)}} q_\mu^{(\alpha)} + (s^{(\alpha)} + 1) \frac{\partial \mathcal{L}}{\partial q^{(\alpha)}} q^{(\alpha)} \right\} - 4\mathcal{L} \quad \sum_\alpha \eta_0^{(\alpha)} \mathcal{L}_0^{(\alpha)}(m), \tag{2.23}$$

with the total lagrangian density $\mathcal{L}$. Making use of the field equation, we obtain

$$\eta_l \mathcal{L}^l = \frac{\partial \mathcal{L}}{\partial q_\mu^{(\alpha)}} q_\mu^{(\alpha)} - 4\mathcal{L} - \eta_0^{(\alpha)} \mathcal{L}_0^{(\alpha)}(m) \,, \tag{2.24}$$

with the neglect of the divergence term in (22.3).

Thus, we have

$$T_{\mu\mu} = -\eta_l \mathcal{L}^l - \eta_0^{(\alpha)} \mathcal{L}_0^{(\alpha)}(m) \,, \tag{2.25}$$

[6] S. Sakata, H. Umezawa and S. Kamefuchi: *Prog. Theor. Phys.*, **7**, 377 (1952); W. Heisenberg, *Solvay Ber.*, Kap. III, IV (1939).

and

$$\overline{p} - \frac{\overline{\varepsilon}}{3} = -\frac{1}{3V}\eta_l \left\langle \int \mathcal{L}^l(x)\, \mathrm{d}^3x \right\rangle - \frac{1}{3V}\eta_0^{(\infty)} \left\langle \int \mathcal{L}_0^{(\infty)}(m, x)\, \mathrm{d}^3x \right\rangle . \tag{2.26}$$

This is of importance because this shows that the relation

$$\overline{p} = \tfrac{1}{3}\overline{\varepsilon}$$

can hold only when we can neglect the mass term $\mathcal{L}_0(m)$ and *the interactions* $\mathcal{L}_l$ *with* $\eta_l \neq 0$.

We can give another elucidation for this fact by means of the following simple dimensional analysis. As will be shown later, $\overline{p}$ and $\bar{\varepsilon}$ do not depend on the volume V. When there is an interaction whose coupling constant λ is of the dimension $[L]^\eta$, $\bar{\varepsilon}$ and $\overline{p}$ are of the form

$$\bar{\varepsilon} = (kT)^4 f(\lambda(kT)^\eta,\ m/kT) , \tag{2.27a}$$

$$\overline{p} = (kT)^4 g(\lambda(kT)^\eta,\ m/kT) . \tag{2.27b}$$

Thus, the Stefan-Boltzmann law (*) holds only when there is no interaction with $\eta \neq 0$ and the mass m is disregarded.

Writing $\bar{\varepsilon}$ (or, $\overline{p}$) as a power series in λ (+).

$$\bar{\varepsilon} = (kT)^4 \left\{ a_0 + a_1 \lambda (kT)^\eta + a_2 [\lambda (kT)^\eta]^2 + \ldots \right\}, \tag{2.27'}$$

with the neglect of mass which, in the high temperature state, is less effective than the kinetic energy. Therefore, in the case $\eta \leqslant 0$ the Stefan-Boltzmann law is approximately valid in the high temperature state. Contrary to this, in the case $\eta > 0$ the Stefan-Boltzmann law does not hold any more in the high temperature state. We know that Dyson's renormalization procedure cannot be successfully applied to the cases of interactions with $\eta > 0$, while the interactions with $\eta \leqslant 0$ are renormalizable (6). The interactions with $\eta \leqslant 0$ and with $\eta > 0$ are called of the first and second kind respectively. We now see that the effects of the interactions of the second kind are more predominant than those of the kinetic energy in the high tem-

---

(*) By means of thermodynamical relation, $\bar{\varepsilon}$, $\overline{p} \propto (kT)^4$ is equivalent to the relation $\overline{p} = \frac{1}{3}\bar{\varepsilon}$.

(+) Here, it is assumed that the zero-point of the coupling constant λ is a regular point. When this is not true, arguments being based on (2.27') have to be changed and we should go back to 2.27 *a*, *b*).

perature state, and, in this way, the relation $\bar{p} = \frac{1}{3}\bar{\varepsilon}$ or the Stefan-Boltzmann law is not valid for this case. The relation (2.26) shows that

$$\bar{p} - \frac{\bar{\varepsilon}}{3} = \frac{\gamma_0^{(\alpha)}}{3V} \left\langle \int H_{(\alpha)}(m, x)\, \mathrm{d}^3x \right\rangle , \tag{2.28}$$

when there is no interaction of the second kind. The quantity $H(m, x)$ is the mass term of the hamiltonian and therefore its expectation values are positive. Thus, we see that $\bar{p} - \frac{1}{3}\bar{\varepsilon}$ *is always negative for the system of the spin zero- and* $\frac{1}{2}$*-particles whose interactions belong to the first kind* (cf. Fig. 2).

So far we have considered the thermal equilibrium of quantum fields in the space at rest. When the space moves with the four velocity $u_\mu(\boldsymbol{v}/\sqrt{1-v^2},\ \mathrm{i}/\sqrt{1-v^2})$ ($\boldsymbol{v}$: the velocity of the system), the Lorentz transformation leads to the relation

$$\left\langle \frac{1}{V} \int T_{\mu\nu}(x)\, \mathrm{d}^3x \right\rangle = \bar{p}\, \delta_{\mu\nu} + (\bar{p} + \bar{\varepsilon}) u_\mu u_\nu \tag{2.29}$$

on account of (2.7) and (2.18), i.e.

$$\bar{p} = \left\langle \frac{1}{3V^0} \int T^0_{ii}(x^0)\, \mathrm{d}^3x^0 \right\rangle , \qquad \bar{\varepsilon} = -\left\langle \frac{1}{V^0} \int T^0_{44}(x^0)\, \mathrm{d}^3x^0 \right\rangle .$$

Here it is assumed that

$$\left\langle \frac{1}{V_0} \int T^0_{\mu\nu}(x^0)\, \mathrm{d}^3x^0 \right\rangle = 0 \qquad (\mu \neq \nu), \tag{2.30}$$

which are the quantities in the space at rest. When we can devide the whole volume into small cells V which is, on the one hand, small enough to regard (2.29) as the localized quantity at x, but not so small, on the other hand, as to destroy the notion of thermal equilibrium, (2.29) can be regarded as the energy-momentum tensor of the relativistic ideal fluid. In this case, the whole set of the cells will behave like the fluid. The condition (2.30) corresponds to the case where the viscosity is zero. We should notice that to consider the above mentioned cells is only an assumption, we don't yet know its validity.

3. – Methods of Calculations and the Renormalization.

To calculate the density matrix ϱ, MATSUBARA introduced the representation [4] where the field quantities $\varphi^{(\alpha)}(\boldsymbol{x}, t)$ are

$$\varphi^{(\alpha)}(\boldsymbol{x}, t) = \exp[tH_0]\, \varphi^{(\alpha)}(\boldsymbol{x}) \exp[-tH_0] . \tag{3.1}$$

Here, H_0 denotes the hamiltonian for the free fields and $\varphi^{(\nu)}(\boldsymbol{x})$ are the field operators in the Schrödinger representation. It has been shown that the density matrix ϱ can be written as

$$\varrho = \varrho_0 S(\beta) \tag{3.2}$$

with

$$\varrho_0 = \exp[-\beta H_0] . \tag{3.3}$$

The $S(\beta)$ satisfies the relation

$$-\frac{\partial S(\beta)}{\partial \beta} = H'(\beta) S(\beta) , \tag{3.4}$$

with

$$H'(\beta) = \exp[\beta H_0] \int H'(\boldsymbol{x}) \, \mathrm{d}^3x \exp[-\beta H_0] . \tag{3.5}$$

$H'(\boldsymbol{x})$ is the interaction part of the hamiltonian density in the Schrödinger representation. The equation (3.4) tells that $S(\beta)$ can be calculated by means of the relation

$$S(\beta) = \sum_n \frac{(-1)^n}{n!} \int_0^\beta \mathrm{d}t_1 \ldots \int_0^\beta \mathrm{d}t_n \int \mathrm{d}^3x_1 \ldots \int \mathrm{d}^3x_n \, \mathrm{P}[H'(\boldsymbol{x}_1 t_1) \ldots H'(\boldsymbol{x}_n t_n)] , \tag{3.6}$$

where

$$H'(\boldsymbol{x}, t) = \exp[tH_0] H'(\boldsymbol{x}) \exp[-tH_0] . \tag{3.7}$$

and P is the t-ordering operator.

To extend this to calculate $\overline{A}$ (cf. (2.2)), we shall introduce the operator

$$A(t) = \exp[tH_0] A \exp[-tH_0] . \tag{3.8}$$

Here, A is the operator in the Schrödinger representation. The relation (2.2) can now be rewritten as

$$\begin{cases} \overline{A} = \mathrm{Tr}\,(A\varrho_0 S(\beta))/\mathrm{Tr}\,(\varrho_0 S(\beta)) \\ \quad = \mathrm{Tr}\,(\varrho_0 A(\beta) S(\beta))/\mathrm{Tr}\,(\varrho_0 S(\beta)) \\ \quad = \langle A(\beta) S(\beta)\rangle_0 / \langle S(\beta)\rangle_0 \end{cases} \tag{3.9}$$

where $\langle A\rangle_0$ means

$$\langle A\rangle_0 = \frac{\mathrm{Tr}\,(\varrho_0 A)}{\mathrm{Tr}\,(\varrho_0)} \,. \tag{3.10}$$

To calculate $\bar{A}$, we use the relation

$$A(\beta)S(\beta) = \sum_n \frac{(-1)^n}{n!}\int_0^\beta \mathrm{d}t_1 \ldots \int_0^\beta \mathrm{d}t_n \int \mathrm{d}^3x_1 \ldots \int \mathrm{d}^3x_n P[A(\beta), H'(\boldsymbol{x}_1 t_1), \ldots H'(\boldsymbol{x}_n t_n)], \tag{3.11}$$

which can be derived from (3.6).

We shall consider, as an example, a scalar field $\varphi(\boldsymbol{x})$,

$$\varphi(\boldsymbol{x}) = \sum_{\boldsymbol{k}} (2\omega_{\boldsymbol{k}} V)^{-\frac{1}{2}} (a_{\boldsymbol{k}}^+ \exp[i(\boldsymbol{k}\boldsymbol{x})] + a_{\boldsymbol{k}}^- \exp[-i(\boldsymbol{k}\boldsymbol{x})]) \,, \tag{3.12}$$

with

$$\omega_{\boldsymbol{k}} = \sqrt{\boldsymbol{k}^2 + m^2} \,.$$

The operators $a_{\boldsymbol{k}}^+$ and $a_{\boldsymbol{k}}^-$ are the annihilation and creation operator respectively. It is not difficult to prove the relations

$$\exp[tH_0]\, a_{\boldsymbol{k}}^+ \exp[-tH_0] = \exp[t \sum_{\boldsymbol{k}'} n_{\boldsymbol{k}'}\omega_{\boldsymbol{k}'}] a_{\boldsymbol{k}}^+ \exp[-t \sum n_{\boldsymbol{k}'}\omega_{\boldsymbol{k}'}] \tag{3.13a}$$

$$= a_{\boldsymbol{k}}^+ \exp[-\omega_{\boldsymbol{k}} t] \,,$$

$$\exp[tH_0] a_{\boldsymbol{k}}^- \exp[-Ht_0] = a_{\boldsymbol{k}}^- \exp[\omega_{\boldsymbol{k}} t] \,. \tag{3.13b}$$

Thus, we have

$$\varphi(\boldsymbol{x}, t) = \sum_{\boldsymbol{k}} (2\omega_{\boldsymbol{k}} V)^{-\frac{1}{2}} (a_{\boldsymbol{k}}^+ \exp[i\boldsymbol{k}\boldsymbol{x} - \omega_{\boldsymbol{k}} t] + a_{\boldsymbol{k}}^- \exp[-i\boldsymbol{k}\boldsymbol{x} + \omega_{\boldsymbol{k}} t]) \,. \tag{3.14}$$

This shows that $\varphi(\boldsymbol{x}, t)$ satisfies the equation

$$\left(\Delta + \frac{\partial^2}{\partial t^2} - m^2\right)\varphi(\boldsymbol{x}, t) = 0 \,. \tag{3.15}$$

The same is true for any field; writing the ordinary field equation of the free (α)-field as

$$A(\partial, \partial_4)\varphi^{(\alpha)}(x) = 0 \,, \tag{3.16}$$

we can prove that $\varphi^{(\alpha)}(\boldsymbol{x}, t)$ satisfies the same equation with $\partial = (\partial_1, \partial_2, \partial_3)$ and $\partial_4 = \partial/\partial t$. To calculate (3.9) with (3.6) and (3.11) we need to evaluate the terms of the form

$$\mathrm{Tr}\,(\varrho_0 T[\varphi^{(\alpha)}(x_1), \varphi^{(\beta)}(x_2), \ldots])/\mathrm{Tr}\,(\varrho_0)\,, \tag{3.17}$$

here T is Wick's ordering operator ([7]).

It has been pointed out by MATSUBARA that (3.17) can be evaluated by means of all the possible Feynman diagrams of the vacuum type, each of whose lines connecting x with x' corresponds to

$$\langle T[\varphi^{(\alpha)}(x), \varphi^{(\alpha)}(x')]\rangle_0\,. \tag{3.18}$$

One of the simplest proofs for this fact may be given as follows. (3.17) contains a term

$$\left\langle n^{(\alpha)}_{\boldsymbol{k}_1}, n^{(\alpha)}_{\boldsymbol{k}_2}, \ldots, n^{(\beta)}_{\boldsymbol{k}'_1} \ldots \middle| \frac{\varrho_0 \varphi^{(\alpha)}(x)\varphi^{(\alpha)}(x) \cdots}{\mathrm{Tr}\,(\varrho_0)} \middle| n^{(\alpha)}_{\boldsymbol{k}_1}, \ldots n^{(\beta)}_{\boldsymbol{k}'_1} \ldots \right\rangle \tag{3.19}$$

with $t > t' > \ldots$. Here $|n^{(\alpha)}_{\boldsymbol{k}_1} \ldots n^{(\beta)}_{\boldsymbol{k}'_1} \ldots\rangle$ denotes the state where numbers of the (α)-particle in $\boldsymbol{k}_{k_1}$, $\boldsymbol{k}_{k_2}$, ... states are $n^{(\alpha)}_{\boldsymbol{k}_1}$, $n^{(\alpha)}_{\boldsymbol{k}_2}$, ..., those of the (β)-particle $n^{(\beta)}_{\boldsymbol{k}'_1}$ ... and so on. Operators in (3.19) may be grouped in pairs

$$(\varphi^{(\alpha)}(\boldsymbol{k}_1)^+, \varphi^{(\alpha)}(\boldsymbol{k}_1)^-)\,, \qquad (\varphi^{(\alpha)}(\boldsymbol{k}_2)^-, \varphi^{(\alpha)}(\boldsymbol{k}_2)^+)\,, \qquad (\varphi^{(\beta)}(\boldsymbol{k}_3)^+, \varphi^{(\beta)}(\boldsymbol{k}_3)^-)\,.$$

of annihilation and creation operators for the same particles in the same states. Since the contributions from the terms whose n-pairs correspond to the same momentum, are smaller than that from the term, none of whose pairs have the same momentum by the factor $1/V^n$. Neglecting the former contributions, the two operators of each pair can be written in succession only by interchanges among the operators of particles in different states. Then $\varrho_0/\mathrm{Tr}\,(\varrho_0)$ in (3.19) leads to the following factor for each pair $(\varphi^+(\boldsymbol{k})\varphi^-(\boldsymbol{k}))$.

$$\exp\left[-\beta n_{\boldsymbol{k}}\omega_{\boldsymbol{k}}\right]/\sum_{m_{\boldsymbol{k}}} \exp\left[-\beta m_{\boldsymbol{k}}\omega_{\boldsymbol{k}}\right]\,.$$

This factor can be written as

$$\exp\left[-\beta n_{\boldsymbol{k}}\omega_{\boldsymbol{k}}\right] \prod_i{}' \left(\sum_{n_{\boldsymbol{k}_i}} \exp\left[-\beta n_{\boldsymbol{k}}\omega_{\boldsymbol{k}_i}\right]\right)/\mathrm{Tr}\,(\varrho_0)\,.$$

([7]) G. C. WICK: *Phys. Rev.*, **80**, 268 (1950).

Here $\prod'$ denotes the product of the terms whose $\boldsymbol{k}_i$ runs over all the momenta except $\boldsymbol{k}$. In this way we can prove that each pair leads to the contribution of the form (3.18).

Since each field operator is proportional to $1/\sqrt{V}$ and the summation over the momentum is proportional to V:

$$\sum_{\boldsymbol{k}} \to \frac{V}{(2\pi)^3}\int \ldots \mathrm{d}^3k\,,$$

we see that each line of the diagram gvies us the contribution independent of the volume V. As the diagrams are the closed ones, the volume integrations except one correspond to the momentum conservations at all the vertices of the diagram. The last volume integration leads to the factor . We now see that when A has the form of $\int a(x)\,\mathrm{d}^3x$ with $a(x)$ made up of the field operators, $\overline{A}$ depends on V linearly, for example, th Helmholtz free energy F does so.

For the scalar field $\varphi(x)$, (3.18) can be evaluated to give

$$\text{(3.20)}\qquad \langle \mathrm{T}[\varphi(x), \varphi(x')]\rangle_0 = \frac{1}{(2\pi)^3}\int \frac{\mathrm{d}^3k}{2\omega_{\boldsymbol{k}}}\cdot$$

$$\cdot\left\{(f_{\boldsymbol{k}}+1)\exp\left[i(\boldsymbol{k}\cdot\boldsymbol{x}-\boldsymbol{x}') - \omega_{\boldsymbol{k}}|t-t'|\right] + f_{\boldsymbol{k}}\exp\left[-i(\boldsymbol{k}\cdot\boldsymbol{x}-\boldsymbol{x}') + \omega_{\boldsymbol{k}}|t-t'|\right]\right\}.$$

where

$$\text{(3.21)}\qquad f_{\boldsymbol{k}} = \frac{\sum_{n_{\boldsymbol{k}}=0}^{\infty} n_{\boldsymbol{k}}\exp\left[-\beta n_{\boldsymbol{k}}\omega_{\boldsymbol{k}}\right]}{\sum_{n_{\boldsymbol{k}}=0}^{\infty}\exp\left[-\beta n_{\boldsymbol{k}}\omega_{\boldsymbol{k}}\right]} = \frac{1}{\exp\left[\beta\omega_{\boldsymbol{k}}\right]-1}\,.$$

This can be extended to the case of arbitrary fields $\varphi^{(\alpha)}(x)$ as

$$\text{(3.22)}\qquad \langle \mathrm{T}[\varphi^{(\alpha)}(x), \overline{\varphi^{(\alpha)}}(x')]\rangle_0 = \mathrm{d}(\partial, \partial_t)\,\frac{1}{(2\pi)^3}\int \frac{\mathrm{d}^3k}{2\omega_{\boldsymbol{k}}}\cdot$$

$$\cdot\left\{sf_{\boldsymbol{k}}+1)\exp\left[i(\boldsymbol{k}\cdot\boldsymbol{x}-\boldsymbol{x}') - \omega_{\boldsymbol{k}}|t-t'|\right] + sf_{\boldsymbol{k}}\exp\left[-i(\boldsymbol{k}\cdot\boldsymbol{x}-\boldsymbol{x}') + \omega_{\boldsymbol{k}}|t-t'|\right]\right\}.$$

Here $\mathrm{d}(\partial, \partial_t)$ is defined by

$$\text{(3.23)}\qquad \mathrm{d}(\partial, \partial_t)\Lambda(\partial, \partial_t) = \Delta + \partial_t^2 - m^2,$$

$f_{\boldsymbol{k}}$ denotes

$$\text{(3.24)}\qquad \begin{cases} f_{\boldsymbol{k}} = \dfrac{1}{\exp\left[\beta\omega_{\boldsymbol{k}}\right]-1} & \text{for the integer spin field} \\ \quad = \dfrac{1}{\exp\left[\beta\omega_{\boldsymbol{k}}\right]+1} & \text{for the half-integer spin field} \end{cases}$$

and s denotes the sign constant

$$s = \begin{cases} +1 & \text{for the integer spin field} \\ -1 & \text{for the half-integer spin field.} \end{cases}$$

The s in (3.22) comes from the anticommutation property for the half-integer spin field. In general, $q^{(\nu)}(x)$ is an one-column matrix, and therefore, $\mathrm{d}(\partial, \hat{c}_t)$ is a square matrix. As an example, we shall consider the Dirac field $\psi(x)$. The free lagrangian density for this field is known to be

$$-\psi^* \gamma_4 (\gamma_\mu \partial_\mu + m)\psi \,.$$

This shows that

$$\Lambda(\partial, \partial_t) = -(\gamma_k \partial_k + \gamma_4 \partial_t + m)\,, \tag{3.25a}$$

$$\mathrm{d}(\partial, \partial_t) = -(\gamma_k \hat{c}_k + \gamma_4 \hat{c}_t - m)\,. \tag{3.25b}$$

Thus we have

$$\langle \mathrm{T}[\psi(x), \overline{\psi}(x')] \rangle_0 = (\gamma_k \partial_k + \gamma_4 \partial_t - m) \frac{1}{(2\pi)^3} \int \frac{\mathrm{d}^3 k}{2\omega_{\boldsymbol{k}}} \cdot$$

$$\cdot \left\{ (f_{\boldsymbol{k}} - 1) \exp[i(\boldsymbol{k}\cdot\boldsymbol{x} - \boldsymbol{x}') - \omega_{\boldsymbol{k}} |t - t'|] + f_{\boldsymbol{k}} \exp[-i(\boldsymbol{k}\cdot\boldsymbol{x} - \boldsymbol{x}') + \omega_{\boldsymbol{k}} |t - t'|] \right\}.$$

This is slightly different from Matzubara's result, because he did not take account of contributions due to the positrons. We don't give the proof for (3.22), because this can be done in a way similar to the derivation of the Green function for the arbitrary fields by extending the Δ_F-function [8].

Although, using these propagators, the Feynman diagrams of vacuum type yield the divergent integrals, we can remove them, by the renormalization procedure quite in the same way as in the S-matrix theory. -We introduce the Fourier transform of the propagator (3.22):

$$G(\boldsymbol{k}, k_{0n}) \equiv \int_{-\beta}^{\beta} \exp[-ik_{0n}t]\,\mathrm{d}t \int \exp[-i\boldsymbol{k}\boldsymbol{x}]\,\mathrm{d}^3 x\, G(\boldsymbol{x}, t)\,, \tag{3.27}$$

where, t-transformation is in the finite domain $(-\beta, \beta)$, and accordingly

$$k_{0n} = \frac{n\pi}{\beta}\,, \qquad (n = 0, \pm 1, \pm 2, \ldots)\,.$$

[8] H. UMEZAWA and A. VISCONTI: *Nuclear Physics*, **1**, 348 (1956); Y. TAKAHASHI and H. UMEZAWA: *Prog. Theor. Phys.*, **9**, 14 (1953).

For example, we have for the scalar field:

$$D(\boldsymbol{k}, k_{0n}) = \begin{cases} 1/(\omega_{\boldsymbol{k}}^2 + k_{0n}^2) & (n = \text{even}) \\ 0 & (n = \text{odd}). \end{cases} \tag{3.28}$$

For the general field:

$$G(\boldsymbol{k}, k_{0n}) = \begin{cases} 0 & (n = \text{even}) \\ \mathrm{d}(i\boldsymbol{k}, ik_{0n})(1/(\omega_{\boldsymbol{k}}^2 + k_{0n}^2)) & (n = \text{odd}) \end{cases} \tag{3.29}$$

for the Fermi field,

$$\begin{cases} \mathrm{d}(i\,\boldsymbol{k}, ik_{0n})(1/(\omega_{\boldsymbol{k}}^2 + k_{0n}^2)) & (n = \text{even}) \\ 0 & (n = \text{odd}) \end{cases}$$

for the Bose field,

Conversely, we have

$$D(x - x') = \frac{1}{\beta} \sum_{k_0 = 2n\pi/\beta} \frac{1}{V} \sum_{\boldsymbol{k}} \frac{1}{\omega_{\boldsymbol{k}}^2 + k_0^2} \exp\left[i(\boldsymbol{k}\cdot\boldsymbol{x} - \boldsymbol{x}') + ik_0(t - t')\right], \tag{3.30}$$

$$G(x - x') = \mathrm{d}(\partial, \partial_i)\frac{1}{\beta} \cdot \sum_{k_0 = m\pi/\beta} \frac{1}{V} \sum_{\boldsymbol{k}} \frac{1}{\omega_{\boldsymbol{k}}^2 + k_0^2} \exp\left[i(\boldsymbol{k}\cdot\boldsymbol{x} - \boldsymbol{x}') + ik_0(t - t')\right] \tag{3.31}$$

$$\left\{ \begin{array}{l} m\text{: odd for the Fermi field} \\ \quad\ \text{even for the Bose field} \end{array} \right\}.$$

In the limit $\beta \to \infty$, these tend to Feynman functions with replacement $\omega_{\boldsymbol{k}} \to i\omega_{\boldsymbol{k}}$.

Since these propagation functions are arranged according to the Feynman diagrams to calculate (3.6), the space integration at each corner results in the δ-function of momentum conservation. As to t-integration, the reader may be perplexed by the following situation; while the Fourier transformation was done in $(-\beta, \beta)$, the integration in (3.6) is only over $(0, \beta)$. Notice, however, that the boson energy $k_{0,n}$ is an even multiple of π/β, and that, though the fermion energy $k_{0,n}$ is an odd multiple of π/β, there comes always a even number of fermions at a vertex. So $\exp\left[i(\sum k_0)t\right]$ satisfies the periodic boundary condition even in $(0, \beta)$, and on integrating, results in the Kronecker delta of energy conservation. Thus the transition from $(\boldsymbol{x}, t)$ space to $(\boldsymbol{k}, k_0)$ space can be done in the same way as in the S-matrix theory.

Now, for the first kind of interactions, our renormalization prescription is to determine the renormalization constants so that they cancel the divergent integral in the limit $\beta \to \infty$. The constants so determined have evidently the same expression as in the S-matrix theory (*). The procedure is, shortly speaking, as follows. If our vacuum type Feynman diagrams give a divergent integral, we cut their internal lines and replace them by the external lines till the divergence is lowered to the so called primitive one. The subtraction of the mass or coupling constant renormalization term determined as above can make the integral finite. If, closing the external lines again, we have a divergence, we must continue the procedure. From the divergence, which arises on closing the last external lines, we subtract the part of itself that remains in the limit $\beta \to \infty$ as a vacuum contribution (+). The finiteness of the result is obvious.

In this way, we have established a parallelism between the renormalization procedures in the statistical mechanics and in the S-matrix theory, which will be a strong support to our prescription.

Now, we will describe an equivalent but more practical way for renormalization. We separate (3.22) into two parts (−):

$$G(x - x') = G^{(e)}(x - x') + G^{(i)}(x - x') \,. \tag{3.32}$$

with

$$G^{(e)}(x - x') = \mathrm{d}(\partial, \partial_t) \frac{1}{(2\pi)^3} \cdot \int \frac{\mathrm{d}^3 k}{2\omega_{\boldsymbol{k}}} s f_{\boldsymbol{k}} \exp\left[i(\boldsymbol{k}\cdot\boldsymbol{x} - \boldsymbol{x}')\right] \left(\exp\left[-\omega_{\boldsymbol{k}} | t - t' |\right] + \exp\left[\omega_{\boldsymbol{k}} | t - t' |\right]\right) ,$$

$$G^{(i)}(x - x') = \mathrm{d}(\partial, \partial_t) \frac{1}{(2\pi)^3} \frac{\mathrm{d}^3 k}{2\omega_{\boldsymbol{k}}} \exp\left[i(\boldsymbol{k}\cdot\boldsymbol{x} - \boldsymbol{x}') - \omega_{\boldsymbol{k}} | t - t' |\right] ,$$

(*) It is not so serious that we must replace $\omega_{\boldsymbol{k}} \to i\omega_{\boldsymbol{k}}$ to make our propagation functions coincide with those of Feynman in the limit $\beta \to \infty$. In the $(\boldsymbol{k}, k_0)$ space integration now concerned, if we change the contour of k_0-integration from the real to the imaginary axis, we get the same integrand as in the S-matrix theory. And, this change of contour can be done without crossing undisplaced poles. Moreover, it has been known that the contribution from displaced poles is finite. See, R. J. EDEN: *Proc. Roy. Soc.*, A **210**, 388 (1952).

(+) This corresponds to the vacuum expectation value of the hamiltonian, and would be zero from the begining if the hamiltonian were so determined that the vacuum energy be zero. In other words, when the vacuum expectation value $(H)_v$ of H is not zero, we should replace H in (2.1) by $H - (H)_v$.

( ) As is implied in the renormalization prescription described above in $(\boldsymbol{k}, k_0)$-space.

$G^{(i)}$ is obtained from (3.22) by taking $\beta \to \infty$, or $f_k = 0$, and is regarded as coming from the vacuum effect. Note that $G^{(i)}$ goes over into a Feynman function by the replacement $\omega_k \to i\omega_k$, so, that it is $G^{(i)}$ to which (3.30) or (3.31) tend in the limit $\beta \to \infty$. We write $G^{(i)}$ and $G^{(e)}$ by dotted and wavy lines in the diagram and call them the (i)- and (e)-lines respectively. In this way, each diagram with n lines will be splitted into 2^n diagrams. Then, cutting all the (e)-lines to make them external lines, we obtain the diagrams whose internal lines are (i)-lines. The divergence to be renormalized originates from the (i)-lines.

We shall illustrate the renormalization procedure for the case of the $\lambda\varphi^4$-interaction, taking for example a second order diagram. See Fig. 1.

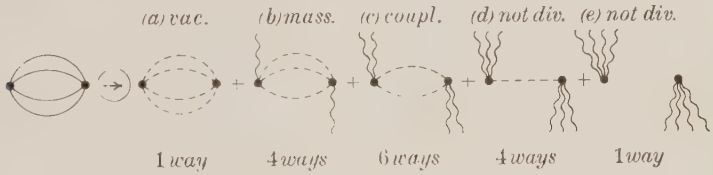

Fig. 1.

We separate the lines and cut the (e)-lines. The number of ways of splitting is shown below each diagrams, the sum of which amounts in this case to $2^4 = 16$. The diagram (a) shows the vacuum effect, and can be disregarded from the beginning. The divergences occurring in the diagram (b) and (c) can be subtracted as a mass and coupling constant renormalization. After the renormalization has been done, we close the (e)-lines again and accomplish the integrations with respect to (e)-lines. The contributions of the diagram (d) and (e) are finite.

The performance of the renormalization shall be exemplified in Sect. 5 and in the Appendix B.

4. – The Multiple Production of Mesons.

We shall now consider the effects of the interactions to the multiple production phenomena by nuclear collision. In Fermi-Landau's theory, the relation $\overline{p} = \frac{1}{3}\overline{\varepsilon}$ leads to

$$N \propto E'^{\frac{1}{4}}, \tag{4.1}$$

the limes $\beta \to \infty$, where the subtraction is made, should be taken after the t-integration in (3.6). In this sense, the separation $G \to G^{(e)} + G^{(i)}$ should not be taken seriously. In fact, $G^{(e)}$ sometimes yields divergence, but it is camcelled out by a part of contributions from $G^{(i)}$. (See Appendix B, Eq. (B.3)).

where N is the number of the mesons produced in the collision of two particles, whose energy in the laboratory system is E'. As was shown in Sect. 2, the relation $\overline{p} = \frac{1}{3}\overline{\varepsilon}$ would not hold any more, if there would exist the interactions of the second kind. The fact that (4.1) is not very different from the experimental result seems to show that the interactions appearing in our subject belong to the first kind i.e. the renormalizable ones. However, since the experimental results are not accurate enough and their energy region not high enough to exclude the second kind interaction, we cannot yet draw the decisive conclusion. Anyhow, as far as we adopt Fermi and Landau's viewpoint it may be possible to decide whether or not the interactions are renormalizable.

When we have only interactions of the first kind, by writing the relation between $\overline{p}$ and $\overline{\varepsilon}$, i.e. the equation of states, in the form

$$\overline{p} = a\left(\lambda, \frac{m}{kT}\right)\frac{1}{3}\overline{\varepsilon} + b\left(\lambda, \frac{m}{kT}\right). \tag{4.2}$$

We see from the discussion in Sect. 2 that ,

$$\lim_{T\to\infty} a\left(\lambda, \frac{m}{kT}\right) = 1\,, \tag{4.3a}$$

$$\lim_{T\to\infty} b\left(\lambda, \frac{m}{kT}\right)\Big/\overline{\varepsilon} = 0\,. \tag{4.3b}$$

When the interactions are of the second kind, the relations (4.3) are not fulfilled. We shall evaluate in Sect. 5 the functions $a(\lambda, m/kT)$ and $b(\lambda, m/kT)$ by means of the perturbation calculation. When a and b can be regarded as the constants over a wide interval of T, we obtain

$$N \propto \left(E' + \frac{3}{a+3}V^0 b\right)^{3/(a+3)}\Big/E'^{\frac{1}{2}}, \tag{4.4}$$

where $V^0 = (4\pi/3)(1/\mu)^3$ is the volume of the meson cloud around the nucleon at rest. (See Appendix A).

In this way, we may possibly estimate a and b from the experimental results. The same is true for the angular distribution of the produced mesons. As was shown in Sect. 2, $\overline{p} - \frac{1}{3}\overline{\varepsilon}$ is always negative for the spin zero- and spin-$\frac{1}{2}$ particle, to which case we shall confine ourselves, and for interactions of the first kind. The $(\overline{p}, \overline{\varepsilon})$-curve for this case can appear only below the line (a) $\overline{p} - \frac{1}{3}\overline{\varepsilon} = 0$ in Fig. 2, and approaches the line (a) in the limit $T\to\infty$.

In other words, the $(\overline{p}, \overline{\varepsilon})$-curve can be above the line (a) only in case of interactions of the second kind. In such a case, we have seen that the $(\overline{p}, \overline{\varepsilon})$-curve does not approach the line (a) in the limit $T \to \infty$. When there are no interactions of the second kind, it is clearly seen from (2.28) that, the mass being smaller, the $(\overline{p}, \overline{\varepsilon})$-curve comes near the line (a). The line (b) in Fig. 2 denotes the $(\overline{p}, \overline{\varepsilon})$-curve for the free fields. When the interaction is repulsive, the interaction energy is positive and, therefore, the mass term in the total hamiltonian is less effective than it is in the case of the free fields. Then, (2.28) shows that in the limit where the mass is zero, the $(\overline{p}, \overline{\varepsilon})$-curve coincides with curve (a). Therefore, the curve for the repulsive interaction lies in the region between the curves (a) and (b). In a similar way, we can show that the region below the curve (b) is for the attractive interaction. This may give us the way to decide the sign of the interaction, as far as we can obtain the precise experimental results.

Fig. 2. – $a)$ $\overline{p} - \frac{1}{3}\overline{\varepsilon} = 0$; (b) The curve for $\lambda = 0$.

We have discussed the multiplicity of mesons by means of the theory of thermal equilibrium. This is true in Landau's theory where the entropy conserves in the expansion process. As was pointed out in Sect. **2**, Landau's application of the hydrodynamics to the description of the expansion process may be justified when (2.29) can be regarded as the local quantity (1.1). In other words, the process is like the expansion of a system of cells, each of which is in thermal equilibrium state. In this case the equation (1.2) leads to the conservation of the total entropy:

$$\partial_\nu(s u_\nu) = 0 .$$

However, it is not clear how the transition from the initial thermal equilibrium state to the system of the cells goes on. Furthermore it is quite doubtful if the entropy of mesons is conserved during the process in which the mesons crystallize to be particles. To derive the definite results from the experiments, the whole of the process seems to need consideration under a new light.

5. – Calculation.

As an example we shall now consider the π-meson field with π-π interaction $\lambda\varphi^4$ only which is of the first kind.

We regard this as the phenomenological π-π interaction which may come either from the π-nucleon interaction or from the direct π-π interaction. Although we know that the perturbation calculation may not be any nice approximation in the case of the interaction λq^4 [9], we apply this calculation method only to get a rough idea about the interaction effects on the multiple production phenomena.

5·1. *Perturbation calculation.* – The hamiltonian is

$$H = H_0 + H_1 \tag{5.1}$$

$$H_0 = \frac{1}{2}\int [\pi^2(x) + (\nabla\varphi(x))^2 + \mu^2\varphi^2(x)]\,\mathrm{d}^3x\,,$$

$$H_1 = \lambda\int \varphi^4(x)\,\mathrm{d}^3x - \frac{1}{2}\,\delta\mu^2\int\varphi^2(x)\,\mathrm{d}^3x - \delta\lambda\int\varphi^4(x)\,\mathrm{d}^3x\,,$$

where μ, λ, $\delta\mu^2$ and $\delta\lambda$ are observed mass, observed coupling constant, mass renormalization term and coupling constant renormalization term respectively. We now calculate the partition function

$$\Xi = \mathrm{Tr}\,(\varrho) = \mathrm{Tr}\,(\exp[-\beta H])\,. \tag{5.2}$$

From this quantity, the Helmholtz free energy F, pressure $\overline{p}$ and energy density $\overline{\varepsilon}$ are derived as

$$F = -\frac{1}{\beta}\log\Xi\,, \tag{5.3a}$$

$$\overline{p} = -\frac{\partial F}{\partial V}\,, \tag{5.3b}$$

$$\overline{\varepsilon} = -\frac{1}{V}\frac{\partial}{\partial\beta}\log\Xi\,. \tag{5.3c}$$

Denoting the zeroth-order partition function by Ξ_0:

$$\Xi_0 = \mathrm{Tr}\,(\exp[-\beta H_0]) = \sum_{n_k}\exp[-\beta\sum_k n_k\omega_k]) = \prod_k\frac{1}{1-\exp[-\beta\omega_k]}\,, \tag{5.4}$$

we expand Ξ/Ξ_0 in power series of the coupling constant λ:

$$\Xi/\Xi_0 = 1 + \xi_1 + \xi_2 + \dots\,. \tag{5.5}$$

[9] W. THIRRING: *Helv. Phys. Acta*, **26**, 33 (1953); A. PETERMAN: *Helv. Phys. Acta*, **26**, 465 (1953).

Here,

$$\xi_n = \frac{(-1)^n}{n!}\int \dots \int \langle \mathrm{P}[H_1(x_1), \dots, H_1(x_n)]\rangle \, \mathrm{d}^4x_1 \dots \mathrm{d}^4x_n \,. \tag{5.6}$$

It was shown in Sect. **3** that these quantities can be calculated by a graphical method. The first order quantity due to the $\lambda\varphi^4$ term is

$$\xi_1' = -\lambda \left\langle \int \varphi^4(x)\, \mathrm{d}^3x \right\rangle = -3\lambda \int D^2(0)\, \mathrm{d}^4x = -3\lambda\beta V\, D^2(0) \,. \tag{5.7}$$

Here $D(x-x')$ is given by (3.20):

$$D(x-x') = \sum_k \frac{1}{2V\omega_k} \left\{ (f_k+1) \exp\left[i(\boldsymbol{k}\cdot\boldsymbol{x} - \boldsymbol{x}') - \omega_k |t-t'| \right] + \right. \tag{5.8}$$
$$\left. + f_k \exp\left[-i(\boldsymbol{k}\cdot\boldsymbol{x} - \pi') + \omega_k |t-t'| \right] \right\} .$$

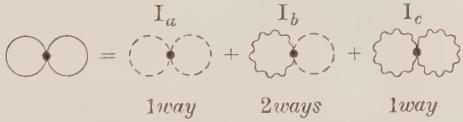

Fig. 3. – First order diagram.

Substituting (5.8) into (5.7), we obtain

$$\xi_1' = -3\lambda\beta V \left\{ \left(\frac{1}{2V} \sum_k \frac{1}{\omega_k} \right)^2 + 2 \left(\frac{1}{V} \sum_k \frac{f_k}{\omega_k} \right) \left(\frac{1}{2V} \sum_\kappa \frac{1}{\omega_\kappa} \right) + \left(\frac{1}{V} \sum_k \frac{f_k}{\omega_k} \right)^2 \right. . \tag{5.9}$$

Each term in ξ_1' corresponds to each diagram i.e. I_a, I_b and I_c in Fig. 3. Renormalizing the mass

$$\frac{1}{2}(\delta\mu^2)_1 = \frac{3\lambda}{V} \sum_k \frac{1}{\omega_k} \tag{5.10}$$

and deducting the vacuum energy

$$v_1 = 3\lambda \left(\frac{1}{2V} \sum_k \frac{1}{\omega_k} \right)^2 , \tag{5.11}$$

we have a finite result

$$\xi_1 = -3\lambda\beta V \left(\frac{1}{V} \sum_k \frac{f_k}{\omega_k} \right)^2 . \tag{5.12}$$

The mass renormalization term (5.10) coincides exactly with that in the S-matrix theory. From (5.3), (5.4), (5.5) and (5.12) we obtain the following results in the first order approximation:

$$\bar{p} = \bar{p}_0 + \bar{p}_1 ,$$

$$\bar{\varepsilon} = \bar{\varepsilon}_0 + \bar{\varepsilon}_1 .$$

where

$$(5.12a_0) \qquad \bar{p}_0 = \frac{1}{3}\frac{1}{(2\pi)^3}\int \frac{1}{\exp[\beta\omega_k]-1}\frac{k^2}{\omega_k}\,4\pi k^2\,\mathrm{d}k ,$$

$$= \frac{1}{2\pi^2}\beta^{-4}\sum_{\nu=1}^{\infty}\frac{\mathrm{K}_2(\nu\mu\beta)}{\nu^2}\,\mu^2\beta^2,$$

$$(5.12a_1) \qquad \bar{p}_1 = -3\lambda\left[\frac{1}{(2\pi)^3}\int\frac{1}{\exp[\beta\omega_k]-1}\frac{4\pi k^2}{\omega_k}\,\mathrm{d}k\right]^2$$

$$- -\frac{3\lambda}{(2\pi^2)^2}\beta^{-4}\left[\sum_{\nu=1}^{\infty}\mu\beta\frac{\mathrm{K}_1(\nu\mu\beta)}{\nu}\right]^2 ,$$

$$(5.12b_0) \qquad \varepsilon_0 = \frac{1}{(2\pi)^3}\int\frac{\omega_k}{\exp[\beta\omega_k]-1}\,4\pi k^2\,\mathrm{d}k ,$$

$$= \frac{3}{2\pi^2}\beta^{-4}\left[\sum_{\nu=1}^{\infty}\mu^2\beta^2\frac{\mathrm{K}_2(\nu\mu\beta)}{\nu^2} - \frac{1}{3}\mu^2\beta^2\sum_{\nu=1}^{\infty}\mu\beta\frac{\mathrm{K}_1(\nu\mu\beta)}{\nu}\right],$$

$$(5.12b_1) \qquad \varepsilon_1 = -3\lambda\left\{\left(\frac{1}{(2\pi)^3}\int\frac{1}{\exp[\beta\omega_k]-1}\frac{4\pi k^2}{\omega_k}\,\mathrm{d}k\right)^2 +\right.$$

$$\left. 2\left(\frac{1}{(2\pi)^3}\int\frac{1}{\exp[\beta\omega_k]-1}\frac{4\pi k^2}{\omega_k}\,\mathrm{d}k\right)\left(\frac{1}{(2\pi)^3}\int\frac{1}{\exp[\beta\omega_k]-1}\,4\pi k^2\,\mathrm{d}k\right)\right\}$$

$$= -9\lambda\frac{1}{(2\pi^2)^2}\beta^{-4}\left\{\left[\sum_{\nu=1}^{\infty}\mu\beta\frac{\mathrm{K}_1(\nu\mu\beta)}{\nu}\right]^2 +\right.$$

$$\left. + \frac{2}{3}\mu^2\beta^2\left(\sum_{\nu=1}^{\infty}\mu\beta\frac{\mathrm{K}_1(\nu\mu\beta)}{\nu}\right)\left(\sum_{\nu=1}^{\infty}\mathrm{K}_0(\nu\mu\beta)\right)\right\}$$

and

$$(5.12c) \qquad \bar{p} - \frac{1}{3}\bar{\varepsilon} = -\mu^2\frac{1}{3(2\pi)^3}\left[\int\frac{1}{\exp[\beta\omega_k]-1}\frac{4\pi k^2}{\omega_k}\,\mathrm{d}k\right]\cdot$$

$$\cdot\left[1-\frac{6\lambda}{(2\pi)^3}\int\frac{1}{\exp[\beta\omega_k]-1}\frac{4\pi}{\omega_k}\,\mathrm{d}k\right] = -\frac{\mu^2\beta^2}{3(2\pi^2)}\left(\sum_{\nu=1}^{\infty}\mu\beta\frac{\mathrm{K}_1(\nu\mu\beta)}{\nu}\right)\left\{1-\frac{6\lambda}{2\pi^2}\sum_{\nu=1}^{\infty}\mathrm{K}_0(\nu\mu\beta)\right\}.$$

Here,

$$K_n(x) = \int_0^\infty \exp[-z\cosh t]\cosh nt\,dt\,. \tag{5.13}$$

(5.12)'s show that, for $\mu = 0$, $\bar{p} = \bar{\varepsilon}/3$ is realized exactly in each stage of the perturbation approximation, which could be foreseen from our general argument in Sect. 2. We show the $(\bar{p}, \bar{\varepsilon})$-curves in Fig. 4 which are given by numerical calculation. (a) is the line for $\mu = 0$, i.e. $\bar{p} = \bar{\varepsilon}/3$ and (b) for $\lambda = 0$, i.e. $(\bar{p}_0, \bar{\varepsilon}_0)$-curve. (c) is the curve for the attractive interaction $(\lambda < 0)$ and this is consistent with the prediction of our general argument in Sect. 2, which says that, in this case, the curve should be below the curve (b), (cf. Fig. 2). On the contrary, for the repulsive interaction $(\lambda > 0)$, the $(\bar{p}, \bar{\varepsilon})$-curve crosses the curve (a) to contradict the general discussion. As is seen from eq. (5.12c) this situation cannot be remedied, however small we assume λ. Moreover, for $\lambda > \lambda_c > 0$, $\bar{p}$, $\bar{\varepsilon}$ are negative for high temperature. Here, the critical value λ_c is derived from the quantities with $\mu = 0$, which describe the behavior at extremely high temperature in the following way:

$$\bar{p}(\mu = 0, \lambda_c) = \frac{1}{3}\bar{\varepsilon}(\mu = 0, \lambda_c) = \frac{\pi^2}{90}\beta^{-4}\left(1 - \frac{15}{8\pi^2}\lambda_c\right) = 0\,. \tag{5.14}$$

We see from Fig. 4 that the first order term overcomes the zero-th order ones for high temperature.

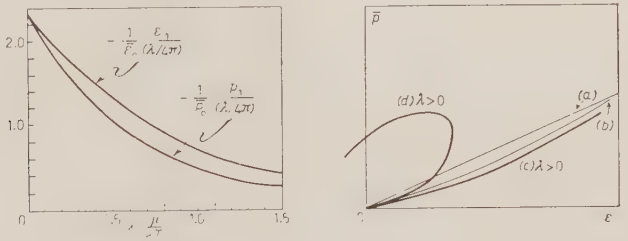

Fig. 4. – $x = \mu/kT$.

Any how these facts may show that the perturbation calculation is not valid in our case. Therefore, we should carry out the above calculation by means of non-perturbational treatment in order that we get the results to be compared with experiment. This consequences may be related with the argument by THIRRING and PETERMAN [10] that the zero point of λ is not a regular point in S-matrix. In Appendix B, we give the result of the second

order approximation, but only to illustrate the method of calculation and renormalization.

5·2. *Non-perturbational method.* – Postponing the application to a forthcoming paper, we briefly consider the path integral formula (*) and the variational method.

A simple derivation of the path integral formula is the following one. Introducing the c-number source $J(x)$, we write $\mathrm{Tr}\,(\varrho)$ in the form,

$$\mathrm{Tr}\,(\varrho) = \lim_{J\to 0} \mathrm{Tr}\,(\exp[-\beta H]U(\infty))\,. \tag{5.15}$$

The operator $U(t)$ satisfies the relation

$$-\frac{\partial U(t)}{\partial t} = \int \varphi(x) J(x)\,\mathrm{d}^3x \cdot U(t)\,, \tag{5.16}$$

with

$$\varphi(x) = \exp[tH]\varphi(\boldsymbol{x})\exp[-tH] \qquad x = (\boldsymbol{x}, t) \tag{5.17}$$

and

$$U(0) = 1\,.$$

The relation (5.16) leads to [10]

$$\frac{\delta^n U(\infty, t_0)}{\delta J(x) \ldots \delta J(x)} = (-1)^n U(\infty, t)[\varphi(x)]^n\, U(t, t_0)\,, \tag{5.18}$$

where $U(t, t_0)$ is the solution of (5.16) for the initial condition $U(t_0, t_0) = 1$, e.g. $U(t, t_0) = U(t)$. It is not difficult to prove the relation

$$\begin{aligned} \pi(x) &= \exp[tH]\pi(\boldsymbol{x})\exp[-tH]\,, \\ &= i\frac{\partial}{\partial t}\varphi(x)\,. \end{aligned} \tag{5.19}$$

Thus, we obtain

$$\mathrm{Tr}\,(\varrho) = \lim_{J\to 0} \varrho\left[\frac{\delta}{\delta J}\right] \mathrm{Tr}\,(U(\infty))\,, \tag{5.20}$$

(*) Path integral method in quantum statistics has been applied by FEYNMAN (*Phys. Rev.*, **91**, 1291 (1953)) to the problem of Liquid Helium, where the particles interact with each other through the potential interaction.

[10] H. UMEZAWA and A. VISCONTI: *Nuovo Cimento*, **1**, 1079 (1955).

where

$$\varrho\left[\frac{\delta}{\delta J}\right] = \exp\left[\beta H\left(\hat{c}\,\frac{\delta}{\delta \bar{J}},\ -\frac{\delta}{\delta J}\right)\right]. \tag{5.21}$$

The operator $H[-\hat{c}(\delta/\delta J),\ -\delta/\delta J]$ denotes the hamiltonian with the replacement

$$\begin{cases} \varphi(x) \to -\dfrac{\delta}{\delta J(x)}\,, \\ \varphi_k(x) \to -\partial_k \dfrac{\delta}{\delta J(x)}\,, \\ \pi(x) \to -i\,\dfrac{\hat{c}}{\partial t}\,\dfrac{\delta}{\delta J(x)}\,. \end{cases} \tag{5.22}$$

Applying (5.21) to the pseudoscalar field φ whose hamiltonian is

$$H = \frac{1}{2}\int \mathrm{d}^3x\,(\pi^2(x) + (\partial_k\varphi(x))^2 + \mu^2\varphi^2(x)) + \lambda\int\varphi^4(x)\ \mathrm{d}^3x\,,$$

we obtain

$$[\Delta + \partial_t^2 - \mu^2 - 4\lambda\varphi^2(x)]\varphi(x) = 0\,. \tag{5.23}$$

This with (5.20) leads to

$$\left(\Delta + \hat{c}_t^2 - \mu^2 - 4\lambda\,\frac{\delta^2}{\delta J(x)\,\delta J(x)}\right)\frac{\delta}{\delta J(x)}\,U(\infty) = \cdots J(x)\,U(\infty)\,. \tag{5.24}$$

and consequently

$$\mathrm{Tr}\left(\Delta + \hat{c}_t^2 - \mu^2 - 4\lambda\,\frac{\delta^2}{\delta J(x)\,\delta J(x)}\right)\frac{\delta}{\delta J(x)}\,U(\infty) = -\,\mathrm{Tr}\,[J(x)\,U(\infty)]\,. \tag{5.25}$$

This can be solved to give

$$\mathrm{Tr}\,[U(\infty)] = \int \delta a\,u(a)\,\exp\left[\left(-i\int_0^\infty \mathrm{d}t\int \mathrm{d}^3x\,a(x)\,J(x)\right)\right], \tag{5.26}$$

where

$$u(a) = \frac{1}{N}\exp\left[\int_0^\infty \mathrm{d}t\int \mathrm{d}^3x\,\mathcal{L}(ia)\right], \tag{5.27}$$

with

$$\mathcal{L}(ia) = -\frac{1}{2}a(x)\left(\Delta + \frac{\partial^2}{\partial t^2} - \mu^2\right)a(x) - \lambda a^4(x) \tag{5.28}$$

and

$$N = \int \delta a\, u(a)\,. \tag{5.29}$$

The last equation comes from the relation

$$\lim_{J\to 0} U(\infty) = 1\,. \tag{5.30}$$

Thus, we have

$$\begin{aligned} \mathrm{Tr}\,(\varrho) &= \lim_{J\to 0} \varrho\left[\frac{\delta}{\delta J}\right] \mathrm{Tr}\,(U(\infty)) \\ &= \frac{1}{N}\int \delta a(x) \exp\left[-\beta \int H(i\partial_\mu a,\, i\,a)\,\mathrm{d}^3x + \int_0^\infty \mathrm{d}t \int \mathrm{d}^3x\, \mathcal{L}(x)\right], \end{aligned} \tag{5.31}$$

with

$$H(i\partial_\mu a,\, ia) = -\frac{1}{2}\left[-\left(\frac{\partial}{\partial t}a(x)\right)^2 + (\partial_k a(x))^2 + \mu^2 a(x)^2 + \lambda(a(x))^4\right]. \tag{5.32}$$

This is the path integral formula for Tr (ϱ).

The Peierls theorem [11] may be useful to calculate Tr (ϱ) by means of the variational method. This theorem says that

$$\sum_n (\Psi_n,\, \exp[-\beta H]\Psi_n) \leqslant \mathrm{Tr}\,(\varrho)\,. \tag{5.33}$$

Here the summation is taken over any set of the elements in the complete set (Ψ_n). The equality in (5.33) holds when we take all the elements of the complete set. Taking a suitable trial function (φ_n), we may apply the variational method to calculate Tr (ϱ).

---

[11] R. E. PEIERLS: *Phys. Rev.*, **54**, 918 (1938).

Appendix A.

Multiplicity of Mesons.

According to Landau's assumption, multiplicity N is proportional to the entropy of the system in thermal equilibrium state:

$$N \propto S = sV ,$$

where s is the entropy density and V is the volume of the meson cloud around the nucleon. By using the thermodynamical relations

$$d\varepsilon = T\,ds$$

$$\varepsilon + p = Ts$$

and the equation of state,

$$p = f(\varepsilon)$$

we derive the formula

$$s = \exp\left[\int^{\varepsilon} \frac{d\varepsilon}{f(\varepsilon) + \varepsilon}\right] .$$

Now, we have the relations

$$\varepsilon = \frac{E}{V} - \frac{E'}{V^0} , \qquad E = \sqrt{2ME'} ,$$

$$V = V^0 \frac{2M}{E} = V^0 \frac{E}{E'} ,$$

where E, E' are the energies of the two nucleons in the barycentric system and in the laboratory system respectively, and V^0 is the volume of the meson cloud around the nucleon at rest i.e. $\sim (4\pi/3)(1/\mu)^3$. When $p = f(\varepsilon) = \frac{1}{3}a\varepsilon + b$ with the constants a, b, we obtain

$$N \propto \left[\left(\frac{a}{3} + 1\right)\varepsilon + b\right]^{3/(a+3)} V$$

$$\propto \left[E' + \frac{3V^0}{a+3}\, b\right]^{3/(a+3)} E'^{-\frac{1}{2}} .$$

For $(a/3)\varepsilon \gg b$, this goes over into

$$N \propto E'^{\frac{1}{2}(3-a)/(a+3)} .$$

This leads to

$$N \propto E'^{\frac{1}{4}}$$

for $a = 1$, $b = 0$. This is the result of Fermi and Landau.

Appendix B.

Renormalization Methods (Second Order Approximation).

We are now concerned with the second order terms in (5.5):

$$\xi_2 = \left\langle \frac{1}{2}\lambda^2 \int \mathrm{P}[\varphi^1(x), \varphi^1(x')]\,\mathrm{d}^4x\,\mathrm{d}^4x' - \frac{\lambda}{2}(\delta\mu^2)_1 \int \mathrm{P}[\varphi^1(x), \varphi^2(x')]\,\mathrm{d}^4x\,\mathrm{d}^4x' + \right.$$
$$+ \frac{1}{2}\left\{\frac{1}{2}(\delta\mu^2)_1\right\}^2 \int \mathrm{P}[\varphi^2(x), \varphi^2(x')]\,\mathrm{d}^4x\,\mathrm{d}^4x' +$$
$$\left. + \frac{1}{2}(\delta\mu^2)_2 \int \varphi^2(x)\,\mathrm{d}^4x + \delta\lambda \int \varphi^4(x)\,\mathrm{d}^4x \right\rangle - \langle\ \rangle_{\mathrm{vac}}\,, \tag{B.1}$$

where $(\delta\mu^2)_i$, $(\delta\lambda)_i$ are the i-th order quantities in λ, and $\langle\ \rangle_{\mathrm{vac}}$ is the vacuum effect. The first term of ξ_2 comes from the following diagrams:

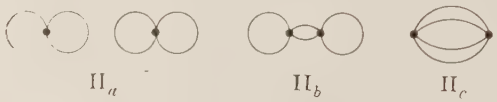

Fig. 5.

The diagrams in II_a are the repeated graphs of the first order one and therefore we dont consider them. We rewrite the graphs II_b and II_c in therms of the (e)- and (i)-line:

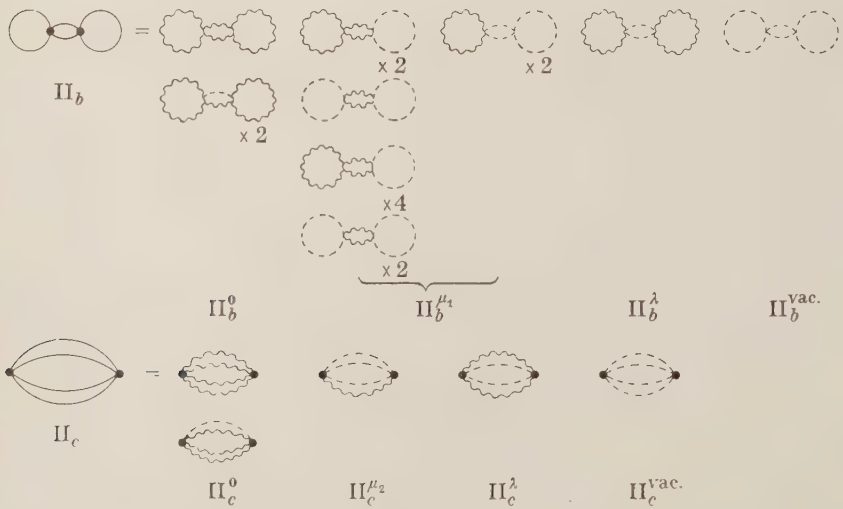

Fig. 6.

The suffixes of Π_a, Π_b, i.e. μ_i, λ, vac. and 0 mean that diagrams correspond to the i-th order mass renormalization, the charge renormalization, vacuum effect and converging terms.

To visualize the renormalization procedure, we calculate the terms of the Π_b and Π_c, we have

$$\text{(B.2)} \qquad \xi'_{2b} = 6\times 6\times 2\times \frac{\lambda^2}{2!} D(0)^2 \int D(x-x')^2 \,\mathrm{d}^4x\,\mathrm{d}^4x' =$$

$$\cdot 36\lambda^2 \left\{\sum_k \frac{1}{2V\omega_k}(2f_k+1)\right\}^2 \left\{\frac{\beta^2}{2}\sum_k \frac{f_k(f_k+1)}{\omega_k^2} + \frac{\beta}{4}\sum_k \frac{(f_k+1)}{\omega_k^3} - \frac{\beta}{4}\sum_k \frac{f_k^2}{\omega_k^3}\right\},$$

$$\text{(B.3)} \qquad \xi'_{2c} = 4!\,\frac{\lambda^2}{2!}\int D(x-x')^4\,\mathrm{d}^4x\,\mathrm{d}^4x' = \frac{3}{2}\lambda^2\beta V \sum_{p+q+r+s=0} \frac{1}{V^3\omega_p\omega_q\omega_r\omega_s}\cdot$$

$$\cdot\left[(f_p+1)(f_q+1(f_r+1)(f_s+1)\frac{1}{\omega_p+\omega_q+\omega_r+\omega_s}+\right.$$

$$+ 4f_p(f_q+1)(f_r+1)(f_s+1)\frac{1}{-\omega_p+\omega_q+\omega_r+\omega_s}+$$

$$+ 6f_pf_q(f_r+1)(f_s+1)\frac{1}{-\omega_p-\omega_q+\omega_r+\omega_s}+$$

$$\left.+ 4f_pf_qf_r(f_s+1)\frac{1}{-\omega_p-\omega_q-\omega_r+\omega_s} + f_pf_qf_rf_s\frac{1}{-\omega_p-\omega_q-\omega_r-\omega_s}\right].$$

Here, some terms have cancelled each other on account of $f_k+1-f_k\exp[\beta\omega_k]$.

The factors f_k's and 1's correspond respectively to the wavy and dotted lines of the splitted diagrams, and therefore the meaning of each term in (B.2) and (B.3) is obvious.

As an example, we consider the second order mass renormalization terms. One of them comes from the diagram $\Pi_c^{\mu_2}$ (the 1-st and 2-nd term in (B.3)),

$$\text{(B.4)} \qquad \xi_{2c}^{\mu_2} = 6\lambda^2\beta V \sum_{p+q+r+s=0} \frac{f_p}{V^3\omega_p\omega_q\omega_r\omega_s}\cdot$$

$$\cdot\left\{\frac{1}{\omega_p+\omega_q+\omega_r+\omega_s}+\frac{1}{-\omega_p+\omega_q+\omega_r+\omega_s}\right\}.$$

We define the counter term for the mass renormalization in the diagram Π_c:

$$\text{(B.5)} \qquad (\delta\mu^2)_{2c} = -12\lambda^2 V \sum_{p+q+r+s=0} \frac{1}{\omega_q\omega_r\omega_s}\cdot$$

$$\cdot\left\{\frac{1}{\omega_p+\omega_q+\omega_r+\omega_s}+\frac{1}{-\omega_p+\omega_q+\omega_r+\omega_s}\right\}.$$

This is just the mass renormalization term in the S-matrix theory. As is known in the S-matrix theory, (B.5) is independent of ω_p (i.e. constant). This can be seen from the covariant calculation.

The other mass renormalization term in the second order stems from the charge renormalization counter term $-\delta\lambda\int\Phi^4(x)\,\mathrm{d}^3x$. As is seen from Fig. 7, it gives

Fig. 7.

the mass renormalization

$$(\delta\mu^2)_{2\lambda} = +6\delta\lambda\sum_k \frac{1}{V\omega_k}\,. \tag{B.6}$$

Finally we have for the second order mass renormalization constant

$$(\delta\mu^2)_2 = (\delta\mu^2)_{2c} + (\delta\mu^2)_{2\lambda}\,. \tag{B.7}$$

Next, we consider the charge renormalization. The second bracket in (B.2) corresponding to the diagram II_b gives the term to be subtracted from charge renormalization term $(\delta\lambda)_b\varphi^4$, on setting $f_k = 0$. The 1-st, and, and 4-th term in (B.3) also calls for $(\delta\lambda)_c\varphi^4$. Summing them,

$$\begin{cases} \delta\lambda = (\delta\lambda)_b + (\delta\lambda)_c\,, \\ (\delta\lambda)_b = -3\lambda^2\left(\sum_k \frac{1}{V\omega_k^3}\right), \\ (\delta\lambda)_c = -9\lambda^2\left(\sum_{\substack{r,s \\ p+q+r+s=0}} \frac{1}{\omega_r\omega_s}\left[\frac{1}{\omega_p+\omega_q+\omega_r+\omega_s} + \right.\right. \\ \qquad \left.\left. + \frac{2}{-\omega_p+\omega_q+\omega_r+\omega_s} + \frac{1}{-\omega_p-\omega_q+\omega_r+\omega_s}\right]\right). \end{cases} \tag{B.8}$$

Thus we have the finite result,

$$\begin{cases} \xi_2 = \xi_{2a} - \xi_{2b} + \xi_{2c} \\ \xi_{2a} = \frac{1}{2!}(\xi_1)^2\,, \\ \xi_{2b} = 18\lambda^2\beta V\left\{\sum_k \frac{f_k}{V\omega_k}\right\}^2\left\{\sum_\kappa\left(\beta\frac{f_k(f_k+1)}{V\omega_k^2} + \frac{f_k}{V\omega_k}\right)\right\}, \\ \xi_{2c} = 6\lambda^2\beta V\sum_{p+q+r+s=0}\frac{1}{V^3\omega_p\omega_q\omega_r\omega_s} f_p f_q f_r\left\{\frac{1}{\omega_p+\omega_q+\omega_r+\omega_s} + \right. \\ \left. + \frac{3}{-\omega_p+\omega_q+\omega_r+\omega_s} + \frac{3}{-\omega_p-\omega_q+\omega_r+\omega_s} + \frac{1}{-\omega_p-\omega_q-\omega_r+\omega_s}\right\}. \end{cases} \tag{B.9}$$

Note that this result is not the same as that obtained by replacing simply $f_k + 1 \to f_k$ from the beginning.

RIASSUNTO (*)

Si discutono le relazioni termodinamiche nella teoria quantistica dei campi. È offerta così la possibilità di decidere se le interazioni siano rinormalizzabili o meno, cioè se siano di prima o di seconda specie. Si illustra il procedimento di rinormalizzazione formulando il calcolo perturbativo. Si mette anche in evidenza la possibilità di procedere con metodo non perturbativo. Queste considerazioni d'indole generale si applicano alla ricerca degli effetti d'interazione nei fenomeni di produzione multipla, effetti che furono trascurati nella teoria statistica di Fermi-Landau.

(*) *Traduzione a cura della Redazione.*

Sulle variazioni delle proprietà magnetiche e meccaniche causate dall'idrogeno disciolto nel ferro (*).

A. Ferro (°) e G. Montalenti

Centro Studi Elettrofisica, Istituto Elettrotecnico Nazionale « Galileo Ferraris » - Torino
(°) *Laboratorio Ricerche e Controlli Auto Avio FIAT - Torino*

(ricevuto il 25 Novembre 1956)

Riassunto. — Si dà un'interpretazione degli effetti meccanici e magnetici dovuti all'idrogeno che si discioglie nel ferro. Si dimostra che, per spiegare i fatti, è necessario ammettere che il gas contenuto nel metallo allo stato atomico tenda a precipitare in molecola biatomica entro cavità ellittiche dell'ordine di grandezza di almeno alcune decine di diametri atomici, determinando nell'interno delle lacune reticolari stesse una forte pressione; questa forte pressione nei materiali duri può produrre la rottura spontanea, nei materiali dolci l'accrescimento delle cavità sino a produrre sulla superficie del metallo delle bollicine, spesso visibili ad occhio nudo e accompagnate da notevole deformazione plastica che determina a sua volta, nei materiali ferromagnetici con permeabilità sufficientemente alta, un aumento del campo coercitivo di saturazione. Si riferisce su alcune esperienze eseguite su ferro caricato con idrogeno a paragone con ferro deformato plasticamente. L'andamento del campo coercitivo di saturazione, misurato a temperatura ambiente, in funzione della temperatura di ricottura è identico nei due casi. Pertanto le ipotesi poste alla base della spiegazione dei fatti su accennati hanno conferma sperimentale. Da considerazioni tratte dalla teoria della precipitazione si stima la distanza media dei centri di precipitazione dell'idrogeno ottenendo valori di circa $2 \cdot 10^{-3}$ cm in accordo coi dati sperimentali disponibili.

1. – Premessa.

Come è noto i gas disciolti nei metalli possono alterarne notevolmente le proprietà, ad esempio l'idrogeno nel ferro aumenta la fragilità e nei materiali ad alta permeabilità il campo coercitivo ([1,2]). I gas possono disciogliersi nei

(*) Presentato al Congresso di Torino, 11-16 Settembre 1956.
([1]) D. P. Smith: *Hydrogen in Metals* (Chicago, 1947).
([2]) C. R. Cupp: *Gases in Metals - Progress in Metal Physics*, **4** (London, 1953).

metalli esotermicamente od endotermicamente. Nel primo caso si ha tendenza a formare composto tra gas e metallo, nel secondo caso no. Questa distinzione è di fondamentale importanza per le diverse conseguenze che il gas disciolto può avere nelle proprietà elastiche e magnetiche del metallo. In particolare l'idrogeno non forma composto nel ferro e da considerazioni termodinamiche sul relativo diagramma di equilibrio si deduce [1-3] che questo gas si discioglie endotermicamente entrando nel metallo allo stato atomico. Le esperienze di COEHN, di SEITH e KUBAČEWSKI (ricordate da CUPP [2]) mostrano tra l'altro che, in alcuni casi, il gas è disciolto allo stato di ione.

Più recentemente [4,5] per il caso dell'idrogeno è stato dimostrato con misure di attrito interno meccanico, a temperatura dell'aria liquida, che l'idrogeno è, almeno in parte, disciolto allo stato atomico interstiziale nella matrice del ferro, oppure allo stato atomico ancorato nelle dislocazioni, come dimostra l'esistenza di due picchi caratteristici nella curva dell'attrito interno in funzione della temperatura. I risultati, in tutto analoghi a quelli del carbonio o dell'azoto allo stato interstiziale nel ferro, sono stati interpretati da uno degli autori [6].

È poi importante osservare che la quantità di idrogeno che può disciogliersi nel ferro aumenta in seguito all'incrudimento [7]: in un monocristallo perfetto, se riesce ad entrare, si trova in piccolissime quantità. La spiegazione di ciò è da ricercarsi nel fatto che il metallo incrudito contiene un numero molto elevato di vacanze, dislocazioni e lacune reticolari, in cui l'idrogeno può raccogliersi, come dimostra il fatto che la densità diminuisce leggermente con l'incrudimento [8].

Come è noto uno dei mezzi per sciogliere una certa quantità di idrogeno in un metallo è per via elettrolitica. In questo processo la quantità che si può sciogliere, o che invece si ricombina in superficie e si riassocia in molecole per evadere dal bagno sotto forma di bollicine, dipende fortemente dalle impurezze che si trovano alla superficie del metallo. Nel presente lavoro non si trattano queste questioni rimandando il lettore alle numerose memorie sull'argomento [9,10]. Giova soltanto osservare che la equazione di Nernst [11] indica che le pressioni sotto le quali può entrare il gas per via elettrolitica o per attacco

[3] W. JOST: *Diffusion* (New York, 1952).
[4] L. C. CHANG e M. GENSAMER: *Acta Metallurgica*, **1**, 482 (1953).
[5] C. BAIN: *Journ. Iron and Steel Inst.*, **181**, 193 (1954).
[6] A. FERRO: *Teoria della diffusione interstiziale* (in corso di pubblicazione).
[7] J. H. ANDREW e H. LEE: *Inst. of Metal London, Symposium on Internal Stress in Metals and Alloys* (1948), pag. 265.
[8] W. BOAS: *Report of the Conf. on Defects in Cristalline Solids* (London, 1955).
[9] J. H. DE BOER e J. D. FAST: *Rec. Trav. Chim. Pays-Bas*, **58**, 584 (1939).
[10] G. BIANCHI e R. ZOIA: *Ric. Scient.*, **18**, 101 (1948).
[11] G. BORELIUS e J. LINDBLOM: *Ann. der Phys.*, **82**, 201 (1927).

in bagno acido possono essere molto elevate: dell'ordine delle decine di migliaia di atmosfere. Alcune valutazioni sperimentali di dette pressioni sono state fatte da BORELIUS, LINDBLOM [11] e SMITHELLS [12].

2. - Effetti dell'idrogeno sulle proprietà magnetiche del ferro.

Il fatto che il ferro depositato per via elettrolitica possegga alto campo coercitivo ed elevata intensità di magnetizzazione residua è stato segnalato nel secolo scorso da MATTHIESSEN. L'unica successiva indagine sistematica su materiali non ottenuti da deposito elettrolitico ma saturati in idrogeno è stata eseguita da REBER [13]. Questo autore conclude che facendo entrare idrogeno per via elettrolitica, su ferro Armco allo stato di fornitura e su ferro Armco laminato a freddo e ricotto, si osserva un'incremento nel campo coercitivo, una diminuzione dell'intensità di magnetizzazione residua e del valore della permeabilità massima. Si può ritenere che le variazioni delle grandezze magnetiche siano una funzione crescente del contenuto di idrogeno. In fig. 1 ed in fig. 2 sono riportati i dati ricavati nel presente lavoro idrogenando del ferro

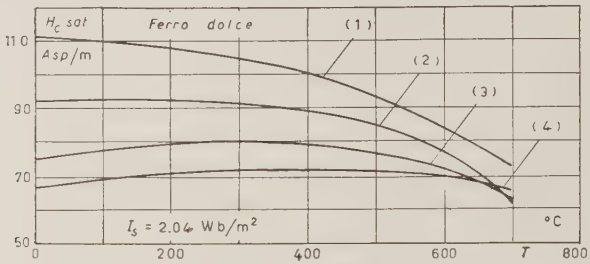

Fig. 1. - Variazione del campo coercitivo di saturazione, misurato a temperatura ambiente su campioni di ferro dolce, in funzione della temperatura di ricottura. Curva 1: campione laminato del 5%. Curva 2: campione idrogenato per 48 ore. Curva 3: campione idrogenato per 24 ore. Curva 4: campione che non ha subito nè idrogenazione nè laminazione. Un campione idrogenato per 96 ore ha dato risultati coincidenti con la curva 2.

dolce ricotto. L'idrogeno è fatto entrare ponendo una striscia di lamiera in un bagno [14] di HCl al 10% con il 0.03% di Na_2S per diverse ore. Dopo idrogenazione appaiono nel materiale le caratteristiche « bollicine » (blister) che denotano la notevole deformazione plastica subita. Sulle lamiere caricate di idro-

[12] C. J. SMITHELLS: *Gases in Metals* (London, 1937).
[13] R. K. REBER: *Physics*, **5**, 297 (1934).
[14] P. BASTIEN e P. AZOU: *Rev. Met.*, **45**, 301 (1948).

geno per 48 ore si hanno variazioni del campo coercitivo intorno al 65 % e tempi di idrogenazione più lunghi non modificano apprezzabilmente questo valore; viceversa per un trattamento di sole 24 ore la variazione nel campo coercitivo è di circa la metà.

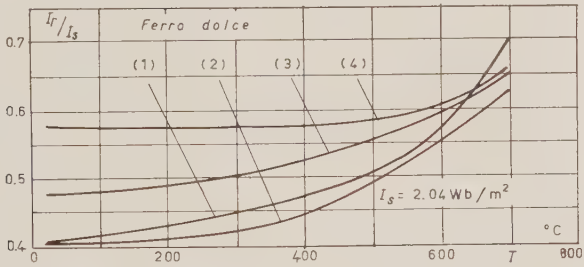

Fig. 2. – Variazione del rapporto I_r/I_s (induzione residua di saturazione diviso induzione di saturazione) misurato a temperatura ambiente, sugli stessi campioni di cui a Fig. 1., in funzione della temperatura di ricottura.

L'intensità di magnetizzazione a saturazione è, entro i limiti di precisione delle misure (1%), costante, in accordo col fatto che comunque la quantità di atomi di idrogeno disciolti è molto piccola (ad es. 10 cc di H_2 per 100 g, che è già una quantità piuttosto elevata, corrispondono ad una concentrazione in atomi di $5 \cdot 10^{-4}$).

Sui provini così preparati si è esaminato come varia il campo coercitivo di saturazione e l'intensità di magnetizzazione residua in funzione della temperatura di ricottura a tempo costante mettendo in evidenza che è necessario raggiungere una temperatura intorno a 700 °C affinchè scompaia, nel materiale, l'effetto dell'idrogeno. La ricottura è eseguita in vuoto.

La curva (1) della fig. 1 rappresenta per confronto la variazione degli stessi parametri magnetici rilevati su un campione dello stesso ferro dolce laminato di circa il 5%. Come si vede l'andamento delle curve è strettamente analogo.

Queste esperienze permettono quindi di concludere che l'effetto dell'idrogeno nel ferro è quello di deformare plasticamente il ferro stesso creando tensioni interne che, come ordine di grandezza, equivalgono a quelle ottenute con una deformazione plastica di qualche percento. Queste tensioni interne aumentano, come è ben noto il campo coercitivo ([15]) ed orientano i domini in modo tale da creare una diminuzione nella induzione residua; infatti, nel nostro caso, il materiale di partenza era anisotropo, mentre le tensioni interne indotte dal-

([15]) R. M. Bozorth: *Ferromagnetism* (New York, 1951).

l'idrogeno sono distribuite a caso e pertanto tendono a riportare l'induzione residua a circa la metà del valor massimo ([16]).

In sintesi, sul ferro dolce, introdurre idrogeno o deformare plasticamente conduce a conseguenze identiche sulle proprietà magnetiche.

Poichè le tensioni interne e l'incrudimento prodotti dall'idrogeno sono piccoli è ovvio che una variazione delle proprietà magnetiche e in particolare del campo coercitivo è osservabile solo su materiali ad alta permeabilità: nessuna variazione è stata infatti osservata su provini incruditi o acciai in cui il campo coercitivo è sempre relativamente alto. Viceversa variazioni sensibili delle proprietà magnetiche si sono di nuovo osservate ad esempio su lamierini al 3.5% di silicio ricotti.

3. Effetti dell'idrogeno sulle proprietà meccaniche del ferro dolce e degli acciai.

L'interesse tecnico su queste questioni (l'idrogeno può dare in certe condizioni luogo a rottura fragile degli acciai) è così vivo che esiste una estesissima bibliografia al riguardo. Per un'ampia rassegna si veda: ([1,2,7,17]). Si cerca qui di riassumere schematicamente i fatti fondamentali. Sul ferro dolce caricato in idrogeno appaiono delle «bollicine» (blister) e la fragilità, intesa come riduzione della capacità di deformazione plastica, è fortemente aumentata: i materiali duri possono anche rompersi spontaneamente. Il modulo di Young ([18]), il punto di snervamento, ([19]) la durezza ([20]) e la curva carichi deformazioni ([20,21]) non subiscono, normalmente, variazioni per effetto dell'idrogeno disciolto: la rottura avviene di regola, invece, per un valore più basso della tensione reale e un corrispondente aumento della sezione di rottura del provino; perchè però si osservi questa diminuzione nella contrazione laterale occorre produrre la rottura, applicando il carico con la velocità bassa in un tempo di almeno 2-3 minuti primi. Se il fenomeno avviene in un tempo dell'ordine di 10^{3} secondi non si nota viceversa aumento alcuno dell'area della sezione di rottura rispetto al metallo non caricato di idrogeno, come dimostrano le esperienze di Bastien e Azou ([22]), di Troiano ([23]) e d'altri ([20]). Di norma si può ritenere che, qualitati-

([16]) R. M. Bozorth: *Zeits. f. Phys.*, **124**, 519 (1948).

([17]) F. de Kazinczy: *Journ. Iron and Steel. Inst.*, **177**, 85 (1954).

([18]) P. Bastien e P. Azou: *Compt. Rend.*, **231**, 147 (1950).

([19]) J. H. Andrew, H. Lee, A. K. Mallik e A. G. Quarrell: *Journ. Iron Steel Inst.*, **153**, 67 (1946).

([20]) J. B. Leabrook, N. J. Grant e D. Carney: *Trans. Amer. Inst. Min. Met. Eng.*, **188**, 1317 (1950).

([21]) P. Bastien e P. Azou: *Rev. Met.*, **49**, 837 (1952).

([22]) P. Bastien e P. Azou: *Compt. Rend.*, **232**, 69 (1951).

([23]) R. P. Frohmberg, W. J. Barnett e A. R. Troiano: *Trans. of Am. Soc. for Metals*, **47**, 892 (1955).

vamente, l'aumento della fragilità cresce al crescere del contenuto di idrogeno come dimostrano le misure di DUFLOT [24] e di altri. Lo stesso autore dimostra, con accurate misure di microdurezza su ferro caricato con idrogeno, che vi è anche un piccolo aumento di durezza che però si osserva soltanto nell'intorno delle bollicine. Ad una temperatura dell'ordine di grandezza di — 100 °C l'aumento di fragilità causata dall'idrogeno scompare [25].

Inoltre le esperienze più recenti hanno permesso di mettere in luce differenze, rispetto al materiale non caricato, assai significative dal punto di vista fisico:

1) Il ferro dolce ricotto [26,27] caricato con idrogeno anche per tempi relativamente brevi se provato subito non presenta più il punto di snervamento caratteristico dovuto agli atomi interstiziali di carbonio e azoto ancorati nelle dislocazioni. Lasciando che il materiale non perda l'idrogeno il ginocchio caratteristico ricompare.

2) Viceversa caricando un materiale leggermente incrudito in modo che le dislocazioni presenti siano libere da carbonio e da azoto e lasciandolo invecchiare per qualche ora si osserva un aumento del limite di snervamento e a — 100 °C un caratteristico ginocchio analogo, se pure di intensità minore, a quello dovuto al carbonio ed all'azoto. Poichè questi ultimi non hanno avuto tempo di riprecipitare nelle dislocazioni tale comportamento deve venire attribuito al fatto che l'idrogeno si comporta come gli altri atomi interstiziali e tende anche esso ad ancorarsi nelle dislocazioni; la sua velocità di diffusione è però assai più alta e l'energia di legame con le dislocazioni assai più bassa: quindi il ginocchio caratteristico si verifica soltanto molto al di sotto della temperatura ambiente.

4. – Interpretazione dei fatti.

L'idrogeno nel ferro si trova in parte allo stato atomico interstiziale nel reticolo in parte ancorato nelle dislocazioni, ma pur sempre allo stato atomico, come dimostrano le esperienze di attrito interno di GENSAMER [4] citate anche da C. BAIN [5]. L'idrogeno può evolvere dallo stato atomico allo stato molecolare se trova una cavità opportuna. Bisogna ora decidere se anche le posizioni interstiziali allargate intorno ad una dislocazione o le vacanze sono cavità idonee per la precipitazione.

---

[24] J. DUFLOT: *Thèse*, Paris (1950).
[25] P. BASTIEN e P. AZOU: *Compt. Rend.*, **229**, 549 (1949).
[26] H. C. ROGERS: *Acta Metallurgica*, **4**, 114 (1956).
[27] H. F. VAUGHAN e M. E. DE NORTON: *Acta Metallurgica*, **4**, 224 (1956).

Per rispondere a questa domanda occorre valutare la pressione massima alla quale può trovarsi, nell'interno del ferro, l'idrogeno molecolare e valutare se essa è sufficiente a vincere le forze che si oppongono al progredire della cavità.

La pressione si potrebbe calcolare mediante la costante di equilibrio della dissoluzione nel ferro supponendo misurata la quantità di idrogeno nell'interno del materiale e supponendo inoltre che la soluzione sia diluita. Poichè per forti pressioni, questa ipotesi non si è verificata conviene servirci della formula data da Phragmén e riportata da Kazinczy [17]:

$$T = \frac{3\,000 - 0.062\,p}{\log p - 2\log x_1 + 3.60}, \tag{1}$$

ove T è la temperatura in gradi assoluti; x_1 la concentrazione di idrogeno nel metallo in $cm^3/100\,g$; p la pressione in atmosfere dell'idrogeno gassoso in equilibrio termodinamico con una data quantità x_1 di gas disciolto nel ferro.

Il termine $0.062\,p$ tiene conto del fatto che, per pressioni molto elevate, ci si allontana dalle condizioni valide per i gas perfetti. Eseguendo i calcoli, per una quantità di idrogeno disciolto di $5\ cm^3/100\,g$, si ottiene che a 20 °C la pressione del gas idrogeno è di 17 000 atmosfere. Comunque la pressione non può mai superare 48 000 atmosfere poichè a questa pressione il numeratore della (1) si annulla. Se si tiene conto che anche l'idrogeno eventualmente già raccolto in cavità viene misurato come idrogeno disciolto, mentre in realtà nella (1) occorrerebbe tener conto soltanto dell'idrogeno che si trova nel ferro allo stato atomico si può concludere che certamente la pressione data dalla (1) è sempre calcolata in eccesso.

Il valore della tensione di decoesione teorica [28] (quella che si dovrebbe avere in un cristallo privo di difetti) è di circa un decimo del modulo elastico: nel caso dell'ordine di $2 \cdot 10^{11}$ dine/cm^2. Orbene se si considera una sfera mancante in un insieme di sfere poste a contatto anche intuitivamente si vede che la cavità sferica non può accrescersi senza che almeno alcune sfere si stacchino fra loro. Quindi una cavità sferica di diametro uguale al diametro di un atomo, una vacanza cioè, non può aumentare il suo volume se non staccando l'uno dall'altro gli atomi che la delimitano. Tenendo conto che la sollecitazione nel metallo al contorno della cavità è doppia della pressione nell'interno, è necessario pertanto avere pressioni maggiori almeno della metà della tensione di decoesione teorica, perchè una cavità di un diametro uguale al diametro atomico possa accrescersi.

Le stesse considerazioni valgono identicamente per le cavità interstiziali e quelle allargate nell'intorno delle dislocazioni. Nel ferro caricato con idrogeno il valore della massima pressione dato dalla (1) risulta sempre inferiore al va-

[28] N. J. Petch: *Progress in Metals Physics*, vol. 5 (London, 1954), p. 7.

lore della tensione teorica di rottura che per il ferro è dell'ordine di $2 \cdot 10^{11}$ dine/cm^2. Si deve pertanto concludere che le vacanze e le dislocazioni non sono centri idonei della formazione di cavità capaci di accrescersi, ove cioè possa precipitare in moto continuo l'idrogeno, ma si deve postulare, come si vedrà meglio in seguito, la esistenza di microcavità aventi almeno una dimensione di un ordine di grandezza che, per le pressioni più alte, può ridursi ad alcune decine di diametri atomici. In questo caso infatti la cavità può accrescersi fino a lunghezza tale da poter dar luogo a deformazione plastica o proseguire fino a produrre la rottura del materiale ([29]). L'esistenza di queste microcavità non deve considerarsi come ipotesi ad hoc poichè, come è ben noto, è essenziale ammetterne l'esistenza per spiegare la rottura per decoesione dei materiali fragili. Un ruolo importante per la precipitazione dell'idrogeno possono anche avere le superfici dei precipitati e in particolare dei carburi e degli ossidi. È comunque probabile che le discontinuità del reticolo dell'interfase facilitano la precipitazione ed effettivamente si osserva che le bollicine sono generalmente allineate in prossimità delle eterogeneità.

Rottura per decoesione – L'ultimo atto della rottura anche nel ferro dolce, dopo una prima fase di deformazione plastica è sempre, sostanzialmente, una rottura per decoesione. Come è ben noto ([28]) per spiegare, nella rottura per decoesione, la differenza tra la resistenza teorica del materiale e quella osservata sperimentalmente si deve ammettere l'esistenza di microcavità di forma molto allungata con un corrispondente elevato fattore di concentrazione di sforzo alle estremità. L'espressione della tensione massima al bordo di una fessura praticata in un continuo elastico indefinito sottoposto a tensione uniforme è nel caso piano data dalla ([28,30]).

$$\sigma_{max} = 2\sigma \sqrt{\frac{l}{c}}, \tag{2}$$

ove σ è la tensione applicata; σ_{max} la massima tensione al bordo della cavità; l la lunghezza della fessura; c la curvatura all'estremo della fessura. Questa stessa formula vale, con sufficiente approssimazione, per una pressione uniforme esercitata nell'interno della cavità ([30]). Poichè il minimo raggio di curvatura possibile è dell'ordine del diametro atomico, per il ferro, con un valore di σ_{max} di circa $2 \cdot 10^{11}$ dine/cm^2 ed ammettendo un carico di rottura tecnico di $3 \cdot 10^9$ dine/cm^2, si trova applicando la (2) che la minima lunghezza l della microcavità, affinchè si possa provocare la rottura con il carico tecnico, deve essere dell'ordine di circa 1000 diametri atomici.

([29]) A. H. Cottrell: *Dislocations and Plastic Flow in Crystals* (Oxford, 1953).
([30]) S. Timoshenko: *Theory of Elasticity* (New York, 1951), p. 197.

Chaudron ([31]) ritiene che l'aumento di fragilità (sempre intesa come diminuzione dell'allungamento plastico a rottura) del ferro caricato con idrogeno sia dovuto alla diminuita possibilità di scorrimento dei piani cristallini, ma questa ipotesi non spiega il meccanismo delle rotture spontanee sotto carico insistente. Petch ([32]) ritiene che l'idrogeno, concentrato nelle cavità del ferro, diminuisca la tensione superficiale e quindi abbassi la resistenza con un meccanismo del tipo proposto da Griffith: ma questa ipotesi è in contrasto col fatto che gli effetti osservati sono proporzionali alla quantità di idrogeno assorbito e col fatto che il calore di assorbimento superficiale dell'idrogeno nel ferro è di poche migliaia di calorie per mole; questa quantità di calore, modesta rispetto al calore di sublimazione del ferro (96000 cal/mole) non può alterare che di poco il calore di sublimazione del ferro caricato di idrogeno e quindi, in ultima analisi, la tensione superficiale del ferro con idrogeno assorbito rispetto a quella del ferro puro. Bastien, Azou ([21]) e Kazinczy ([17]) ritengono invece che tutti gli effetti osservati siano imputabili alla pressione esercitata dall'idrogeno che precipita nelle microcavità.

Si vuole mostrare come questa ipotesi non è contradditoria con i fatti sperimentali e consente di valutare alcuni parametri entro qualche ordine di grandezza. La teoria della elasticità garantisce che, anche per una pressione esercitantesi nell'interno di una cavità, si può ritenere valga con sufficiente approssimazione la (2) ([30]). Sostituendo in essa i valori dati dalla (1) si ottiene che per una pressione di 20000 atmosfere è sufficiente una cavità la cui dimensione massima sia almeno dell'ordine delle decine di diametri atomici per avere la rottura. Questo dato coincide, entro qualche ordine di grandezza, con le microcavità postulate da Griffith e valutate come sopra applicando la (2) al ferro puro. L'aumentata fragilità del ferro caricato con idrogeno, la comparsa di « blister » nel ferro dolce, la rottura spontanea negli acciai duri sotto tensione rimane dunque spiegata in modo semiquantitativo come dovuta all'elevata pressione esercitata nelle microcavità di Griffith dall'idrogeno che precipita dallo stato atomico allo stato molecolare.

Per spiegare il fatto che alla temperatura di circa — 100 °C l'aumento di fragilità scompare è sufficiente ricordare che a temperatura ambiente è necessario, per osservare l'effetto causato dall'idrogeno, provocare la rottura in qualche primo ([20,22]) e che il coefficiente di diffusione D dell'idrogeno atomico nel metallo varia con la temperatura con la legge ben nota:

$$D = D_0 \exp\left[-\frac{Q}{RT}\right]. \tag{3}$$

([31]) G. Chaudron e F. Moreau: *Arch. f. Metallkunde*, **2**, 308 (1948).
([32]) N. J. Petch e P. Stables: *Nature*, **169**, 842 (1952).

ove i valori dei parametri sono $Q = 9000$ cal/mole ([33]); $R = 1.98$ cal/mole; $D_0 = 1.35 \cdot 10^{-2}$ cm^2 s^{-1}. Alla temperatura di 20 °C D vale $2.5 \cdot 10^{-9}$ cm^2 s^{-1} ([33]) alla temperatura di — 110 °C D vale circa 10^{-14}. Ne segue che a questa temperatura occorrerebbero tempi dell'ordine di 10^5 minuti primi per osservare quei fenomeni che a temperatura ambiente avvengono in tempi dell'ordine del minuto.

Altro problema al quale si può dare risposta è la stima della distanza media tra le microcavità ove può avvenire la precipitazione. La teoria della precipitazione degli atomi interstiziali ([3,33]) applicabile anche al caso dell'idrogeno ove in prima approssimazione si ammetta che la pressione dell'idrogeno nella cavità rimanga costante al crescere della cavità stessa, fornisce la seguente espressione per la concentrazione in funzione del tempo nell'intorno del punto ove avviene la precipitazione:

$$\frac{C(t) - C_0}{C_0} = 1 - \exp\left[\frac{t \cdot D_0 \exp[-Q/RT]}{L^2}\right]^n , \tag{4}$$

ove C_0 è la concentrazione al tempo zero; t il tempo nel quale avviene la precipitazione, L la distanza tra i precipitati, n un esponente che dipende dalla forma dei precipitati. Si sa dall'esperienza che, a temperatura ambiente, l'azoto nel ferro precipita in 10^3 minuti primi ([34]) in precipitati distanti tra loro 300 Å circa: il coefficiente di diffusione dell'N a 20 °C vale ([34]) $4.8 \cdot 10^{-17}$ cm^2 sec^{-1}. Non esistono valutazioni precise del tempo di precipitazione dell'idrogeno nel ferro ma dall'esperienza di alcuni autori ([20,22]) si può ritenere compreso tra uno e sessanta primi. Poichè il coefficiente di diffusione dell'H a 20 °C vale circa $2.5 \cdot 10^{-9}$ cm^2 s^{-1} ([3]), se si ammette, ipotesi ragionevole, che in ambedue i casi valga la (4) con valori di n non troppo diversi e ricordando la (3) si può, per confronto con l'azoto, ricavare il valore incognito L della distanza dei precipitati dell'idrogeno nel ferro. Eseguendo i calcoli, assumendo come tempo di precipitazione dell'idrogeno il valore medio di 10 minuti primi, si ottiene per L un valore di $2 \cdot 10^{-3}$ cm. Da alcune micrografie di DUFLOT ([24]) e da altre osservazioni da noi eseguite si ottiene una distanza media dei precipitati dell'ordine di $10 \cdot 10^{-3}$ cm con buon accordo tra valore calcolato e valore osservato.

Si può pertanto concludere che, nonostante l'elevata velocità di diffusione dell'idrogeno rispetto a quella dell'azoto, i tempi di precipitazione dei due gas sono ancora comparabili perchè il cammino che deve compiere l'idrogeno per trovare un centro di precipitazione è molto maggiore di quello che deve compiere l'azoto.

([33]) C. WERT: *Phys. Rev.*, **79**, 601 (1950).
([34]) C. WERT: *Journ. Appl. Phys.*, **20**, 943 (1949).

Questo risultato costituisce un'ulteriore conferma dal fatto che l'idrogeno può precipitare soltanto in cavità relativamente grandi e pertanto meno frequenti, cioè più distanti tra loro, che non le vacanze o le posizioni interstiziali distorte intorno alle dislocazioni.

5. – Conclusione.

Le esperienze eseguite sulle proprietà magnetiche del ferro dolce, caricato con idrogeno per via elettrolitica, in funzione della temperatura di ricottura dimostrano che l'effetto dell'idrogeno equivale a produrre nel ferro dolce una deformazione plastica. Negli acciai o nei materiali incruditi per laminazione a freddo non si osserva alcuna variazione delle proprietà magnetiche per effetto dell'idrogeno. Queste esperienze confermano l'ipotesi che, l'idrogeno, entrato allo stato atomico tenda a precipitare dallo stato interstiziale allo stato molecolare.

Si dimostra inoltre con considerazioni semiquantitative come, quale centro di precipitazione, sia necessaria una microcavità che abbia almeno una dimensione dell'ordine di alcune decine di diametri atomici. Tutti i fatti inerenti alle variazioni di proprietà meccaniche e magnetiche nel ferro caricato con idrogeno sono interpretati in modo semiquantitativo come dovuti alla forte pressione che l'idrogeno allo stato molecolare esercita nelle microcavità di GRIFFITH.

Dai dati relativi al coefficiente di diffusione dell'idrogeno nel ferro e da considerazioni suggerite dalla teoria della precipitazione si calcola la distanza dei precipitati: il valore trovato di $2 \cdot 10^{-3}$ cm è in accordo coi dati sperimentali disponibili.

Come si vede tutta questa serie di fatti è interpretabile sotto la sola ipotesi che l'idrogeno non si combini chimicamente con il ferro, ma precipiti allo stato molecolare in microcavità preesistenti nei singoli grani ed aventi almeno una dimensione dell'ordine di grandezza di alcune decine di diametri atomici.

SUMMARY

An interpretation of variations of mechanical and magnetic properties due to hydrogen in iron is given. The gas contained in the metal in solid solution tends to precipitate as diatomic molecules in elliptical cavities of a length of the order of at least several tens atomic diametres thus giving rise to a strong pressure in the cavities themselves.

This pressure can produce delayed breakage in the case of harder metals under an applied stress, and in case of softer materials, the formation of blisters often visible by eye. These blisters are accompanied by rather large plastic slip which, as to magnetic properties, mainly increases the coercitive force. The magnetic properties of hydrogen chargen iron and cold worked specimens of the same material are compared. In both cases the same behavior of coercitive field versus annealing temperature has been found. Therefore the assumptions made receive further evidence. Moreover the average distance among hydrogen precipitation centres in iron is evaluated from the precipitation theory. The values obtained ranging about $2 \cdot 10^{-3}$ cm are in agreement with the available experimental data.

An Observed Cosmic-Ray Flux of Light Elements at 41° N. Geomagnetic Latitude.

J. H. Noon, A. J. Herz and B. J. O'Brien

The F.B.S. Falkiner Nuclear Research and Adolph Basser Computing Laboratories, School of Physics (*), The University of Sydney - Sydney, N.S.W., Australia

(ricevuto il 27 Novembre 1956)

Summary. — The relative abundances of the different charge groups of heavy cosmic-ray nuclei under less than 12 g/cm² of atmosphere and packing, were measured in a stripped-emulsion stack flown at geomagnetic latitude 41° N. A minimum potential range of 4.5 cm in emulsion was required for the acceptance of any track. Identification was based on measurements of δ-ray density. Charge calibration was obtained from grain counts and gap-length measurements on identified protons and deuterons coming to rest in the emulsion. The flux of beryllium and boron was found to be comparable with that of carbon, nitrogen and oxygen nuclei.

1. – Introduction.

A number of experiments with nuclear emulsions ([1-6]) and with ionization chambers, counters and cloud chambers ([7-9]) on the charge distribution of cosmic radiation have given conflicting results on the flux of light-element

(*) Also supported by the Nuclear Research Foundation within the University of Sydney.

([1]) H. L. Bradt and B. Peters: *Phys. Rev.*, **80**, 943 (1950).
([2]) A. D. Dainton, P. H. Fowler and D. W. Kent: *Phil. Mag.*, **43**, 729 (1952).
([3]) K. Gottstein: *Phil. Mag.*, **45**, 347 (1954).
([4]) M. F. Kaplon, J. H. Noon and G. W. Racette: *Phys. Rev.*, **96**, 1408 (1954).
([5]) B. Peters: *Proc. Ind. Acad. Sci.*, A **40**, 230 (1954).
([6]) H. Fay: *Zeits. Naturfor.*, **10***a*, 572 (1955).
([7]) J. A. Van Allen: *Phys. Rev.*, **84**, 791 (1951).
([8]) T. H. Stix: *Phys. Rev.*, **95**, 782 (1954).
([9]) J. Linsley: *Phys. Rev.*, **101**, 826 (1956).

nuclei ($3 \leqslant Z \leqslant 5$), although there is substantial agreement on the magnitude of the medium-element flux ($6 \leqslant Z \leqslant 10$). The early experiments with nuclear emulsions [1-4] performed at relativistic latitudes can be criticized on the grounds that as glass-backed emulsions were used, and identification in these experiments was not possible without tracing tracks from plate to plate for some minimum range, the difficulties of tracing result in a bias against the acceptance of light elements. Experiments at non-relativistic latitudes[2-4] were based on identification by scattering measurements. In these experiments, most tracks accepted were of sufficient length in one plate for identification. Thus tracing was not essential and there was no bias against the acceptance of light elements. However, it has been suggested [10] that the scattering technique leads to an underestimate of momentum in the high-energy region, and thus to an underestimate of charge on multiply-charged particles. Although the energy spectrum derived from such scattering measurements [2] is indeed in disagreement with other work [11], it has not been established that serious distortion of the charge spectrum does result from the scattering method of identification.

An additional uncertainty in estimating the flux of primary nuclei at the top of the atmosphere is the correction necessary for fragmentations occurring in the atmosphere and packing material [1,3,12]. This feature is common to experiments with emulsions, counters and cloud chambers. Experiments involving balloon-borne or rocket-borne counter systems or cloud chambers give results of low statistical accuracy.

Through the use of a large-area stripped-emulsion stack in the present work, many of the uncertainties involved in most earlier experiments have been eliminated. Since the emulsions were in contact, tracing of all tracks was easily carried out. Since the flight was made at a relativistic latitude, it was not necessary to use the scattering method of identification. And since all the tracks selected were those of nuclei which had traversed less than 12 g/cm^2 of residual atmosphere and packing, only a small correction was required for the effects of fragmentations. The results, in agreement with other recent work [4,6], show that for kinetic energies above about 1.3 GeV/nucleon the abundances of primary L nuclei ($3 \leqslant Z \leqslant 5$) and M nuclei ($6 \leqslant Z \leqslant 10$) are comparable. The abundance of H nuclei ($Z = 1$) obtained by us for the flight altitude is higher than the values given by most other workers [3,6,7,12,13].

([10]) S. Biswas, B. Peters and Rama: *Proc. Ind. Acad. Sci.*, A **41**, 154 (1955).

([11]) M. F. Kaplon, B. Peters, H. L. Reynolds and D. M. Ritson: *Phys. Rev.*, **85**, 295 (1952).

([12]) J. H. Noon and M. F. Kaplon: *Phys. Rev.*, **97**, 769 (1955).

([13]) D. Lal, Yash Pal, M. F. Kaplon and B. Peters: *Phys. Rev.*, **86**, 569 (1952).

2. – Experimental Details.

2·1. – *General.* – The emulsion stack used in this experiment consisted of fifteen sheets of 600 μm Ilford G5 stripped emulsion, size 9 in × 10 in., all in

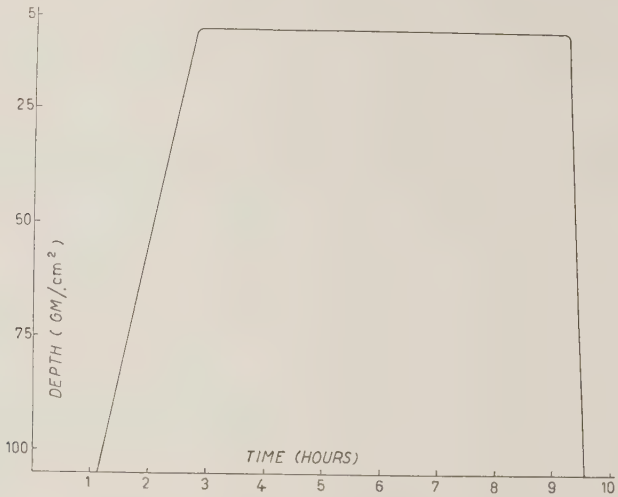

Fig. 1. – Time-altitude curve of balloon flight on February 6th, 1956.

contact. It was flown with vertical orientation of the 9 in. side for around six hours at over 110 000 feet (8.6 g/cm²) at San Angelo (Texas) in February 1956. The flight curve is given in Fig. 1. To the amount of atmosphere above the stack must be added the thickness of the packing material which was 2 g/cm². After the flight the emulsions were mounted on glass and processed with amidol-bisulphite developer (Bristol type) and alcohol drying. The grain density at plateau ionization (g_{pl}) was found to be 8 grains per 100 μm in these plates.

Each plate was cut into fifteen sections 3 in. × 2 in., and these were mounted on perspex frames and aligned using the tracks of heavy nuclei as markers.

2·2. *Scanning Criteria.* – Sections of one outer plate were scanned for tracks satisfying the following criteria:

(1) projected zenith angle $\leqslant 45°$
(2) projected length $\geqslant 2$ mm/plate
(3*a*) grain density $\geqslant 10\, g_{pl}$
(3*b*) grain density $\geqslant 7\, g_{pl}$.

Scanning was done under $\times 100$ magnification for criterion (3*a*), under $\times 250$ magnification for criterion (3*b*).

All such tracks were then traced through the stack. To ensure that any losses due to errors made in applying the criteria were kept to a minimum, a track was accepted for analysis only if its projected angle to the vertical was less than or equal to 30°, and if its length per plate was at least 3 mm. In addition, only those tracks were analyzed which either traversed at least 4.5 cm of emulsion or had this potential range but caused a nuclear disintegration in the emulsion.

Criterion (3*a*) ($g \geqslant 10\, g_{pI}$) was set so that, for tracks satisfying it in the scanning plate, tracing for a distance of 4.5 cm allowed reliable discrimination against background due to slow protons, deuterons, tritons and α-particles. Nearly all such particles have residual ranges less than 4.5 cm of emulsion. The ratio of background tracks to genuine heavy-primary tracks was found to be only of the order of 10%, so that the signal-to-background ratio was extremely satisfactory.

Criterion (3*a*) does, however, exclude a large proportion of relativistic lithium nuclei, and in order to estimate the abundance of these some sections of the scanning plate were also scanned under criterion (3*b*) ($g \geqslant 7\, g_{pI}$). In the region $7\, g_{pI} \leqslant g \leqslant 10\, g_{pI}$, the ratio of confusable background tracks to genuine heavy-primary tracks is of order ten to one so that the need for discrimination against background gives rise to serious problems.

Only 75 cm² were scanned under criterion (3*b*), whereas an area of 231.4 cm² was scanned under criterion (3*a*). Slow singly-charged particles of grain density $7\, g_{pI}$ will change in grain density by more than 50% when traversing 4.5 cm of emulsion, but an α particle of this grain density will only show a grain density change of about 15%. Thus, although background tracks due to singly-charged particles can be rejected easily, it is more difficult to distinguish between slow α particles and fast lithium nuclei. Only two tracks on which a total of 1 500 grains were counted and which changed in grain density by less than 10% over a range of 4.5 cm were accepted as being due to relativistic lithium.

2·3. *Delta-Ray Counting.* – Since the cut-off kinetic energy per nucleon of heavy nuclei at 41° N geomagnetic latitude is more than 1.3 GeV/nucleon for angles of incidence less than 30° to the vertical ([14]), all primary heavy nuclei observed at the flight depth (< 12 g/cm²) will be relativistic. Their δ-ray

([14]) R. A. Alpher: *Journ. Geophys. Res.*, **55**, 437 (1950); J. A. Simpson, K. B. Fenton, J. Katzmann and D. C. Rose: *Phys. Rev.*, **102**, 648 (1956).

density should, therefore, vary according to the relation

$$n_\delta(Z) = Z^2 a + b\,, \qquad (\delta\text{-rays per } 100\ \mu\text{m}),$$

where $n_\delta(Z)$ is the observed δ-ray density of a relativistic nucleus of charge Z, a is the true δ-ray density of a relativistic singly-charged particle, and b is the spurious δ-ray density.

The spurious δ-ray density b arises partly from electron tracks randomly distributed throughout the emulsion, and partly from chance configurations of background grains which are interpreted by the observer as δ rays.

The convention adopted for δ-ray counting was the well-known four-grain convention according to which all electron tracks containing four or more grains and apparently originating from the track of the primary are counted. In the present work the δ-ray counting was done by four observers who were standardized against each other by counting standard tracks in several charge regions, and by periodic check counts during the course of the experiment.

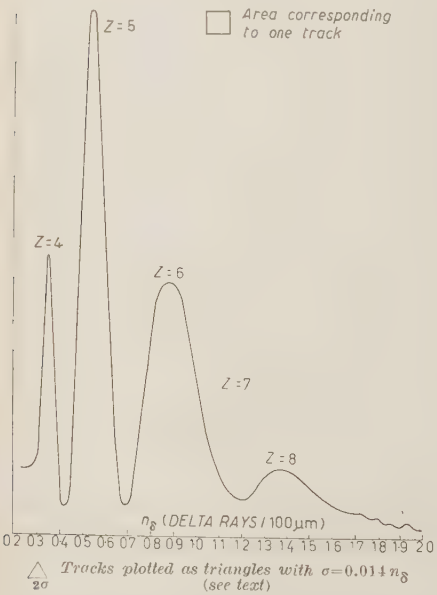

Fig. 2. – Frequency distribution of δ-ray counts (δ rays/100 μm) for tracks with grain density $\geqslant 10\ g_{p1}$.

δ-ray counts were made on 106 tracks which satisfied the scanning and tracing criteria with $g \geqslant 10\, g_{p1}$. A total of fifty δ rays was counted on each track, giving a statistical standard deviation of 14% for each count. Repeat counts to check consistency were made on twenty-six tracks, and in 80% of these repeat counts the largest deviation from the mean of the two counts was less than 14%.

The resolution obtained by the four observers was the same, and their combined results are plotted in Fig. 2. In this figure, each value is plotted as a triangle of unit area with a base width equal to two standard deviations. This type of weighted plotting results in a considerable improvement in the resolution between charges; similar methods have been used by other workers ([15]).

([15]) R. E. DANIELSON, P. S. FREIER, J. E. NAUGLE and E. P. NEY: *Phys. Rev.*, **103**, 1075 (1956).

Because of the low sensitivity of our G5 emulsion, the δ-ray densities for particles of a given charge are quite low. However, it is clear from Fig. 2 that for densities up to about 1 per 100 μm there is practically complete resolution between the peaks corresponding to different charges. This shows that the δ-ray counts were internally consistent, and that, as expected, the background of non-relativistic particles was small.

From the two tracks of relativistic Li nuclei, one of which was 9 cm long in one plate, the δ-ray density for lithium was found to be (0.19 ± 0.03) per 100 μm. δ-ray counts on α particles gave a value of order 0.11, but showed rather wide fluctuations. These values suggest that the spurious δ-ray count b at very low values of Z is about 0.05. The positions of the peaks in Fig. 2 show that the spurious count must be a function of Z. It is not more than 0.1 δ rays per 100 μm at low Z. The highest observed δ-ray density was (13 ± 2) per 100 μm, consistent with that of a relativistic iron nucleus ($Z = 26$) on the basis of the charge calibration as described in Sect. 2·6.

2·4. *Grain Counting.* – For the purpose of assigning scanning criteria, and for the identification of nuclei of very low charge, the grain density g_{pl} corresponding to plateau ionization was determined from an unbiassed sample of π-μ-e decays in the plate in which the scanning was done. The grain density at plateau was found to be 8 grains per 100 μm.

Grain counts were also made on protons which stopped in the emulsion in order to establish the grain densities at residual ranges corresponding to $16\times$ and $25\times$ the plateau value of the restricted rate of energy loss ([16]). These grain densities were about 110 and 125 grains per 100 μm respectively. Sample tracks whose δ-ray densities lay in the intervals 0.25 to 0.45 and 0.45 to 0.65 had grain densities in the ranges 90 to 120 and 115 to 125 so that charges 4 and 5 could be tentatively assigned to tracks within these two intervals of δ-ray density. However, because of the low degree of resolution achieved, these assignments were not sufficiently reliable for calibration purposes.

2·5. *Gap-Length Measurements.* – In order to establish an absolute charge calibration for relativistic nuclei in the range $5 \leqslant Z \leqslant 7$, gap-length measurements were carried out on identified proton and deuteron tracks which ended in the emulsion. Gap-length measurements are much less subjective than grain counts if the tracks are very dense, and good resolution can be obtained from measurements on only 500 μm of track.

([16]) W. H. Barkas and D. M. Young: *Heavy Particle Functions.* Univ. of California Radiation Laboratory Report UCRL-2579 Rev. (Berkeley, Calif.: Univ. of Calif., 1954).

Gap-length measurements were made on ten heavy-primary tracks whose δ-ray densities fell into the range $0.5 < n_\delta < 1.4$. The gap lengths obtained (length of gap per 100 μm of track, from total track lengths of about 500 μm) are plotted against the δ-ray densities in Fig. 3, showing three clusters of

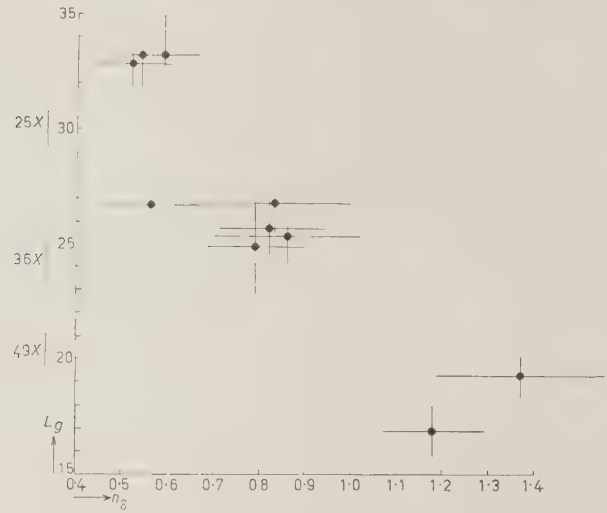

Fig. 3. – Integral gap length I_g (length of gap per 100 μm of track) as function of δ-ray density per 100 μm for ten tracks of heavy primaries. Errors given are statistical standard deviations. On the left of gap-length scale are given the values obtained from calibration tracks at 49×, 36× and 25× plateau ionization.

points. The calibration protons and deuterons were selected in the same areas of the scanning plate, and measurements were made over regions around residual ranges at which the restricted energy-loss rates ([16]) had, respectively, 25, 36 and 49 times the plateau values. As can be seen, the clusters of points due to the heavy-primary tracks correspond to $Z = 5$, 6 and 7, and the standard deviation of the individual points is of the order of one third of the separation between charges Z and $Z + 1$.

2·6. *Charge Calibration.* – Combining the results of grain counting and gap-length measurements with the δ-ray counts displayed in Fig. 2, we now have an absolute charge calibration for δ-ray counts in the range $3 \leqslant Z \leqslant 7$. These charge assignments are shown in Fig. 2. Estimation of higher charges on the basis of δ-ray density can be made using the relation $n_\delta = 0.022Z^2 + 0.1$.

An independent check on the correctness of the calibration comes from the interaction shown in Fig. 4 where a primary nucleus of δ-ray density

← Fig. 4. – Calibration interaction: $B \rightarrow p + \alpha + \alpha$.

(0.57 ± 0.08) per 100 μm breaks up into three closely-collimated fragments one of which has a grain density corresponding to plateau ionization for a singly-charged particle, while the other two have the grain density of relativistic α particles over a range of more than 12 g/cm². No further tracks originating from this interaction were found in a careful search made by four different observers, and the event therefore confirms the assignment $Z = 5$ for δ-ray density 0.54 per 100 μm.

3. – Results.

3·1. *Charge Spectrum at Flight Altitude.* – The charge spectrum obtained is shown in Fig. 5. The value for $Z = 3$, also given in Fig. 5, was obtained from scanning an area of 75 cm² with criterion (3*b*) (see Sect. 2·2). Two Li nuclei were found in this area, indicating that about six Li nuclei should have been present in the area of 231.4 cm² from which the results for $Z \geqslant 4$ were taken. Because of the poor charge resolution in the region $Z \geqslant 7$, the values for $Z \geqslant 7$ are drawn with broken lines, and charges 9 and 10 have been lumped together. A total of 20 tracks of nuclei with $Z > 10$ were also found in the scanning area.

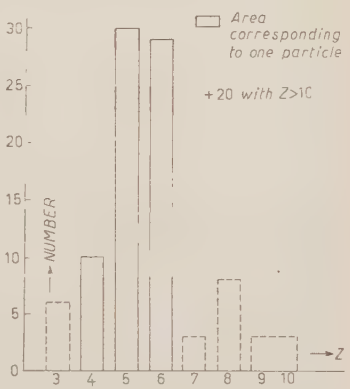

Fig. 5. – Charge distribution. The value for Li is uncertain (see text); charges 9 and 10 have been lumped together.

3·2. *Relative and Absolute Abundances.* – The results on the abundances of the three charge groups are summarized in Table I. The data at flight altitude are the numbers of tracks found in the various charge groups with their r.m.s. errors, except in the case of Li where the number is

normalized to an area of 231.4 cm² and the errors are fiducial limits for the 68% probability level ([17]).

These abundances can be extrapolated to the top of the atmosphere by the use of the diffusion equations given by KAPLON *et al.* ([4]). A correction of order ten percent must also be made for nuclei which entered the stack during the ascent and descent of the balloon. Ionization loss may be neglected

TABLE I.

	$Z = 3$	$Z = 4, 5$	$3 < Z < 5$	$6 < Z < 10$	$Z > 10$
Flight altitude: Numbers found	6^{+8}_{-4} (+)	40 ± 6	46^{+10}_{-7}	46 ± 7	20 ± 4
Relative to M group			1.00	1.00	0.43
At top of atmosphere: Flux (*) with					
$p = 0.45$			3.5	5.5	2.6
$p = 0.23$			4.2	5.5	2.6
Relative to M group					
$p = 0.45$			0.64	1.00	0.47
$p = 0.23$			0.76	1.00	0.47
Relative cosmic abundances ([18])			—	1.00	0.08

(*) Flux is given in particles $m^{-2} s^{-1} sr^{-1}$.
(+) From scanning 75 cm², normalized to 231.4 cm².

since all the heavy nuclei have traversed less than 12 g/cm² before entering the stack. The amount of material above our stack was considerably less than that present in previous nuclear-emulsion experiments and the correction for fragmentation of incident primary nuclei is not very great. Two different values of the average fragmentation probability p, 0.23 and 0.45, are given in the literature ([3,12]), and results obtained with both are given in Table I As will be seen, the difference is within the limits of experimental uncertainty

([17]) V. H. REGENER: *Phys. Rev.*, **84**, 161 (1951).
([18]) H. E. SUESS and H. C. UREY: *Rev. Mod. Phys.*, **28**, 53 (1956).

For comparison we also show in Table I the relative cosmic abundances obtained from astrophysical data ([18]).

3·3. *Interaction Mean Free Paths.* – The observed mean free paths of the different charge groups in emulsion are given in Table II. The values for γ_L and γ_H are in agreement with previous work ([12]). The fact that γ_M appears to be somewhat higher than previously reported is not significant in view of the low statistical weight of the results.

TABLE II. – *Interaction Mean Free Paths in Emulsion* (*in* g/cm²).

$4 \leqslant Z \leqslant 5$	$\lambda_L = \dfrac{906}{11^{+4.4}_{3.3}} = 82^{+36}_{-23}$
$6 \leqslant Z \leqslant 10$	$\lambda_M = \dfrac{1091}{12^{+4.5}_{-3.4}} = 91^{+36}_{-25}$
$Z > 10$	$\lambda_H = \dfrac{354}{9^{+4.1}_{-2.9}} = 39^{+19}_{-12}$

All errors given are fiducial limits for the 68% probability level ([17]).

4. – Discussion and Conclusions.

The present experiment was designed for the purpose of deciding whether an appreciable abundance of light-element nuclei is present in the cosmic radiation or not. No corrections were made for possible scanning and tracing inefficiencies, for such inefficiencies could only increase the relative abundance of L nuclei. The charge resolution achieved in the critical region around $Z = 5$ and $Z = 6$ is very good, and we are certain that the charges assigned to the various δ-ray densities are correct.

The grain-density criteria adopted were such that it is certain that no slow α particles have been included in the light-element group. Any inclusion of slow particles of charge greater than two would have the result that these particles would be classified as having a charge greater than their real charge, thus, for example, boron would be wrongly classed as carbon. Like scanning inefficiencies, therefore, this type of error would lead to an underestimate of the real abundance of L nuclei. We stress this point in view of the recent work ([14,19]) which indicates that cosmic-ray geomagnetic latitudes in the U.S.A. are several degrees higher than previously believed.

([19]) C. J. WADDINGTON: *Nuovo Cimento*, **10**, 930 (1956).

While the absolute flux of M nuclei observed is in agreement with the results of earlier work, the abundance of heavy-element nuclei is somewhat greater than has been reported previously ([3,6,7,12,13]). As most of the earlier work was done under appreciably more than 12 g/cm^2 of material, and the mean free path of H nuclei is only about 18 g/cm^2, the results on their abundance obtained in this work should be rather more reliable than those obtained earlier.

The ratio of the abundances of the light and medium groups of nuclei, extrapolated to the top of the atmosphere, we find to be of the order of 0.7. This figure is not affected very much by the exact values of the fragmentation probabilities, and we are confident that the light-element group is present in the primary cosmic-ray beam with an abundance comparable to that of the medium group. Thus, unless some time variation exists in the primary light-element cosmic-ray flux, previous experimental results giving a low figure for this quantity must be incorrect.

As boron is by far the most abundant member of the light-element group in cosmic rays, and carbon is similarly predominant in the medium-element group, the light-to-medium abundance ratio will be largely determined by the boron-to-carbon ratio. Any error in the charge calibration, resulting in an erroneous classification of some boron nuclei as carbon, or viceversa, can therefore strongly affect the abundance ratio obtained.

As was already pointed out by BRADT and PETERS ([1]), it is not necessary to conclude from the presence of light elements in the primary cosmic radiation that these elements are present in the source region. They can be produced by collisions of heavier elements with interstellar matter. The amount of lithium, beryllium and boron present in the primary radiation entering the earth's atmosphere sets a definite upper limit to the time of travel of cosmic rays in interstellar space. This figure is of the order of a few million years ([4,8]) if the average density of interstellar hydrogen in the galaxy is taken to be 1 atom/cm^3, and no account is taken of the very wide fluctuation in this quantity. However, if one assumes that some fragmentation occurs during the acceleration period, or that light elements are present in the source region, the life time of the cosmic rays will be less than this upper limit.

It is now evident that the detailed charge distribution of the primary cosmic radiation is not the same as that of matter in the universe as obtained from astronomical data ([18]). To relate the charge distribution in any assumed source region to that in the observed cosmic rays requires detailed knowledge of the fragmentation probabilities, and better statistics than have been obtained up to now on the complete charge distribution.

* * *

The team of scanners who have taken part in this work consisted of Mrs. B. CHARTRES, Mrs. I. DOCHERTY, Mrs. M. RABBITT, Mrs. A. THOW, Mrs.

K. WOODGER and Miss M. WOODWARD. The figures and the photomicrograph were prepared by Miss S. A. O'REILLY. Our thanks are due to the U. S. Office of Naval Research who arranged the balloon exposure, and to Professor H. MESSEL and the Nuclear Research Foundation within the University of Sydney for the excellent facilities put at our disposal. One of us (B. J. O'B.) is indebted to the Research Committee of the University of Sydney for a Research Studentship.

RIASSUNTO (*)

In un pacco di emulsioni nude esposto alla latitudine geomagnetica di 41° N si sono misurate le abbondanze relative dei differenti gruppi di carica sotto meno di 12 g/cm² di atmosfera e copertura. Per l'accettazione delle tracce fu richiesto un percorso potenziale minimo di 4.5 cm in emulsione. L'identificazione fu basata sulle misure di densità dei raggi δ. La misura delle cariche fu eseguita col conteggio dei granuli e la misura dei gas su protoni identificati e deutoni arrestati nell'emulsione. Si è trovato che il flusso dei nuclei di berillio e di boro è confrontabile con quello dei nuclei di carbonio, azoto ed ossigeno.

(*) *Traduzione a cura della Redazione.*

IL NUOVO CIMENTO Vol. V, N. 4 1° Aprile 1957

Separability of a Covariant Wave Equation.

H. S. Green

University of Adelaide - Australia

(ricevuto il 4 Dicembre 1956)

Summary. — Separable solutions are obtained of a covariant wave equation proposed by Wick, who conjectured that such solutions do not exist. The solutions are in a simpler form and more easily obtained than those obtained by Wick and Cutkosky, whose conclusions on the energy spectrum are, however, confirmed. The separability of the covariant wave equation is shown to be connected with the existence of a constant of motion which does not appear in non-relativistic approximation, but is analogous to the « strangeness » or dionic quantum number which has already been proposed.

1. – Introduction.

A modification of the Salpeter-Bethe equation (1), which describes the interaction of two fermions, has been proposed by Wick (2). The spin of the fermions is neglected, so that all propagators appearing in the equation are for bosons. The resulting equation may be regarded as an approximation to the original S-B equation, or as describing, for instance, the electromagnetic interaction of two π-mesons (*). It might also be expected to throw light on some of the special properties of covariant wave equations which are lost in non-relativistic approximation. Wick and Cutkosky (3) have found exact

(*) It has been shown by Dr. S. N. Biswas that, for a special choice of the arbitrary parameter in the renormalization of scalar or pseudo-scalar meson theory, the nuclear interaction of two π-mesons is, at short distances, of the same type.

(1) E. E. Salpeter and H. A. Bethe: *Phys. Rev.*, **84**, 350 (1951).

(2) G. C. Wick: *Phys. Rev.*, **96**, 1124 (1954).

(3) R. E. Cutkosky: *Phys. Rev.*, **96**, 1135 (1954).

solutions of Wick's equation, when the mass of the interaction particle is either zero or can be neglected. But the solutions which they obtained were of a non-separable type, expressed as definite integrals involving Heun's functions, integrals whose properties are not easily discernible and have already been the source of some confusion. (See SCARF [4]; GEFFEN and SCARF [5]; CUTKOSKY and WICK [6]).

The import of this note is to point out that, contrary to Wick's conjecture, his equation is separable, and that the separable solutions are simpler and much more easily obtained than those deduced by WICK and CUTKOSKY. The conclusions of WICK and CUTKOSKY concerning the spectrum of Wick's equation do not require modification. But the fact that separation is possible has a physical significance, implying the existence of a constant of the motion which does not appear in non-relativistic approximation. It has been shown by GREEN and BISWAS [7] that the original Salpeter-Bethe equation has similar characteristics, and that the new constant has properties similar to the « strangeness » or dionic number (cf. PAIS [8], GOLDHABER [9]), which has been postulated to explain properties of hyperons and heavy mesons.

2. – Solution of Wick's equation.

Two bosons of masses m_1 and m_2 will be considered, interacting *via* a field of electromagnetic type. Adopting a metric with $g_{44}=1$ and $g_{11}=g_{22}=g_{33}=-1$, Wick's equation may be written

$$\{(p_4+E_1)^2-\boldsymbol{p}^2-m_1^2\}\{(p_4-E_2)^2-\boldsymbol{p}^2-m_2^2\}\Phi(p)=\Psi(p)\,, \tag{1}$$

where $p=(\boldsymbol{p}, p_4)$ is the relative momentum 4-vector, $E_1+E_2=2E$ is the total energy of the system in the centre of mass frame, and

$$\Psi(p)=i\pi^{-2}\lambda\int\{(p-k)^2-i\varepsilon\}^{-1}\Phi(k)\,\mathrm{d}^4k \tag{2}$$

where the limit $\varepsilon\to+0$ is intended.

The difference E_1-E_2 can be chosen at will, and is conveniently fixed

(4) F. L. SCARF: *Phys. Rev.*, **100**, 912 (1955).
(5) D. A. GEFFEN and F. L. SCARF: *Phys. Rev.*, **101**, 1829 (1956).
(6) R. E. CUTKOSKY and G. C. WICK: *Phys. Rev.*, **101**, 1830 (1956).
(7) H. S., GREEN and S. N. BISWAS: *Phys, Rev.*, in press.; also *Nuclear Phys.*, **2**, 177 (1956).
(8) A. PAIS: *Proc. Nat. Acad. Sci.*, **40**, 835 (1954).
(9) M. GOLDHABER: *Phys. Rev.*, **101**, 433 (1956).

by taking

$$2E(E_1 - E_2) = m_1^2 - m_2^2 . \tag{3}$$

From (2) it follows (see GREEN [10]) that

$$\Box\Psi = \frac{\partial^2\Psi}{\partial p_4^2} - \frac{\partial^2\Psi}{\partial \boldsymbol{p}^2} = 4\lambda\Phi . \tag{4}$$

This differential form of the original integral equation is equivalent to (2) only when supplemented by boundary conditions: $p^2\Psi(p)$ must remain finite for large values of p and $\Psi(p)$ must be finite when $p = 0$.

It will be shown that Wick's equation is separable in the bipolar co-ordinates (cf. MAGNUS and OBERHETTINGER [11], p. 153) defined by $p_1 = p_s \sin\theta\cos\varphi$, $p_2 = p_s \sin\theta\sin\varphi$, $p_3 = p_s\cos\theta$,

$$p_4 = \frac{c\sin\alpha}{\cos\alpha - \cos\beta} , \quad p_s = \frac{c\sin\beta}{\cos\alpha - \cos\beta} \tag{5}$$

where

$$c^2 = m_1^2 - E_1^2 = m_2^2 - E_2^2 . \tag{6}$$

The whole of the relative momentum-energy space is contained within various finite ranges of θ, φ, α and β, in particular within the ranges $0 \leqslant \theta \leqslant \pi$, $0 \leqslant \varphi < \pi$, $-\pi < \alpha < \pi$, $0 < \beta \leqslant \pi$. Positive values of p_s are obtained for $\beta > |\alpha|$, and negative values for $\beta < |\alpha|$. Large values of p_s are attained by allowing β to approach zero at a rate proportional to $|\alpha|^{\frac{1}{2}}$; large values of p_4 are attained by allowing $\pi - |\alpha|$ to approach zero at a rate proportional to $(\pi - \beta)^{\frac{1}{2}}$. When $p_4 = 0$, $\alpha = 0$, and when $p_s = 0$, $\beta = \pi$.

In the new co-ordinates, separable solutions exist of the type

$$\Psi = f(\alpha)\, g(\beta)\, Y_{l,m}(\theta, \varphi)/p_s , \tag{7}$$

where $Y_{l,m}$ is a spherical harmonic. For (1) reduces to

$$\frac{4c^2(E_1 \sin\alpha - c\cos\alpha)(E_2\sin\alpha + c\cos\alpha)\Phi}{(\cos\alpha - \cos\beta)^2} = \Psi \tag{8}$$

[10] H. S. GREEN: *Phys. Rev.*, **97**, 540 (1955).

[11] W. MAGNUS and F. OBERHETTINGER: *Special Functions of Mathematical Physics* (Chelsea, New York, 1949).

and (4) to

$$(9)\qquad \frac{(\cos\alpha-\cos\beta)^2}{c^2p_s}\left\{\frac{\partial^2}{\partial\alpha^2}-\frac{\partial^2}{\partial\beta^2}+\frac{l(l+1)}{\sin^2\beta}\right\}(p_s\Psi)=4\lambda\Phi\,,$$

so (7) will satisfy the equations provided

$$(10)\qquad \frac{\mathrm{d}^2f}{\mathrm{d}\alpha^2}+\left\{n^2+\frac{\lambda}{(E_1\sin\alpha-c\cos\alpha)(E_2\sin\alpha+c\cos\alpha)}\right\}f=0$$

and

$$(11)\qquad \frac{\mathrm{d}^2g}{\mathrm{d}\beta^2}+\left\{n^2-\frac{l(l+1)}{\sin^2\beta}\right\}g=0\,.$$

To be certain of the meaning of the boundary conditions in the new coordinates, one can substitute Φ from (9) into (2), which is satisfied provided $f(-\pi)=f(\pi)$, $f'(-\pi)=f'(\pi)$, $g(0)=g(\pi)$, and $f(\alpha)$ and $g(\beta)$ are finite within the ranges $|\alpha|<\pi$ and $\pi>\beta>0$ respectively. The general solution of (11) is

$$(12)\qquad g=g_{n(l)}=\mathrm{const}\times\sin^{l+1}\beta\left(\frac{1}{\sin\beta}\frac{\mathrm{d}}{\mathrm{d}\beta}\right)^l\frac{\sin(n\beta+\delta)}{\sin\beta}\,.$$

If Ψ, given by (7) is to be finite at $\beta=0$, the phase angle δ must vanish, and the condition $g(0)=g(\pi)$ then requires that n should be an integer. For $g\neq 0$ one must have $n\geqslant l+1$. The conditions $f(-\pi)=f(\pi)$ and $f'(-\pi)=f'(\pi)$ mean that only solutions of (10) with period 2π are acceptable.

Equation (10) can be written

$$\frac{\mathrm{d}^2f}{\mathrm{d}\alpha^2}+\left\{n^2+\frac{2\lambda(m_1m_2)^{-1}}{p-\cos(2\alpha+\theta)}\right\}f=0\,,$$

$$p=(m_1m_2)^{-1}(E_1E_2-c^2)\,,$$

$$(13)\qquad \sin\theta=(m_1m_2)^{-1}c(E_1-E_2)\,,\qquad \cos\theta=(m_1m_2)^{-1}(E_1E_2+c^2)\,,$$

which has the form of a generalized Lamé equation, reducible to Heun's equation (see Erdelyi [12]) by the substitution $z=\frac{1}{2}\{1+\cos(2\alpha+\theta)\}$. The eigenvalue problem is determinate when it is required that f should be a periodic function of α.

---

[12] A. Erdelyi: *Quart. Journ. Math.*, **13**, 107 (1942); **15**, 64 (1944).

3. – Significance of Separability.

It has been seen that separable solutions of Wick's equation exist in the form $\rho_s\Psi = f_{E(n)}(\alpha)g_{n(l)}(\beta)P_l^m(\cos\theta)\exp[im\varphi]$. Now the mere possibility of separation has physical implications which deserve to be noticed. The important point is that each factor of a separable solution is the eigenfunction of an operator which commutes with total energy ($2E$) and is therefore a constant of the motion. The fact that $P_l^m(\cos\theta)$ and $\exp[im\varphi]$ are eigenfunctions corresponding to the orbital and azimuthal angular momentum is well known. In the above calculation $f_{E(n)}(\alpha)$ could be regarded as the eigenfunction of the total energy, since the equation which it satisfies determines the eigenvalues of E. The feature of the covariant wave equation which distinguishes it from the corresponding Schrödinger equation is the appearance of a fourth factor $g_{n(l)}(\beta)$ in the separable solutions, which is an eigenfunction of the operator $\mathcal{M}_l$ defined by

$$\mathcal{M}_l^2 = \left\{-\frac{\partial^2}{\partial\beta^2} + \frac{l(l+1)}{\sin^2\beta}\right\} \tag{14}$$

in the special representation which has been adopted. This operator must represent a constant of the motion, and therefore an observable of special physical importance.

It has been noticed by WICK and CUTKOSKY that solutions in non-relativistic approximation correspond to $n = l+1$, the lowest of the admissible eigenvalues; for $n > l+1$, there is no non-relativistic analogue, but an operator N_l^+ exists such that

$$\mathcal{M}_l^+ g_{n(l)} = g_{n(l+1)} \quad \left[\mathcal{M}_l^+ = \frac{\partial}{\partial\beta} - (l+1)\cot\beta\right], \tag{15}$$

so that if $n = l+2$, the operator $\mathcal{M}_l^+$, applied to the eigenfunction, will produce a non-relativistic eigenfunction. The effect of this operator is nearly reversed by the operator $\mathcal{M}_l^-$ satisfying

$$\mathcal{M}_l^-\mathcal{M}_l^+ = \mathcal{M}^2 - (l+1)^2,$$

$$\left[\mathcal{M}_l^- = \frac{\partial}{\partial\beta} + (l+1)\cot\beta\right]. \tag{16}$$

Operators with similar properties are found in the theory of the relativistic

angular momentum tensor (see e.g., BORN and FUCHS ([13])) which was used by PAIS ([8]) to correlate the properties of the « strange » particles. The operator $\mathcal{M}_l^2$ is not exactly constructed from the angular momentum tensor, but from a non-unitary transformation of it.

It seems likely that an additional constant of the motion will appear in the solution of any covariant wave equation for two-particle systems, on account of the additional degree of freedom, afforded by the relative time. This constant of the motion is quantized, and has its minimum eigenvalue in processes which occur at non-relativistic energies. Transitions between states with different eigenvalues are forbidden except in weak (e.g. FERMI - type) interactions. It may well be identical with the « strangeness » number or « dionic » number which has already been postulated to account for properties of hyperons and heavy mesons.

([13]) M. BORN and K. FUCHS: *Proc. Roy. Soc. Edin.*, **60**, 141 (1939).

RIASSUNTO (*)

Si ottengono soluzioni separabili di un'equazione d'onda covariante proposta da WICK che pensava che tali soluzioni non esistessero. Le soluzioni sono di forma più semplice e più facilmente ottenibili di quelle di Wick e Cutkosky le cui conclusioni sullo spettro energetico risultano, tuttavia, confermate. Si dimostra che la separabilità dell'equazione d'onda covariante è connessa all'esistenza di una costante di moto che non compare nell'approssimazione non relativistica ma è analoga alla « stranezza », o numero quantico, che è già stata proposta.

(*) *Traduzione a cura della Redazione.*

IL NUOVO CIMENTO Vol. V, N. 4 1° Aprile 1957

Bilocal Field Theories and their Experimental Tests - II.

J. Rayski

Institute of Theoretical Physics, Nicholas Copernicus University - Toruń
Institute of Physics of the Polish Academy of Sciences - Warsaw

(ricevuto il 4 Dicembre 1956)

Summary. — A theory of heavy particles accounting for the existence and characteristic properties of hyperons and heavy mesons is presented. It offers a qualitative and quantitative explanation of the mass spectra. A physical interpretation of mass, charge, isotopic spin, attribute, and of Gell-Mann's selection rules is proposed.

1. – Field Equations and Mass Spectra.

In the Part I [1] we investigated four alternatives of field equations two of them applying to fermions, and two to bosons: fermion-isofermion (abbreviate notation fif), fermion-isoboson (fib), as well as boson-isofermion (bif), and boson-isoboson (bib). These equations, supplemented by an auxiliary condition, yield formulae for the mass spectra of the respective particle families. In the case of fermions the agreement between the theoretical eigenvalues m_n (in units $c = \hbar = l = 1$, where l is the Compton wave length of the nucleon) and the experimental ratios of the Λ and Ξ masses to the nucleon mass was remarkably good. However, a mass eigenvalue corresponding to the hyperon Σ was lacking. Meanwhile we have found an alternative field equation for fermions-isobosons where the (first non-vanishing) mass eigenvalue m_1 is close to the experimental mass value for Σ. Now we believe, that there are not four but five different alternatives: Three for fermions (denoted in short as fif, fib I and fib II) and two for bosons (denoted in short as bif, and bib).

We assume that the elementary particles are described by means of two

[1] J. Rayski: *Nuovo Cimento*, **4**, 1231 (1956).

sets of variables: the usual position variables x and the « isotopic » variables u forming a manifold of points on a sphere that is embedded in a metrical, euclidean, three-dimensional space. The points in this space are denoted by means of a radius vector $\boldsymbol{u}$. The equation of the sphere representing the particle with mass m is

$$u^2 - l^2 m^2 = 0 \,, \tag{1}$$

where $u = (\boldsymbol{u}\boldsymbol{u})^{\frac{1}{2}}$ and l means a constant with dimension of length. Let us introduce the following notations

$$k_j = -i\frac{\partial}{\partial u_j} \,, \qquad k = \frac{1}{2}\left(\frac{1}{u}\boldsymbol{u}\boldsymbol{k} + \boldsymbol{k}\boldsymbol{u}\frac{1}{u}\right), \qquad \tau = \frac{\boldsymbol{u}\boldsymbol{\tau}}{u} \,, \tag{2}$$

where τ_j are Pauli matrices for the u-space.

A straightforward generalization of the Dirac equation is [2]

$$(\gamma_\mu p_\mu + \tau\boldsymbol{\tau}\boldsymbol{k})\psi = -k\psi \,, \tag{A}$$

where the term to the right has been introduced in order to ensure the compatibility with the auxiliary condition (1). This term may be understood as the effect of the reaction forces brought about by the constraints (1).

A straightforward generalization of the Klein-Gordon equation is [3]

$$(p_\mu p_\mu + \boldsymbol{k}\boldsymbol{k})\psi = kk\psi \,. \tag{B}$$

(A) obviously applies to fermions-isofermions, while (B) to bosons-isobosons. A straightforward generalization for the case of fermions-isobosons is a partly linearized equation of the form [4]

$$(i\gamma_\mu p_\mu + l\boldsymbol{k}\boldsymbol{k})\psi = lkk\psi \,. \tag{C}$$

At the first sight it seems that all possibilities have been already taken into account but there are still two further possibilities as will be seen from the following discussion. The equations (A), (B), (C) are separable and may be

---

[2] A reversed sign of the terms with τ matrices is also possible. But replacing $\tau \to i\tau$ would lead to imaginary masses. The formulae in the Part I are erroneous by a factor i.

[3] A reversed sign of the terms with the k's would lead to imaginary masses.

[4] The other alternative $[lp_\mu p_\mu + i(\boldsymbol{\tau}\boldsymbol{k} - \tau k)]\psi = 0$ (for bosons-isofermions) is ruled out as the eigenvalues of $i(\boldsymbol{\tau}\boldsymbol{k} - \tau k)$ are positive as well as negative whereas $\gamma_\mu p_\mu$ must be negative.

written in the following form

$$(a) \qquad (i\gamma_\mu p_\mu + m)\chi = 0\,, \qquad [i(\tau\tau\boldsymbol{k} - k) - m]\eta = 0\,,$$

$$(b) \qquad (p_\mu p_\mu + m^2)\chi = 0\,, \qquad [\boldsymbol{kk} - kk - m^2)\eta = 0\,,$$

$$(c) \qquad (i\gamma_\mu p_\mu + m)\chi = 0\,, \qquad [l(\boldsymbol{kk} - kk) - m]\eta = 0\,,$$

where χ is merely a function of x_μ, and η is merely a function of $\boldsymbol{u}$. It is immediately seen that we are also allowed to combine the equations (a) and (b) differently

$$(d) \qquad (i\gamma_\mu p_\mu + m)\chi = 0\,, \qquad [\boldsymbol{kk} - kk - m^2]\eta = 0\,,$$

$$(e) \qquad (p_\mu p_\mu + m^2)\chi = 0\,, \qquad [i(\tau\tau\boldsymbol{k} - k) - m]\eta = 0\,.$$

By squaring the first order equations appearing in (d) and (e) the constant m may be eliminated and the equations may be fused again into single (second order) equations [5]. The alternative (d) applies to fermions-isobosons, and (e) to bosons-isofermions. Thus we have two fermion-isoboson alternatives (c) and (d) which will be denoted in short as fib I and fib II.

The second equations in (a)–(e) are nothing else but eigen-equations for the mass parameter. With the aid of the supplementary equation (1) they yield the following mass eigenvalues (computed in the Appendix). For fermions we have from (a), (c), (d) respectively

$$lm_a = \begin{cases} [a + \frac{1}{2}]^{\frac{1}{2}} & \text{(the case fif)} \quad (3') \\ [a(a+1)]^{\frac{1}{2}} & \text{(the case fib I)} \quad (3'') \\ [a(a+1)]^{\frac{1}{2}} & \text{(the case fib II)} \quad (3''') \end{cases}$$

and for bosons we have from (b), (e) respectively

$$lm_a = \begin{cases} [a + \frac{1}{2}]^{\frac{1}{2}} & \text{(the case bif)} \quad (4') \\ [a(a+1)]^{\frac{1}{2}} & \text{(the case bib)} \quad (4'') \end{cases}$$

where $a = 0, 1, \ldots$ for isobosons and $a = \frac{1}{2}, \frac{3}{2}, \ldots$ for isofermions. In this way all possibilities of field equations involving only the first or the second deri-

[5] We rule out the alternative

$$(p_\mu p_\mu + m^2)\chi = 0\,, \qquad [l(\boldsymbol{kk} - kk) - m]\eta = 0\,,$$

since the elimination of m would lead in this case to a fourth order equation.

vatives have been exploited except perhaps some further possibilities taking advantage of the Duffin-Kemmer algebra.

In order to compare the mass spectra with experiment we have to adjust the value of l from the lowest non-vanishing mass term. It appears that we have to use different l-values for fermions and bosons: l_b is about $2 \cdot l_f$. The value l_f is adjusted by assuming that the nucleon is the lowest fermion-isofermion. By taking the arithmetic mean of the proton and the neutron mass we have from (3′)

$$m_{\frac{1}{2}} = l_{(f)}^{-1} = 1\,837.4 \,. \tag{5}$$

Thus, l_f si the Compton wave length of the nucleon. With this l-value we compute from (3′) the remaining values $m_{\frac{3}{2}}$, $m_{\frac{5}{2}}$, ... and with the same l we compute also the m-values from (3″) and (3‴). The lowest mass eigenvalues are given in the table. The values $m_{\frac{3}{2}}$ and $m_{\frac{5}{2}}$ (in the case fif) as well as the values m_1 in the case fib I and m_1 in the case fib II agree remarkably well with the experimental values 2586, 3220, 2327, and 2181.7 for the hyperons Ξ, Y_E, Σ and Λ respectively.

TABLE I.

	Well established						Presumable		
name	π	K	N	Λ	Σ	Ξ	K_1	K_2	Y_E
type	bib	bif	fif	fib II	fib I	fif	bif	bif	fif
a	0	$\frac{1}{2}$	$\frac{1}{2}$	1	1	$\frac{3}{2}$	$\frac{3}{2}$	$\frac{5}{2}$	$\frac{5}{2}$
m_a	0	adjusted		2185	2315	2598	1370	1670	3180
Q/e	$-1, 0, +1$	$-1, 0$	$0, +1$	0	$-1, 0, +1$	$-1, 0$	$-2, -1$	$-3, -2$	$-2, -1$

In order to describe bosons we adjust the value l_b from the lowest non-vanishing mass eigenvalue which is probably identical with the mass of the K-meson. Thus, from (4′) we have

$$m_{\frac{1}{2}} = l_{(b)}^{-1} = 966 \,. \tag{6}$$

The next mass eigenvalues for the boson-isofermion family are

$$m_{\frac{3}{2}} = 1\,370 \,, \qquad m_{\frac{5}{2}} = 1\,670 \,, \quad \ldots \,. \tag{7}$$

From (4″) we see that the lowest mass eigenvalue m_0 in the boson-isoboson family is zero. This value corresponds to the pion whose mass is only a field mass (compare Part I). A vanishing value m_0 appears also in the fib families. In order to prevent a decay of heavy fermions into the light fermions we have to assume that the fib families are restricted by a condition e.g. $\eta(-u) = -\eta(u)$ so that only odd values $a = 1, 3, \ldots$ come into play in the Λ- and Σ-families. If it is so, there exist no hyperons with masses intermediate between 2600 and 3180.

2. – The Charge and the Attribute.

Characterization of heavy particles (including the pion) by means of a number expressing a relation between the charge and the isospin and called attribute (or strangeness) is not unique. The question is whether the choice of NISHIJIMA, GELL-MANN, or SACHS are the most favourable for a subsequent physical interpretation. Since the sum of the attribute a and of the isotopic spin component T_3 determines a physical quantity (the charge), both a and T_3 must be of the same nature. In particular, since T_3 is a projection of the isospin, also the attribute must be interpretable as a projection (of something) upon the third axis in the isospace. But the attribute defined by previous authors seems to have no connection whatsoever with the iso-character of the particles. This is surely unsatisfactory. A more intelligible scheme is obtained by changing slightly the definition of a

$$Q = -e(a + T_3 - M)\,, \tag{8}$$

where Q is the charge, e is the absolute value of the elementary charge, and M is $+1$ for a fermion, -1 for its antiparticle, and 0 for a boson. With this definition the attribute is integer for isobosons, and half-integer for isofermions which establishes a connection of a with the iso-character of particles.

With the aid of (8) we may attach uniquely the values a to the best known particles according to their charge multiplets. These values are given in the table. Except for the pion whose $a = 0$, the attributes of all particles are positive and ascend monotonously with the mass. The attributes of all antiparticles are negative (the absolute values $|a|$ are equal for each particle and its antiparticle. $K^{0,+}$ is an antiparticle of $K^{0,-}$).

The rule of Gell-Mann holds in the following form:

1) Interactions are strong for $\Delta a = 0$.

2) Interactions are weak for $|\Delta a| = \frac{1}{2}$.

3) Interactions are still weaker for $|\Delta a| > \frac{1}{2}$.

By comparing the results of Sect. **1** and **2** we notice the following striking fact: the number a labelling the mass eigenvalues m_a coincides with the attribute defined by (8). It is hard to believe that the above described regularities and coincidences are accidental. The probability of an accidental coincidence of the three theoretical mass eigenvalues 2185, 2315, 2598 with the experimental masses (2181.7; 2327; 2586) is less than 1/2000. Moreover, their iso-character (isofermion or isoboson) is also predicted correctly: we found that N, Ξ and K must be isofermions but Λ, Σ and π must be isobosons. Finally, there is a remarkable coincidence of the attribute a defined by means of (8) with the quantum number a characterizing the mass eigenvalues. A simultaneous accidental coincidence of all these facts is very improbable. We estimate the probability of such an accidental coincidence to be less than 10^{-6}.

3. – A Formalistic Interpretation.

The most straightforward but formalistic and, as it seems, superficial interpretation of our field equations and their connection with the notion of attribute and charge may be summarized as follows:,

1) There exists an euclidean, three-dimensional space (isospace) having nothing to do with the usual space.

2) Particles are represented by rotators in this space.

3) In addition to an orbital angular momentum (of the rotator) the particle can possess also a spin in this space. This spin manifests itself in experiment as the isotopic spin (isospin). Both, the isospin and the orbital angular momentum combine into the total angular momentum in the isospace.

4) Mass and charge are manifestations of the rotational motion of the particle in the isospace.

5) There is a privileged direction in the isospace. The axes of all particles (rotators) are parallel to this direction.

In order to have a clear (anschaulich) picture of the details let us think as if all particles were bosons-isobosons. With this simplification we may say that the square of the mass is nothing else but the absolute value of the orbital angular momentum in the isospace (in the units $c = \hbar = l = 1$). The postulate 5) means that there exists a system of co-ordinates u_1, u_2, u_3 such that the state of each rotator is given by a sectorial spherical harmonic, i.e. one with equal upper and lower indices Y_n^n. Thus, the same index $a = n$ denotes both, the square of the orbital angular momentum $n(n+1)$ and its projection

n upon the priviledged direction. There follows from (8) a clear physical meaning of the attribute and the charge of bosons-isobosons: the attribute is simply a projection of the orbital angular momentum, whereas the charge is a projection of the total angular momentum upon the priviledged axis. Since all rotators point in the same direction, there is an algebraic additivity of both, charge and attribute. The law of charge conservation is nothing else but the law of conservation of (the projection of) the total angular momentum. Gell-Mann's rule means that the interactions are strong if the projection of the orbital angular momentum is conserved $\Delta n = 0$. But it is not an absolute selection rule. Transitions which do not conserve the orbital angular momentum are also possible but their probability is small (6).

The above assumptions providing a simple interpretation of mass, charge, and attribute are attractive but, at the same time, they constitute a source for new problems as to the nature of the isospace itself. In particular, the assumption 5) was introduced *ad hoc* in order to secure an additive character of charge and attribute and seems very artificial. Therefore we shall try to abandon this assumption and admit that:

5) The axes of the rotators are distributed at random. At the same time we secure the additivity of charge and attribute by assuming that:

6) The particles interact only if their axes are parallel to each other.

At first sight this assumption seems strange but it is very similar to the assumption of a local (contact) interaction. The assumption of a contact interaction may be stated as follows. Let us introduce for each point-particle its « proper » system of reference with the origin at the point occupied by the particle. The interaction between two or more particles is local if they do not interact unless the origins of their proper systems of reference coincide. Now, when the particles are represented by rotators (in isospace), we may introduce for each of them its « proper » system of reference. In this case the system will be called « proper » if the state of the particle is given (in it) by a sectorial spherical harmonic Y_n^n. Our new assumption 6) means that the particles do not interact unless their proper systems of reference coincide. Thus, our assumption is a very natural extension of the assumption of a local interaction for the case where the particles possess an extension and an axial symmetry. In this way the strange assumption of a priviledged direction in

(6) *Note added in proofs*: In order to secure a commutability of mass with the projection of isospin it seems necessary to reformulate the formalism and define the square of the mass M^2 as a function of the total (instead of the orbital) momentum. Then M^2 commutes with the radial component of isospin, and the attribute is a maximal projection of the total angular momentum. T_3 is to be reinterpreted as $T_4 \quad (1/\mu)\boldsymbol{uT}$.

the isospace has been circumvented. There is no priviledged direction in the isospace itself but there is a priviledged direction in the particles. The algebraic additivity is secured by means of a generalized postulate of a « contact interaction ».

4. – An Attempt of Eliminating the Concept of Isospace.

The next problem is whether the isospace itself is to be regarded as a primary concept or whether it may be reduced to more familiar concepts. We notice that the isospace is quite similar to the ordinary space and that our field equations are distinguished by a remarkable symmetry of the roles played by the x-variables and the u-variables. Therefore, there must exist an intimate relation between the two spaces. This relation is to be clarified.

It will be suggestive to assume that there exists no autonomous isospace. Instead, the particle is to be regarded no more as a point but as a body with an internal structure, whereby the u-variables should describe its internal degrees of freedom in the ordinary space. A stumbling block is that (i) the formalism suggests the particle to be a rotator but (ii) it cannot be a rotator in the usual space since it would contribute to the usual spin instead of the isospin (obviously both spins must be independent). This seems to be an unsoluble dilemma, and yet, there exists a very simple way out of it.

If there exists a rotational motion of the particle in the usual space which does not contribute to the usual spin, the particle cannot be represented by a single rotator but, instead, by a pair of rotators rotating in an opposite sense so that their resultant angular momentum is zero. Such a pair of rotators will be called isotor. A particle whose model is the isotor will be called isoparticle.

The isotor possesses a privileged axis (axis of rotation) and two internal degrees of freedom since an infinitesimal change of the position of one of the rotators determines a corresponding change of the position of the other rotator. The two degrees of freedom may be identified with (the two independent of) the u-variables. With this interpretation the « rotations in isospace » are nothing else but relative rotations of one of the rotators against the other.

The above described intrinsic rotations of the isotor form a group isomorphic with the group of (ordinary) rotations in three dimensions. The field quantity describing the isoparticle is, in general, endowed with a suffix which means a set of field quantities spanning a representation of the group of rotations. According to the order of this (irreducible) representation the particle possesses a corresponding isospin. The isospin is to be distinguished from the total angular iso-momentum which is composed of both, the isospin and the orbital angular iso-momentum. In this way we get a physical interpretation

of the isospin as well as of the rest mass, of the attribute, and of the charge within the framework of the usual space. This interpretation may be summarized as follows:

1) The isoparticle is a body with an internal structure called isotor. It is capable of an internal rotation which does not contribute to the usual angular momentum (the resultant angular momentum of the constituents of the isotor vanishes).

2) Rest mass, charge, attribute, and isospin are different manifestations of this internal motion.

3) Two or more isoparticles interact with each other only if their isotors are oriented in the same direction.

Such interpretation, avoiding a mystical conception of an isospace, constitutes (at least in the case of bosons-isobosons) a really « anschaulich » explanation of the conceptions of mass and charge, hitherto regarded as primary. At the same time it provides a justification for the necessity of suitable generalizations of the traditional Dirac and Klein-Gordon equations. Indeed, all degrees of freedom (all generalized co-ordinates and momenta) of the particle have to be treated on the same footing.

But still, the conception of isotor may be regarded as quite artificial. To meet this objection I should like to present some arguments in favour of this new idea.

5. – Speculations About Elementarity.

First of all we should like to point out that an isotoric motion (or something similar to the isotoric motion) appears even in the traditional theory of elementary particles. To see this let us consider the pion. According to the current theories the pion is actually a « dressed » particle to be distinguished from the fictitious point-particle, the « naked » pion which plays only a subsidiary role. The state of the « dressed » pion is a superposition of the state of the « naked » pion and of a cloud of nucleon pairs. Since the total angular momentum of the pion (at rest) is zero, the spins and the orbital angular momenta of the virtual nucleons must compensate exactly. Thus, the cloud of virtual nucleons actually possesses a property assumed for the isotor: there exists undoubtedly an intrinsic rotation (of the constituents forming the cloud) which does not contribute to the total angular momentum of the entity — the dressed particle.

The agreement with experiment achieved by our formalism may be understood in the following way: the dressed particle is a complicated cluster with

properties very different from those of a material point (but reminding rather of a small non-rigid body). Our formalism means a (fortunate) simplification of the (very complicated) properties of the cluster-particles and is to be regarded as a schematic picture of the particles including the main effects of their self-action.

But it is also possible to believe that the effects accounted for by our formalism are not secondary but primary and that the formalism does not mean an idealization of secondary, complicated effects (of the interactions) but describes some truly elementary properties of elementary particles (7). If the latter alternative is true, the isotor has to be regarded as a primary, fundamental conception.

The traditional theory investigated exclusively the point model of elementary particles. This was supported by a conviction that only the point model is compatible with the notion of elementarity. This traditional viewpoint seems to be too narrow and the notion of elementarity is to be refined. It is conceivable that the elementary particle (instead of being a material point) is an object (body) with an extension and with a structure, provided its structure is of an elementary character. In order to find a criterion for the elementarity of a structure let us consider the motion of a body from a general point of view. It will be natural to classify the motions with respect to the group of space-transformations. From this point of view we may classify the motions of a body into 1) these which are equivalent to a translation of the system of reference (connected with the macroscopic observer), 2) these which are equivalent to a rotation of this system of reference, and 3) those which cannot be compensated neither by a translation nor by a rotation of this system of reference. These last are general motions of a non-rigid body. In order to be quite general we should accept that the particle is able to perform (observable) motions of the three above mentioned types (i.e. that it is an anisotropic, non-rigid body). But it should be also elementary. In order to be elementary it should possess the simplest structure necessary and sufficient for the execution of the above mentioned motions. The simplest structure necessary and sufficient for a translational motion is the point. The simplest structure necessary and sufficient for a purely rotational motion is a rotator (with a fixed point). The simplest structure for both, translational and rotational motions is a rotator without a fixed point (i.e. a composition of a free point and of a rotator « fixed » to this point). Similarly, the simplest structure for a purely internal (non-rigid) motion is the isotor. The simplest structure

(7) The self-effects of interactions exist too but we believe that they are comparatively weak and may be « absorbed » by means of a charge renormalization and a renormalization of the constant l (which replaces the traditional mass renormalization except for the case of a vanishing mechanical mass.)

able to perform motions of any type will be a composition of a point, a rotator, and an isotor. A general model of elementary particle may involve these elementary structure elements. Thus, in general, the field quantity is expected to be a function $\psi(x, r, u)$ where the x-variables denote the position of the « centre » of the particle in space-time, the r-variables are relative variables of the first kind denoting the direction of a rotator, whereas, the u-variables are relative variables of the second kind describing the degrees of freedom of an isotor. The x-variables are influenced in the well known way by translations and rotations, the r-variables are not influenced by translations but are still influenced by rotations. Two independent of the r-degrees of freedom may be expressed in the system of rest (of the centre) and denote a unit vector determining the direction of the rotator in the 3-dimensional space. Finally, the u-variables, denoting the relative position of the two rotators constituting the isotor (in a system of reference with the origin at the centre of the particle) are neither influenced by translations nor by rotations. The displacements of the x-variables contribute to the total momentum as well as to the total angular momentum. The displacements of the r-variables contribute only to the total angular momentum. The displacements of the u-variables neither contribute to the total momentum nor to the total angular momentum. This seems to be a complete list of variables for a general but elementary physical entity.

Such speculations may help to understand why a general model of the elementary particle is not so simple as a material point. By neglecting the r- and u-variables we have the defective traditional theory. By taking account of the r-variables we have a theory of Yukawa that includes automatically the particles with higher spins. By taking account of the u-variables we have the present theory. The x- and r-variables may be called « extrinsic » in contradistinction to the « intrinsic » u-variables. These last are necessary to describe intrinsic properties of particles such as their mass, charge, isospin, and attribute.

6. – Some Rare Events.

We should like to emphasize that, apart from a striking agreement with experiment in the case of well established particles, the above formalism is able to account also for some rare events.

The existence of unusual particles (mesons heavier than the usual K-mesons, or hyperons heavier than the cascade hyperon Ξ) has been suggested several times. Most of these findings appeared to be a statistical fluctuation or an overestimation of the exactitude of the mass measurements, but still some of them give strong support for the real existence of new particles.

An event of FRY *et al.* [8] constitutes an evidence for the existence of either a new meson with a mass not smaller than 1100, or a new hyperon with a mass not smaller than 2900. If it is a meson, it may be our K_1 i.e. a particle of the type bif with $a=\frac{3}{2}$, or a particle of the type bib with $a=1$. If it is a hyperon, it may be our particle of the type fif with $a=\frac{5}{2}$.

The event of EISENBERG [9] constitutes an evidence for the existence of a hyperon with mass 3200 ± 700 with a decay mode $Y_E^- \to K^- + ?^0$ According to the selection rule $|\Delta a| = \frac{1}{2}$ this event may be interpreted as a decay of our hyperon of the type fif (with a $a=\frac{5}{2}$ and $m_a = 3180$) into a neutron ($a=\frac{1}{2}$) and a heavy meson K_1 ($a=\frac{3}{2}$, $m_a = 1370$). Apart from a sufficiently good agreement of the predicted masses with the energy balance in this event, we notice that also the negative sign of the charge is correct.

Finally, we call attention to an event of a particular interest [10] interpreted as a doubly charged particle with a mass close to that of the nucleon ($m = 1960^{+450}_{-270}$). This event fits very well to our K_2 being the lightest particle whose charge cannot be less than two. A search for further examples of this type is very important for a final confirmation of the present theory.

APPENDIX

The supplementary condition (1) shows that $u = |\boldsymbol{u}|$ is a redundant variable. Thus, the solutions η of the mass eigenequations (a)-(c) are homogeneous functions of degree zero $H(u_1 u_2 u_3)$. However, the eigensolutions may be multiplied by an arbitrary constant factor f, or $f(u)$ as u assumes a constant value. It will be particularly convenient to use $f(u) = u^{-1}$, or

$$\eta = \frac{1}{u} H(u_1, u_2, u_3) \tag{A.1}$$

since

$$k u^{-1} = -i \left(\frac{\partial}{\partial u} + \frac{1}{u} \right) u^{-1} = 0 , \tag{A.2}$$

so that, for this class of functions (A.1), we may simply omit the terms involving the k. Thus, the solutions of the mass eigenequation (a) are equivalent to

---

[8] W. F. FRY, J. SCHNEPS and M. S. SWAMI: *Phys. Rev.*, **99**, 1570 (1955).
[9] Y. EISENBERG: *Phys. Rev.*, **96**, 541 (1954).
[10] G. ASCOLI: *Phys. Rev.*, **90**, 1079 (1953).

the solutions of the equation

$$(i\tau\boldsymbol{\tau}\boldsymbol{k} - m)\eta = 0\,, \tag{A.3}$$

and the solutions of (b) or (c) are equivalent to the solutions of the equation

$$[\boldsymbol{k}\boldsymbol{k} - m^2]\eta = 0 \quad \text{or} \quad [l\boldsymbol{k}\boldsymbol{k} - m]\eta = 0 \tag{A.4}$$

if η is of the form (A.1).

Let us investigate the set of solutions of the form

$$\eta_n = \frac{c_{i_1\ldots i_n} u_{i_1} u_{i_2} \ldots u_{i_n}}{u^{n+1}}\,, \tag{A.5}$$

where $i_1 \ldots i_n$ are tensor indices, $i = 1, 2, 3$. In the case (A.3) the $c_{i_1\ldots i_n}$ possess also a spinor index $\varrho = 1, 2$. We assume in the case of isofermions

$$\tau_{i_k} c_{i_1\ldots i_k \ldots} = 0\,, \tag{A.6}$$

which is a condition of irreducibility. In the case of isobosons we assume correspondingly

$$c_{i_1\ldots i_k \ldots i_k \ldots} = 0\,. \tag{A.7}$$

In the isofermion case we have

$$(i\tau\boldsymbol{\tau}\boldsymbol{k} - m)\eta_n = \left(-\tau\tau_j \frac{\partial}{\partial u_j} + m\right)\eta_n = \left[(n+1)\boldsymbol{\tau}\frac{\tau_j u_j}{u^2} + m\right]\eta_n = 0\,, \tag{A.8}$$

where use has been made of (A.6). With the aid of (2) and (1) we have further

$$\left(\frac{n+1}{u}\tau^2 - m\right)\eta_n = 0\,, \qquad [(n+1) - l^2\,|\,m\,|\,m]\eta_n = 0\,. \tag{A.9}$$

Since the eigenvalues of the matrix τ are ± 1 we find

$$m_n = \frac{1}{l}\sqrt{n+1} = \frac{1}{l}(a + \tfrac{1}{2})^{\frac{1}{2}} \tag{A.10}$$

where $a = n + \frac{1}{2}$.

In the case of isobosons we have, with the aid of (A.7)

$$\boldsymbol{k}\boldsymbol{k}\eta_n = \frac{n(n+1)}{u^2}\eta_n\,, \tag{A.11}$$

whence (A.4) yields the eigenvalues $(3'')$ or $(3''')$ with $a = n$.

RIASSUNTO (*)

Si presenta una teoria sulle particelle pesanti che tiene conto dell'esistenza e delle proprietà caratteristiche degli iperoni e dei mesoni pesanti. La teoria offre una spiegazione qualitativa e quantitativa degli spettri di massa. Si propone un'interpretazione fisica della massa, della carica, dello spin isotopico, dell'attributo e delle regole di selezione di Gell-Mann.

(*) *Traduzione a cura della Redazione.*

IL NUOVO CIMENTO Vol. V, N. 4 1° Aprile 1957

Mass Measurements of Particles Stopping in the Emulsion by the Constant Sagitta Method.

B. Judek

Division of Pure Physics, National Research Council - Ottawa, Canada

(ricevuto il 5 Dicembre 1956)

Summary. — Scattering measurements by the Constant Sagitta method, using a scattering scheme based on the Göttingen tables [4], were made on tracks of particles stopping in the emulsion and at least 3 cm long. The following general results were obtained: (i) The mean value of the sagitta, $\bar{D}$, for protons was found to be about 3% in excess of the theoretical value. (ii) The spread of the experimental observations of $\bar{D}$ corresponds quite closely to its expected statistical value calculated on the basis of the $75/\sqrt{N}$ % formula for the standard error. A good resolution for proton and deuteron groups was obtained on the basis of 3 cm and 2 cm track lengths. (iii) The range-energy exponent deduced from the observations on deuteron/proton and triton/proton mass ratios and from the variation of the value of $\bar{D}$ with residual range was found to be in good agreement with the value 0.568 of Fay *et al.* [4] and Vigneron [12]. (iv) No particle corresponding to a 1450 m_e meson suggested by Fowler and Perkins [9] was observed, although the present statistics are not sufficient to exclude definitely the existence of such a particle.

1. Introduction.

The Constant Sagitta method [1-3] of measurement of multiple scattering against the residual range is widely used for the determination of masses of particles stopping in the emulsion. Most of the measurements, however, have

[1] C. Dilworth, S. J. Goldsack and L. Hirschberg: *Nuovo Cimento*, **11**, 113 (1954).

[2] T. Holtebekk, N. Isachsen and S. O. Sörensen: *Phil. Mag.*, **44**, 1037 (1953).

[3] S. Biswas, E. C. George and B. Peters: *Proc. Ind. Acad. Sci.*, **38**, 418 (1953).

been made on comparatively short tracks, with a variety of scattering schemes employed by different authors prior to the appearance of the Göttingen tables [1] and only a few systematic calibration measurements have been reported [5-8].

The present work, whose original purpose was to investigate the existence of a group of mesons of mass of about 1450 m_e (*) which was at one time suggested by FOWLER and PERKINS [9], comprises systematic measurements on particles with masses of the order of proton mass. The tracks selected for measurements were at least 3 cm long and were « flat », each being wholly contained in one emulsion layer (1000 μm thickness). Consequently a higher statistical precision has been attained than in most of the previous work in the same mass region [1-3,5,7,8].

The scattering scheme for protons of the Göttingen tables [1] was essentially adopted. This is based on the values of scattering constants calculated from Molière's theory [10] (taking into account the variation of the scattering constant with velocity of the particle and cell length), and on the range energy relations readjusted on the basis of the up to date experimental data.

2. Experimental Details.

The plates were developed by the temperature cycle method using amidol developer with boric acid. Different degrees of development were obtained by varying the time of the warm stage of development from 10 to 50 minutes. The appearance of steep, heavy tracks indicated that little or no distortion was present.

Tracks were selected from six plates, all from the same batch of Ilford G-5 emulsion, 1000 μm thick, 4 in. × 4 in. in area, flown for 8.5 hours at a height of 102 000 feet (+). Measurements were made by two observers on two Leitz

---

([4]) H. FAY, K. GOTTSTEIN and K. HAIN: *Suppl. Nuovo Cimento*, **11**, 2 (1954).

([5]) M. DI CORATO, D. HIRSCHBERG and B. LOCATELLI: *Suppl. Nuovo Cimento*, **12**, 2, 381 (1954).

([6]) SHIN-ICHI KANEKO: *Journ. Phys. Soc. of Japan*, **10**, 325 (1955).

([7]) A. ORKIN-LECOURTOIS: *Suppl. Nuovo Cimento*, **1**, 3, 222 (1955).

([8]) B. ROEDERER: *Nuovo Cimento*, **10**, 135 (1955).

(*) The method proposed was to obtain a mass spectrum by constant sagitta measurements on particles coming to rest in the emulsion, having a minimum range and hence a pre-determined minimum energy. It should be noted that this method is independent of ionization and so, of any fading of tracks.

([9]) P. H. FOWLER and D. H. PERKINS: *Suppl. Nuovo Cimento*, **12**, 236 (1954).

([10]) K. GOTTSTEIN, M. G. K. MENON, J. H. MULVEY, C. O'CEALLAIGH and O. ROCHAT: *Phil. Mag.*, **42**, 708 (1951).

(+) We are indebted to the Office of Naval Research for making this exposure possible in a Minnesota balloon flight.

Ortholux microscopes specially adapted for scattering measurements. The Leitz Ks 100× apochromatic oil immersion objective, and later on the Koritska 100 · fluorite oil immersion objective (on account of its greater working distance which covered the whole thickness of the 1000 μm emulsion) were used in conjunction with the Leitz 12.5× micrometer eyepieces.

The scattering scheme employed for measurements is given in Appendix I, and is based on Table VI of the Göttingen tables ([4]) which gives for protons the nominal value of the mean sagitta ($\bar{D}$) of 0.5 μm (about 4× the noise level on our microscopes) extended to cover ranges up to 3 cm. It was modified in such a way that the cell length was increased in steps of 5 μm instead of 1 μm as in the original scheme. This modification helped to speed up the measurements considerably especially with the type of micrometer screw used for controlling the stage movement of the microscope, while any errors introduced in this way were found negligible except possibly at the end of the track where comparatively short cells are used and varied more frequently and the alignment of the track is not likely to be as good as over the straighter portions. It was estimated in the way indicated in Appendix II that the errors due to these causes would amount to about 2% for the first 35 cells but their effect averaged over the whole length of the track would not exceed 0.5%.

Because of the comparatively high grain density of the tracks it was possible to make each eyepiece micrometer setting averaged over a few grains within 1 to 3 μm along the track. Since this is only as mall fraction of even the shortest (15 μm) cell used one can say that the settings were essentially made at a point and the 0.96 smoothing ([11]) correction which some authors ([3,6]) introduce into their calculations of the scattering schemes need not be applied here.

The tracks were realigned whenever their inclination to the direction of stage motion exceeded 3/100 radians. A good alignment is important in this work since, as is shown in Appendix II, the effect of apparent scattering occurring at sudden changes of the cell length varies with the square of alignment.

No correction for steepness was considered necessary since only « flat » tracks were selected for measurements.

The usual $4x$ cut-off procedure was applied to the observations. The noise level correction was determined by the usual method of elimination, from measurements at full and half cell lengths of the scheme. In calculations account was taken of the difference in the values of the scattering constants for full and half cell lengths, while the noise level itself was assumed to remain constant. The resultant value obtained from measurements on 7 proton,

([11]) Y. Goldschmidt-Clermont, D. T. King, H. Muirhead and D. M. Ritson: *Proc. Phys. Soc.* (*London*), **61**, 183 (1948).

3 deuteron, and one triton tracks was $(.132 \pm .005)$ μm. No significant variation of the noise level with residual range (or cell length) was detected, and neither did it differ significantly for proton, deuteron or triton tracks. Details of the calculation are shown in Appendix III. For comparison the noise level was also determined by a direct application of the scheme to a relativistic alpha track aligned with a 3 100 slope. This yielded a value of $(.140 \pm .006)$ μm which is considered in satisfactory agreement with the first determination. The value of .132 μm was accepted for correction of all the measurements on one microscope, while the value of .115 μm was found for the other microscope.

3. Results.

3·1. *The estimation of the values of* $\bar{D}$. – Altogether 16 tracks were measured. The distributions of the mean values of $\bar{D}$ (corrected for the noise level only) for the individual tracks for 3 cm, 2 cm and one cm of the residual ranges are shown in Figs. 1*a*, 1*b*, and 1*c* respectively. They were tentatively analysed

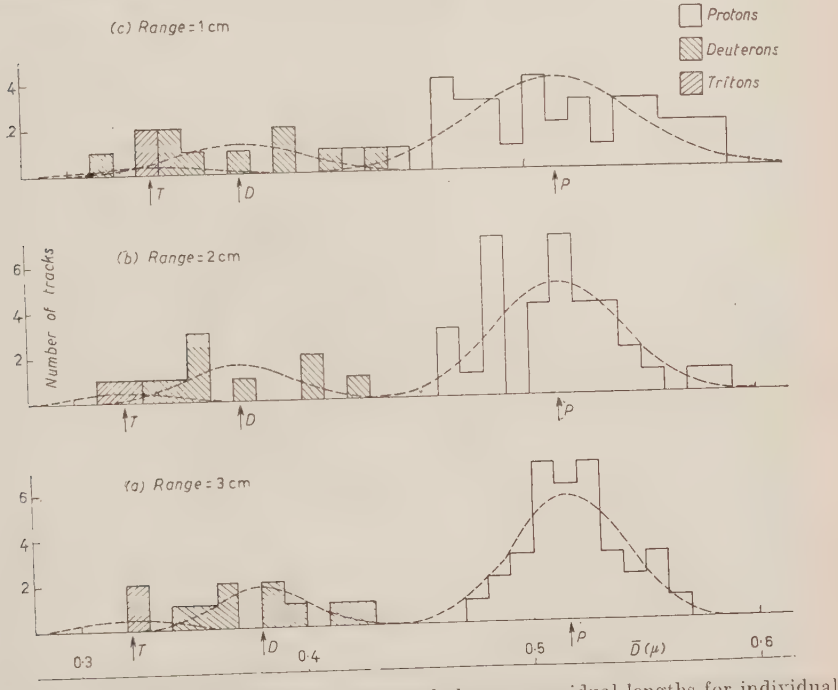

Fig. 1. – Distributions of $\bar{D}$ for one, two and three cm residual lengths for individual tracks measured. Arrow indicate mean values of $\bar{D}$ for each individual group.

into groups of 35 protons, 9 deuterons and 2 tritons. It can be seen that a good resolution for protons and deuterons has been obtained with 3 cm and even 2 cm tracks while with track length of 1 cm they tend to overlap. The dotted curves indicate the Gaussian distributions centred about the mean values of $\bar{D}$ for each group and with widths corresponding to the expected spreads calculated on the basis of the $.75/\sqrt{N}$ formula (with correction for the effect of the noise level). The comparison between the theoretical and experimental spreads of observations (from the usual calculation of the standard deviation) showed excellent agreement for the 3 cm and 2 cm proton tracks, while the experimental values were 20-40 % higher than the theoretical values for the one cm and deuteron tracks, but still much lower than in most of the results reported by other workers ([5,7,8]).

The mean value of $\bar{D}$ (corrected for noise level) for the proton group is $(.516 \pm .004)$ μm which is about 3 % higher than the expected values of .500 μm. This difference lies outside the estimated statistical error but it is too small to be certain of any definite disagreement, at least at this stage. It is quite possible that some of the quantities used in the calculation of the scattering scheme require a small correction, but at the same time one cannot exclude the possibility that an accumulation of small measuring errors (distortion, alignment, inaccuracy of the noise determination, etc.), which are difficult to estimate with any accuracy, may be responsible, at least partially, for this discrepancy between experimental and theoretical values. These results are generally in agreement with other workers ([6,8]) who used scattering schemes based on Göttingen tables, and also tend to give high experimental values for $\bar{D}$.

3·2. *Mass distribution.* – The mass distribution derived from the values of $\bar{D}$ for 3 cm tracks is shown in Fig. 2. The Gaussian distributions indicated by the dotted curves have widths corresponding to the theoretical statistical spreads of observations. The mean mass value for the proton group (M_0) was assumed as 1837 m_e, and all the other masses were calculated on its basis by the relation:

$$M = M_0 \left(\frac{\bar{D}_0}{\bar{D}}\right)^{\frac{1}{1-n}}, \tag{1}$$

where $\bar{D}_0$ is the mean value of $\bar{D}$ for the proton group, and n is the range-energy exponent whose value was taken here as .568. Equation (1), however, contains the non-relativistic approximation $p\beta = 2E_{\text{Kin}}$, and also no account is taken of the differences in the variation of velocity with residual range for particles of different masses and its effect on the scattering constant K. Since in this work comparatively long tracks were selected for measurement the

appropriate correction for this approximation was estimated as shown in Appendix IV. In fact the correction to the values of K is in the opposite

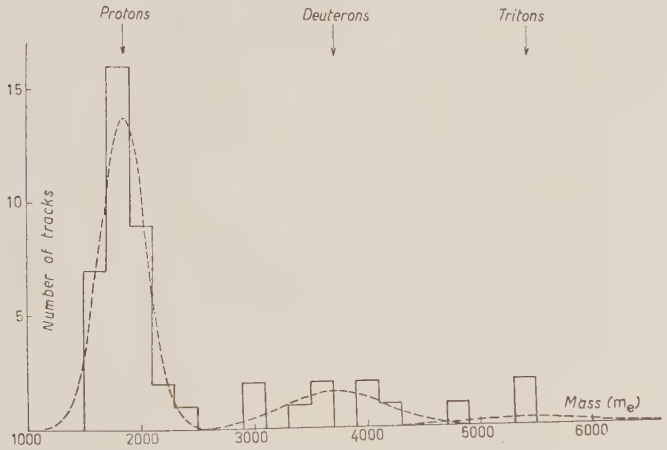

Fig. 2. – Mass distribution.

sense to that for the departure of the value of $p\beta/2E_{\mathrm{Kin}}$ from unity, so that the resultant correction is only of order of .5% for both deuterons and tritons. After application of this correction the experimental values of $\bar{D}$ of (.516 .004) μm for protons, .380 ± .008 μm for deuterons and (.322 ± .012) μm for tritons become .516 μm, .3815 μm and .324 μm respectively, and the mean deuteron/proton and triton/proton mass ratios are found as 2.01 ± .10 and 2.94 ± .30.

No particle with scattering corresponding to a mass $\leqslant 1500\ m_e$ was observed although if a group of mesons of mass of about $1450\ m_e$ and of 8% intensity of the proton group existed, as was originally suggested by Fowler and Perkins [9], one might expect two or three such particles here.

3·3. *Variation of the value of $\bar{D}$ with the residual range.* – Figs 3 (*a*) and (*b*) show the variation of $\bar{D}$ with residual range for the proton and deuteron tracks respectively. The points on the curves were obtained by dividing each track into sections each containing 35 successive second differences and averaging over all the tracks measured. All points are corrected for noise level while an additional small correction, described in Appendix IV, was applied to the points on the deuteron curve. The dotted lines indicate the best lines through the points determined by the « least squares » method. Their slopes were found to be — (.002 ± .004) μm per cm for protons and (0.01 ± .007) μm per cm

residual range for deuterons. Thus one can safely conclude that the value of $\bar{D}$ remains constant within the limits of experimental error, which is also in agreement with the results of other workers. The first points seem to lie rather high on both curves. This might be just a statistical fluctuation or it may be due to higher experimental errors connected with alignments and approximations in the scattering scheme, as indicated in Appendix II.

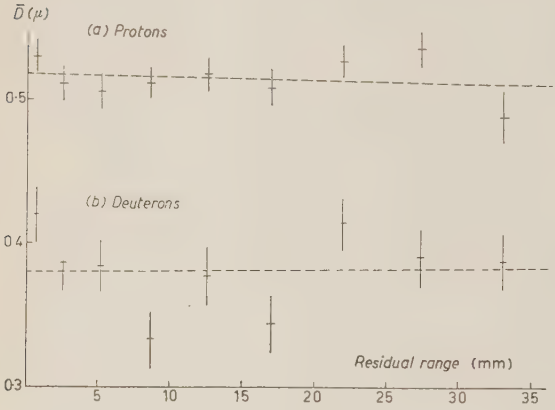

Fig. 3. – Variation of $\bar{D}$ with residual range.

3·4. *The value of the range-energy exponent.* – The best value of the range-energy exponent, n, can be deduced from our observations in two ways: (i) from the mean values of $\bar{D}$ for particles of known masses (i.e. protons, deuterons and tritons) using equation (1): (ii) from the variation of the values of $\bar{D}$ with residual range for protons and deuterons (see Sect. **3·3**) by evaluating by the usual statistical methods the logarithmic slope of the « best » line through the observations.

By the first method the value of $.564 \pm .036$ was obtained from the deuteron proton mass ratio, and $.576 \pm .036$ from the triton/proton mass ratio with a mean of $.570 \pm .026$. The second method has shown that the value of n consistent with our observations does not differ significantly from the accepted value of .568 within the limits of error of $\pm .01$.

These results indicate that our experimental observations are in better agreement with the value n of .568 of FAY *et al.* [4] and VIGNERON [12] than with .581, the value of BRADNER *et al.* [13] or .607 obtained more recently by GLASSER [14].

---

[12] L. VIGNERON: *Journ. de Phys. et Rad.*, **14**, 145 (1953).

[13] H. BRADNER, F. M. SMITH, W. H. BARKAS and A. S. BISHOP: *Phys. Rev.*, **77**, 462 (1950).

[14] R. G. GLASSER: *Phys. Rev.*, **98**, 174 (1955).

* * *

I wish to thank Dr. E. PICKUP for suggesting this investigation and for helpful discussions. I also thank Mr. J. P. BERNIER, a Summer Student in this laboratory, for assisting in the measurements.

APPENDIX I

The Scattering Scheme Employed.

Residual range (μm)	Cell length (μm)	Number of Cells	Residual range (μm)	Cell length (μm)	Number of Cells
40	15	2	5 940	95	10
70	20	3	6 890	100	10
130	25	3	7 890	105	11
205	30	4	9 045	110	11
325	35	5	10 255	115	12
500	40	5	11 635	120	12
700	45	5	13 075	125	12
925	50	6	14 575	130	12
1 225	55	7	16 135	135	12
1 610	60	7	17 755	140	15
2 030	65	7	19 855	145	14
2 485	70	8	21 885	150	14
3 045	75	8	23 985	155	14
3 645	80	9	26 155	160	16
4 365	85	9	28 715	165	15
5 130	90	9	31 190	170	16
5 940			33 910		

APPENDIX II

(i) A difference Δt between the actual cell length used, t, and its exact theoretical value introduces an error in D, given by

$$\Delta D/D = \tfrac{3}{2}\Delta t/t \qquad \text{since} \qquad D \propto t^{\frac{3}{2}},$$

and this averaged over N cells becomes

$$(\Delta D/D)_{\text{Av.}} = (3/2N) \sum \Delta t/t .$$

The quantity $\Delta t/t$ was evaluated for each successive cell of the scattering scheme, and it was found that the resultant error has its largest value of about 1% at the end of the track (for the first 35 second differences), and averages to about .25% for 3 cm of track length.

(ii) A discontinuity Δt between two successive cell lengths introduces an apparent scattering given by

$$d = m\Delta t ,$$

where m is the inclination of the track to the direction of the stage movement.

If there are n such discontinuities in a total number of $N+1$ cells this effect would be approximately equivalent to an additional noise given by

$$\delta = \overline{m}\Delta t\sqrt{n/N} ,$$

and the error introduced in D — $(\frac{1}{2}\overline{m}^2(\Delta t)^2/\overline{D})(n/N)\cdot 100\%$ where $\overline{m}$ is the mean absolute value of m.

For $\Delta t = 5$ μm and for the worst alignment allowed in our observations, i.e. for $m = 3/100$, the value of δ was estimated as .07 μm for the first 35 second differences, and .05 μm averaged over 3 cm of track length.

Appendix III

The noise level, ε, was calculated from the values of $\overline{D}$, at full cells, $\overline{D}(t)$, and half cells, $\overline{D}(t/2)$, using the equation

$$\varepsilon^2 = \frac{8\left[\frac{K(t)}{K(t/2)}\right]^2\overline{D}^2(t/2) - \overline{D}^2(t)}{8\left(\frac{K(t)}{K(t/2)}\right)^2 - 1} .$$

Where $K(t)$ and $K(t/2)$ are the values of scattering constants for full, and half cells, averaged over the whole length of track. The value of the ratio $K(t)/K(t/2)$ was found to be 1.04 for protons, deuterons and tritons alike.

It was assumed that the noise level remained constant for the range of cell lengths used (15 μm to 165 μm).

Appendix IV

For a particle of mass M at a residual range R we have the standard relations

$$D = \frac{K(\beta, t)M^2Z}{p\beta} , \tag{1}$$

and

$$E_{\mathrm{Kin}} = \mathrm{const}\ M^{1-n}R^{n}Z^{2n}\ . \tag{2}$$

Hence

$$D = \mathrm{const}\ K(\beta, t)M^{n-1}Z^{1-2n}R^{-n}t^{\frac{2}{3}}(E_{\mathrm{Kin}}/p\beta)\ , \tag{3}$$

where $K(\beta, t)$, the scattering constant, assumes slightly different values for particles of different masses, on account of the difference in variation of velocity with residual range.

For comparison of the mass, M_x, of an unknown particle with the known particle, M_0, (both of unit charge), for which the scattering scheme has been calculated, we have

$$\frac{M_x}{M_0} = \left[\frac{\bar{D}_0}{\bar{D}_x}\frac{(E_{\mathrm{Kin}}/p\beta)_x}{(E_{\mathrm{Kin}}/p\beta)_0}\frac{K_x}{K_0}\right]^{1/(1-n)} = \left(\frac{\bar{D}_0}{\bar{D}'_x}\right)^{1/(1-n)}\ , \tag{4}$$

where

$$\bar{D}'_x = \bar{D}_x\frac{(E_{\mathrm{Kin}}/p\beta)_0}{(E_{\mathrm{Kin}}/p\beta)_x}\frac{K_0}{K_x}\ , \tag{5}$$

and $\bar{D}_0$ and D_x are the experimental values of D for the two particles respectively and K_0 and K_x the corresponding values of the scattering constants averaged for the whole length of the track.

The correction for the values of $E_{\mathrm{Kin}}/p\beta$ was found to be 0.84% for deuterons, 1.2% for tritons, and the correction for the values of K — 0.45% for deuterons and — 0.53% for tritons, when measured using a proton scheme.

The correction (5) should also be applied when the variation of $\bar{D}$ with residual range for particles other than protons is considered since its value varies for different parts of the track.

RIASSUNTO (*)

Su tracce di particelle arrestantisi in emulsione e lunghe almeno 3 cm, si sono eseguite misure di scattering per mezzo del metodo della saetta costante usando uno schema di scattering basato sulle tabelle di Göttingen (4). Si ottennero i seguenti risultati: (i) Il valor medio della saetta, $\bar{D}$, pei protoni fu trovato eccedere di circa il 3% il valore teorico. (ii) La dispersione delle osservazioni sperimentali di $\bar{D}$ corrisponde assai strettamente al presunto valore statistico calcolato con la formula $75/\sqrt{N}$ % per l'errore medio. Si ottenne una buona risoluzione per gruppi di protoni e di deutoni con lunghezze di traccia di 3 e 2 cm. (iii) L'esponente range-energia dedotto dalle osservazioni dei rapporti di massa deutone/protone e tritone/protone e dalla variazione del valore di $\bar{D}$ col percorso residuo fu trovato in buon accordo col valore 0.568 di Fay *et al.* (4) e di Vigneron (12). (iv) Non è stata osservata alcuna particella corrispondente a un mesone di 1450 m_e come preconizzato da Fowler e Perkins (9); nonpertanto le presenti statistiche non sono sufficienti ad escludere definitivamente l'esistenza di tale particella.

(*) *Traduzione a cura della Redazione.*

IL NUOVO CIMENTO Vol. V, N. 4 1º Aprile 1957

Some Relations Among Green's Functions.

K. Hiida and M. Sawamura

Department of Physics, University of Hiroshima - Hiroshima

(ricevuto il 10 Dicembre 1956)

Summary. — Starting from several physically reasonable assumptions, taken by Källén and Lehmann, various Green's functions are transformed into the parametrical integral form with spectral functions. Then a method is presented to convert the equations connecting various Greens' functions into those among the corresponding spectral functions alone.

1. – Introduction.

The method to treat the quantum field theory which was originally used by Källén [1] and then by Lehmann [2] has manifested its own usefullness in investigating the formal structure and properties of the Green's function, without recourse to the conventional perturbation theory. It consists in making explicit use of the following postulates introduced from the physical point of view, that is,

(i) The theory is Lorentz-invariant.

(ii) There exists an energy-momentum four-vector P_μ such that

$$\frac{\partial}{\partial x_\mu} 0(x) = i[0(x), P_\mu], \qquad [P_\mu, P_\nu] = 0,$$

where $0(x)$ stands for any Heisenberg operator.

[1] G. Källén: *Helv. Phys. Acta*, **25**, 417 (1952).
[2] H. Lehmann: *Nuovo Cimento*, **11**, 342 (1954).

(iii) We can define the vacuum state for which the energy operator takes the smallest eigenvalue.

(iv) The positive energy states form a complete set in the Hilbert space.

(v) The following two operations are permissible:

(*a*) when we calculate an expectation value, for example,

$$\langle \varphi(x)\varphi(y)\rangle_0 = \sum_p \langle 0|\varphi(x)|p\rangle\langle p|\varphi(y)|0\rangle ,$$

summation over states belonging to the same eigenvalue of P_μ can be taken first;

(*b*) when the Green's function is expressed in a parametrical integral form, the parameter integrations can be performed at the end.

(vi) The Theory is also invariant under such transformations as the gauge transformation, or the charge conjugation.

Now it seems of significance to put the following questions: Can these postulates be consistent with each other? Even when this is the case, what are the magnitudes of the renormalization constants and can the renormalized coupling constant take the value just equal to the observed one? One of the approaches to these ends may be given by the method of Y. NAMBU [3]. Invoking exclusively the postulates mentioned above one transforms the various kinds of Green's functions into the parametrical integral form with the spectral functions. Then the equations of motion for the Green's functions may be converted into the equations among the corresponding spectral functions alone. The problems are now to investigate whether these equations for the spectral functions are consistent or not. To this end we shall develop in this note a method to transform the equations of motion for the Green's functions into those for the corresponding spectral functions with recourse to the above mentioned postulates alone, and to obtain certain conditions necessary for the consistency.

For illustrative purposes we shall take the pseudo-scalar meson coupled with the nucleon in the pseudo-scalar type, neglecting for simplicity's sake the φ^4-term. The Lagrangian density L of the whole meson-nucleon system and the commutation relations for the field operators are given as

[3] Y. NAMBU: *Phys. Rev.*, **100**, 394 (1955); **101**, 459, 1183 (1956).

follows:

$$L = -z^2\bar{\psi}(\gamma_\mu\partial_\mu + m_0)\psi - \frac{z_3}{2}(\partial_\mu\varphi_i\partial_\mu\varphi_i + \mu_0^2\varphi_i\varphi_i) - igz_1\bar{\psi}\gamma_5\tau_i\varphi_i\psi\,, \tag{1.1}$$

and

$$\begin{cases} \{\psi_\alpha(\boldsymbol{x}, 0), \bar{\psi}_\beta(\boldsymbol{x}', 0)\} = (\gamma_4)_{\alpha\beta}\delta(\boldsymbol{x} - \boldsymbol{x}')Z_2^{-1}\,, \\ \left[\varphi_i(\boldsymbol{x}, 0), \frac{\partial}{\partial x_0'}\varphi_j(\boldsymbol{x}', x_0')\Big|_{x_0'=0}\right] = i\delta_{ij}\delta(\boldsymbol{x} - \boldsymbol{x}')z_3^{-1}\,, \end{cases} \tag{1.2}$$

where φ, ψ and $\bar{\psi}$ are respectively the operators of the meson and the nucleon fields in the Heisenberg representation. The equations of motion for the field operator φ, ψ and $\bar{\psi}$ are derived from (1.1), as

$$(\gamma_\mu\partial_\mu + m_0)\psi = -igz_1z_2^{-1}\gamma_5\tau_i\varphi_i\psi\,, \qquad (-\gamma_\mu^T\partial_\mu + m_0)\bar{\psi} = -igz_1z_2^{-1}\bar{\psi}\gamma_5\tau_i\varphi_i \tag{1.3}$$

and

$$(\Box - \mu_0^2)\varphi_i = igz_1z_3^{-1}\bar{\psi}\gamma_5\tau_i\psi\,.$$

The simplest example of the equations of motion for the Green's functions may be provided, using (1.2) and (1.3), by

$$(\Box_x - \mu_0^2)\langle T(\varphi_j(x)\varphi_i(z))\rangle_0 = i\delta_{ij}z_3^{-1}\delta(x - z) - \\ - igz_1z_3^{-1}\,\mathrm{Tr}\,[\gamma_5\tau_j\langle T((\psi(x)\bar{\psi}(x)\varphi_i(z))\rangle_0\,, \tag{1.4}$$

the relation connecting the modified meson propagator Δ_F' and the 3-rd order Green's functions $\langle\psi\bar{\psi}q\rangle_0$ etc. The quantity on the left hand side of the equation is already obtained by LEHMANN [2] in the parametrical integral form, namely

$$\langle T(q_j(x)q_i(z))\rangle_0 = -\frac{i\delta_{ij}}{(2\pi)^4}\int \mathrm{d}k\,\exp[ik(x - z)]\int_0^\infty \mathrm{d}\omega\,\frac{\varrho(\omega)}{k^2 + \bar{\omega}}\,, \qquad \bar{\omega} = \omega - i\varepsilon\,,$$

where

$$\varrho(\omega) = \delta(\omega - \mu^2) + \sigma(\omega) \qquad \text{and} \qquad \sigma(\omega) \geqslant 0\,. \tag{1.5}$$

As for the quantity on the right hand side we shall express it in the parametrical integral from in the following section, and the equation (1.4) is converted into that between the spectral function of the 2-nd order and those of the 3-rd order, ϱ and $\nu_{\lambda\lambda'}$ respectively. The method to be developed in Sects. 2–4 will equally be applicable to the equations for the more complicated Green's functions.

2. – The Parametrical Integral Representation of the Third Order Green's Function.

In this section, invoking the postulates exclusively, we shall derive the 3-rd order Green's functions $\langle \psi\bar{\psi}q \rangle_0$, etc., in the parametrical integral forms.

Postulates (ii) and (iv) permit us to write

$$(2.1)\qquad \langle \psi_\alpha(x)\,\bar{\psi}_\beta(y)\varphi_i(z)\rangle_0 = \\ = \sum_{p,k} \langle 0|\psi_\alpha|p\rangle\langle p|\bar{\psi}_\beta|k\rangle\langle k|\varphi_i|0\rangle \exp[ipx]\exp[i(k-p)y]\exp[-ikz]\,,$$

where $|p\rangle$, $|k\rangle$ are the members of the complete system of states over which the summations should be taken. p_μ and k_μ are then time-like vectors with positive 4-th component by virtue of the postulates (i) and (iii). Using (i) and (v-*a*), we obtain

$$(2\pi)^6 \sum_p{}' \sum_k{}' \langle 0|\psi_\alpha|p\rangle\langle p|\bar{\psi}_\beta|k\rangle\langle k|\varphi_i|0\rangle = \\ = \theta(-p^2)\theta(p_0)\theta(-k^2)\theta(k_0)[(i\gamma p)^\lambda i\gamma_5\tau_i(i\gamma(p-k))^{\lambda'}]_{\alpha\beta}\cdot \\ \cdot \{\theta[-(k-p)^2]\theta(k_0-p_0)\nu^1_{\lambda\lambda'}[-p^2,-(k-p)^2,-k^2] + \\ + \theta[-(k-p)^2]\theta(-k_0+p_0)\nu^2_{\lambda\lambda'}[-p^2,-(k-p)^2,-k^2] + \\ + \theta[(k-p)^2]\nu^3_{\lambda\lambda'}[-p^2,-(k-p)^2,-k^2]\}, \quad (\lambda,\lambda'=0,1),$$

where

$$(2.2)\qquad \theta(p_0) = \begin{cases} 1 & \text{for } p_0 > 0\,, \\ 0 & \text{for } p_0 < 0\,, \end{cases}$$

and by the primed summation $\sum_t{}'$ we mean the sum over the states belonging to the same eigenvalue t_μ of P_μ, and γ_5 reflects the pseudoscalar nature of the field φ. Substituting (2.2) into (2.1) and referring to (v-*b*) we get

$$(2.3)\qquad \langle \psi_\alpha(x)\bar{\psi}_\beta(y)\varphi_i(z)\rangle_0 = \\ = \frac{1}{(2\pi)^6}\int \mathrm{d}p\,\mathrm{d}q\,\mathrm{d}k \exp[ipx]\exp[iqy]\exp[ikz]\theta(p_0)\theta(-k_0)\delta(p+q+k)\cdot \\ \cdot[(i\gamma p)^\lambda i\gamma\tau_i(-i\gamma q)^{\lambda'}]_{\alpha\beta}\int_0^\infty \mathrm{d}u\,\mathrm{d}w\int_{-\infty}^{\infty}\mathrm{d}v\,\delta(p^2+u)\delta(q^2+v)\delta(k^2+w)\cdot \\ \cdot[\theta(v)\theta(q_0)\nu^1_{\lambda\lambda'}(uvw) + \theta(v)\theta(-q_0)\nu^2_{\lambda\lambda'}(uvw) + \theta(-v)\nu^3_{\lambda\lambda'}(uvw)]\,,$$

where $\nu^i_{\lambda\lambda'}$ may generally be complex functions.

The theory should be invariant under charge conjugation. The field operators are then transformed as follows

$$(2.4)\qquad \begin{cases} \overline{\psi} \to c^{-1}\psi\,, \\ \psi \to c\overline{\psi} \\ \varphi_1 \to \varphi_1\,, \\ \varphi_2 \to -\varphi_2\,, \\ \varphi_3 \to \varphi_3\,, \end{cases} \qquad \text{where} \quad \begin{cases} c^{-1}\gamma_\mu c = -\gamma_\mu^T, \\ c^{-1}\tau_i c = \tau_i\,. \end{cases}$$

We thus get a relation;

$$(2.5)\qquad \langle\overline{\psi}_\beta(y)\,\psi_\alpha(x)\varphi_i(z)\rangle_0 = -\,\varepsilon_i c^{-1}_{\beta\beta'}\langle\psi_{\beta'}(y)\,\overline{\psi}_{\alpha'}(x)\varphi_i(z)\rangle_0 c_{\alpha'\alpha}\,,$$

where

$$\varepsilon_i: \begin{cases} \varepsilon_1 = 1\,, \\ \varepsilon_2 = -1\,, \\ \varepsilon_3 = 1\,. \end{cases}$$

From eqs. (2.3) and (2.5) there results

$$(2.6)\qquad \langle\overline{\psi}_\beta(y)\psi_\alpha(x)\varphi_i(z)\rangle_0 =$$

$$= -\frac{-1}{(2\pi)^6}\int \mathrm{d}p\,\mathrm{d}q\,\mathrm{d}k\,\exp[ipx]\exp[iqy]\exp[ikz]\delta(p+q+k)\theta(q_0)\theta(-k_0)\cdot$$

$$\cdot[(i\gamma p)^\lambda i\gamma_5\tau_i(-i\gamma q)^{\lambda'}]_{\alpha\beta}\int_0^\infty \mathrm{d}v\,\mathrm{d}w\int_{-\infty}^{\infty}\mathrm{d}u\,\delta(p^2+u)\delta(q^2+v)\delta(k^2+w)\cdot$$

$$\cdot[\theta(u)\theta(p_0)\nu^1_{\lambda'\lambda}(vuw)+\theta(u)\theta(-p_0)\nu^2_{\lambda'\lambda}(vuw)+\theta(-u)\nu^3_{\lambda'\lambda}(vuw)]\,.$$

Recalling

$$(27)\qquad \begin{cases} \langle\varphi_i(z)\,\psi_\alpha(x)\,\overline{\psi}_\beta(y)\rangle_0 = \langle\psi_{\beta'}(y)\,\psi^+_\alpha(x)\varphi_i(z)\rangle^*_0\,(\gamma_4)_{\beta'\beta}\,, \\ \langle\varphi_i(z)\,\overline{\psi}_\beta(y)\,\psi_\alpha(x)\rangle_0 = \langle\psi^+_\alpha(x)\,\psi_{\beta'}(y)\varphi_i)z)\rangle^*_0\ \ (\gamma_4)_{\beta'\beta}\,, \\ (^+\text{: Hermitian conjugate, } {}^*\text{: Complex conjugate}) \end{cases}$$

and substituting (2.3) and (2.6) into the right hand side of (2.7), we have

$$(2.8)\qquad \langle\varphi_i(z)\psi_\alpha(x)\overline{\psi}(y)\rangle_0 =$$

$$= \frac{1}{(2\pi)^6}\int \mathrm{d}p\,\mathrm{d}q\,\mathrm{d}k\,\exp[ipx]\exp[iqy]\exp[ikz]\delta(p+q+k)\theta(-q_0)\theta(k_0)\cdot$$

$$\cdot[(i\gamma p)^\lambda i\gamma_5\tau_i(-i\gamma q)^{\lambda'}]_{\alpha\beta}\int_0^\infty \mathrm{d}v\,\mathrm{d}w\int_{-\infty}^{\infty}\mathrm{d}u\,\delta(p^2+u)\delta(q^2+v)\delta(k^2+w)\cdot$$

$$\cdot[\theta(u)\theta(-p_0)\nu^{1*}_{\lambda'\lambda}(vuw)+\theta(u)\theta(p_0)\nu^{2*}_{\lambda'\lambda}(vuw)+\theta(-u)\nu^{3*}_{\lambda'\lambda}(vuw)]\,.$$

and

$$(2.9)\qquad \langle\varphi_i(z)\overline{\psi}_\beta(y)\psi_\alpha(x)\rangle_0 =$$

$$= -\frac{1}{(2\pi)^6}\int \mathrm{d}p\,\mathrm{d}q\,\mathrm{d}k\,\exp[ipx]\exp[iqy]\exp[ikz]\delta(p+q+k)\,\theta(-p_0)\,\theta(k_0)\cdot$$

$$\cdot[(i\gamma p)^\lambda i\gamma_5\tau_i(-i\gamma q)^{\lambda'}]_{\alpha\beta}\int_0^\infty \mathrm{d}u\,\mathrm{d}w\int_{-\infty}^{\infty}\mathrm{d}v\,\delta(p^2+u)\delta(q^2+v)\delta(k^2+w)\cdot$$

$$\cdot[\theta(v)\,\theta(-q_0)v^{1*}_{\lambda\lambda'}(uvw)+\theta(v)\,\theta(q_0)v^{2*}_{\lambda\lambda'}(uvw)+\theta(-v)v^{3*}_{\lambda\lambda'}(uvw)]\,.$$

In a similar way we can also obtain parametrical integral forms for $\langle\psi\varphi\overline{\psi}\rangle_0$ and $\langle\overline{\psi}\varphi\psi\rangle_0$.

3. Relation between the Modified Propagator and the Third Order Green's Function.

We have obtained in the preceding section the parametrical integral representation of the 3-rd order Green's function. Now we shall, using it, transform the eq. (1.4) into the momentum space. By virtue of (1.2) and $\langle\varphi\rangle_0 = 0$,

$$(3.1)\qquad \langle T(\psi_\alpha(x)\,\overline{\psi}_\beta(x)\varphi_i(z))\rangle_0 = \theta(x_0-z_0)\langle\psi_\alpha(x)\,\overline{\psi}_\beta(x)\varphi_i(z)\rangle_0 -$$

$$-\theta(z_0-x_0)\langle\varphi_i(z)\,\overline{\psi}_\beta(x)\,\psi_\alpha(x)\rangle_0\,.$$

After the substitution of expressions (2.3) and (2.9) into (3.1), we get

$$(3.2)\qquad (\gamma'_5\tau_j)_{\beta\alpha}\int \mathrm{d}(x-z)\exp[ik(x-z)]\langle T(\psi_\alpha(x)\overline{\psi}_\beta(x)\varphi_i(z))\rangle_0 =$$

$$= \frac{8}{(2\pi)^3}\,\delta_{ij}\int \mathrm{d}\boldsymbol{p}\int_0^\infty \mathrm{d}u\,\mathrm{d}w\int_{-\infty}^{\infty}\mathrm{d}v\,\frac{1}{2\sqrt{\boldsymbol{p}^2+u}\cdot 2\sqrt{k^2+w}}\cdot$$

$$\cdot\begin{pmatrix}1 & 0\\ 0 & p^2+\boldsymbol{p}\cdot\boldsymbol{k}+\sqrt{\boldsymbol{p}^2+u}\sqrt{\boldsymbol{k}^2+w}\end{pmatrix}_{\lambda\lambda'}\delta[(\boldsymbol{p}+\boldsymbol{k})^2-(\sqrt{\boldsymbol{p}^2+u}-\sqrt{\boldsymbol{k}^2+w})^2+v]\cdot$$

$$\cdot\Big\{\frac{1}{k_0+\sqrt{\boldsymbol{k}^2+w}-i\varepsilon}[\theta(v)\,\theta(\sqrt{\boldsymbol{k}^2+w}-\sqrt{\boldsymbol{p}^2+u})v^1_{\lambda\lambda'}(uvw)+$$

$$+\theta(v)\,\theta(-\sqrt{\boldsymbol{k}^2+w}+\sqrt{\boldsymbol{p}^2+u})v^2_{\lambda\lambda'}(uvw)+\theta(-v)v^3_{\lambda\lambda'}(uvw)]+$$

$$+\frac{1}{\sqrt{\boldsymbol{k}^2+w}-k_0-i\varepsilon}[\theta(v)\,\theta(\sqrt{\boldsymbol{k}^2+w}-\sqrt{\boldsymbol{p}^2+u})v^{1*}_{\lambda\lambda'}(uvw)+$$

$$+\theta(v)\,\theta(-\sqrt{\boldsymbol{k}^2+w}+\sqrt{\boldsymbol{p}^2+u})v^{2*}_{\lambda\lambda'}(uvw)+\theta(-v)v^{3*}_{\lambda\lambda'}(uvw)]\Big\}\,.$$

Provided that the k_μ in (3.2) is a time-like vector, we can take a special Lorentz frame where $k = (0, 0, 0, k_0)$, and then the remaining $\boldsymbol{p}$ integrations in (3.2) are easily evaluated.

Putting

$$\nu^{i}_{\lambda\lambda'}(uvw) = \nu^{iR}_{\lambda\lambda'}(uvw) + i\nu^{iI}_{\lambda\lambda'}(uvw) \qquad (i\,, = 1, 2, 3), \tag{3.3}$$

where $\nu^{iR}_{\lambda\lambda'}$ and $\nu^{iI}_{\lambda\lambda'}$ are real functions, we obtain, after the $\boldsymbol{p}$ integration in (3.2) and the substitution of the results into (1.4), the following equation:

$$\begin{aligned}(3.4)\ (*)\qquad (k^2 + \mu^2 - \delta\mu^2)\int_0^\infty \mathrm{d}w\,\frac{\varrho(\omega)}{k^2 + \bar{w}} = \\ = z_3^{-1}\left\{1 - \frac{2gz_1}{(2\pi)^2}\int_0^\infty \mathrm{d}u\,\mathrm{d}w\int_{-\infty}^{\infty}\mathrm{d}v\,\frac{\sqrt{(w+u-v)^2 - 4uw}}{w}\right. \cdot \\ \cdot\begin{pmatrix} 1 & 0 \\ 0 & \dfrac{w-u-v}{2}\end{pmatrix}_{\lambda\lambda'}\left.\left[\frac{A_{\lambda\lambda'}(uvw)}{k^2 + \bar{w}} - \frac{ik_0}{\sqrt{k^2 + w}}\,\frac{B_{\lambda\lambda'}(uvw)}{k^2 + \bar{w}}\right]\right. \quad \text{for} \quad k^2 < 0\,,\end{aligned}$$

where

$$\left\{\begin{aligned} A_{\lambda\lambda'}(uwv) &= \theta(v)\theta[\sqrt{w} - (\sqrt{u} + \sqrt{v})]\nu^{1R}_{\lambda\lambda'}(uvw) + \\ &\quad + \theta(v)\,\theta[\sqrt{w} - (\sqrt{v} + \sqrt{w})]\nu^{2R}_{\lambda\lambda'}(uvw) + \theta(-v)\nu^{3R}_{\lambda\lambda'}(uvw) \\ &\text{and} \\ B_{\lambda\lambda'}(uvw) &= \theta(v)\theta[\sqrt{w} - (\sqrt{u} + \sqrt{v})]\nu^{1I}_{\lambda\lambda'}(uvw) + \\ &\quad + \theta(v)\theta[\sqrt{u} - (\sqrt{v} + \sqrt{w})]\nu^{2I}_{\lambda\lambda'}(uvw) + \theta(-v)\nu^{3I}_{\lambda\lambda'}(uvw)\,. \end{aligned}\right. \tag{3.5}$$

4. – Relations between the Spectral Functions ϱ and $\nu^{i}_{\lambda\lambda'}$.

Remarking the identity

$$\frac{1}{k^2 + \bar{w}} = \frac{1}{w - \mu^2} - \frac{k^2 + \mu^2}{w - \mu^2}\,\frac{1}{k^2 + \bar{w}}\,,$$

(*) The 2-nd term in the bracket [ ] on the right hand side of (3.4) may be dropped, for this is an odd function of k_μ, while the other terms in the equation are exclusively the even functions of the same variable.

we can expand each term in (3.4) in powers of $(k^2+\mu^2-i\varepsilon)$. The equation may be considered to be satisfied in every power of $(k^2+\mu^2-i\varepsilon)$. Thus comparing both sides we get the following relations, from the coefficients of $(k^2+\mu^2-i\varepsilon)^{-1}$, $(k^2+\mu^2-i\varepsilon)^0$ and $(k^2+\mu^2-i\varepsilon)^n$ for $n \geqslant 1$,

$$
(4.1)\qquad \begin{cases} \dfrac{2z_1 z_3^{-1}}{(2\pi)^2} g^2\mu^2 X^{(1)}\,, \\ z_3 = \left[1 - \dfrac{2z_1 g}{(2\pi)^2}\int_0^\infty \mathrm{d}w\, \dfrac{X^{(2)}(w)}{w-\mu^2}\right] \Big/ \left[1 - \delta\mu^2 \int_0^\infty \mathrm{d}w\, \dfrac{\sigma(w)}{w-\mu^2}\right] \\ \text{and} \\ \sigma(w)\left[1+\dfrac{\delta\mu^2}{w-\mu^2}\right] = \dfrac{2z_1 z_3^{-1} g}{(2\pi)^2}\,\dfrac{X^{(2)}(w)}{w-\mu^2}\,, \end{cases}
$$

respectively, where the functions $X^{(1)}$ and $X^{(2)}$ are defined as

$$
(4.2)\,(*)\quad X(w) = \int_0^\infty \mathrm{d}u \int_{-\infty}^\infty \mathrm{d}v\, \frac{\sqrt{(w-u-v)^2-4uw}}{w} \begin{pmatrix} 1 & 0 \\ 0 & \dfrac{w-u-v}{2} \end{pmatrix}_{\lambda\lambda'} A_{\lambda\lambda'}(u\,v\,w) =
$$

$$
= \mu^2\delta(w-\mu^2)X^{(1)} + X^{(2)}(w)\,,
$$

the part proportional to $\delta(w-\mu^2)$ in $X(w)$ being denoted by $X^{(1)}$ and the one independent of it being exclusively contained in $X^{(2)}(w)$.

The 3-rd of (4.1) is the desired relation for the spectral functions. A glance at (3.3), (3.5), (4.1) and (4.2) shows that $\sigma(w)$ is related with the real parts of $\nu^i_{\lambda\lambda}$ alone and thus it is real. As for the magnitude of the real parts of $\nu^i_{\lambda\lambda'}$ unfortunately we can not give any further statements such that they are positive definite or negative definite and so on. Therefore the 3-rd of (4.1) itself is not enough to investigate if the method given by G. KÄLLÉN and H. LEHMANN is self-consistent or not.

The 2-nd and the 3-rd of (4.1) lead to

$$
(4.3)\qquad z_3^{-1} = 1 + \int_0^\infty \mathrm{d}w\, \sigma(w)\,.
$$

This is already obtained by LEHMANN to express z_3 in terms of $\sigma(w)$. How-

(*) In the Appendix we shall evaluate $A_{\lambda\lambda'}$ in g'-approximation and substitute them in the 3-rd of (4.1) to obtain the $\sigma(w)$ up to g^2-order.

ever (4.1), is not sufficient to derive a relation between $\delta\mu^2$ and $\sigma(w)$. On the other hand if the postulates are self-consistent, it must be such that

$$\delta\mu^2 = -z_3\int_0^\infty \mathrm{d}w(w-\mu^2)\sigma(w)\,, \tag{4.4}$$

which was previously derived by LEHMANN [2]. Combining this with (4.1) and (4.2), we have

$$\delta\mu^2 = -\frac{2z_1z_3^{-1}g}{(2\pi)^2}\int_0^\infty \mathrm{d}wX^{(1)}(w)\,. \tag{4.5}$$

If we recall (4.2), then (4.5) and the 1-st of (4.1) are incorporated into

$$\int_0^\infty \mathrm{d}wX(w) = 0\,, \tag{4.6}$$

a necessary condition to be satisfied by the spectral functions for the consistency of the postulates.

To summarize, it has been shown by taking one of the simplest examples how one can derive the relations linking the spectral functions which are the reflections of the corresponding Green's functions, and how one can get certain subsidiary conditions to be satisfied by them for the consistency of the postulates. One is also able to derive the relations among the more general spectral functions in the same way. Then there will further be obtained among the spectral functions a number of subsidiary conditions which are necessary for the consistency mentioned above. In the present paper, however, this consistency problem will be not traced any further. What the magnitude of z_i-factors should be, was not checked over too, to be left for future investigation.

* * *

The authors wish to thank Prof. K. SAKUMA for his continual encouragements. Their thanks are also due to Prof. R. UTIYAMA and the members of the institutes for theoretical physics in Nagoya and Osaka for fruitful discussions.

APPENDIX

The 3rd order Green's function $\langle \psi_\alpha(x)\bar{\psi}_\beta(y)\varphi_i(z)\rangle_0$ is rewritten, up to the first order in g, as

$$
\begin{aligned}
(A.1)\quad & \langle \psi_\alpha(x)\bar{\psi}_\beta(y)\varphi_i(z)\rangle_0 = \\
& = -g\int_{-\infty}^{\infty} dx_1 \big\{[S_F(x-x_1)+iS^{(-)}(x-x_1)](\gamma_5\tau_i)S^{(+)}(x_1-y)\Delta^{(+)}(x_1-z)+ \\
& + S^{(+)}(x-x_1)(\gamma_5\tau_i)[S_F(x_1-y)-iS^{(+)}(x_1-y)]\Delta^{(+)}(x_1-z)- \\
& - S^{(+)}(x-x_1)(\gamma_5\tau_i)S^{(-)}(x_1-y)[\Delta_F(z-x_1)-i\Delta^{(+)}(x_1-z)]\big\}_{\alpha\beta} = \\
& = -\frac{g}{(2\pi)^6}\int dp\, dq\, dk \exp[ipx]\exp[iqy]\exp[ikz]\cdot \\
& \cdot \delta(p+q+k)\theta(p_0)\,\theta(-k_0)[(i\gamma p)^\lambda i\gamma_5\tau_i(-i\gamma q)^{\lambda'}]_{\alpha\beta}\cdot \\
& \cdot \begin{pmatrix} m^2 & -m \\ -m & 1 \end{pmatrix}_{\lambda\lambda'}\left[\theta(-q_0)\frac{1}{p^2+m^2}\delta(q^2+m^2)\delta(k^2+\mu^2)+\right. \\
& \left. + \delta(p^2+m^2)\frac{1}{q^2+m^2}\delta(k+\mu^2)+\theta(q_0)\delta(p^2+m^2)\delta(q^2+m^2)\frac{1}{k^2+m^2}\right].
\end{aligned}
$$

In (A.1) the terms which contain the product of four δ-functions

$$\delta(p+q+k)\delta(p^2+m^2)\delta(q^2+m^2)\delta(k^2+\mu^2)$$

have been omitted, for the case where $p+q+k=0$, $p^2+m^2=0$, $q^2+m^2=0$ and $k^2+\mu^2=0$ would never be realized. Comparing this with (2.3) we obtain for $\nu^i_{\lambda\lambda'}$

$$
(A.2)\,(*)\quad \begin{cases}
\nu^{1R}_{\lambda\lambda'} = -g\begin{pmatrix} m^2 & -m \\ -m & 1 \end{pmatrix}_{\lambda\lambda'}\delta(u-m^2)\left[\frac{1}{v-m^2}\delta(w-\mu^2)+\delta(v-m^2)\frac{1}{w-\mu^2}\right], \\
\nu^{2R}_{\lambda\lambda'} = g\begin{pmatrix} m^2 & -m \\ -m & 1 \end{pmatrix}_{\lambda\lambda'}\delta(w-\mu^2)\left[\frac{1}{u-m^2}\delta(v-m^2)+\delta(u-m^2)\frac{1}{v-m^2}\right], \\
\nu^{3R}_{\lambda\lambda'} = g\begin{pmatrix} m^2 & -m \\ -m & 1 \end{pmatrix}_{\lambda\lambda'}\delta(u-m^2)\frac{1}{v-m^2}\delta(w-\mu^2) \\
\text{and} \qquad \nu = 0\,.
\end{cases}
$$

(*) We are very grateful to Prof. S. TOMONAGA who kindly pointed out an error in the original manuscript for the expressions of $\nu^i_{\lambda\lambda'}$.

From these and (3.3) and (4.2), we have

$$X^{(2)}(w) = \frac{g}{2}\,\theta(w - 4m^2)\,\frac{\sqrt{w^2 - 4m^2 w}}{w - \mu^2}\,. \tag{A.3}$$

(A.3) is substituted into the 3-rd of (4.1) to give

$$\sigma(w) = \frac{g^2}{(2\pi)^2}\,\theta(w - 4m^2)\,\frac{\sqrt{w^2 - 4m^2 w}}{(w - \mu^2)^2}\,. \tag{A.4}$$

The same result (A.4) can also be attained from another approach which was taken by H. LEHMANN when he calculated the spectral functions ϱ_1 and ϱ_2 of the nucleon propagator S'_F (2).

RIASSUNTO (*)

Partendo da alcune ipotesi di Källén e Lehmann, ammissibili dal punto di vista fisico, si trasformano varie funzioni di Green nella forma integrale parametrica con funzioni spettrali. Si presenta poi un metodo per convertire le equazioni che collegano varie funzioni di Green in quelle fra le sole funzioni spettrali corrispondenti.

(*) *Traduzione a cura della Redazione.*

IL NUOVO CIMENTO Vol. V, N. 4 1° Aprile 1957

Phase shift Analysis of Proton-Proton Scattering Experiments.

II - Analysis of the Scattering Data from 18 to 260 MeV (*).

E. Clementel, C. Villi (°) and L. Jess

Istituti di Fisica dell'Università di Padova e di Trieste (°)
Istituto Nazionale di Fisica Nucleare - Sezione di Padova
(°) *Istituto Nazionale di Fisica Nucleare - Gruppo di Trieste*

(ricevuto l'11 Dicembre 1956)

Summary. — The experimental data on proton-proton scattering in the energy interval 18÷260 MeV are discussed by using an analytical method and limiting the analysis to the contribution of the S and P states. The polarization data at high energy allow a double set of phase shifts which reproduce the angular distributions in the considered energy interval. The two sets follow from the behaviour of the singlet S phase shift, which can either become negative at about 220 MeV or be simply a decreasing function of the energy without assuming negative values. The stability of the solutions thus found against the introduction of the $^1D_2$ and $^3F_2$ states is also discussed. Finally, the present results are compared with the solutions already obtained in proton-proton scattering analysis by different Authors.

Introduction.

Many attempts have been made in the last few years to analyze the proton-proton scattering data in terms of phase shifts. Most of them are of graphical nature ([1-3]) and limited to high energy scattering data, which have been dis-

(*) The results of this paper have been reported at the *USSR* Conference on high energy particles, Moscow, May 1956.

([1]) R. M. Thaler and J. Bengston: *Phys. Rev.*, **94**, 679 (1953); R. M. Thaler, J. Bengston and G. Breit: *Phys. Rev.*, **94**, 683 (1954).

([2]) A. Garren: *Phys. Rev.*, **101**, 419 (1956).

([3]) C. A. Klein: *Nuovo Cimento*, **1**, 581 (1955); **2**, 38 (1955).

cussed assuming that the proton-proton interaction is due only to S and P states of orbital angular momentum. The effect of the ${}^3F_2$ state has been considered both with ([1]) and without ([4]) coupling to the ${}^3P_2$ state. Higher order waves can be introduced into the analysis only by using electronic computers, and this has been done with the 300 MeV data of the Berkeley group([5,6]) Unfortunately, all these attempts do not give a unique answer, and many sets of phase shifts do fit not only the angular distributions, but even the double (polarization) and triple scattering data ([6]).

In a recent attempt to fit the nucleon-nucleon scattering data from zero to 274 MeV by means of a boundary-condition approximation ([7]), FESHBACH and LOMON ([8]) have produced in two different alternatives (either S, P and D states only or S, P, D and ${}^3F_2$ states) a unique set of phase shifts, having continuity versus energy. We shall show below that this uniqueness is only apparent, and that in each one of the two alternatives there exist according to our results, at least two sets which, still with continuity versus energy, fit the angular and the available polarization data.

In a previous paper ([9]) we have given already a formal discussion of the method used in the present analysis, which is intended, and we hope it to be, a clear up of the phase shift analysis problem in the lowest approximation, i.e. with S and P waves only. The method used is completely analytical, and the main difference with similar calculations lies in the introduction of a new parameter, the continuity versus energy, which was found essential in selecting the « correct » set. It will be seen how the continuity excludes several solutions, which could not be eliminated by considering the data referring to one energy only. These spurious solutions will automatically spoil any analysis carried at a given energy, as long as the sets are chosen according to the criterion to fit differential and polarization data.

The extension of this analysis to include higher order waves requires computing facilities which are not at present at our disposal.

In Sect. 1 we shall give a brief outline of the method with some formulas needed for the analysis in S and P waves. In Sect. 2 the solutions for 170 and 260 MeV will be discussed and the « correct » sets will be fixed according to

([4]) S. OHNUMA and D. FELDMAN: *Phys. Rev.*, **102**, 1641 (1956). We thank the Authors for a prereprint of their work.

([5]) M. H. HULL, jr., J. B. FERMAN, R. D. HATCHER and L. DURANT: *Phys. Rev.*, **103**, 1047 (1956).

([6]) H. P. STAPP, T. J. YPSILANTIS and N. METROPOLIS: *Proceedings of the Rochester Conference*, (1956, II, 15).

([7]) G. BREIT and W. BOURICIUS: *Phys. Rev.*, **75**, 1029 (1949).

([8]) H. FESHBACH and I. LOMON: *Phys. Rev.*, **102**, 891 (1956).

([9]) E. CLEMENTEL and C. VILLI: *Nuovo Cimento*, **2**, 1165 (1955). We shall refer to this paper as I.

the continuity versus the S phase shift using the polarization data. The chosen sets will be followed in Sect. **3** down to 18 and 30 MeV, and by using continuity in S and P phase shifts the solutions at 75 and 95 MeV will be given in Sect. **4**. In Sect. **5** we shall consider the stability of the solutions thus found against introduction of $^1D_2$ and $^3F_2$ (without coupling to $^3P_2$) waves. Finally, Sect. **6** will contain some concluding remarks. Unless otherwise stated, throughout this paper we shall use the same symbols and notation as in I. Phase shifts and angles will be given in degrees.

1. – Formalism of the Phase shift Analysis.

It follows from Eqs. (I; 19, 20, 21) that the difference $\Delta\sigma(\vartheta) = \sigma(\vartheta) - \sigma_c(\vartheta)$ can be expressed in the S and P wave approximation as

$$(1)\quad k^2\Delta\sigma(\vartheta) = [1 + (\eta/2)\boldsymbol{Y}_0]\sin^2 K_0 - (\eta/2)\boldsymbol{X}_0 \sin K_0 \cos K_0 + \\ + [1 + (\eta/2)\boldsymbol{Y}_1 P_1(\cos\vartheta)]z_1 - (\eta/2)\boldsymbol{X}_1 P_1(\cos\vartheta)z_2 + P_2(\cos\vartheta)z_3\,,$$

where the quantities z_i, given by Eq. (I; 22), are combinations of the P state phase shifts δ_0, δ_1 and δ_2. At a given energy, fixing the values of the phase shifts K_0 and using the experimental values for $\Delta\sigma(\vartheta)$, from Eq. (1) the quantities z_i can be derived with the least squares method as a function of K_0. Once the combinations z_i are given, the system of Eqs. (I; 22) can be solved, and, as it has already been shown ([9,10]), it presents a fourfold degeneracy, i.e. for a given K_0 four sets of P-phase shifts exist fitting the angular distribution equally well. These four sets, which we shall distinguish with the letters A, B, C and D, are associated two by two in the sense that they satisfy the relation

$$(2)\qquad (\delta_i - \delta_j)_{A,C} = (\delta_j - \delta_i)_{B,D} \qquad (i, j = 0, 1, 2).$$

From Eq. (2) it follows that

$$(3)\qquad \sum_{N=A,\ldots D} \delta_i^{(N)} = \text{const} \qquad (i = 0, 1, 2),$$

which supplies a very useful and quick check of the calculations. At this stage, the polarization data provide an automatic selection of the possible values for the phase shift K_0. In fact, one has only to select those sets of P phase shifts (and consequently the corresponding K_0), which reproduce the experimental

([10]) E. Clementel and C. Villi: *Nuovo Cimento*, **2**, 352 (1955). Both for mechanical or graphical solution of the equation system in δ_0, δ_1 and δ_2 it is convenient to divide by 4 the relation (2) of this note, which corresponds to Eq. (I; 28).

value of the quantity (see (I; 32))

$$(4) \qquad p(\vartheta) = \frac{k^2\sigma(\vartheta)P(\vartheta, \varphi = 0)}{\sin 2\vartheta} = 3(\delta_0|\delta_1) + \frac{9}{2}(\delta_1|\delta_2),$$

having defined $(\delta_i|\delta_j) \equiv \sin\delta_i \sin\delta_j \sin(\delta_i - \delta_j)$.

A further reduction of the sets fitting the differential and polarization data can be obtained by imposing continuity versus energy. Because the polarization has been so far measured only at high energies, we shall start our analysis discussing the Berkeley ([11]) experiments at 170 and 260 MeV.

2. – Analysis of Scattering Data at 170 and 260 MeV.

Although the S and P wave approximation has doubtless greater validity at lower energies, we have been forced to start with the high energy data, where polarization measurements, which are needed to select the S phase-shift K_0, are available.

Having assumed, according to Eq. (4), the polarization $P(\vartheta)$ to be a pure $\sin 2\vartheta$ curve, the function $p(\vartheta)$ reduces to the constant term on the right hand side of Eq. (4) for $\vartheta = 45°$. Using the experimental results at 130, 170, 210, and 300 MeV ([12-15]), given in Table I, it is seen that in the energy range 130÷300 MeV, the polarization at $\vartheta = 45°$ is a linear function of the incident

TABLE I. – *Proton-proton polarization at* $\vartheta = 45°$.

E_{lab} (MeV)	$P(45°)$	$k^2\sigma(\vartheta)$	$p(45°)$
300	0.31 (± 0.02)	1.41	0.44
260	0.28	1.20	0.34
210	0.23 (± 0.04)	0.95	0.23
170	0.213 (± 0.032)	0.79	0.17
130	0.180 (± 0.042)	0.67	0.12
95	0.15	0.55	0.08

([11]) O. CHAMBERLEIN and J. D. GARRISON: *Phys. Rev.*, **95**, 1349 (1954). For reader's convenience we refer to: L. BERETTA, C. VILLI and F. FERRARI: *Suppl. Nuovo Cimento*, **12**, 499 (1954), where all the experimental data used in our analysis can be found collected.

([12]) J. M. DICKINSON and D. C. SALTER: *Nature*, **173**, 946 (1954).

([13]) D. FISHER and J. BALDWIN: *Phys. Rev.*, **100**, 1445 (1956).

([14]) C. L. OXLEY, W. F. CARTWRIGTH and J. ROUVINA: *Phys. Rev.*, **93**, 806 (1954).

([15]) D. FISHER and G. GOLDHABER: *Phys. Rev.*, **95**, 1350 (1954); O. CHAMBERLAIN, G. PETTENGILL, E. SEGRE and C. WIEGAND: *Phys. Rev.*, **95**, 1348 (1954).

energy, and can be represented by the equation $P(45°) - 0.08 + 0.77 \cdot 10^{-3} E_{lab}$. According to this relation the value of $P(45°)$ has been interpolated at 260 MeV and extrapolated down to 95 MeV. The value of $k^2\sigma(45°)$ at 130 and 210 MeV has been also interpolated.

The least squares values of the quantities z_1 and z_2 are given in Table II for some values of K_0 between $-45°$ and $45°$. The combination z_3 does not depend practically on K_0, and its average value is shown in parenthesis. The values of z_1 and z_2 of Table II follow from the central values of the differential data. We have calculated the errors of these quantities in few cases, and we have seen that this amounts to change the final results of no more than about 10 percent. Furthermore, all the P phase shifts listed below have been approximated to the nearest half degree, and derived using the mechanical analyser already described ([10]).

The behaviour of the sets A and D following from Table II for 170 MeV is shown in Fig. 1. The associated solutions B and C are mirror sets (change of sign of all the phase shifts) only if z_2 is equal to zero: this is just the case for $K_0 = 45°$ and practically for $K_0 = 30°$. It is interesting to observe that for $K_0 = -15°$ the set D satisfies the condition $\delta_2 > \delta_1 > \delta_0$, which corresponds to the level inversion required by the nuclear shell model. At 260 MeV none of the solutions satisfy again this condition.

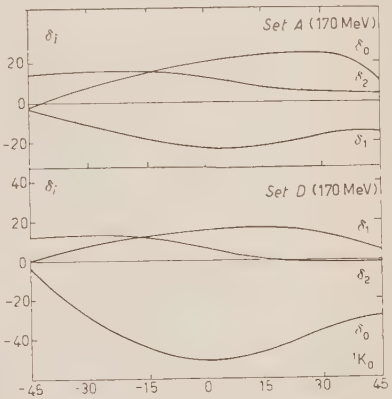

Fig. 1. – Behaviour of the P phase shifts (set A and D) at 170 MeV for $-45° \leqslant K_0 \leqslant 45°$.

Both at 170 and 260 MeV we have calculated the quantity $p(\vartheta)$ for $\vartheta = 45°$ as a function of K_0, and the results are reproduced for the four possible sets in Fig. 2. Because at 170 MeV only the solutions A and D cross the experi-

TABLE II. – *Values of* z_1 *and* z_2 *at* 170 *and* 260 MeV *as function of* K_0.

E_{lab} (MeV)	$K_0 =$	$-45°$	$-30°$	$-15°$	0	15°	30°	45°
170	z_1	0.228	0.480	0.667	0.739	0.679	0.501	0.253
($z_3 = 0.076$)	z_2	0.964	0.902	0.724	0.476	0.224	0.037	−0.001
260	z_1	0.630	0.881	1.068	1.140	1.078	0.898	0.650
($z_3 = 0.054$)	z_2	0.538	0.482	0.306	0.059	−0.194	−0.384	−0.461

mental line, while at 260 MeV the experimental value of $p(45°)$ can be fitted only with the solutions A and C, for continuity reasons we have to select solution A as the « correct » one. From Fig. 2 it is clear that in either case, if we had limited our analysis to a single energy, we could not disregard one of the two solutions, and therefore wehad been left wite four possible values for K_0. The solution A crosses the experimental value of $p(45)°$ for $K_0 = 19°$ and $K_0 = -18°$ at 170 MeV, while at 260 MeV the crossing occurs for $K_0 = 11°$ and $K_0 = -22°$. We believe that the value $K_0 = -18°$ at 170 MeV is not a realistic one because it would imply a far too large core radius for the proton-proton central interaction. The other value $K_0 = 19°$ at 170 MeV can be thought of as continuously linked either to the value $K_0 = 11°$ or $K_0 = -22°$ at 260 MeV. With the latter choice, the S phase shift K_0 changes sign somewhere between 215 and 220 MeV, implying a repulsive core radius of about $0.4(\hbar/\mu c)$. Although this behavior of the S phase shift reflects current ideas on the two-body potential, the other way of joining the phase shift K_0 at 260 MeV cannot be excluded on the basis of the available experimental data concerning the

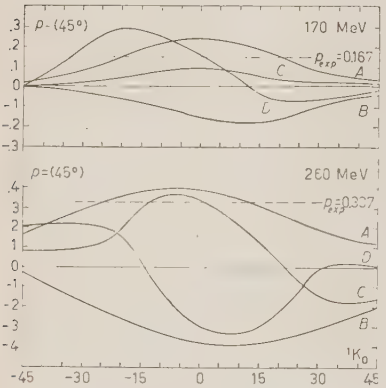

Fig. 2. – Behaviour of the function $p(\vartheta)$ for $\vartheta = 45°$ at 170 MeV and 260 MeV with the four sets of Table III for $-45° \leqslant K_0 \leqslant 45°$.

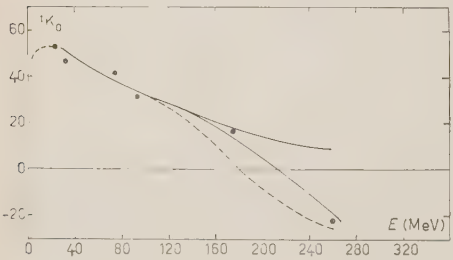

Fig. 3. – The S phaseshift K_0 versus energy. The two upper tracks differ for the choise of K_0 at 260 MeV. The dotted track corresponds to the choise $K_0 = 0$ at 170 MeV.

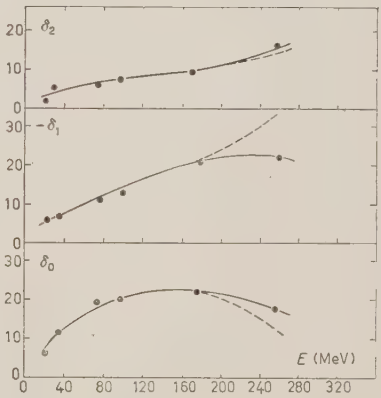

Fig. 4. – The triplet P phaseshifts (set A) versus energy. The continuous track corresponds to the choise $K_0 = -22$, the dotted one to the choise $K_0 = 11$ at 260 MeV.

proton-proton scattering. On the contrary, a positive value for K_0 at 260 MeV seems to be required by the continuity of the neutron-proton phase shifts versus energy ([16]). The four solutions corresponding to the two alternatives are given in Table III and IV.

TABLE III. – *Energy dependence of the singlet S phase shift K_0 and of the correspoding four sets of triplet P phase shifts δ_0, δ_1 and δ_2.*

E_{lab} (MeV)	18 ($K_0=52°$)			30 ($K_0=47°$)			75 ($K_0=19°$)		
Set	δ_0	δ_1	δ_2	δ_0	δ_1	δ_2	δ_0	δ_1	δ_2
A	6.5	— 3.5	2.0	11.5	— 5.0	5.0	19.5	-10.5	6.5
B	— 4.5	5.5	-1.0	— 8.0	8.5	—1.5	—15.0	14.5	— 2.0
C	10.0	— 2.0	1.0	14.5	— 1.5	2.0	28.0	— 6.0	2.0
D	— 9.0	3.5	1.0	—10.0	6.0	2.0	—24.0	10.5	2.0

E_{lab} (MeV)	95 ($K_0=32°$)			170 ($K_0=19°$)			260 ($K_0=-22°$)		
Set	δ_0	δ_1	δ_2	δ_0	δ_1	δ_2	δ_0	δ_1	δ_2
A	20.0	—12.0	7.0	21.5	-20.5	9.5	17.5	—25.0	-15.5
B	—17.0	26.0	—2.5	—18.5	23.5	—7.0	—11.0	31.5	— 8.5
C	32.0	— 6.5	2.5	50.5	— 9.5	2.5	81.0	0.5	3.0
D	—26.0	12.0	2.5	—46.0	15.0	3.0	—74.0	6.5	3.5

In view of a further discussion of the results obtained by FESHBACH and LOMON, we give in Table V the solutions at 170 MeV corresponding to the

TABLE IV. – *Triplet P phase shifts at 260 MeV corresponding to $K_0 = 11°$.*

Set	δ_0	δ_1	δ_2
A	16.5	— 32.0	11.5
B	— 19.0	30.0	— 14.0
C	78.0	— 14.0	4.0
D	— 79.5	12.0	— 6.0

TABLE V. – *Triplet P phase shifts 170 MeV corresponding to $K_0 = 0$.*

Set	δ_0	δ_1	δ_2
A	20.5	— 20.0	13.5
B	— 13.0	27.5	— 6.0
C	58.5	— 4.0	3.0
D	— 50.5	20.2	4.0

([16]) E. CLEMENTEL and C. VILLI: see the forthcoming paper on neutron-proton scattering to be published in the *Nuovo Cimento*.

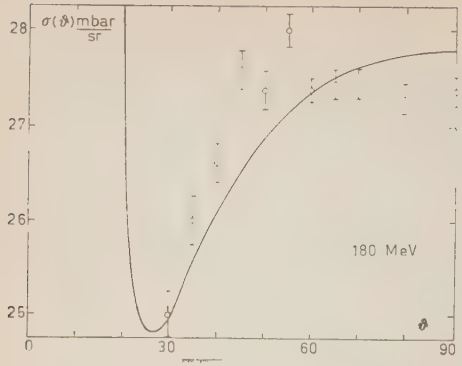

Fig. 5. – Differential cross-section at 18 MeV. The theoretical curve follows from the phase shifts given in Table III.

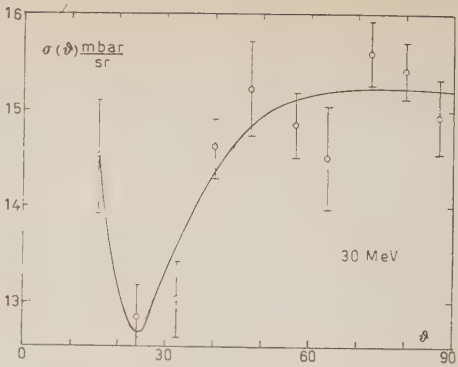

Fig. 6. – Differential cross-section at 30 MeV. The theoretical curve follows from the phase shifts given in Table III.

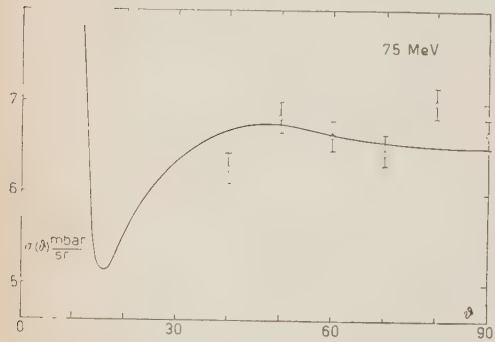

Fig. 7. – Differential cross-section at 75 MeV. The theoretical curve follows from the phase shifts given in Table III.

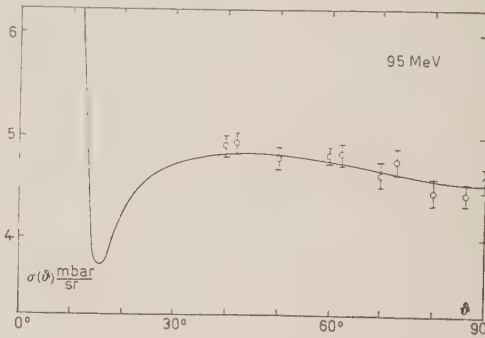

Fig. 8. – Differential cross-section at 95 MeV. The theoretical curve follows from the phase shifts given in Table III.

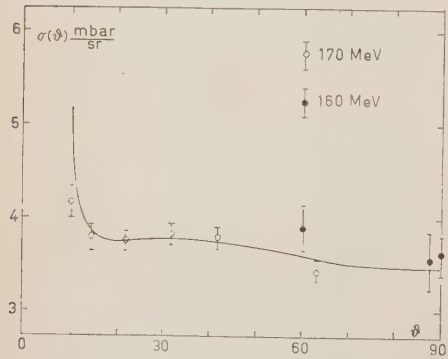

Fig. 9. – Differential cross-section at 170 MeV. The theoretical curve follows from the phase shifts given in Table III.

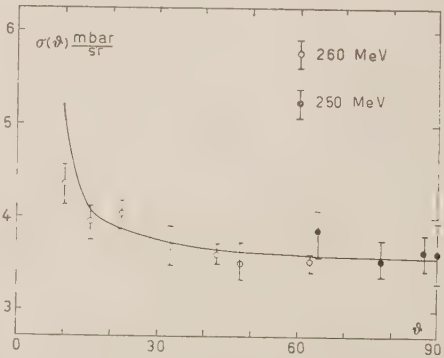

Fig. 10. – Differential cross-section at 260 MeV. The theoretical curve follows from the phase shifts given in Table III.

choice $K_0 = 0$, where solution D crosses $p_{exp}(45°)$. It is seen from Fig. 2 that this solution does not fit the polarization at 260 MeV and the best one could do is to join the value $K_0 = 0$ at 170 MeV with a value of K_0 equal or lower than $-20°$ at 260 MeV.

3. – Analysis of the Scattering Data at 18 and 30 MeV.

The analysis of the data at 18 and 30 MeV ([17,18]) is facilitated mainly because the phaseshift K_0 at 18 MeV must join the results of the effective range theory at lower energies. The choice of the solution at 30 MeV is bound to the condition to have a lower K_0 and higher P phase shifts. This condition is restrictive only in the sense that, being the two energies rather close each other, the range of variability of K_0 cannot be very wide.

The least squares values of the quantities z_1 and z_2 are given in Table VI for some positive values of K_0.

TABLE VI. – *Least squares values of z_1 and z_2 at 18 and 30 MeV as functions of K_0.*

E_{lab} (MeV)	$K_0 =$	0	15°	30°	45°	55°
18 ($z_3 = 0.009$)	z_1	0.623	0.574	0.407	0.164	−0.022
	z_2	0.806	0.549	0.310	0.125	0.120
30 ($z_3 = 0.035$)	z_1	0.565	0.511	0.340	0.094	0.082
	z_2	0.836	0.588	0.388	0.306	0.315

Being z_1 necessarily a positive quantity, it follows from Table VI that both for 18 and 30 MeV the phase shift K_0 must be less than 55°. The effective range theory ([17]) suggests for K_0 a value of $53 \div 54°$ at 18 MeV. In Table VII we give the P phase shifts for $K_0 = 52°$ and 15° at 18 MeV, and $K_0 = 47°$ and 40° at 30 MeV. In these intervals the P phase shifts depend practically linearly on K_0. The analysis of the deuteron photo-disintegration experiments ([20])

([17]) J. L. YNTEMA and M. G. WIGHT; *Phys. Rev.*, **95**, 1226 (1956).
([18]) F. L. FILLMORE: *Phys. Rev.*, **83**, 1252 (1951).
([19]) J. D. JACKSON and J. M. BLATT: *Rev. Mod. Phys.*, **22**, 77 (1950).
([20]) S. HSIEH: *Prog. Theor. Phys.*, **15**, 79 (1956); **16**, 68 (1956); *Nuovo Cimento*, **4**, 138 (1956). We are very much indebted to Dr. HSIEH of Nagoya University for a useful correspondence, of great help to us in analyzing the low energy scattering data. The polarization of nucleons from the photo disintegration of the deuteron has been

TABLE VII. – *Triplet P phase shifts at* 18 *and* 30 MeV *as functions of* K_0.

	$E_{lab} = 18$ MeV							$E_{lab} = 30$ MeV						
Set	$K_0 = 52°$			$K_0 = 45°$			Set	$K_0 = 47°$			$K_0 = 40°$			
	δ_0	δ_1	δ_2	δ_0	δ_1	δ_2		δ_0	δ_1	δ_2	δ_0	δ_1	δ_2	
A	6.5	−3.5	2.0	14.0	−9.5	4.0	*A*	11.5	−5.0	5.0	17.5	−8.0	5.0	
B	−4.5	5.5	−1.0	−12.5	11.5	−2.5	*B*	− 8.0	8.5	−1.5	−16.5	9.5	−4.0	
C	10.0	−2.0	1.0	23.0	−6.0	1.0	*C*	14.5	−1.5	2.0	24.5	−4.5	2.0	
D	−9.0	3.5	1.0	−21.0	7.5	1.5	*D*	−10.0	6.0	2.0	−20.5	8.5	2.0	

would suggest a value of K_0 near to the lower limit, which corresponds to a larger separation among the *P* phase shifts. In our final results (Table III) we have chosen the solutions corresponding to the upper value of K_0, although many other combinations would be possible, without destroying the phase shift continuity.

The upper limit solutions given in Table VI are rather close to the solutions derived by MARTIN and VERLET [21], using Levy potential in Born approximation; more exact calculations [22] have later shown that this potential cannot possibly fit the experimental data at 30 MeV [23].

4. – Phase shifts at 75 and 95 MeV.

The knowledge of the *S* and *P* phase shifts at 18, 30, 170 and 260 MeV fixes in an unique way the solutions at 75 and 95 MeV [24,25] because, apart from the fit of the angular distribution data, one must have continuity both in the phase shifts and in the quantities z_1, z_2, z_3. The sets thus found are

recently investigated using the phase shifts of the present paper by W. CŻYZ and J. SAWICKI (*Nuovo Cimento*, **5**, 45 (1957). We thank the Authors for a preprint of their work.

[21] A. MARTIN and L. VERLET: *Phys. Rev.*, **89**, 519 (1953).

[22] A. MARTIN and L. VERLET: *Nuovo Cimento*, **12**, 483 (1954).

[23] As one should expect on theoretical grounds, this failure has been confirmed at higher energies by a recent exact calculations done by M. S. WERTHEIM, M. H. HULL and A. M. SAPERSTEIN (*Phys. Rev.*, **104**, 764 (1956)). We thank Prof. BREIT for letting us know the results before publication.

[24] H. W. BIRGE, U. E. KRUSE and N. F. RAMSEY: *Phys. Rev.*, **83**, 274 (1951).

[25] U. E. KRUSE, J. M. TEEM and N. F. RAMSEY: *Phys. Rev.*, **94**, 1795 (1954); **101**, 1079 (1956).

given in Table III and they do not depend practically from the choice of K_0 at 170 MeV mainly because of the stability of the P phase shifts (see Table III and V) at this energy against variations of K_0. The set A at 95 MeV gives $p(45°) = 0.064$, which is lower than the value listed in Table I, but it is out of doubt that the linear extrapolation used overestimates $p(45°)$ at 95 MeV. The set D at 95 MeV corresponds to $p(45°) = 0.034$.

5. – Stability of the S and P Wave Solutions.

We have checked the stability of some sets at 170 MeV against the introduction of the ${}^1D_2(K_2)$ and the ${}^3F_2(\delta_{23})$ phase shifts using the following procedure, analogous to the one used by OHNUMA and FELDMAN ([4]).

If we ignore the Coulomb effects, we can consider the two expansions

$$k^2\sigma(\vartheta) = A_0 + A_2P_2(\cos\vartheta) + A_4P_4(\cos\vartheta)\,, \tag{5a}$$

$$\frac{k^2\sigma(\vartheta)P(\vartheta)}{\sin\vartheta} = B_1P_1(\cos\vartheta) + B_3P_3(\cos\vartheta)\,. \tag{5b}$$

The expansion coefficients in terms of the phase shifts in the approximation in which the ${}^3P_2 - {}^3F_2$ coupling is neglected, are given by the following expressions ([8-16])

$$A_0 = (K_0, K_0) + 5(K_2, K_2) + \sum_{j=0}^{2}(2j+1)(\delta_{j1}, \delta_{j1}) + 5(\delta_{23}, \delta_{23})\,, \tag{6a}$$

$$\begin{aligned} A_2 = {} & (50/7)(K_2, K_2) + 10(K_0, K_2) + (3/2)(\delta_{11}, \delta_{11}) + \\ & + (7/2)(\delta_{21}, \delta_{21}) + 4(\delta_{01}, \delta_{21}) + 9(\delta_{11}, \delta_{21}) + (32/7)(\delta_{23}, \delta_{23}) + \\ & + 6(\delta_{01}, \delta_{23}) + 6(\delta_{11}, \delta_{23}) + (6/7)(\delta_{21}, \delta_{23})\,, \end{aligned} \tag{6b}$$

$$A_4 = (90/7)(K_2, K_2) + (10/7)(\delta_{23}, \delta_{23}) + (120/7)(\delta_{21}, \delta_{23})\,, \tag{6c}$$

$$B_1 = 6\,[(\delta_{01}\,|\,\delta_{21}) - (\delta_{01}\,|\,\delta_{23}) + (3/2)(\delta_{11}\,|\,\delta_{21}) - (3/2)(\delta_{11}\,|\,\delta_{23}) - (5/7)(\delta_{21}\,|\,\delta_{23})]\,, \tag{7a}$$

$$B_3 = -30(\delta_{21}\,|\,\delta_{23})\,, \tag{7b}$$

where we have used the notation $(\delta_i, \delta_j) \equiv \sin\delta_i \sin\delta_j \cos(\delta_i - \delta_j)$.

To neglect the coupling at 170 MeV is probably not too serious, because it has been shown ([6]) that at 300 MeV the effect of the coupling is practically negligible. From B_3, using the known value of δ_{21} as first approximation, the phase shift δ_{23} follows. Then, introducing in the expression of B_1 the values

of δ_{01} and δ_{11} corresponding to the value of δ_{21} already used, the theoretical B_1 is calculated. If this step does not reproduce the «experimental» B_1, one moves along the curves giving the behaviour of the three P phase shifts versus energy (Fig. 4), up or down as the case may be. Once B_1 has been reproduced, the phase shift K_2 follows from A_4 while its sign is fixed by A_2. Finally the coefficient A_0 gives K_0, and its sign has been chosen according to the results of the S and P wave analysis.

We have used the parameters $B_1 = 0.103 \pm 0.048$ and $B_2 = 0.419 \pm 0.104$ given by FISHER and BALDWIN [13]; from the Berkeley data [11] we have derived the least squares parameters $a_0 = 0.749$, $a_2 = 0.057$, $a_4 = 0.031$. For $K_0 = 19°$ the new A solution at 170 MeV is found to be

$$K_0 = 16°, \quad K_2 = -7°.8, \quad \delta_{01} = 21°.8, \quad \delta_{11} = -18°.5, \quad \delta_{21} = 8°.7, \quad \delta_{23} = -4°.9,$$

which is of the same type and rather close to the solutions labelled as C and D, found by OHNUMA and FELDMAN [1] in the analysis of 150 MeV proton-proton scattering data. The solution A for $K_0 = 0$ gives instead

$$K_0 = 13°.5, \quad K_2 = -7°.7, \quad \delta_{01} = 21°.1, \quad \delta_{11} = -17°.7, \quad \delta_{21} = 10°.8, \quad \delta_{23} = -3°.8 .$$

It is seen that the value of K_0 is raised to a value near to the one of the previous solution, while the P phase shifts are practically stable. The reverse happens for our D solution ($K_0 = 19°$); in fact we obtain:

$$K_0 = 0, \quad K_2 = 4°.5, \quad \delta_{01} = -24°.5, \quad \delta_{11} = 12°.8, \quad \delta_{21} = 2°.0, \quad \delta_{23} = -16°.4 .$$

Finally, the D solution corresponding to $K_0 = 0$ gives

$$K_0 = 0, \quad K_2 = 4°.5, \quad \delta_{01} = -25°.9, \quad \delta_{11} = 11°.8, \quad \delta_{21} = 2°.0, \quad \delta_{23} = -16°.4 .$$

The order of magnitude of the phase shift δ_{23} of the two solutions A is in agreement with the results of Feshbach and Lomon, while the phase shift K_2 corresponding to the two D sets has the same sign but a higher value. In the case of the solutions D, the small value of the phase shift δ_{21} is responsible for the high value of the phase shift δ_{23}.

6. – Concluding Remarks.

It is clear from the previous analysis that, even in the lowest approximation, with the available scattering and polarization data is it not possible to give a unique answer to the problem of finding a set of phase shifts reproducing

with continuity the experimental data over the range of energy from 18 to 260 MeV. Polarization experiments at energies lower than 170 MeV should in principle allow a selection of the correct P set, because in this region the ambiguity on the sign of the phase shift K_0 disappears, and furthermore the lower the energy the more reliable the application of the method. We feel that as long as the correct P set has not been fixed at energies of the order of 100 MeV, it will be difficult to find out a criterion for selecting the correct solution among the several ones found at higher energies, considering besides the S and P states the contribution of higher order waves. The S and P states are certainly dominant in proton-proton scattering, and therefore they should be « isolated » performing scattering and polarization experiments in the region of 100 MeV. The attempt done at Berkeley and Yale University to analyze the 300 MeV data with electronic computers is rather discouraging, because no one common solution has been found. This is not the case in the S and P wave approximation, not only because there are less ambiguities due to the limited number of waves, but also because the problem can be handled mathematically and the choise of the set of phase shifts can be reduced to the solution of graphical or analytical relations. This explains why some of our sets are in agreement with sets given by GARREN, KLEIN, FESHBACH and LOMON and OHNUMA and FELDMAN.

We can compare the solutions given by GARREN at 200 MeV with our solutions at 170 MeV. Referring to Table II of Garren, the set A corresponds to our set D of Table V, while sets B'' and B''' are our sets D and A. In fact, for $K_0 = -38°$ we find for the P phase shifts of the set D the values $\delta_0 = -18°$, $\delta_1 = 4°$, $\delta_2 = 13°$, and for $K_0 = -30°$ the P phaseshifts of the set A are $\delta_0 = 9°$, $\delta_1 = -10°.5$, $\delta_2 = 15°.2$.

The sets given by KLEIN at 170 MeV for $K_0 = 26°$ and $-26°$ are of the type A, those for $K_0 = 7°$ and $-37°$ of the type D (the latter one corresponds to the solution B'' of Garren), while those for $K_0 = 27°$ and $-13°$ are of the type B. The sets given at 260 MeV for $K_0 = 23°$ and $-35°$ are of the type A, the set for $K_0 = -43°$ is of the type D and finally those for $K_0 = 35°$ and $-27°$ are both of type B. All the previous sets follow from the parameters given in Table II.

The triplet P phase shift given by FESHBACH and LOMON corresponds practically to our set D, having the phase shift δ_{01} negative throughout the energy region up to 260 MeV. This solution fits the polarization data at 170 MeV provided $K_0 = 0$ (alternative A of Feshbach and Lomon), but it appears rather unstable against introduction of the $^1D_2$ and $^3F_2$ phase shifts (Sect. 5).

In agreement with OHNUMA and FELDMAN we find that the $^1S_1$, $^1D_2$ and $^3P_2$, $^3F_2$ pairs of phase shifts have opposite sign. The negative sign for the $^1D_2$

phase shift is required to fit the neutron-proton scattering data ([16]) using the same partial wave approximation as in Sect. **5**.

In spite of the fact that the information obtained from the experimental data do not give so far a satisfactory set of phase shifts, mainly because of the lack of uniqueness, the results obtained by any approach which avoids a potential model can be used to derive and discuss some phenomenological parameters, like the real and imaginary part of the nucleon-nucleus potential ([26,27]). Although the fit of these parameters is less critical than the fit of the original scattering data, it may nevertheless help in excluding some of the ambiguities connected with any phase shift analysis. For instance, the real part of the potential should change sign nearby the scattering energy at which the S singlet phase shift becomes negative ([27]).

* * *

We acknowledge the Electronic Computing Center of the Politecnico of Milan for a very helpful cooperation in various stages of this analysis, and Dr. L. Beretta for computational assistance in the early stage of this work. We like to thank also Mr. A. Dozza for many ingenious mechanical improvements devised in the construction of the P-triplet phase shift analyzer.

Note added in proof.

Recent phase shift calculations performed by J. L. Gammel, R. S. Christian and R. M. Thaler (*Phys. Rev.*, **105**, 311 (1957)), using a phenomenological two-nucleon potential of Yukawa type, are in good agreement with the behaviour of the singlet S phase shift changing sign at about 220 MeV and with the set A for the triplet P state given in the present paper.

([26]) J. S. Bell and T. H. R. Skyrme: to be published. We thank the Authors for a preprint of their work.

([27]) W. B. Riesenfeld and K. M. Watson: *Phys. Rev.*, **102**, 1157 (1956).

RIASSUNTO

I dati sperimentali sulla diffusione protone-protone fra 18 e 260 MeV vengono discussi sulla base di un metodo analitico limitando l'analisi al contributo dei soli stati S e P. Usando le misure di polarizzazione alle alte energie viene ottenuto un doppio sistema di fasi che riproducono le sezioni d'urto differenziali nell'intervallo energetico considerato. I due sistemi corrispondono a due diversi andamenti della fase del singoletto S, la quale può annullarsi a circa 220 MeV oppure decrescere con l'energia senza assumere valori negativi. Viene discussa la stabilità delle soluzioni trovate considerando il contributo delle onde relative agli stati $^1D_2$ e $^3F_2$. Infine le soluzioni vengono confrontate con quelle date da altri Autori.

IL NUOVO CIMENTO Vol. V, N. 4 1° Aprile 1957

On the Scattering of Particles by a Force Centre According to the Radiation Damping Theory.

A. Sokolov and B. Kerimov

State University - Moscow

(ricevuto il 17 Dicembre 1956)

Summary. — The elastic scattering of particles by a force centre at rest is investigated with the help of the radiation damping theory. Formulas are obtained both for the effective cross-sections and for the phase shifts of the scattering by the short-range force centre. In conclusion a comparison is given of the formulas obtained by different methods.

1. – Introduction.

The radiation damping theory in the continuous spectrum was developed [1-5] in order to investigate the meson-nucleon scattering. The perturbation theory may be used to calculate the elastic scattering effective cross-section σ only in the region of comparatively large de Broglie wavelength, $\lambda^2 > \sigma$. But the perturbation theory gives as a rule the unlimited increase of cross-sections with the energy in the region of small $\lambda^2 \ll \sigma$. The difficulty of the unlimited increase of cross-sections is removed when one takes into consideration the influence of the damping. In [1] the normalization-like relation was established:

$$C^+C + \sum_k{}' C'^+C' = 1 \,, \tag{1}$$

[1] A. Sokolov: *Journ. of Phys. USSR*, **5**, 231 (1941).
[2] W. Heitler: *Proc. Cambr. Phil. Soc.*, **37**, 291 (1941).
[3] A. H. Wilson: *Proc. Cambr. Phil. Soc.*, **37**, 301 (1941).
[4] W. Heitler: *The Quantum Theory of Radiation* (Oxford, 1954), p. 159-174.
[5] W. Pauli: *Meson Theory of Nuclear Forces* (New York, 1946), p. 41.

i.e., according to the damping theory, at any moment t the total sum of incident and scattered particles is constant. Therefore the damping theory may also be used to investigate the elastic scattering phenomena ([6,7]) connected with the so-called strong coupling.

In recent years the damping theory was applied to the investigation of the scattering and photoproduction of π-mesons on nucleons taking into account the nucleon's excited states (isobars). By suitable choice of the four empirical constants it became possible to explain ([8-10]) the resonance character of the cross section-energy dependence, in good agreement with experiments.

2. – The Fundamental Equations of Damping Theory.

The Dirac equation without external forces has the form

$$\left(-\frac{\hbar}{i}\cdot\frac{\partial}{\partial t} - H\right)\psi = 0\,, \tag{2}$$

where

$$H = \frac{\hbar c}{i}(\boldsymbol{\alpha}\nabla) + \varrho_3 mc^2\,, \tag{3}$$

is the Hamiltonian of the free Dirac particles; $\boldsymbol{\alpha} = \varrho_1\boldsymbol{\sigma}$ and ϱ_3 are the well-known Dirac matrices, m is the rest mass of the particle.

The general solution of equation (2) can be represented in the form:

$$\psi = L^{-\frac{3}{2}} \sum_{\boldsymbol{k},s,\varepsilon} C_{s\varepsilon}(\boldsymbol{k}) b_{s\varepsilon}(\boldsymbol{k}) \exp\left[-i\varepsilon cKt + i\boldsymbol{kr}\right], \tag{4}$$

where L^3 is the fundamental volume; the coefficients $C_{s\varepsilon}(\boldsymbol{k})$ determine the probability of finding the particle in the state $(\boldsymbol{k}, s, \varepsilon)$; $b_{s\varepsilon}(\boldsymbol{k})$ is the one column four row matrix. If one wishes to take the spin state ($\frac{1}{2}s = \pm\frac{1}{2}$) explicitly into consideration it is convenient to write down this matrix in spherical

---

([6]) A. SOKOLOV and B. KERIMOV: *Dokl. Akad. Nauk SSSR*, **105**, 961 (1955).
([7]) A. SOKOLOV and B. KERIMOV: *Dokl. Akad. Nauk SSSR*, **108**, 611 (1956).
([8]) S. MINAMI, T. NAKANO, K. NISHIJIMA, H. OKONOGI and E. YAMADA: *Progr. Theor. Phys.*, **8**, 531 (1952).
([9]) I. TAMM, J. GOLFAND and B. FAINBERG: *Žu. Éksper. Teor. Fiz.*, **26**, 649 (1954).
([10]) V. RITUS: *Žu. Éksper. Teor. Fiz.*, **27**, 660 (1954).

co-ordinates $\boldsymbol{k}(k, \theta, \varphi)$ as (see [11]):

$$b_{\varepsilon}(\boldsymbol{k}) = \frac{1}{\sqrt{2}} \begin{pmatrix} f(\varepsilon K)\cos\theta_s \\ f(\varepsilon K)\sin\theta_s \exp[i\varphi] \\ s\varepsilon f(-\varepsilon K)\cos\theta_s \\ s\varepsilon f(-\varepsilon K)\sin\theta_s \exp[i\varphi] \end{pmatrix} \tag{5}$$

where $\hbar\boldsymbol{k}$ is the momentum of the particle, $k_0 = mc/\hbar$

$$f(\varepsilon K) = \sqrt{1 + \frac{k_0}{\varepsilon K}}, \qquad \theta_s = \frac{\theta}{2} - \frac{\pi}{4}(1 - s), \tag{6}$$

and the quantity $\varepsilon = \pm 1$ characterizes the sign of the energy:

$$E = \varepsilon c\hbar K = \varepsilon c\hbar\sqrt{k^2 + k_0^2}. \tag{7}$$

One gets a similar solution for the conjugated equation, when $b^{+}_{s\varepsilon}(\boldsymbol{k})$ is the one row matrix.

Considering the elastic scattering of Dirac particles (electrons, nucleons) by a spherically symmetrical force field it is convenient to treat the interaction energy by the Fourier analysis

$$V(r) = L^{-3}\sum_{\varkappa} V_{\varkappa}\exp[-i\boldsymbol{\varkappa r}]. \tag{8}$$

We shall seek the solution of the Dirac equation in the presence of the scattering centre in the form:

$$\psi = L^{-\frac{3}{2}}\sum_{\boldsymbol{k}'',s''} C''_{s''}(t) b''_{s''}\exp[-icK''t + i\boldsymbol{k}''\boldsymbol{r}]. \tag{9}$$

Hence we get the following system of integro-differential equations for the coefficients $C'_{s'}$:

$$-\frac{1}{ic}\dot{C}'_{s'} = \frac{1}{c\hbar L^3}\left(H^{s's}_{\boldsymbol{k}',\boldsymbol{k}}\exp[icI''t]C_s + \sum'_{\boldsymbol{k}'',s''} H^{s's''}_{\boldsymbol{k}',\boldsymbol{k}''}\exp[ic(I' - I'')t]C''_{s''}\right), \tag{10}$$

$$-\frac{1}{ic}\dot{C}_s = \frac{1}{c\hbar L^3}\sum'_{\boldsymbol{k}'',s''} H^{ss''}_{\boldsymbol{k},\boldsymbol{k}''}\exp[-icI''t]C''_{s''} + \frac{V_0}{c\hbar L^3}C_s, \tag{11}$$

---

[11] A. Sokolov: *Journ. of Phys. USSR*, **9**, 363 (1945).

where

$$(12)\qquad \begin{cases} H^{s's''}_{\boldsymbol{k}',\boldsymbol{k}''} = b^{\prime +}_{s'} V_{|\boldsymbol{k}'-\boldsymbol{k}''|} b''_{s''}\,, & \text{etc.} \\ C'_{s'} = C_{s'_1}(\boldsymbol{k}', t)\,, & \text{etc.} \\ b^{\prime +}_{s'} = b^{+}_{s'_1}(\boldsymbol{k}')\,, \quad \Gamma' = K' - K, & \text{etc.} \\ V_0 = V_\varkappa \qquad \text{at} \qquad \varkappa = 0\,. \end{cases}$$

The coefficient C_s, describing the initial state of particles is written down separately in the system of equations (10), (11). The negative energy states ($\varepsilon = -1$) may generally not be taken into consideration as far as in this work we do not consider the influence of vacuum effects on the scattering.

If we assume that at the beginning of the interaction with the scattering centre ($t = 0$) the particle was in the state ($\boldsymbol{k}, s, \varepsilon = 1$), the coefficients C_s must satisfy the following initial conditions

$$(13)\qquad C'_{s'} = \delta_{\boldsymbol{k}'\boldsymbol{k}}\delta_{s's}\,,$$

at $t = 0$. We shall seek the solution of Eqs. (10), (11) satisfying the condition (13) in the form:

$$(14)\qquad C_s = \exp\left[-c\beta_1 t + ic\beta_2 t\right],$$

$$(15)\qquad C'_{s'} = \begin{cases} \dfrac{1}{c\hbar L^3}\cdot\dfrac{1-\exp\left[-c\beta_1 t + ic(\Gamma'+\beta_2)t\right]}{\Gamma'+\beta_2+i\beta_1}\sum\limits_j \varepsilon_j H^{s's}_{j,\boldsymbol{k}',\boldsymbol{k}}\,, & \text{at} \quad |\Gamma'| < |\Gamma_0|\,, \\ 0 & \text{at} \quad |\Gamma'| > |\Gamma_0|\,, \end{cases}$$

where

$$(16)\qquad \sum_j H^{s's}_{j,\boldsymbol{k}',\boldsymbol{k}} = H^{s's}_{\boldsymbol{k}',\boldsymbol{k}}\,.$$

One must choose so large a quantity Γ_0 that the oscillating function $\exp[\mp icI'_0 t]$ may be considered as practically zero. The quantities ε_j, β_1 and β_2 will be found from equations (10), (11).

To pass from the damping theory to the usual perturbation theory one must put

$$\beta_1 = \beta_2 = 0\,, \qquad \varepsilon_j = 1\,.$$

We make use of the following formula for the further computation (see, for

example, the formula (35.15) in ([12]))

$$\frac{\exp[c\beta_1 t - ic(\Gamma'' + \beta_2)t] - 1}{\Gamma'' + \beta_2 + i\beta_1} \approx \frac{\pi}{i}\delta(\Gamma'' + \beta_2)\,, \tag{17}$$

which is valid for the relatively narrow frequency interval

$$\beta_1 \ll \Gamma_0 \ll K\,. \tag{18}$$

To show this we make use of the relation:

$$I = \int_{K-\Gamma_0}^{K+\Gamma_0} \frac{\exp[c\beta_1 t - ic(K'' - K + \beta_2)t] - 1}{K'' - K + \beta_2 + i\beta_1} f(K'')\,\mathrm{d}K'' = \tag{19}$$

$$= \left[\frac{\pi}{i} + O\left(\frac{\beta_1}{i\Gamma_0}\,,\ \frac{\Gamma_0}{K}\right)\right] f(K - \beta_2)\,.$$

Neglecting the small quantities (see inequality (18)) in the right-hand side of (19), we obtain the relation (17). In a similar way one can also obtain the following relation:

$$\frac{\partial}{\partial t}\left|\frac{1 - \exp[-c\beta_1 t + ic(\Gamma' + \beta_2)t]}{\Gamma' + \beta_2 + i\beta_1}\right|^2 \approx 2\pi c \exp[-2c\beta_1 t]\delta(\Gamma' + \beta_2)\,. \tag{20}$$

Likewise one has also to make the anologous assumption of taking into account only the resonance terms when solving the analogous problems by perturbation theory ([13]).

Substituting (14), (15) into (10), (11) and taking (17) into account one obtains the equations for the determination of the quantities ε_j, β_1, β_2 ($|\Gamma''| < |\Gamma_0|$) ([1-3])

$$\sum_j (\varepsilon_j - 1)H^{s's}_{j,\boldsymbol{k}',\boldsymbol{k}} = \frac{kK}{8\pi^2 c\hbar i}\sum_{j,j',s''} \varepsilon_{j'} \oint \mathrm{d}\Omega'' H^{s's''}_{j,\boldsymbol{k}',\boldsymbol{k}''} H^{s''s}_{j',\boldsymbol{k}'',\boldsymbol{k}}\,, \tag{21}$$

$$\beta_1 - i\beta_2 = \frac{kK}{8\pi^2 c^2\hbar^2 L^3}\sum_{j,j',s''} \varepsilon_{j'} \oint \mathrm{d}\Omega'' H^{ss''}_{j,\boldsymbol{k},\boldsymbol{k}''} H^{s''s}_{j',\boldsymbol{k}'',\boldsymbol{k}} + \frac{iV_0}{c\hbar L^3}\,, \tag{22}$$

where $K'' = K - \beta_2 \approx K$, $\beta_1 \sim \beta_2 \sim 1/L^3$, $\mathrm{d}\Omega''$ is the elementary solid angle of the vector $\boldsymbol{k}''$.

([12]) A. Sokolov and D. Ivanenko: *Quantum Theory of Fields* (Moscow-Leningrad, 1952), p. 260.

([13]) V. Ginzburg: *Dokl. Akad. Nauk SSSR*, **24**, 130 (1939).

According to (15) we have $C' = 0$ at $|\Gamma'| > |\Gamma_0|$. In this case one obtains the following relation, instead of (21):

$$-\exp[ic\Gamma' t]\sum_j H^{s's}_{j,\boldsymbol{k},\boldsymbol{k}} = \frac{kK}{8\pi^2 c\hbar i}\exp[ic\Gamma' t]\sum_{j,j',s''}\varepsilon_{j'}\oint \mathrm{d}\Omega'' H^{s's''}_{j',\boldsymbol{k}',\boldsymbol{k}''}H^{s''s}_{j',\boldsymbol{k}'',\boldsymbol{k}}\,.$$

This is also valid since, as was pointed out, the oscillating function $\exp[\pm ic\Gamma' t]$ may be practically put equal to zero for comparatively large values of $c\Gamma' t$.

The equations (21), (22) constitute the foundation of the damping theory for the elastic particle scattering. It is seen from (22) that these equations cannot directly describe the scattering by a Coulomb centre (long-range forces) since in this case the quantity V_0 tends to ∞ (see formula (54) below).
In this case the effective cross-section may be obtained by the formula

$$\mathrm{d}\sigma_{ss'} = \frac{1}{N}\frac{\partial}{\partial t}\sum_{\boldsymbol{k}''} C'^{+}_{s'}C'_{s'} = \frac{K^2}{4\pi^2 c^2\hbar^2}\sum_{j',j}\varepsilon^{+}_{j'}\varepsilon_j H^{+ss'}_{j',\boldsymbol{k}',\boldsymbol{k}}H^{s's}_{j,\boldsymbol{k}',\boldsymbol{k}}\,\mathrm{d}\Omega'\,, \tag{23}$$

where $N = N_0 C^{+}_{s} C_{s} = (ck/L^3K)\exp[-2c\beta_1 t]$ is the number of a particles falling on unit area per unit time.

For the investigation of the elastic scattering of the spinless relativistic particles by a force centre at rest we shall use the Klein-Gordon scalar equation which may be represented by a system of two first-order equations:

$$\left(-\frac{\hbar}{i}\frac{\partial}{\partial t} - V(r)\right)\psi - \chi = 0\,, \tag{24}$$

$$\left(-\frac{\hbar}{i}\frac{\partial}{\partial t} - V(r)\right)\chi + c^2\hbar^2\nabla^2\psi - m_0^2c^4\psi = 0\,. \tag{25}$$

In this case we should seek the solution of Eqs. (24), (25) in the form:

$$\begin{cases} \psi = L^{-\frac{3}{2}}\sum_{\boldsymbol{k}''} C''(t)\dfrac{1}{\sqrt{E''}}\exp[-icK''t + i\boldsymbol{k}''\boldsymbol{r}]\,, \\ \chi = L^{-\frac{3}{2}}\sum_{\boldsymbol{k}''} C''(t)\sqrt{E''}\exp[-icK''t + i\boldsymbol{k}''\boldsymbol{r}]\,, \end{cases} \tag{26}$$

where $E'' = chK''$ and the charge density will be determined by the expression:

$$\varrho = \tfrac{1}{2}(\chi^{+}\psi + \psi^{+}\chi)\,. \tag{27}$$

Then for the determination of the coefficients C, as well as for the calculation of the effective cross-section, we may use the previous results which have been obtained for the Dirac particles (see (14)–(23)), if we limit ourselves to consider

one zero-value ($s = s' = s'' = 0$) of the parameter s, determining the spin state. In this case one must omit the spin indices (s) in the indicated equations.

3. – Scattering of Particles by a δ-Potential.

It is rather difficult to solve the system of Eqs. (21), (22) in the general case. Therefore we limit ourselves to the investigation of the scattering of the Dirac particle by a potential of the form:

$$V(r) = V_0\,\delta(\boldsymbol{r}) = L^{-3}V_0 \sum_{\boldsymbol{\varkappa}} \exp[-i\boldsymbol{\varkappa}\boldsymbol{r}], \tag{28}$$

$\delta(\boldsymbol{r})$ being the usual δ-function.

In this case, two spin states being present, one must divide the matrix element of interaction energy in two parts ($j, j' = 1, 2$) (*):

$$H^{s's}_{\boldsymbol{k}',\boldsymbol{k}} = H^{s's}_{1,\boldsymbol{k}',\boldsymbol{k}} + H^{s's}_{2,\boldsymbol{k}',\boldsymbol{k}}, \tag{29}$$

where

$$\begin{cases} H^{s's}_{1,\boldsymbol{k}',\boldsymbol{k}} = \dfrac{V_0}{2} f(K) f(K')(\cos\theta_s \cos\theta'_{s'} + \exp[i(\varphi - \varphi')] \sin\theta_s \sin\theta'_{s'}), \\ H^{s's}_{2,\boldsymbol{k}',\boldsymbol{k}} = \dfrac{V_0}{2} s s' f(-K) f(-K')(\cos\theta_s \cos\theta'_{s'} + \exp[i(\varphi - \varphi')] \sin\theta_s \sin\theta'_{s'}), \\ f(\pm K) = \sqrt{1 \pm \dfrac{k_0}{K}}. \end{cases} \tag{30}$$

Further, making us of the following orthogonality-conditions for the matrix elements

$$\begin{cases} \sum\limits_{s''} \oint \mathrm{d}\Omega'' H^{s's''}_{j,\boldsymbol{k}',\boldsymbol{k}''} H^{s''s}_{j',\boldsymbol{k}'',\boldsymbol{k}} = 2\pi V_0 \left[1 - (-1)^j \dfrac{k_0}{K}\right] H^{s's}_{j,\boldsymbol{k}',\boldsymbol{k}} \delta_{jj'}, \\ \sum\limits_{s''} \oint \mathrm{d}\Omega'' H^{ss''}_{j,\boldsymbol{k},\boldsymbol{k}''} H^{s''s}_{j',\boldsymbol{k}'',\boldsymbol{k}} = \pi V_0^2 \left[1 - (-1)^j \dfrac{k_0}{K}\right]^2 \delta_{jj'}, \end{cases} \tag{31}$$

and taking into account the Eqs. (29), (30), (31) one obtains the values of ε_1 and ε_2

$$\varepsilon_1 = \frac{1}{1 + i\vartheta_1}, \qquad \varepsilon_2 = \frac{1}{1 + i\vartheta_2}, \tag{32}$$

(*) The method of solving the problems of the damping theory by means of introducing several values of ε_i was examined in [1].

where

$$\delta_1 = \frac{V_0}{4\pi c\hbar} k(K + k_0)\,, \qquad \delta_2 = \frac{V_0}{4\pi c\hbar} k(K - k_0)\,. \tag{33}$$

By substituting the Eqs. (29), (32) in (23) one obtains the following expression for the differential cross-section for the elastic scattering of the Dirac particles:

$$\frac{\mathrm{d}\sigma_{ss'}}{\mathrm{d}\Omega'} = \frac{V_0^2 K^2}{32\pi^2 c^2\hbar^2}\left(1 + ss'\frac{(\boldsymbol{k}\boldsymbol{k}')}{kk'}\right)\cdot \left[\frac{(1 + (k_0/K))^2}{1 + \delta_1^2} + \frac{(1 - (k_0/K))^2}{1 + \delta_2^2} + 2ss'\frac{k^2}{K^2}\cdot\frac{1 + \delta_1\delta_2}{(1 + \delta_1^2)(1 + \delta_2^2)}\right]. \tag{34}$$

Summing over final spin states (s') and averaging over initial spin states (s), one obtains the following expression for the elastic differential cross-section:

$$\mathrm{d}\sigma = \frac{1}{2}\sum_{s,s'=\pm 1}\mathrm{d}\sigma_{ss'} = \frac{V_0^2 K^2}{16\pi^2 c^2\hbar^2}\cdot \left[\frac{(1 + (k_0/K))^2}{1 + \delta_1^2} + \frac{(1 - (k_0/K))^2}{1 + \delta_2^2} + 2\frac{k^2}{K^2}\cdot\frac{1 + \delta_1\delta_2}{(1 + \delta_1^2)(1 + \delta_2^2)}\cdot\frac{\boldsymbol{k}\boldsymbol{k}'}{kk'}\right]\mathrm{d}\Omega'\,. \tag{35}$$

Hence the integral elastic cross-section becomes:

$$\sigma = \frac{V_0^2 K^2}{4\pi c^2\hbar^2}\left[\frac{(1 + (k_0/K))^2}{1 + \delta_1^2} + \frac{(1 - (k_0/K))^2}{1 + \delta_2^2}\right]. \tag{36}$$

The values of β_1 and β_2 can be found with the help of the Eqs. (31), (32) and (22):

$$c\beta_1 = \frac{\sigma N_0}{2}\,, \quad c\beta_2 = \frac{\sigma N_0}{2}\cdot\frac{\gamma_1\delta_1 + \gamma_2\delta_2}{\gamma_1 + \gamma_2} - \frac{V_0}{\hbar L^3}\,, \quad \gamma_j = \frac{[1 - (-1)^j\sum'_{\boldsymbol{k}',s'}(k_0/K)]^2}{1 + \delta_j^2}\,. \tag{37}$$

It follows from the formulas (37) that the quantities β_1 and β_2 tend to zero if $L \to \infty$.

By means of the Eqs. (14), (37) and (36) one can show that the coefficients C will satisfy the normalization relation (1):

$$C_s^+ C_s + \sum'_{\boldsymbol{k}',s'} C_{s'}'^+ C'_{s'} = \exp[-\sigma N_0 t] + \sigma N_0\int_0^t \exp[-\sigma N_0 t]\,\mathrm{d}t = 1\,. \tag{38}$$

Making use of the perturbation theory we find the following expression for

the elastic scattering cross-section of a Dirac particle by a δ-potential:

$$\sigma_0 = \frac{1}{N_0}\frac{\partial}{\partial t}\frac{1}{2}\sum_{\boldsymbol{k}',s,s} C'^{*}_{s'} C'_{s'} - \frac{V_0^2}{2\pi c^2\hbar^2}(2k_0^2 + k^2)\,. \tag{39}$$

This relation can be obtained from the eqs. (36) if one puts there

$$\delta_1^2 = \delta_2^2 = 0\,. \tag{40}$$

The relation (39) is valid only in the range of comparatively low energies. At comparatively high energies $k \gg (1\pi c\hbar/V_0)^{\frac{1}{2}}$ of the incident particle the quantities δ_1^2, δ_2^2 increase very rapidly ($\delta_1^2 \gg 1$, $\delta_2^2 \gg 1$) and therefore the influence of damping cannot be neglected. In this case the cross-section begins to decrease when the energy increases:

$$\sigma = \frac{8\pi}{k^2} = 8\pi\lambda\!\!\!^{-2}\,. \tag{41}$$

The cross-section for the elastic scattering of the spinless relativistic particle by a δ-potential can be found in a similar way:

$$\sigma = \frac{V_0^2K^2}{\pi c^2\hbar^2}\cdot\frac{1}{1+\delta^2}\,, \tag{42}$$

where

$$\delta = \frac{kKV_0}{2\pi c\hbar}\,.$$

4. – Scattering of Particles by a Short-Range Force Centre.

In the general case of the short-range force we were able to get the solution of the equations (21) and (22) only for the spinless particles ($s = s' = s'' = 0$).

In this case, let us expand the components of potential energy in terms of Legendre functions $P_l(\cos\theta')$:

$$H_{\boldsymbol{k}',\boldsymbol{k}'} = V_{|\boldsymbol{k}''-\boldsymbol{k}'|} = \sum_{l=0}^{\infty} V_l''' = \sum_{l=0}^{\infty} b_l P_l(\cos\theta''')\,, \qquad \text{etc.} \tag{43}$$

where $l = j$, $H_{l,\boldsymbol{k}',\boldsymbol{k}'} = V_l'''$, θ''' is the angle between the vectors $\boldsymbol{k}'$ and $\boldsymbol{k}''$,

$$\cos\theta''' = \frac{(\boldsymbol{k}'\boldsymbol{k}'')}{k'k''} = \cos\theta'\cos\theta'' + \sin\theta'\sin\theta''\cos(\varphi' - \varphi'')\,,$$

and for the coefficients b_l one obtains

$$b_l = 2\pi(2l+1)\int_0^{\pi} P_l(\cos\theta''')\sin\theta'''\,\mathrm{d}\theta'''\int_0^{\infty} rV(r)\,\frac{\sin\left(\sqrt{2k^2(1-\cos\theta''')}\,r\right)\mathrm{d}r}{\sqrt{2k^2(1-\cos\theta''')}}\,. \tag{44}$$

Let us call the angles between the vector $\boldsymbol{k}$ directed along the $\bar{Z}$-axis and the vectors $\boldsymbol{k}'$ and $\boldsymbol{k}''$ directed as θ' and θ'' respectively. The corresponding values for the component of the potential will be designated as V_l' and V_l''. Integrating over the solid angle one can obtain the following orthogonality conditions

$$\oint \mathrm{d}\Omega'' V_l''' V_{l'}'' = \frac{4\pi b_l}{2l+1}\,V_l'\delta_{l'l}\,, \tag{45}$$

$$\oint \mathrm{d}\Omega'' V_l'' V_{l'}'' = \frac{4\pi b_l^2}{2l+1}\,\delta_{l'l}\,. \tag{46}$$

Taking into consideration the last expressions one finds for the quantities ε_l (see (21)):

$$\varepsilon_l = \frac{1}{1+ic_l}\,, \qquad l = 0, 1, 2, \ldots \tag{47}$$

where

$$c_l = \frac{kK}{2\pi c\hbar}\cdot\frac{b_l}{2l+1}\,. \tag{48}$$

Further taking into account the Eqs. (20) and (23) one obtains the following expressions for the differential cross-section (see [7]) (*)

$$\frac{\mathrm{d}\sigma}{\mathrm{d}\Omega'} = \frac{1}{k^2}\sum_{l,l'}\frac{c_l c_{l'}(1+c_l c_{l'})(2l+1)(2l'+1)P_l(\cos\theta')P_{l'}(\cos\theta')}{(1+c_l^2)(1+c_{l'}^2)}\,, \tag{49}$$

and for the total cross-section of elastic scattering according to the damping theory:

$$\sigma = \frac{4\pi}{k^2}\sum_{l=0}^{\infty}(2l+1)\sin^2\eta_l\,, \tag{50}$$

where (see [7] and [14]):

$$\sin^2\eta_l = \frac{c_l^2}{1+c_l^2}\,. \tag{51}$$

(*) In a similar way, it is easy to compute with the help of (49) the quantities:

$$\int_0^{\pi} P_n(\cos\theta')\,\frac{\mathrm{d}\sigma}{\mathrm{d}\Omega'}\sin\theta'\,\mathrm{d}\theta'\,, \qquad (n = 0, 1, 2, \ldots)$$

which can also characterize the angular distribution of scattering.

[14] H. A. BETHE and F. HOFFMAN: *Mesons and Fields*, Vol. II (New York, 1955), p. 212; B. LIPPMANN and J. SCHWINGER *Phys. Rev.*, **79**, 469 (1950).

with the help of the Eqs. (44), (48) one obtains for the coefficients c_l determining the phase of the scattered wave:

$$c_l = \operatorname{tg} \eta_l = -\frac{\pi K}{c\hbar} \int_0^\infty r V(r) J^2_{l+\frac{1}{2}}(kr)\, \mathrm{d}r \,, \tag{52}$$

$J_{l+\frac{1}{2}}$ being the Bessel function.

In the case of small values of c_l the expression (52) turns into the one which can easily be obtained by the perturbation theory ($\operatorname{tg} \eta_l \approx \eta_l$).

With the help of the last relations and taking into account also the Eq. (22), one obtains for β_1 and β_2:

$$c\beta_1 = \frac{\sigma N_0}{2}; \qquad c\beta_2 = \frac{\sigma N_0}{2} \cdot \frac{\sum_{l=0}^{\infty} (2l+1) \sin^2 \eta_l \operatorname{tg} \eta_l}{\sum_{l=0}^{\infty} (2l+1) \sin^2 \eta_l} - \frac{V_0}{\hbar L^3} \,. \tag{53}$$

Hence it follows that the coefficients C will satisfy the normalization relation (1).

5. – Scattering of Particles by a Yukawa Potential.

Let us apply the formulas obtained to the investigation of the scattering of a spinless relativistic particle by a force centre, when the potential energy is:

$$V(r) = -g^2 \frac{\exp[-\varkappa_0 r]}{r}, \quad \text{that is} \quad V_\varkappa = -\frac{4\pi g^2}{\varkappa_0^2 + \varkappa^2} \,. \tag{54}$$

By substituting (54) in (52) one obtains the following expression for the phase shift:

$$c_l = \operatorname{tg} \eta_l = \gamma \cdot Q_l(x) \,, \tag{55}$$

where

$$\gamma = \frac{g^2}{c\hbar} \cdot \frac{K}{k}, \qquad x = 1 + \frac{\varkappa_0^2}{2k^2} \,, \tag{56}$$

and

$$Q_l(x) = \frac{1}{2} \int_{-1}^{+1} \frac{P_l(y)\, \mathrm{d}y}{x - y} \,, \tag{57}$$

is the l-th Legendre spherical function of the second kind. According to the

formulas (50) and (55) one finds the value for the total elastic cross-section:

$$\sigma = \frac{4\pi}{k^2} \sum_{l=0}^{\infty} (2l+1) \frac{\gamma^2 Q_l^2(x)}{1 + \gamma^2 Q_l^2(x)} . \tag{58}$$

In the case of low energies of the incident particles, when the de Broglie wavelength is much greater than the force range, one may use the well-known asymptotic representation of the function $Q_l(x)$ which is valid for large x $(x \gg 1)$:

$$Q_l(x) \approx \frac{\Gamma(l+1)}{\Gamma(l+\frac{3}{2})} \cdot \frac{\sqrt{\pi}}{(2x)^{l+1}} \approx \frac{\sqrt{\pi}}{(2x)^{l+1} \sqrt{l+\frac{1}{2}}} . \tag{59}$$

Then the expression (58) can be transformed as follows

$$\sigma = \frac{V_0^2 K^2}{\pi c^2 \hbar^2} \left\{ \frac{1}{1+\delta^2} + \frac{4}{3} \cdot \frac{(k/\varkappa_0)^4}{1 + (4/9)(k/\varkappa_0)^4 \delta^2} + \cdots \right\}, \tag{60}$$

where $\delta^2 = V_0^2 k^2 K^2 / 4\pi^2 c^2 \hbar^2$. In the sum (60) there remains only the first term $(l = 0)$ describing the s-scattering at $\varkappa_0^2 \to \infty$ and $V_a = -4\pi g^2/\varkappa_0^2$. Then the formula (60) gives the cross-section for the scattering by a δ-potential already established for the spinless particle (see (42)).

On the contrary in investigating the scattering in the high energy region, we shall be especially interested in the case $x \to 1 + 0$.

In order to determine the asymptotic behaviour of the function $Q_l(x)$ in this case we shall make use of the method worked out in [15].

To this end we make the change of variable $x = \cosh\varphi$ $(x > 1)$ in the differential equation for the polynomial $Q_l(x)$:

$$(x^2 - 1) Q_l''(x) + 2x Q_l'(x) - l(l+1) Q_l(x) = 0 \tag{61}$$

and we shall seek the solution in the form:

$$Q_l(x) = F(\varphi) I(\varphi) , \tag{62}$$

$I(\varphi)$ being a cylindrical function the order of which is to be determined later. Then we obtain the following equation for the determination of the unknown

---

[15] A. SOKOLOV: *Vestnik Moskovskogo Gosudarstvennogo Universiteta*, **4**, 77 (1947); see also D. IVANENKO and A. SOKOLOV: *Classical Theory of Fields* (Moscow-Leningrad, 1951), p. 273.

functions F and I

$$I'' + \frac{1}{\varphi} I' - (l + \tfrac{1}{2})^2 (1 - \varepsilon) I + \frac{I'}{F}\left[\left(\operatorname{ctgh}\varphi - \frac{1}{\varphi}\right) F + 2F'\right] = 0 , \tag{63}$$

where

$$\varepsilon = (l + \tfrac{1}{2})^{-2} \cdot \left(\frac{1}{4} + \frac{F'}{F} \operatorname{ctgh}\varphi + \frac{F'}{F}\right) .$$

Choosing the function F so that the coefficient at $I' = \mathrm{d}I/\mathrm{d}\varphi$ shall vanish one has:

$$F = \sqrt{\frac{\varphi}{\sinh\varphi}} . \tag{64}$$

Then one finds

$$\varepsilon - \frac{1}{4}\left(l + \frac{1}{2}\right)^{-2} \cdot \left(\frac{1}{\sinh^2\varphi} - \frac{1}{\varphi^2}\right) .$$

Hence it is seen that ε is quickly tending towards zero not only at large values of $\varphi(\cosh\varphi \gg 1)$, but at small values $\varphi(\cosh\varphi \to 1)$, too. Indeed, when $\varphi \to 0$

$$\varepsilon \approx -\frac{1}{12}\left(l + \frac{1}{2}\right)^{-2} , \tag{65}$$

i.e. when $l > 0$ for the all considered range of the argument x, we see that $\varepsilon \ll 1$. Neglecting the quantity ε in the equation (63) we see that the function $I(\varphi)$ is the Bessel function of imaginary argument of the order zero (I_0 and K_0), which in the general case can be represented in the form:

$$I(\varphi) = D_1 I_0((l + \tfrac{1}{2})\varphi) + D_2 K_0((l + \tfrac{1}{2})\varphi) . \tag{66}$$

To determine the unknown coefficients D_1 and D_2, in accordance with the method described in [15] we have to write the Eqs. (62) for large values of x, the asymptotic values of functions coming into this equality being easy to obtain. Indeed the expression for the polynomial $Q_l(x)$ at $x > 1$ is determined by the formula (59), and the Bessel functions at large $\varphi \approx \ln 2x$ have the form:

$$\begin{cases} \sqrt{\dfrac{\varphi}{\sinh\varphi}}\, K_0((l + \tfrac{1}{2})\varphi) \approx \dfrac{\sqrt{\pi}}{\sqrt{l + \tfrac{1}{2}}(2x)^{l+1}} \\ \sqrt{\dfrac{\varphi}{\sinh\varphi}}\, I_0((l + \tfrac{1}{2})\varphi) \approx \dfrac{(2x)^l}{\sqrt{l + \tfrac{1}{2}}\sqrt{\pi}} . \end{cases} \tag{67}$$

Hence it follows that $D_1 = 0$, $D_2 = 1$.

Therefore in the case $x = \operatorname{chos}\varphi > 1$ the asymptotic behaviour of the function $Q_l(x)$ can be represented in the form:

$$Q_l(\cosh\varphi) \approx \sqrt{\frac{\varphi}{\sinh\varphi}}\, K_0((l+\tfrac{1}{2})\varphi)\,. \tag{68}$$

The behaviour of the function $Q_l(x)$ at $x=1+0$ ($\varphi=\operatorname{arc\,cosh} x \approx \sqrt{x^2-1}$) is determined by a simpler asymptotic formula:

$$Q_l(x) \approx K_0((l+\tfrac{1}{2})\sqrt{x^2-1})\,. \tag{69}$$

In a similar way it is easy to get, in the case $x = \cos\varphi < 1$:

$$Q_l(\cos\varphi) \approx -\frac{\pi}{2}\sqrt{\frac{\varphi}{\sin\varphi}}\, Y_0((l+\tfrac{1}{2})\varphi)\,, \tag{70}$$

and the function (70) is the analytical continuation of the function (68) as it is seen from the relation:

$$\frac{1}{2}\int_0^\infty \cos\left(t - \frac{(l+\tfrac{1}{2})^2(x^2-1)}{4t}\right)\frac{\mathrm{d}t}{t} =$$

$$= \begin{cases} K_0((l+\tfrac{1}{2})\sqrt{x^2-1})\,, & \text{at} \quad x = 1+0\,, \\ -\dfrac{\pi}{2}\, Y_0((l+\tfrac{1}{2})\sqrt{1-x^2})\,, & \text{at} \quad x = 1-0\,. \end{cases}$$

In a similar way it is easy to get the following asymptotic values for the first Legendre function $P_l(x)$:

$$\begin{cases} P_l(\cosh\varphi) \approx \sqrt{\dfrac{\varphi}{\sinh\varphi}}\, I_0((l+\tfrac{1}{2})\varphi) & \text{at} \quad x=\cosh\varphi>1, \\ P_l(\cos\varphi) \approx \sqrt{\dfrac{\varphi}{\sin\varphi}}\, J_0((l+\tfrac{1}{2})\varphi) & \text{at} \quad x=\cos\varphi<1, \end{cases} \tag{71}$$

where J_0 and Y_0 are the well-known Bessel functions of real argument of the order zero.

Thus at high energies ($x \to 1+0$) the phases η_l for the Yukawa potential have the following asymptotic values:

$$c_l = \operatorname{tg}\eta_l \approx \gamma K_0((l+\tfrac{1}{2})\sqrt{x^2-1})\,. \tag{72}$$

In this case the terms with comparatively large values of l in the sum (58) play a main role and accordingly passing from the summation to the integration with respect to y ($y = l \cdot \sqrt{x^2 - 1}$) one obtains for cross-section:

$$\sigma \approx \frac{8\pi}{k^2} \frac{1}{x^2 - 1} \int_0^\infty \frac{\gamma^2 y K_0^2(y)\, dy}{1 + \gamma^2 K_0^2(y)}. \tag{73}$$

Hence it is seen that one can neglect the influence of damping if in the point $y_0 \approx 0.165$, corresponding to the maximum value of the function $yK_0^2(y)$, the following inequality:

$$\gamma^2 K_0^2(y_0) \ll 1 \tag{74}$$

is valid. Then we obtain for the cross-section:

$$\sigma_{as.} \approx \frac{8\pi}{k^2} \frac{\gamma^2}{x^2 - 1} \int_0^\infty y K_0^2(y)\, dy = \frac{4\pi\gamma^2}{k^2(x^2 - 1)}, \tag{75}$$ (*)

which result coincides with the value obtained by the perturbation theory:

$$\sigma_0 = \frac{4\pi\gamma^2}{k^2} \sum_{l=0}^{\infty} (2l + 1) Q_l^2(x) = \frac{4\pi\gamma^2}{k^2(x^2 - 1)}. \tag{76}$$

In the other limiting case, when $\gamma^2 K_0^2(y_0) \gg 1$ the damping has to play a great role. In this case, according to the Eq. (73) we have for the cross-section:

$$\sigma \approx \frac{8\pi}{k^2} \cdot \frac{1}{x^2 - 1} \int_0^{Z_0} y\, dy = \pi \left(\frac{Z_0}{\varkappa_0} \right)^2, \tag{77}$$

Z_0 being determined from the equation $Z_0 / \pi\gamma^2 \exp[Z_0] = 1$, i.e. $Z_0 \approx \ln[\pi\gamma^2]$.

In other words at high energies ($K \approx k$) the scattering proceeds just as the scattering by a impenetrable sphere of constant radius:

$$\frac{Z_0}{\varkappa_0} = \frac{1}{\varkappa_0} \ln \left[\pi \left(\frac{g^2}{\hbar c} \right)^2 \right].$$

(*) More exactly the lower limit of the integral in (75) must have the value $\frac{1}{2}\sqrt{x^2 - 1}$. Therefore we may put $\sigma_{as.} = \sigma_0$ only if $\frac{1}{2}\sqrt{x^2 - 1} \ll y_0$.

6. – Scattering of Particles by a Uniform Potential Barrier.

Let us consider the scattering of particles by a sphere of radius a, the potential energy being given by:

$$V(r) = \begin{cases} D = \dfrac{3V_0}{4\pi a^3}, & r < a, \\ 0, & r > a. \end{cases} \tag{78}$$

If $a \to 0$, one comes once more to the case of scattering by a δ-potential. According to (52) the phase may be found from the relation:

$$c_l = \operatorname{tg} \eta_l \approx -\frac{\pi DK}{c\hbar k^2} \int_0^{ka} J_{l+\frac{1}{2}}^2(y) y \, dy \, . \tag{79}$$

In the first limiting case $ka \ll 1$ (one assumes that the radius of a sphere a is much smaller than the de Broglie wave length λ) the scattering is practically determined only by the phase of the s-wave: $c_0 = \operatorname{tg} \eta_0 = -\frac{2}{3}(DK/c\hbar)ka^3$. In this case, according to (50), the cross-section is

$$\sigma \approx \frac{4\pi}{k^2} \begin{cases} \gamma_1^2 & \text{at} \quad \gamma_1 = \dfrac{V_0 kK}{2\pi c\hbar} \ll 1 \, , \qquad (80) \\ 1 & \text{at} \quad \gamma_1 \gg 1 \, . \qquad (81) \end{cases}$$

The cross-section of scattering by a potential barrier can also be obtained by means of the adjustment method (i.e. the method of using the continuity condition of the wave function and its derivative at $r = a$) described in [16] (see, p. 28-44).

In the case $ka \ll 1$, only the s-phase ($l = 0$) will not vanish, and this phase, in the non-relativistic approximation ($K \approx k_0$), is given by

$$\eta_0 = \operatorname{arctg}\left[\frac{k}{\sqrt{d^2 - k^2}} \operatorname{tgh}\left(a\sqrt{d^2 - k^2}\right)\right] - ka \quad \text{at} \quad D - \frac{\hbar c d^2}{2k_0} > E - \frac{\hbar c k^2}{2k_0} \, . \tag{82}$$

Then in the case $ad \ll 1$ one obtains for the phase:

$$\eta_0^2 \approx k^2 a^2 \left(\frac{a^2 d^2}{3}\right)^2 \, . \tag{83}$$

---

[16] N. F. MOTT and H. S. W. MASSEY: *The Theory of Atomic Collisions* (Oxford, 1949).

On the contrary, in the case $ad \gg 1$ we shall have:

$$\eta_0^2 \approx k^2 a^2 . \tag{84}$$

Thus, the adjustment method gives, at $ka \ll 1$:

$$\sigma \approx \frac{4\pi}{k^2}\eta_0^2 \approx 4\pi a^2 \begin{cases} \left(\frac{\gamma_1}{ak}\right)^2 & \text{at} \quad \frac{3\gamma_1}{ak} \ll 1 , \quad (85) \\ 1 & \text{at} \quad \frac{3\gamma_1}{ak} \gg 1 . \quad (86) \end{cases}$$

Comparing (85) with (80) we see that both expressions are exactly equal to the one that can be obtained by means of the perturbation theory. However the range of validity of the perturbation theory will be different.

This, for example, leads to the conclusion that according to the adjustment method there should be no scattering by the δ-potential ($a \to 0$, Da^3 is a finite value) in contrast with the radiation damping theory.

At large values of V_0, the cross-section in the damping theory must be proportional to λ^2, while it must generally remain constant ($\sigma = 4\pi a^2$) according to the adjustment method.

In the other limiting case $ka \gg 1$ (the radius a is very much greater than the wave-length λ) the phase η_l in damping theory can be approximately found from the Eq. (79):

$$\operatorname{tg}\eta_l \approx -\frac{3\pi\gamma_1}{2(ka)^3} \begin{cases} \frac{2}{3\pi^2}\int_0^l (l-y)K_{\frac{2}{3}}^2\left[\frac{2^{\frac{2}{3}}}{3l^{\frac{1}{2}}}(l-y)^{\frac{3}{2}}\right] dy + \frac{2}{\pi}\int_l^{ka} \sin^2\left(y - \frac{\pi}{2}l\right) dy , \\ \qquad\qquad \text{at} \quad l < ka, \\ \frac{1}{2\pi}\int_0^{ka} \frac{y}{\sqrt{l^2-y^2}} \exp\left[-\left(l \ln \frac{l+\sqrt{l^2-y^2}}{l-\sqrt{l^2-y^2}} - \sqrt{l^2-y^2}\right)\right] dy , \\ \qquad\qquad \text{at} \quad l > ka, \end{cases}$$

or

$$\operatorname{tg}\eta_l \approx \begin{cases} -\frac{3\pi\gamma_1}{2(ka)^3}\left[\frac{3^{\frac{1}{2}}\Gamma^2(\frac{2}{3})l^{\frac{2}{3}}}{2^{\frac{5}{3}}\pi^2} + \frac{1}{\pi}(ka-l)\right] & \text{at} \quad l < ka, \\ 0 & \text{at} \quad l > ka, \end{cases} \tag{87}$$

where $K_{\frac{1}{3}}$ is the Bessel function of imaginary argument of the order $\frac{1}{3}$.

Therefore the damping theory gives ($ka \gg 1$):

$$\sigma \approx \frac{8\pi}{k^2} \int_0^{ka} \frac{[3\gamma_1/2(ka)^3]^2\, l(ka-l)^2\, \mathrm{d}l}{1 + [3\gamma_1/2(ka)^3]^2\, (ka-l)^2} \approx 4\pi a^2 \begin{cases} \frac{3}{8}\left[\frac{\gamma_1}{(ka)^2}\right]^2 & \text{at} \quad \frac{\gamma_1}{(ka)^2} \ll 1, \\ 1 & \text{at} \quad \frac{\gamma_1}{(ka)^2} \gg 1. \end{cases} \tag{88}$$

Using the adjustment method we find for the case $ka \gg 1$, with the help of the Eqs. obtained in ([16]) in the non-relativistic approximation:

$$\sigma \approx 2\pi a^2 \begin{cases} \frac{9}{4} \cdot \left[\frac{\gamma_1}{(ka)^2}\right]^2 & \text{at} \quad \frac{3}{2} \cdot \frac{\gamma_1}{(ka)^2} \ll 1 \quad \text{and} \quad D \ll E, \\ 1 & \text{at} \quad \frac{3}{2} \frac{\gamma_1}{(ka)^2} \gg 1. \end{cases} \tag{89}$$

Thus at $ka \gg 1$ both theories, including also the criterions of passage to the perturbation theory ($\gamma_1/(ka)^2 \ll 1$), give the same results, differing only by the numerical coefficients.

7. – Discussion.

Let us now make the analysis of the different theories of scattering by considering the case of scattering by a δ-potential. For the sake of simplicity let us limit ourselves to a non-relativistic approximation. Then we have the following wave equation for the description of scattering:

$$(\nabla^2 + k^2)\psi = \frac{2k_0}{c\hbar} V_0 \delta(\boldsymbol{r})\psi\,. \tag{90}$$

The solution of the wave equation (90) with the outgoing waves at large r is to be sought in the form:

$$\psi = A_0 \exp[ikZ] + A_1 \left(\frac{1}{8\pi^3} \int \frac{\exp[i\boldsymbol{\varkappa}\boldsymbol{r}]}{k^2 - \varkappa^2}\, \mathrm{d}^3\varkappa - \frac{i}{4\pi} \cdot \frac{\sin kr}{r}\right). \tag{91}$$

Taking account of the value of the integral

$$\frac{1}{8\pi^3} \int \frac{\exp[i\boldsymbol{\varkappa}\boldsymbol{r}]}{k^2 - \varkappa^2}\, \mathrm{d}^3\varkappa = \begin{cases} -\frac{\cos kr}{4\pi r}, & r > 0, \\ -\frac{\alpha}{\pi^2}, & r = 0, \end{cases} \tag{92}$$

where α determines the interval of k-values ($k-\alpha \leqslant \varkappa \leqslant k+\alpha$) of a scattered particle, we find from the last Eqs. for the cross-section:

$$\sigma = \frac{|A_1|^2}{4\pi |A_0|^2} = \frac{k_0^2 V_0^2}{\pi c^2 \hbar^2 \left[\left(1 + \frac{2k_0 V_0 \alpha}{\pi^2 c\hbar}\right)^2 + \frac{k_0^2 \hbar^2 V_0^2}{4\pi^2 c^2 \hbar^2}\right]}. \tag{93}$$

If one omits the terms depending on V_0 in the denominator of the Eq. (93) then one obtains a value for the cross-section in accordance with the perturbation theory (see, the non-relativistic approximation of the Eq. (39)).

When solving the same problem by the adjustment method, one has to put $\alpha \to \infty$ (more exactly, $\alpha \gg k$, i.e. the non-resonance terms have to give the main contribution to the scattering).

In this case we find that when the potential is of the δ-form, there is no scattering at all, in full agreement with the formulas (85) and (86). After all, if one puts α equal to zero in the denominator of Eq. (93) (more exactly $\alpha \ll k$, i.e. only the resonance terms $\varkappa \sim k$ are taken into account at the scattering) one obtains for the cross-section the value corresponding to the damping theory (see the non-relativistic approximation of formulas (42)).

If we suppose that the leading term may be obtained by perturbation theory ($\alpha = 1/a \neq \infty$, is some effective range of force), then according to (93) the next term of expansion is proportional to V_0^2 according to the damping theory, and is proportional to V_0 according to the adjustment method, i.e. will be explicitly dependent on the sign of the interaction energy.

RIASSUNTO (*)

Coll'ausilio della teoria dello smorzamento della radiazione si esamina lo scattering elastico delle particelle da parte di un centro di forza in riposo. Si ottengono formule sia per le sezioni d'urto effettive che per gli sfasamenti dello scattering dovuti all'azione del centro di forze di breve raggio d'azione. Alla fine si fa un confronto fra le formule ottenute con metodi differenti.

(*) *Traduzione a cura della Redazione.*

Bubble Density Along the Path of Ionizing Particles Crossing a Bubble Chamber.

L. Bertanza, G. Martelli and B. Tallini

Istituto di Fisica dell'Università - Pisa
Istituto Nazionale di Fisica Nucleare - Gruppo Aggregato di Pisa

(ricevuto il 22 Dicembre 1956)

Summary. — The formation of bubbles along the path of charged particles in a bubble chamber is investigated, and the various processes which contribute to the formation of a track are analysed. The dependence of the density of bubbles on the velocity of the particles and on the degree of superheat of the liquid is studied, and it is shown that the contradiction between some experimental results is only apparent and may be explained in terms of different conditions of operation.

---

1. – In a previous paper [1] the conditions under which bubbles may nucleate in ionized overheated liquids, as well as the mechanism of their formation, have been investigated under quite general assumptions with the help of electrodynamical models. The results have been applied to the particular case of a bubble chamber [2] and the operating conditions of the device have been found by working out how the minimum number N_0 of ions, which has to be created within a given volume $\frac{4}{3}\pi R_0^3(N_0)$ in order to give rise to a bubble, depends upon the thermodynamical parameters of the liquid (temperature and pressure). In that investigation, however, no particular hypothesis had been required about the way in which ions are created along the path of the ionizing particle crossing the liquid: it is obvious that if necessary conditions are satisfied, bubbles will form independently of the mechanism of formation of the ions.

[1] L. Bertanza and G. Martelli: *Nuovo Cimento*, **1**, 324 (1955).
[2] L. Bertanza, G. Martelli and A. Zacutti: *Nuovo Cimento*, **2**, 487 (1955).

Theoretical considerations ([3]) show that there is a strict dependence of the density of bubbles along the track of an ionizing particle on the velocity of the particle itself. This fact has been checked experimentally by several authors ([1,5]), but their results do not agree about the form of this dependence, and on the basis of experimental data it is not clear whether the contradiction might be explained only in terms of different methods of operating a bubble chamber.

In the work which is the subject of the present paper, an attempt is made to treat the problem of the density of bubbles along a track in a detailed way, in which some results of our preceeding investigations will be also used.

2. – In overheated liquids bubbles form in those places where a sufficiently large energy density has been created by the passage of the particle, so as to favour the rupture of the metastable equilibrium.

The density of bubbles along the path of a charged particle may be calculated by supposing a fraction of the total number of bubbles to form on the track of δ-electrons (i.e. in those places where the energy transfer due to the interaction of ions prevails) and the remaining fraction to nucleate on the « core » of the track, where the fluctuations both of ionization and other forms of energy losses contribute to the local increase of energy density.

It is convenient to calculate separately the contributions of the two processes, and then to determine what fraction of the total number of bubbles may be ascribed to each of them, under various operating conditions.

3. – To calculate the contribution of δ-electrons, let us divide the total length T of a track of a δ-electron into intervals of equal length $q_0 = 2R_0$, and let $\overline{E}$ be the average energy required for the formation of a single ion. The mean number of ions formed within the i-th interval q_0 may be written as

$$\overline{n}_i = \frac{1}{\overline{E}} \left(\frac{\mathrm{d}E}{\mathrm{d}x} \right)_i q_0 ,$$

(the q_0's are so small, that $\mathrm{d}E/\mathrm{d}x$ may be regarded as a constant over the whole length of each of them). The probability for a cluster with $N \geqslant N_0$ ions to form within the i-th interval q_0 is

$$w_i(N \geqslant N_0, q_0) = 1 - \sum_{k=0}^{N_0 - 1} \frac{\exp[-\overline{n}_i] n_i^k}{k!} = 1 - \Phi(N_0, \overline{n}_i) .$$

([3]) G. A. Askar'ian: *J. Exptl. Theoret. Phys.* (*U.S.S.R.*), **30**, 610 (1956).

([4]) G. A. Blinov, Y. S. Krestnikov and M. F. Lomanov: (CERN Symposium) 1956.

([5]) D. A. Glaser, D. C. Rahm and C. Dodd: *Phys. Rev.*, **102**, 1653 (1956).

Here q_0 depends on N_0, but the final conclusions are independent of the choice cof N_0. $\Phi(N_0, \overline{n}_i)$ may be written as

$$\Phi(N_0, \overline{n}_i) = \Phi_1 + \Phi_2 ,$$

where

$$\Phi_1 = \sum_{\nu=0}^{N^*-1} \frac{\overline{n}_i^{\nu}}{\nu!} \sum_{t=0}^{N^*-(\nu+1)} \frac{(-1)^t \overline{n}_i^t}{t!} = 1$$

$$\Phi_2 = \sum_{\nu=N^*}^{\infty} (-1)^{\nu} \overline{n}_i^{\nu} \sum_{r=0}^{N^*} \frac{(-1)^r}{r!(\nu - r)!} .$$

and $N^* = N_0 - 1$. Hence $w_i(N \geqslant N_0, q_0)$ becomes

$$w_i(N \geqslant N_0, q_0) = \sum_{\nu=N^*}^{\infty} (-1)^{\nu+1} \overline{n}_i^{\nu} \sum_{r=0}^{N^*} \frac{(-1)^r}{r!(\nu - r)!} . \tag{1}$$

In this range of energy $\mathrm{d}E/\mathrm{d}x \sim \alpha/E$ so, after substitution, eq. (1) becoimes

$$w_i(N \geqslant N_0, q_0) = \sum_{\nu=N^*}^{\infty} (-1)^{\nu+1} \frac{1}{E^{\nu}} \left(\frac{\alpha q_0}{E}\right)_i^{\nu} \sum_{r=0}^{N^*} \frac{(-1)^r}{r!(\nu - r)!} .$$

We see that the w_i's are very small everywhere on the track, except near the end of the path of every δ-electron: *to calculate the contribution of δ-electrons to the bubble density along a track, it will be sufficient to take into account only the contribution of the ions formed on the last q_0*, where, to give rise to a bubble, any event corresponding to the formation of $N_0 + k$ ions in an interval $2R_0(N_0 + k) = q_0(N_0 + k)$ has to occur ($k = 0, 1, 2, \ldots$). If we call $\overline{N}_k$ the mean number of ions formed in the last interval $q_0(N_0 + k)$ we get, for the probability of $N_0 + k$ ions to form within $q_0(N_0 + k)$

$$\pi_k = \frac{\exp[-\overline{N}_k]\overline{N}_k^{N_0+k}}{(N_0 + k)!} .$$

Recalling that the average number of δ-electrons having energies between E and $E + \mathrm{d}E$ formed by the particle per unit path is given by

$$\mathrm{d}N = \frac{C}{E^2} \mathrm{d}E ,$$

we can write, for the total number of bubbles formed per unit path of track

by this process

$$(2) \qquad n_1 = \sum_0^k \int_{E_k}^{E_{k+1}} \Big(\sum_0^k{}_i \, \pi_i - 2 \sum_0^k{}_{i,h} \, \pi_i \pi_h + 3 \sum_0^k{}_{i,h,l} \, \pi_i \pi_h \pi_l - \ldots\Big) \frac{C}{E^2} \, \mathrm{d}E \,, \qquad (i < h < l),$$

where E_k is the minimum energy to be transferred to a δ-electron in order to form $N_0 + k$ ions. The sum $\sum_0^k$ extends up to a given $E_{\max}$, the choice of which does not affect, in practice, the final result ($E_{\max} \gg E_0$).

4. – The average energy loss of the primary particle along the « core » of the track is due to various mechanisms of energy transfer, and equals the total energy loss when the energy spent to form δ-electrons of energy larger than E_0 has been subtracted.

The energy T_k required for the formation of a critical bubble (i.e. of a bubble which can evolve freely with a decrease of its total energy) is known [1,6]. We assume that a bubble will form every time that an energy transfer equal or larger than T_k will occur within an interval $q_k = 2R_k$ (R_k being the radius of the critical bubble). If $\bar{\varepsilon}$ is the average energy loss of the primary particle along the core, the probability of a fluctuation for which the above condition is satisfied, may be written as

$$p(\bar{\varepsilon}, 2R_k) \sim \frac{2}{\sqrt{\pi}} \int \exp\left[-t^2\right] \mathrm{d}t \,.$$

Hence, the average number of bubbles formed per unit path because of this process is

$$(3) \qquad n_2 = \frac{1}{R_k \sqrt{\pi}} \int_{T_k/\bar{\varepsilon}\,\frac{1}{2}}^{\infty} \exp\left[-t^2\right] \mathrm{d}t \,.$$

5. – The total number of bubbles per unit path of the primary particle may be written as

$$(4) \qquad n = n_1 + n_2 = \frac{A_\delta}{\beta^2} + n_2 \,,$$

where

$$A_\delta = 2\pi N \frac{Z}{A} z^2 r^2 \delta m c^2 \sum_0^k \int_{E_k}^{E_{k+1}} \Big(\sum_0^k{}_i \, \pi_i - 2 \sum_0^k{}_{i,h} \, \pi_i \pi_h + \ldots\Big) \frac{\mathrm{d}E}{E^2}$$

---

(6) S. TAKAGI: *Journ. Appl. Phys.*, **24**, 1453 (1953).

as it may be seen from Eq. (2), if one substitutes (7)

$$C = 2\pi N \frac{Z}{A} z^2 r^2 \delta mc^2 \frac{1}{\beta^2},$$

where N is Avogadro's number, Z and A are the charge and mass numbers of the medium, z is the charge of the incident particle in terms of the charge of the electron, r and mc^2 are the classical radius and the rest energy of the electron, δ is the density of the liquid and β the velocity of the particle in terms of the velocity of light.

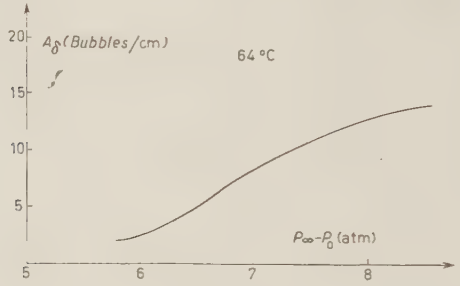

Fig. 1.

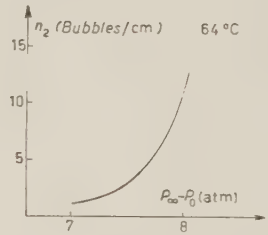

Fig. 2.

To investigate the relative contribution of the two terms appearing in the right side of Eq. (4), A_δ and n_2 have been calculated assuming various operating conditions. The value of A_δ and n_2 calculated in the experimental conditions of BLINOV *et al.* (4) (who worked with a bubble chamber at a definite pressure filled with propane at 64 °C and a degree of superheat $p_\infty - P$ ranging from ~ 6 atm up to ~ 8 atm) are plotted in Fig. 1 and 2. In Fig. 3, $n = n_1 + n_2$ is given together with the experimental points of these authors. It may be seen that A_δ increases with increasing degree of superheat and tends asymptotically to a constant value. This corresponds to the fact that, with increasing sensitivity of the bubble chamber, the probability for a δ-electron to give

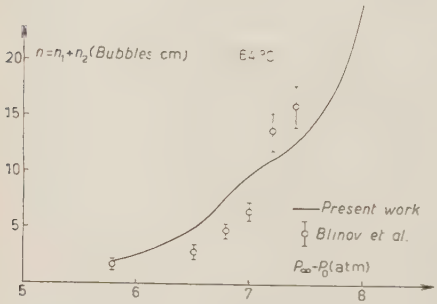

Fig. 3.

(7) B. BOSSI: *High Energy Particles* (New York, 1952), p. 138.

rise to a bubble tends to unity. If the degree of superheat is kept constant, A_δ shows a weak dependence on the temperature, at least within a small range of temperatures.

BLINOV *et al.* have carried out most of their measurements with their bubble chamber operated at very low sensitivity (low degree of superheat): in these conditions the term n_2 becomes negligible and n may therefore be written as $A_\delta \beta^2$. As a matter of fact, n_2 increases with increasing temperature and degree of superheat, because the occurrence of a favourable fluctuation increases with these quantities: under operating conditions other than Blinov's its contribution may become very relevant.

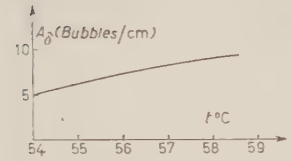

Fig. 4.

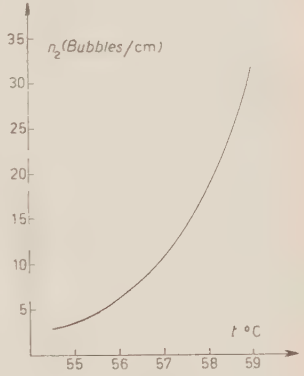

Fig. 5.

A second check of our results has been carried out by calculating A_δ and n_2 under the operating conditions of Glaser *et al.* [5], and by comparing the results obtained in this way with the experimental points given by these authors. In Fig. 4 and 5 A_δ and n_2 are plotted as functions of temperature. In Fig. 6 $n = n_1 + n_2$ is compared with the experimental points obtained by Glaser *et al.* (for pions with $\beta^{-2} = 1.05$). In order to find out the values of the parameters which in eq. (2) and (3) depend on the operating conditions (*), we have normalized our curves to those given by Glaser at one point (58 °C).

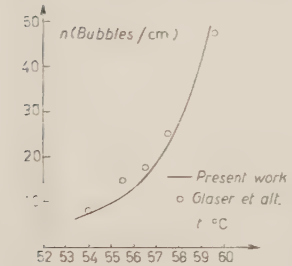

Fig. 6.

The good agreement seems to confirm that, if the sensitivity of the bubble chamber is sufficiently high, a fraction of the total number of bubbles will form on the « core » of the track, and this may explain the term $B(T)$ wich appears in Glaser's results.

From the foregoing discussion, it seems that there is no contradiction between the results obtained by the two groups of authors, and that the differences depend upon the different ways of operating the devices.

(*) The final pressure in the bubble chamber of Glaser, which is operated at defined volume, in not known exactly.

It is worth noticing that, if the bubbles formed by the two different processes could be distinguished experimentally, it should be possible, in principle, to measure velocity and mass of a particle by means only of bubble counts.

* * *

The authors acknowledge with pleasure some interesting discussions on the subject with Proff. M. CONVERSI and L. A. RADICATI. They wish to thank Dr. A. ZACUTTI and Miss C. BARSANTI for valuable help in carrying out numerical calculations.

RIASSUNTO

Si studia la formazione di bolle lungo il percorso di una particella carica in una camera a bolle e si analizzano alcuni processi che possono contribuire alla formazione di una traccia. Si studia la dipendenza della densità di bolle dalla velocità delle particelle e dal grado di surriscaldamento del liquido e si trova che la contraddizione tra alcuni risultati sperimentali è solo apparente e può essere spiegata tenendo conto della diversità delle condizioni di lavoro.

IL NUOVO CIMENTO Vol. V, N. 4 1° Aprile 1957

Interference in the Double Compton Effect.

B. De Tollis and R. S. Liotta

Istituto di Fisica dell'Università - Roma
Istituto Nazionale di Fisica Nucleare - Sezione di Roma

(ricevuto il 28 Dicembre 1956)

Summary. — The differential cross-section by double Compton effect is calculated in the case of identity of the two emitted photons. It results a factor of interference $1/(4\pi)^2$ besides the factor 1/137 due to the perturbative development.

Many authors have studied the double Compton effect. Heitler and Nordheim [1] have calculated according to the usual perturbation methods of quantum electrodynamics the order of magnitude for the double process, reaching the not entirely justified conclusion, that the ratio between the double and the single Compton effect is approximately 1/137 for high energies, while for low energies it is entirely negligible. In any case the process would be favoured when the two photons have the same energy in the final state. Mandl and Skirme [2] have made a new calculation of the cross-section with the most recent methods of Feynman and Dyson and have particularly considered the case where one of the two photons emitted is very weak with respect to the other, and has an energy much lower than the electronic mass. In this case, integrating over all the possible angles of emission of the weak photon they have found a cross-section which for angles of the outgoing photon with the direction of the incident quantum of about 30° and for energies greater than 8 MeV, is larger than that obtained for the single Compton effect. However this result does not mean that the value of the theoretical cross-section

[1] W. Heitler and L. Nordheim: *Physica*, **1**, 1059 (1934); W. Heitler: *The Quantum Theory of Radiation* (1934).

[2] F. Mandl and T. H. R. Skirme: *Proc. Roy. Soc.*, **215**, 497 (1952).

for the single Compton effect is to be modified, since, because of the presence of a factor dk_2/k_2 in the cross-section for the double effect, the high contribution above mentioned is entirely annulled when the radiative corrections on the single Compton effect are considered; in fact these corrections contain the terms of one infrared catastrophe of the type dk_2/k_2 [3].

The above mentioned Authors have also considered the energy spectra in the case that the two photons emitted form an angle of 90° between them and with the direction of the incident photon.

On the other hand, recent experiments with nuclear emulsions exposed to the cosmic radiation [4] reveal the presence of two pairs of electrons with a common origin, with a frequency, with regard to the production of one single pair, which seems to be of the order of the above mentioned ratio 1/137.

HOOPER and KING explain the two very close pairs by an electrodynamic process in which a quantum γ of high energy colliding with a nucleus produces two pairs. According to the theory of perturbation a similar phenomenon is due (in the lowest order) to the term $S^{(3)}$ of the S operator of Dyson, and one of the corresponding Feynman diagrams is drawn on the left. However, it is well known that the term $S^{(3)}$ may produce various processes, such as double bremmsstrahlung or double Compton effect which are closely connected with the replacement of real quanta by virtual ones and of electrons by positrons; and which finally allow the production of two electrons pairs. These considerations have led us to go deeper into the calculation of the cross section for double Compton effect with the aim to achieve, at least in few cases, a numerical result which is definite and compatible with events of the type observed by HOOPER and KING.

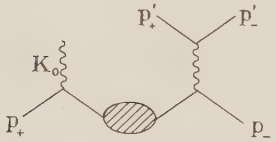

From the physical viewpoint it is possible to think, following the theories of Fermi on the multiple production of mesons, that the electron is surrounded by a cloud of photons in virtual states and that they constitute a Bose gas in thermodynamic equilibrium. In this case, when a perturbation (incident quantum) reaches the electron, it allows a photon to pass into a real state (single Compton effect); more exactly it allows that photon, the state of which has the maximum probability, to pass into a real state.

Since many photons, being bosons, may be in the same state, it can be deduced that if the incident perturbation is of sufficiently high energy, more than one photon will pass into the real state, and if one of these photons is in a state particularly favorable for such a transition the same will happen

---

[3] L. M. BROWN and R. P. FEYNMAN: *Phys. Rev.*, **85**, 231 (1952).
[4] J. E. HOOPER and D. T. KING: *Phyl. Mag.*, **41**, 1194 (1950).

to the other photons which are in the same state. The only limit to the multiplicity of this process being given by the energy balance between the initial and final state. A proof of the correctness of this theory might come from a comparison between the cross sections for the single and double Compton effects. In the case that the higher probability of emission of two photons in the same state does not exist, that ratio should not be remarkably different from 137. In the other case, when the ratio is remarkably lower than 137 it should be possible to think that the virtual photons accumulate preferably in some states, while if the resulting ratio is considerably higher than 137, it would mean that only a few virtual photons stay in a given state.

Furthermore, the work of Heitler and Nordheim permits on the basis of these considerations to calculate the cross section for double Compton effect in the case when the two photons emitted have the same energy.

Such a calculation, when outgoing photons have the same energy but different momenta is practically impossible; in fact in the matrix element we find six different terms and in its quadratic modulus there are 21 traces (different) of matrix products of twelve factors, each of them sum of more than one term. Such traces are not easily computable.

We have therefore limited our study to the case when the two photons emitted are identic, which means, that they have both the same energy and the same momentum. With these limitations the calculation is much simplified and we obtain the experimentally observed case of two pairs of electrons having the same origin.

1. – A few Data on the Calculation of the Cross-Section.

In this calculation we have used the theorems of Wick ([5]) and the formulas of Dyson. In the process under examination we have one photon and one electron in the initial state and two photons and one electron in the final state. Since the radiative corrections are not considered, in the perturbative development of the operator S of Dyson, the term of lower order which might produce the process under examination is:

$$(1) \qquad S^{(3)} = \frac{(ie)^3}{3!} \int T(:\overline{\psi}\widetilde{A}\psi(x)::\overline{\psi}\widetilde{A}\psi(y)::\overline{\psi}\widetilde{A}\psi(z):)\,\mathrm{d}x\,\mathrm{d}y\,\mathrm{d}z\,, \qquad (\hbar=1;\ c=1)$$

where the symbols are those used by Wick.

([5]) G. Wick: *Phys. Rev.*, **80**, 268 (1950).

If we introduce the four vectors:

$$p_0 \equiv (\boldsymbol{p}_0, iE_0) \equiv (p_1^{(0)}, p_2^{(0)}, p_3^{(0)}, p_4^{(0)}) \qquad \text{for the initial electron}$$

$$k_0 \equiv (\boldsymbol{k}_0, i\varepsilon_0) \equiv (k_1^{(0)}, k_2^{(0)}, k_3^{(0)}, k_4^{(0)}) \qquad \text{for the initial photon}$$

$$A_0 \equiv (\boldsymbol{A}_0, 0) \equiv (A_1^{(0)}, A_2^{(0)}, A_3^{(0)}, 0) \qquad \text{for the polarization vector of } k_0$$

$$k_1 \equiv (\boldsymbol{k}_1, i\varepsilon_1) \equiv (k_1^{(1)}, k_2^{(1)}, k_3^{(1)}, k_4^{(1)}) \qquad \text{for one of the emitted photons}$$

$$A_1 \equiv (\boldsymbol{A}_1, 0) \equiv (A_1^{(1)}, A_2^{(1)}, A_3^{(1)}, 0) \qquad \text{for the polarization vector of } k_1$$

$$k_2 \equiv (\boldsymbol{k}_2, i\varepsilon_2) \equiv (k_1^{(2)}, k_2^{(2)}, k_3^{(2)}, k_4^{(2)}) \qquad \text{for the other photon}$$

$$A_2 \equiv (\boldsymbol{A}_2, 0) \equiv (A_1^{(2)}, A_2^{(2)}, A_3^{(2)}, 0) \qquad \text{for the polarization vector of } k_2$$

$$p \equiv (\boldsymbol{p}, iE) \equiv (p_1, p_2, p_3, p_4) \qquad \text{for the final electron}$$

with the conditions that:

$$A_0^2 = 1, \qquad A_1^2 = 1, \qquad A_2^2 = 1,$$
$$A_\lambda^{(0)} k_\lambda^{(0)} = 0, \qquad A_\lambda^{(1)} k_\lambda^{(1)} = 0, \qquad A_\lambda^{(2)} k_\lambda^{(2)} = 0,$$
$$k_0^2 = 0, \qquad k_1^2 = 0, \qquad k_2^2 = 0,$$

which allow to consider the photons real and transversal, we have from formula (1) developing the product T of Wick, for the matrix element of $S^{(3)}$ between the initial and the final states:

$$\langle k_1, k_2, p \,|\, S^{(2)} \,|\, k_0, p_0 \rangle = (2\pi)^{20} i e^3 \, \delta_4(p_0 + k_0 - p - k_1 - k_2) \cdot$$
$$\cdot \left\{ (\overline{u} p) \left[\widetilde{A}_2 \frac{\widetilde{p} + \widetilde{k}_2 + im}{(p + k_2)^2 + m^2} \widetilde{A}_1 \frac{\widetilde{k}_0 + \widetilde{p}_0 + im}{(k_0 + p_0)^2 + m^2} \widetilde{A}_0 u(p_0) + \widetilde{A}_1 \frac{\widetilde{p} + \widetilde{k}_1 + im}{(p + k_1)^2 + m^2} \cdot \right.\right.$$
$$\cdot \widetilde{A}_2 \frac{\widetilde{p}_0 + \widetilde{k}_0 + im}{(p_0 + k_0)^2 + m^2} \widetilde{A}_0 + \widetilde{A}_2 \frac{p + \widetilde{k}_2 + im}{(p + k_2)^2 + m^2} \widetilde{A}_0 \frac{\widetilde{p}_0 - \widetilde{k}_1 + im}{(p_0 - k_1)^2 + m^2} \widetilde{A}_1 -$$
$$+ \widetilde{A}_1 \frac{\widetilde{p} + \widetilde{k}_1 + im}{(p + k_1)^2 + m^2} \widetilde{A}_0 \frac{\widetilde{p}_0 - \widetilde{k}_2 + im}{(p_0 - k_2)^2 + m^2} \widetilde{A}_2 + \widetilde{A}_0 \frac{\widetilde{p} - \widetilde{k}_0 + im}{(p - k_0)^2 + m^2} \cdot$$
$$\left.\left. \cdot \widetilde{A}_1 \frac{\widetilde{p}_0 - \widetilde{k}_2 + im}{(p_0 - k_2)^2 + m^2} \widetilde{A}_2 + \widetilde{A}_0 \frac{\widetilde{p} - \widetilde{k}_0 + im}{(p - k_0)^2 + m^2} \widetilde{A}_2 \frac{\widetilde{p}_0 - \widetilde{k}_1 + im}{(p_0 - k_1)^2 + m^2} \widetilde{A}_1 \right] u(p_0) \right\},$$

where $u(q)$ is the wave function of the electron with momentum q in the mo-

mentum representation which satisfies the equation

$$(\tilde{q} - im)u(q) = 0\,, \tag{2}$$

where m is the electron mass.

If we consider the case where $A_1 = A_2 = A$, $k_1 = k_2 = k$ in the frame of reference in which the initial electron is at rest, in which case $\tilde{A}_0$ and $\tilde{p}_0$ anticommute, we have for the matrix element:

$$\langle k, k, p\,|\,S^{(3)}|\,k_0, p_0\rangle = 2\cdot(2\pi)^{20}ie^3\,\delta_4(p_0 + k_0 - p - 2k)\cdot \tag{3}$$

$$\cdot\,\bar{u}(p)\left\{\frac{\tilde{A}(\tilde{p} + \tilde{k} - im)\tilde{A}\tilde{k}_0\tilde{A}_0}{[(p+k)^2 + m^2][(p_0 + k_0)^2 + m^2]} - \frac{\tilde{A}(\tilde{p} + \tilde{k} - im)\tilde{A}_0\tilde{k}\tilde{A}}{[(p+k)^2 + m^2][(p_0 - k)^2 + m^2]} - \right.$$

$$\left. - \frac{\tilde{A}_0(\tilde{p} - \tilde{k}_0 + im)\tilde{A}\tilde{k}\tilde{A}}{[(p-k_0)^2 + m^2][(p_0 - k)^2 + m^2]}\right\} u(p_0) = H_{fi}\,,$$

$|H_{fi}|^2$ is calculated by summing over the spin direction of the electron in the initial and final state and by using the projection operators

$$(\tilde{p}_0 + im)/2im\,, \qquad (\tilde{p} + im)/2im\,,$$

and putting

$$u_\alpha(p)\bar{u}_\alpha(p) = 1\,, \qquad u_\alpha(p_0)\bar{u}_\alpha(p_0) = 1\,.$$

We also sum over the direction of polarization of the final photons and we average over the direction of polarization of the incident quantum. In this way we obtain for $|H_{fi}|^2$ an expression of the following type:

$$|H_{fi}|^2 = \frac{[2ie^3(2\pi^8)]^2}{4^3m^2}\,F(p_0k_0kp)\{\textstyle\sum_{s,p}\}\delta_4^2(p_0 + k_0 - p - 2k)\,,$$

where $F(p_0k_0kp)$ is a function which takes into account the product of the denominators of (3) while $\{\sum_{s,p}\}$ is a function which takes into account the sum of the spins and the polarizations.

Since $(2\pi\hbar)^4\delta_4(p_0 + k_0 - p - 2k)$ [$\hbar = 1$] is the fourvolume element in which the interaction is possible, the probability of transitions to one simple final state w_s is given by:

$$w_s = \frac{e^6}{1m^2}\,F(p_0k_0kp)\{\textstyle\sum_{s,p}\}(2\pi)^4\delta_4(p_0 + k_0 - p - 2k)\,.$$

To calculate the total transition probability we have still to consider the case where the two final photons have different momenta.

The number of states of each final particle in the respective intervals

$$\mathrm{d}\boldsymbol{p} = \mathrm{d}p_1\,\mathrm{d}p_2\,\mathrm{d}p_3, \qquad \mathrm{d}\boldsymbol{k}_1 = \mathrm{d}k_1^{(1)}\,\mathrm{d}k_2^{(1)}\,\mathrm{d}k_3^{(1)}, \qquad \mathrm{d}\boldsymbol{k}_2 = \mathrm{d}k_1^{(2)}\,\mathrm{d}k_2^{(2)}\,\mathrm{d}k_3^{(2)},$$

is given by

$$(2\pi)^{-3}\frac{m}{E}\,\mathrm{d}\boldsymbol{p}, \qquad (2\pi)^{-3}\frac{1}{2\varepsilon_1}\,\mathrm{d}\boldsymbol{k}_1, \qquad (2\pi)^{-3}\frac{1}{2\varepsilon_2}\,\mathrm{d}\boldsymbol{k}_2.$$

The total transition probability is therefore

$$w = \frac{e^6}{4m^2}F(p_0k_0kp)\{\textstyle\sum_{s,v}\}(2\pi)^{-5}\frac{m}{4E\varepsilon_1\varepsilon_2}\,\delta(E_0+\varepsilon_0-E-\varepsilon_1-\varepsilon_2)\,\mathrm{d}\boldsymbol{k}_1\,\mathrm{d}\boldsymbol{k}_2,$$

where $E = \sqrt{\boldsymbol{p}^2 + m^2}$ is expressed by $\boldsymbol{p}_0$, $\boldsymbol{k}_0$, $\boldsymbol{k}_1$, $\boldsymbol{k}_2$ making use of the conservation of momentum.

Since

$$\delta(E_0+\varepsilon_0-E-\varepsilon_1-\varepsilon_2) = \delta(k_3^{(1)}-k_{3c}^{(1)})\Big/\frac{\mathrm{d}(E+\varepsilon_1+\varepsilon_2)}{\mathrm{d}k_3^{(1)}},$$

where $k_{3c}^{(1)}$ is the particular value of $k_3^{(1)}$ for which we have conservation of momentum and energy, we can write

$$w = \frac{e^6}{4m^2}F(p_0k_0kp)\{\textstyle\sum_{s,v}\}(2\pi)^{-5}\frac{m}{4E\varepsilon_1\varepsilon_2}\,\frac{\mathrm{d}k_1^{(1)}\,\mathrm{d}k_2^{(1)}\,\mathrm{d}k_3^{(1)}}{\mathrm{d}(E+\varepsilon_1+\varepsilon_2)}\,\mathrm{d}\boldsymbol{k}_2,$$

where $k_3^{(1)}$ makes use of the conservative theorems, so that five independent parameters remain: the three components of $\boldsymbol{k}_2$ and the angles of $\boldsymbol{k}_1$ with the frame axes.

Considering again the case where $\boldsymbol{k}_1 = \boldsymbol{k}_2$, in the polar coordinate system, keeping in mind that it:

$$\frac{\mathrm{d}\varepsilon}{\mathrm{d}(E+2\varepsilon)} = \frac{\varepsilon E}{m\varepsilon_0}, \qquad \varepsilon_1 = \varepsilon_2 = \varepsilon,$$

we obtain for the total transition probability

$$w = \frac{e^6}{4m^2}F(p_0k_0kp)\{\textstyle\sum_{s,v}\}(2\pi)^{-5}\frac{\varepsilon^3}{4\varepsilon_0}\,\mathrm{d}\varepsilon_2\,\mathrm{d}\Omega_1\,\mathrm{d}\Omega_2, \tag{4}$$

where $\mathrm{d}\Omega_1\,\mathrm{d}\Omega_2$ are the elements of solid angle in which the final photons are emitted.

The differential cross section is given by:

(5) $\mathrm{d}\sigma = wV_1V_2$,

where V_1 and V_2 are the volumes of normalization of the incident particles

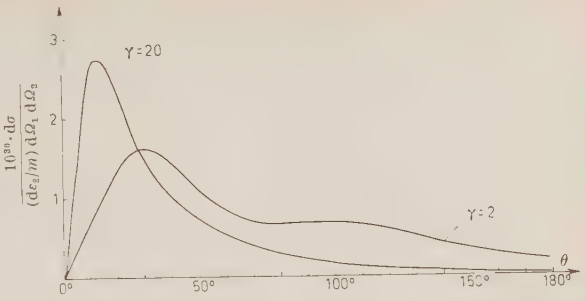

(6) $$V_1 = \frac{m}{E_0} = 1\,, \qquad V_2 = \frac{1}{2\varepsilon_0}\,.$$

From (5), considering the expression (6) and expressing the functions $F(p_0k_0kp)\{\sum_{s,r}\}$ contained in (4), we obtain in the final analysis for the double Compton effect the differential mass section

(7) $$\mathrm{d}\sigma = \frac{1}{2}r_0^2\alpha\frac{\Theta}{a^4}\frac{1}{(4\pi)^2}\frac{\mathrm{d}\varepsilon_2}{m}\mathrm{d}\Omega_1\,\mathrm{d}\Omega_2\,,$$

where

$$\Theta = a^3 + a^2[2\gamma\sin^2\theta - 3] + \\ + a[-3\gamma\sin^2\theta - 4\gamma\sin^2\theta\cos\theta + 8\gamma\sin^2\theta\cos^2\theta + 3] + 2\gamma\sin^2\theta - 1\,,$$

$$a = 1 + \gamma(1-\cos\theta), \qquad (\gamma = \varepsilon_0/m)\,,$$

$$r_0 = e^2/4\pi m \simeq 2.8\cdot10^{-13}\ \mathrm{cm}\,,$$

$$\alpha = e^2/4\pi \simeq 1/137\,.$$

2. – Results and Discussion.

Considering the function Θ/a^4 we see that the differential cross section is zero for $\gamma \to 0$. This result is obvious since the double Compton effect has not a classical correspondence. It results also zero for $\theta = 0$ and the numerical tables show a behaviour with the maximum displaced toward smaller angles with increasing energy of the incident quantum. For very small angles and for $\gamma \to \infty$ the value of this maximum is ~ 4.5. For $\theta = \pi$ the function has a definite value, it tends to zero with increase of the energy.

If we compare the finite parts of (7) and those of the differential cross section of the single Compton effect (HEITLER: loc. cit., formula (40), p. 219) we see

that (7) contains, besides the factor $1/137$ also the factor $1/(4\pi)^2$, from which it follows that the double Compton effect cross section is lower by a factor $\sim 10^{-4}$ than the section for single Compton effect, while decrease of a factor 10^{-2} was expected.

This leads one to think that a destructive interference exists between the emitted photons, and that the cloud of photons surrounding the electrons is constituted only by few pairs for each state.

If we want to generalize this result we would reach the conclusion that the probability of emitting n identical photons decreases not only by a factor 137^{-n} but also by the factors of interference.

The result achieved, the excistence of this interference, might be generalized and applied to the double Bremsstrahlung in the case of the two photons emitted being identical, and with less probability to the radiative production of electron pairs in the field of a nucleus by a quantum.

Due to the relatively high mean free path of a photon, in order to observe two electron pairs with the same origin, we should think that the two photons generating the pairs, have the same direction and the same energy, as otherwise the probability of conversion into pairs at two different points becomes higher.

This consideration has led us to make the present calculation.

As far as the events observed by HOOPER and KING are concerned, the authors do not mention in their work the experimental errors occurred in the observation of two double events out of 1380 single ones; therefore as long as we do not have more complete data a definite comparison with experiment will not be possible.

* * *

We wish to express our gratitude to Prof. B. FERRETTI for useful discussions and helpful advice.

RIASSUNTO

Si calcola la sezione d'urto differenziale per doppio effetto Compton nel caso che i due fotoni emessi siano identici. Si trova un fattore $1/(4\pi)^2$ di interferenza oltre al fattore 137^{-1} dovuto allo sviluppo perturbativo.

The Spin Kinematics for a Charged Particle in a Uniform Magnetic Field.

M. Carrassi

Istituto di Fisica Teorica dell'Università - Genova
Istituto di Fisica Nucleare - Sezione aggregata di Genova

(ricevuto il 5 Gennaio 1957)

Summary. — The influence of a uniform magnetic field on the spin orientation of electrons in a beam is calculated according to the Dirac theory. It is shown that, when the field is perpendicular to the electron beam path, the spin orientation does not change with respect to the direction of propagation. The calculations are performed using the exact solution of Dirac equation.

1. – In order to study the possibility of detecting the states of longitudinal polarization of an electron beam, H. A. Tolhoek and R. S. De Groot have recently given consideration to the kinematics of the electron spin in a uniform magnetic field perpendicular to the direction of motion [1]. By using cartesian co-ordinates and letting the xy plane be the plane of the electron orbit and the z-axis be along the magnetic field, the spin direction was found to precess uniformly around the z-axis by an angle (*) $\Delta\alpha_s = \Delta\alpha_p$ where $\Delta\alpha_p$ is the infinitesimal rotation of the momentum $\boldsymbol{p}$. The authors have made the calculations by taking a plane wave as the starting-point and by calculating the deviation from the plane wave caused by the field in a first approximation.

However this procedure does not allow to establish the order of approximation up to which the equality (*) can be considered true; in other words, the question can be posed whether the equality $\alpha_s = \alpha_p$ is still valid for a finite angle of rotation α_p of the momentum (forgetting of course the effect accountable to the anomalous magnetic moment of the electron). This matter

[1] H. A. Tolhoek and R. S. De Groot: *Physica*, **17**, 17 (1951); H. A. Tolhoek: *Rev. Mod. Phys.*, **28**, 277 (1956).

has a particular interest when one considers the spin kinematics of an electron moving around in an accelerating machine with deflecting magnetic field, where the electron beam performs very many tours. Indeed if for a finite deflection angle, for instance $\alpha_p = \pi$, we have a very small $\alpha_p - \alpha_s$ (but different from zero) this quantity, might become not negligible when the beam comes out from the accelerator. With this in mind, the spin rotation has been calculated, using the exact solutions of Dirac equation in a uniform magnetic field ([2]). The solutions derived in Sect. **2** are essentially already contained in Huff's paper ([2]) and the definition of « spin direction » for a free particle, when referred to the system of coordinates in which the electron is at rest, is the one generally used ([3]).

In Sect. **3**, the spin direction for the electron beam coming out from a magnetic field is derived as a function of the spin direction of the incident beam. The result agrees with that obtained by K. M. Case ([4]), using the Foldy-Wouthuysen transformation.

2. – Let us consider the Dirac equation for steady state problems:

$$\left(\frac{w}{c} + \beta mc + \boldsymbol{\alpha}\cdot\boldsymbol{\pi}\right)\psi = 0\,, \tag{1}$$

where ψ is the Dirac wave function with four components ψ_j $(j = 1, 2, 3, 4)$, α_i and β the usual Dirac matrices, $W = (p^2c^2 + m^2c^4)^{\frac{1}{2}}$, $\boldsymbol{\pi} = -i\hbar\boldsymbol{\nabla} + (e/c)\boldsymbol{A}$. It is known that the set of equations (1) can be reduced to the system of two second order differential equations:

$$\left[\frac{w^2}{c^2} - m^2c^2 - \boldsymbol{\pi}\cdot\boldsymbol{\pi} - \hbar\frac{e}{c}\boldsymbol{H}\cdot\boldsymbol{\sigma}\right]\begin{pmatrix}\psi_3\\ \psi_4\end{pmatrix} = 0\,, \tag{2}$$

considering that, among the four unknown functions ψ_j, exist the relations

$$\begin{cases} \psi_1 = -\dfrac{\pi_x - i\pi_y}{(w/c) + mc}\,\psi_4 - \dfrac{\pi_z}{(w/c) + mc}\,\psi_3\,, \\ \psi_2 = -\dfrac{\pi_z + i\pi_y}{(w/c) + mc}\,\psi_3 + \dfrac{\pi_x}{(w/c) + mc}\,\psi_4\,. \end{cases} \tag{3}$$

([2]) I. I. Rabi: *Zeits. f. Phys.*, **49**, 507 (1928); I. D. Huff: *Phys. Rev.*, **38**, 501 (1931). These two authors found somewhat different solutions for the Dirac equation: the connection between them was derived later by M. H. Johnson and B. A. Lippmann: *Phys. Rev.*, **76**, 828 (1949).

([3]) See. for example, N. F. Mott and S. W. Massey: *The Theory of Atomic Collision*, (Oxford, 1950).

([4]) K. M. Case: *Phys. Rev.*, **95**, 1323 (1954).

The system (2), using div $\boldsymbol{A} = 0$, can be written:

$$(2') \qquad \left[\frac{w^2}{c^2} - m^2c^2 + \hbar^2\boldsymbol{\nabla}^2 + 2i\hbar\frac{e}{c}\boldsymbol{A}\cdot\boldsymbol{\nabla} - \frac{e^2}{c^2}\boldsymbol{A}^2 - \hbar\frac{e}{c}\boldsymbol{H}\cdot\boldsymbol{\sigma}\right]\begin{pmatrix}\psi_3\\ \psi_4\end{pmatrix} = 0\,,$$

where the σ_i $(i = 1, 2, 3)$ are the usual Pauli matrices.

We consider the following case: $H = 0$ for $x < 0$ and $H = H_z$ for $x > 0$. In this case we can put $\pi_z = 0$, and that amounts to suppose the ψ_j independent of z (it is easy to prove that the dependence on z of the ψ_j simply means the conservation of the z component of the momentum). Putting $A_x = -\frac{1}{2}Hy$, $A_y = \frac{1}{2}Hx$, $A_z = 0$, the system (2') is reduced to two independent differential equations:

$$(4) \qquad \left[\frac{w^2}{c^2} - m^2c^2 + \hbar^2\boldsymbol{\nabla}^2 - 2i\hbar\omega\left(y\frac{\partial}{\partial x} - x\frac{\partial}{\partial y}\right) - \omega^2(x^2 + y^2) - 2\hbar\omega\sigma_z\right]\begin{pmatrix}\psi_3\\ \psi_4\end{pmatrix} = 0\,,$$

where $\omega = eH/2c$; equations (3) become:

$$(5) \qquad \psi_1 = -\frac{\pi_x - i\pi_y}{(w/c) + mc}\psi_4; \qquad \psi_2 = -\frac{\pi_x + i\pi_y}{(w/c) + mc}\psi_3\,.$$

We put now in (4) (cfr. [2])

$$(6) \qquad \begin{pmatrix}\psi_3\\ \psi_1\end{pmatrix} = \exp\left[\frac{i}{\hbar}\omega xy + \eta y\right]\begin{pmatrix}\varphi_3(x)\\ \varphi_4(x)\end{pmatrix},$$

and we obtain:

$$\left[\frac{w^2}{c^2} - m^2c^2 + \hbar^2\frac{\mathrm{d}^2}{\mathrm{d}x^2} - 4\omega^2\left(x + \frac{\eta}{2\omega}\right)^2 - 2\hbar\omega\sigma_z\right]\begin{pmatrix}\varphi_3\\ \varphi_4\end{pmatrix} = 0\,.$$

From this equation, with the substitution $\xi = (2x + (\eta/2\omega))\sqrt{\omega/\hbar}$, we have:

$$\left[\frac{\mathrm{d}^2}{\mathrm{d}\xi^2} + \frac{1}{4\omega\hbar}(p^2 - \hbar\omega\xi^2 - 2\hbar\omega\sigma_z)\right]\begin{pmatrix}\varphi_3\\ \varphi_4\end{pmatrix} = 0\,.$$

Putting finally $\nu = p^2/4\omega\hbar$, we can write:

$$(7) \qquad \begin{cases}\dfrac{\mathrm{d}^2\varphi_3}{\mathrm{d}\xi^2} + \left(\nu - \dfrac{1}{2} - \dfrac{1}{4}\xi^2\right)\varphi_3 = 0\,,\\[2ex] \dfrac{\mathrm{d}^2\varphi_4}{\mathrm{d}\xi^2} + \left(\nu + \dfrac{1}{2} - \dfrac{1}{4}\xi^2\right)\varphi_4 = 0\,.\end{cases}$$

We might point out that, if $\lambda = h/p$ is the de Broglie wave-length of the electron and $r = cp/eH$ is the radius of the classical orbit, then ν is the number of the de Broglie wave length in the classical path. Each one of the (7) is the known Weber's equation and the solutions are hence the parabolic cylinder functions usually designed by $D_n(\xi)$. Putting then $\varphi_4 = D_\nu(\xi)$, $\varphi_3 = D_{\nu-1}(\xi)$ and using (5), (6) and the known recurrence formulae of the parabolic cylinder functions [5] we find the solution of the Dirac equation (1) in the case $x > 0$:

$$(8)\qquad \begin{bmatrix} \psi_1 \\ \psi_2 \\ \psi_3 \\ \psi_4 \end{bmatrix} = \begin{bmatrix} i\dfrac{2\sqrt{\hbar\omega}}{(w/c)+mc} B\nu D_{\nu-1}(\xi) \\ -i\dfrac{2\sqrt{\hbar\omega}}{(w/c)+mc} A D_\nu(\xi) \\ A D_{\nu-1}(\xi) \\ B D_\nu(\xi) \end{bmatrix} \exp\left[\frac{i}{\hbar}(\omega x y + \eta y)\right].$$

3. – The solution (8) of the Dirac equation, vanishes for any value of ν, if ξ is large. Therefore a plane wave, describing a polarized electron beam injected in the region $x > 0$ with momentum $\boldsymbol{p}$ (p_x, p_y), is « reflected » by the magnetic field. Hence, the solution of the Dirac equation in the region $x < 0$ $(H = 0)$ will have the following form:

$$(9)\qquad \psi = \begin{vmatrix} -B_1 M(p_x - ip_y) \\ -A_1 M(p_x + ip_y) \\ A_1 \\ B_1 \end{vmatrix} \exp\left[\frac{i}{\hbar}(p_x x + p_y y)\right] + \begin{vmatrix} B_2 M(p_x + ip_y) \\ A_2 M(p_x - ip_y) \\ A_2 \\ B_2 \end{vmatrix} \exp\left[\frac{i}{\hbar}(-p_x x + p_y y)\right],$$

where the temporal factor is omitted and $M = c(W + mc^2)^{-1}$. The constants A_1 and B_1 of the incident plane wave must be considered known and their ratio fixes the state of polarization.

More correctly we shall say that the ratio

$$\frac{B_1}{A_1} = \operatorname{tg}\frac{\chi}{2}\cdot\exp[i\omega],$$

[5] See E. T. Whittaker and G. N. Watson: *Modern Analysis* (Cambridge, 1952), p. 350.

specifies the spin direction; this means that χ and ω are the polar angles of the oriented straight-line with respect to which the component of the spin angular momentum is determined in the coordinate system where the electron is at rest.

Then we shall obtain the solution of the Dirac equation in the full space by matching with continuity for $x = 0$ the solution of type (8) with those of type (9). From this condition it comes out immediately that p_y and that:

$$
(10)\qquad \begin{cases} M[(B_2 - B_1)p_x + i(B_1 + B_2)p_y] = \quad 2iM\sqrt{\hbar\omega}\,B\nu D_{\nu-1}(\delta) \\ M[(A_2 - A_1)p_x - i(A_1 + A_2)p_y] = -2iM\sqrt{\hbar\omega}\,AD_\nu(\delta) \\ A_1 + A_2 = AD_{\nu-1}(\delta) \\ B_2 + B_1 = BD_\nu(\delta)\,, \end{cases}
$$

where $\delta = p_y/\sqrt{\hbar\omega}$. From system (10) we deduce:

$$
(11)\qquad \begin{cases} A_1 = \dfrac{A}{2p_x}[(p_x - ip_y)D_{\nu-1}(\delta) + i\,2\sqrt{\hbar\omega}D_\nu(\delta)\,, \\ B_1 = \dfrac{B}{2p_x}[(p_x + ip_y)D_\nu(\delta) \quad - i\,2\sqrt{\hbar\omega}\;\nu D_{\nu-1}(\delta)]\,, \\ A_2 = \dfrac{A}{2p_x}[(p_x + ip_x)D_{\nu-1}(\delta) - i\,2\sqrt{\hbar\omega}D_\nu(\delta)]\,, \\ B_2 = \dfrac{B}{2p_x}[(p_x - ip_y)D_\nu(\delta) \quad + i\,2\sqrt{\hbar\omega}\;\nu D_{\nu-1}(\delta)]. \end{cases}
$$

From (11) we can derive A and B as well as A_2 and B_2, in terms of the initial data for the incident plane wave. Developing the algebra and using $p^2 = 4\omega\hbar\nu$, we find the simple result:

$$
(12)\qquad \frac{B_2}{A_2} = -\frac{B_1}{A_1}\frac{p_x - ip_y}{p_x + ip_y}\,.
$$

Writing $\alpha_0 = \operatorname{tg}^{-1}(p_y/p_x)$, then, as shown in the figure, the angle between the momentum of the reflected beam and the momentum of the incident beam is

$$
\alpha = \pi - 2\alpha_0\,,
$$

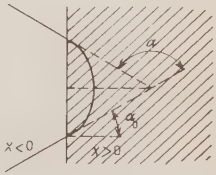

and we obtain:

$$
\frac{p_x - ip_y}{p_x + ip_y} = -\frac{1 - i\operatorname{tg}\alpha_0}{1 + i\operatorname{tg}\alpha_0} = -\cos 2\alpha_0 + i\sin 2\alpha_0 = \exp[i\alpha]\,.
$$

Therefore from (12) we find:

$$\frac{B_2}{A_2} = \frac{B_1}{A_1} \exp[i\alpha] = \operatorname{tg}\frac{\chi}{2} \cdot \exp[i(\omega + \alpha)] . \tag{13}$$

The formula (13) shows that the spin direction of the reflected beam is rotated around the direction of the magnetic field by an angle equal to the rotation angle of the momentum; as an example, if $\alpha = \pi$, one gets, $B_2/A_2 = -B_1/A_1$.

As the momentum rotation occurs with angular velocity $\omega_L = eH\gamma/mc$, the angular velocity of the spin precession is $\omega_s = \omega_L$.

Since the result contained in (13) is independent of the polarization state of the incident beam, one deduces also that if the incident beam is not polarized, the same is true for the reflected one.

* * *

The author wishes to thank Prof. A. Borsellino for suggesting the subject of the present work and for helpful discussions.

RIASSUNTO (*)

Si calcola secondo la teoria di Dirac, l'influenza di un campo magnetico uniforme sull'orientamento dello spin degli elettroni in un fascio. Si dimostra che quando il campo è perpendicolare al fascio degli elettroni, l'orientamento dello spin non varia rispetto alla direzione di propagazione. Si eseguono i calcoli usufruendo della soluzione esatta dell'equazione di Dirac.

(*) *Traduzione a cura della Redazione.*

IL NUOVO CIMENTO Vol. V, N. 4 1° Aprile 1957

Electron Scattering in Nuclear Field with Pair-Creation.

E. MONTALDI

Istituto Nazionale di Fisica Nucleare - Sezione di Milano

M. PUSTERLA

Istituto di Fisica dell'Università - Pavia
Istituto Nazionale di Fisica Nucleare - Sezione di Milano

(ricevuto il 10 Gennaio 1957)

Summary. — By Feynman's graphs, we compute the differential cross-section and indicate the line of calculation of the total one for the following process: electron scattering in nuclear field with pair creation.

1. – Matrix Element.

In order to get the covariant matrix element for the process, we use the graphical technique, as given by DYSON. We use Born's approximation for the external potential and thus obtain the following different graphs:

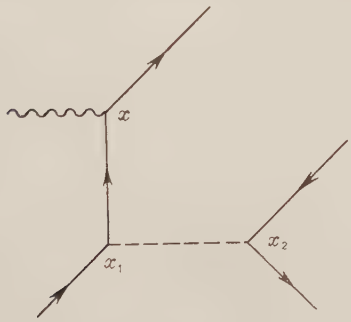

(a)

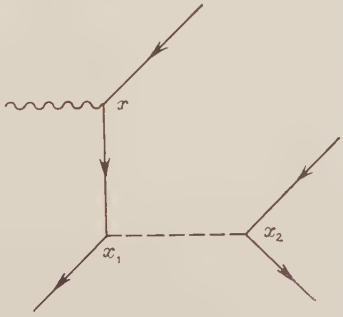

(b)

From these, other two are gotten by interchanging x_1 with x_2, and it is easy to see that their contributions are the same of the first ones (owing to the symmetry of the chronological product in x_1, x_2). Each graph admits two physical interpretations in Feynman's picture. We use these conventional symbols:

Incoming electron: (p, u).

Final state: { electrons (p', u'), (p'', u''); positron (p''', u''').

Furthermore, $\underline{p}$ stands for $\gamma_\mu p_\mu$.

A) This graph can describe the following processes:

a_1) Incoming electron in x_1, outgoing from x after scattering (external interaction); pair created in x_2 by a virtual photon emitted in x_1.

a_2) Incoming electron in x_2, and outgoing from this same point, after emission of the photon; pair created in x_1; electron of the pair scattered in x.

Using Dyson's rules, we easily get the following matrix elements (neglecting, for the moment, the coefficient appearing in the S-matrix at the third order):

$$(1)\ a_1)\quad -\frac{1}{4}\cdot\frac{-2i}{(2\pi)^4}\cdot\frac{2}{(2\pi)^4}\cdot\frac{i}{(2\pi)^3}\,g(\boldsymbol{k})\int\{\overline{u}'\exp[-ip'\cdot x]\gamma_4(\underline{k}'+im)\gamma_\lambda u\exp[ip\cdot x_1]\}\cdot$$
$$\cdot(\overline{u}''\exp[-ip''\cdot x_2]\gamma_\lambda u'''\exp[-ip'''\cdot x_2])(k'^2+m^2)^{-1}(k''^2)^{-1}\exp[i\boldsymbol{k}\cdot\boldsymbol{x}]\cdot$$
$$\cdot\exp[ik'\cdot(x-x_1)]\exp[ik''\cdot(x_1-x_2)]\,\mathrm{d}^4x\,\mathrm{d}^4x_1\,\mathrm{d}^4x_2\,\mathrm{d}^4k'\,\mathrm{d}^4k''=$$
$$=-2\pi g(\boldsymbol{k})\int[\overline{u}'\gamma_4(\underline{k}'-im)\gamma_\lambda u](\overline{u}''\gamma_\lambda u''')(k'^2+m^2)^{-1}(k''^2)^{-1}\cdot$$
$$\cdot\delta^{(3)}(\boldsymbol{p}'-\boldsymbol{k}-\boldsymbol{k}')\delta^{(4)}(p-k'+k'')\delta^{(4)}(p''+p'''+k'')\delta(p_0'-k_0')\,\mathrm{d}^4k'\,\mathrm{d}^4k''=$$
$$=-2\pi g(\boldsymbol{k})[\overline{u}'\gamma_4(\underline{p}-\underline{p}''-\underline{p}'''+im)\gamma_\lambda u](\overline{u}''\gamma_\lambda u''')(p''+p''')^{-2}\cdot$$
$$\cdot[(p-p''-p''')^2+m^2]^{-1}\delta^{(3)}(\boldsymbol{p}+\boldsymbol{k}-\boldsymbol{p}'-\boldsymbol{p}''-\boldsymbol{p}''')\delta(p_0-p_0'-p_0''-p_0'''),$$

$$(2)\ a_2)\quad -2\pi g(\boldsymbol{k})[\overline{u}''\gamma_4(\underline{p}-\underline{p}'-\underline{p}'''+im)\gamma_\lambda u'''](\overline{u}'\gamma_\lambda u)(p-p')^{-2}\cdot$$
$$\cdot[(p-p'-p''')^2+m^2]^{-1}\delta^{(3)}(\boldsymbol{p}+\boldsymbol{k}-\boldsymbol{p}'-\boldsymbol{p}''-\boldsymbol{p}''')\,\delta(p_0-p_0'-p_0''-p_0''').$$

It is to be noted that:

1) Our potential $A_\mu^{\mathrm{ext}}(x)$ is reduced to the fourth component $A_4^{\mathrm{ext}}(\boldsymbol{x})$, without any temporal dependence. Therefore:

$$(3)\qquad A_4^{\mathrm{ext}}(\boldsymbol{x})=\frac{i}{(2\pi)^3}\int\exp[i\boldsymbol{k}\cdot\boldsymbol{x}]g(\boldsymbol{k})\,\mathrm{d}^3\boldsymbol{k}\,.$$

2) We first consider the contribution of a single Fourier component of the external potential, for reasons which will be clear later.

B) We have here the following interpretations:

b_1) Incoming electron in x, where it is scattered, outgoing from x_1; pair creation in x_2.

b_2) Incoming electron in x_2, and outgoing from this same point, after emission of the photon; pair creation in x_1; positron scattered in x.

The matrix elements are:

$$(4)\ b_1) \qquad -2\pi g(\boldsymbol{k})[\overline{u}'\gamma_\lambda(\underline{p}'+\underline{p}''+\underline{p}'''+im)\gamma_4 u](\overline{u}''\gamma_\lambda u''')(p''+p''')^{-2}\cdot$$
$$\cdot[(p'+p''+p''')^2+m^2]^{-1}\delta^{(3)}(\boldsymbol{p}+\boldsymbol{k}-\boldsymbol{p}'-\boldsymbol{p}''-\boldsymbol{p}''')\,\delta(p_0-p_0'-p_0''-p_0''')\,;$$

$$(5)\ b_2) \qquad -2\pi g(\boldsymbol{k})[\overline{u}''\gamma_\lambda(-\underline{p}+\underline{p}'+\underline{p}''+im)\gamma_4 u'''](\overline{u}'\gamma_\lambda u)(p-p')^{-2}\cdot$$
$$\cdot[(-p+p'+p'')^2+m^2)]^{-1}\delta^{(3)}(\boldsymbol{p}+\boldsymbol{k}-\boldsymbol{p}'-\boldsymbol{p}''-\boldsymbol{p}''')\,\delta(p_0-p_0'-p_0''-p_0''').$$

Collecting all these results, and applying well-known rules, we obtain the total matrix element:

$$(6)\quad K=-2\pi e^3 g(\boldsymbol{k})\{f_1[\overline{u}'\gamma_4(\underline{P}_1+im)\gamma_\lambda u](\overline{u}''\gamma_\lambda u''')+f_2[\overline{u}''\gamma_4(P_2+im)\gamma_\lambda u''](\overline{u}'\gamma_\lambda u)+$$
$$+f_3[\overline{u}'\gamma_\lambda(\underline{P}_3+im)\gamma_4 u](\overline{u}''\gamma_\lambda u''')+f_4[\overline{u}''\gamma_\lambda(\underline{P}_4+im)\gamma_4 u'''](\overline{u}'\gamma_\lambda u)-$$
$$-g_1([\overline{u}''\gamma_4(\underline{P}_2+im)\gamma_\lambda u](\overline{u}'\gamma_\lambda u''')-g_2[\overline{u}'\gamma_4(\underline{P}_1+im)\gamma_\lambda u'''](\overline{u}''\gamma_\lambda u)-$$
$$-g_3[\overline{u}''\gamma_\lambda(\underline{P}_3+im)\gamma_4 u](\overline{u}'\gamma_\lambda u''')-g_4[\overline{u}'\gamma_\lambda(\underline{P}_4+im)\gamma_4 u'''](\overline{u}''\gamma_\lambda u)\}\cdot$$
$$\cdot\delta^{(3)}(\boldsymbol{p}+\boldsymbol{k}-\boldsymbol{p}'-\boldsymbol{p}''-\boldsymbol{p}''')\,\delta(p_0-p_0'-p_0''-p_0''')=$$
$$=M\delta^{(3)}(\boldsymbol{p}+\boldsymbol{k}-\boldsymbol{p}'-\boldsymbol{p}''-\boldsymbol{p}''')\,\delta(p_0-p_0'-p_0''-p_0'''),$$

where we have put:

$$(7a)\quad f_1=\frac{1}{(p''+p''')^2[(p-p''-p''')^2+m^2]},\quad g_1=\frac{1}{(p'+p''')^2[(p-p'-p''')^2+m^2]};$$

$$(7b)\quad f_2=\frac{1}{(p-p')^2[(p-p'-p''')^2+m^2]},\quad g_2=\frac{1}{(p-p'')^2[(p-p''-p''')^2+m^2]};$$

$$(7c)\quad f_3=\frac{1}{(p''+p''')^2[(p'+p''+p''')^2+m^2]},\quad g_3=\frac{1}{(p'+p''')^2[(p'+p''+p''')^2+m^2]};$$

$$(7d)\quad f_4=\frac{1}{(p-p')^2[(-p+p'+p'')^2+m^2]},\quad g_4=\frac{1}{(p-p'')^2[(-p+p'+p'')^2+m^2]}.$$

and

$$(8)\qquad \begin{cases} P_1 = p - p'' - p''', & P_2 = p - p' - p''', \\ P_3 = p' + p'' + p''', & P_4 = -p + p' + p''. \end{cases}$$

For convenience, we give also the explicit form of K^*:

$$(9)\qquad \begin{aligned} K^* \cdot\ & 2\pi e^3 g^*(\boldsymbol{k})\{f_1[\bar{u}\gamma_\lambda(\underline{P}_1 - im)\gamma_4 u'](\bar{u}'''\gamma_\lambda u'') - f_2[\bar{u}'''\gamma_\lambda(\underline{P}_2 + im)\gamma_4 u''](\bar{u}\gamma_\lambda u') + \\ & + f_3[\bar{u}\gamma_4(\underline{P}_3 + im)\gamma_\lambda u'](\bar{u}'''\gamma_\lambda u'') + f_4[\bar{u}'''\gamma_4(\underline{P}_4 + im)\gamma_\lambda u''](\bar{u}\gamma_\lambda u') - \\ & - g_1[\bar{u}\gamma_\lambda(\underline{P}_2 + im)\gamma_4 u''](\bar{u}'''\gamma_\lambda u') - g_2[\bar{u}'''\gamma_\lambda(\underline{P}_1 + im)\gamma_4 u'](\bar{u}\gamma_\lambda u'') - \\ & - g_3[\bar{u}\gamma_4(\underline{P}_3 + im)\gamma_\lambda u''](\bar{u}'''\gamma_\lambda u') - g_4[\bar{u}'''\gamma_4(\underline{P}_4 + im)\gamma_\lambda u'](\bar{u}\gamma_\lambda u'')\}\cdot \\ & \cdot \delta^{(3)}(\boldsymbol{p} + \boldsymbol{k} - \boldsymbol{p}' - \boldsymbol{p}'' - \boldsymbol{p}''')\,\delta(p_0 - p_0' - p_0'' - p_0''') = \\ & = M^*\delta^{(3)}(\boldsymbol{p} + \boldsymbol{k} - \boldsymbol{p}' - \boldsymbol{p}'' - \boldsymbol{p}''')\,\delta(p_0 - p_0' - p_0'' - p_0''')\,. \end{aligned}$$

2. – Sums over the Spins.

We have now to sum over the eigenvalues of the final spin states, and mediate over the initial ones. That is, writing for simplicity (compare eq. (6)):

$$(10a)\qquad M = -2\pi e^3 g(\boldsymbol{k})\{\sum_{\lambda=1}^{4} f_\lambda M_\lambda^{(1)} - \sum_{\lambda=1}^{4} g_\lambda M_\lambda^{(2)}\}$$

$$(10b)\qquad M^* = -2\pi e^3 g^*(\boldsymbol{k})\{\sum_{\mu=1}^{4} f_\mu M_\mu^{(1)*} - \sum_{\mu=1}^{4} g_\mu M_\mu^{(2)*}\}$$

and denoting by S the sum over the spins of all particles, we must calculate:

$$(11)\qquad \begin{aligned} \tfrac{1}{2} S\,|M|^2 = 2\pi^2 e^6\,|g(\boldsymbol{k})|^2\{ & \sum_{\lambda,\mu=1}^{4} f_\lambda f_\mu S M_\lambda^{(1)} M_\mu^{(1)*} - \sum_{\lambda,\mu=1}^{4} f_\lambda g_\mu S M_\lambda^{(1)} M_\mu^{(2)*} - \\ & - \sum_{\lambda,\mu=1}^{4} g_\lambda f_\mu S M_\lambda^{(2)} M_\mu^{(1)*} + \sum_{\lambda,\mu=1}^{4} g_\lambda g_\mu S M_\lambda^{(2)} M_\mu^{(2)*}\}\,. \end{aligned}$$

For this purpose, we employ the method of the projection operators, which one finds in Dyson's lectures already cited.

Let us consider, first, the terms f_λ^2 and g_λ^2. For the coefficient of f_1^2, we easily find:

$$(12)\qquad \begin{aligned} & -Sp[\Lambda^{(+)}(p')\gamma_4(P_1 + im)\gamma_\mu\Lambda^{(+)}(p)\gamma_\lambda(\underline{P}_1 + im)\gamma_4]\cdot Sp[\Lambda^{(+)}(p'')\gamma_\mu\Lambda^{(-)}(p''')\gamma_\lambda] = \\ & = -Sp[\Lambda^{(+)}(-\bar{p}')(\underline{P}_1 + im)\gamma_\mu\Lambda^{(+)}(p)\gamma_\lambda(\underline{P}_1 + im)]\cdot Sp[\Lambda^{(+)}(p'')\gamma_\mu\Lambda^{(-)}(p''')\gamma_\lambda]\,, \end{aligned}$$

where

$$\bar{p}'_k = p'_k \quad (k = 1, 2, 3), \qquad \bar{p}'_0 = -p'_0 . \tag{13}$$

After a straightforward calculation, (12) becomes:

$$\begin{aligned} 2m^{-4}\{&2(P_1\cdot\bar{p}')(p\cdot p'')(P_1\cdot p''') + 2(P_1\cdot\bar{p}')(p\cdot p''')(P_1\cdot p'') - P_1^2(p\cdot p'')(\bar{p}'\cdot p''') - \\ &- P_1^2(p\cdot p''')(\bar{p}'\cdot p'') - 2m^2(P_1\cdot p)(P_1\cdot\bar{p}') + 2m^2(p\cdot p'')(P_1\cdot p''') + \\ &+ 2m^2(p\cdot p''')(P_1\cdot p'') - 2m^4(P_1\cdot p) + m^2P_1^2(p\cdot\bar{p}') - m^2(p\cdot p'')(\bar{p}'\cdot p''') - \\ &- m^2(p\cdot p''')(\bar{p}'\cdot p'') + 2m^2(P_1\cdot\bar{p}')(p''\cdot p''') - m^2P_1^2(p''\cdot p''') + \\ &+ m^4(p\cdot\bar{p}') - 4m^4(P_1\cdot\bar{p}') + 2m^4P_1^2 + m^4(p''\cdot p''') - 2m^6\}. \end{aligned} \tag{14}$$

The coefficients of f_2^2, f_3^2 and f_4^2 can be deduced from this result by the following substitutions:

(14*a*) For f_2^2: $\quad p'' \rightleftarrows p'$, $\quad p \rightleftarrows -p'''$,

(14*b*) For f_3^2: $\quad p' \rightleftarrows p$, $\quad p'' \rightleftarrows -p'''$,

(14*c*) For f_4^2: $\quad p'' \rightleftarrows p$, $\quad p' \rightleftarrows -p'''$.

Finally, the coefficients of the terms g_λ^2 are obtained from those of f_λ^2 by interchanging p' and p''.

The evaluation of the coefficients of the mixed terms $f_\lambda g_\mu$ is more involved. Let us consider, for example, the coefficient of $f_1 g_1$, which is given by:

$$\mathrm{Sp}[A^{(+)}(p')\gamma_4(\underline{P}_1 + im)\gamma_\mu A^{(+)}(p)\gamma_\lambda(\underline{P}_2 + im)\gamma_4 A^{(+)}(p'')\gamma_\mu A^{(-)}(p''')\gamma_\lambda]. \tag{15a}$$

Similarly, for the coefficient of $g_1 f_1$, we have:

$$\mathrm{Sp}[A^{(+)}(p')\gamma_\mu A^{(-)}(p''')\gamma_\lambda A^{(+)}(p'')\gamma_4(\underline{P}_2 + im)\gamma_\mu A^{(+)}(p)\gamma_\lambda(\underline{P}_1 + im)\gamma_4], \tag{15b}$$

and it is easy to see that (15*a*) and (15*b*) give rise to the same contributions. Indeed, a typical term in the development of (15*a*) is:

$$\mathrm{Sp}[\underline{p}'\gamma_4\underline{P}_1\gamma_\mu\underline{p}\gamma_\lambda P_2\gamma_4\underline{p}''\gamma_\mu\underline{p}'''\gamma_\lambda], \tag{16a}$$

to which corresponds, in the development of (15*b*), the following expression:

$$\mathrm{Sp}[\underline{p}'\gamma_\mu\underline{p}'''\gamma_\lambda\underline{p}''\gamma_4\underline{P}_2\gamma_\mu\underline{p}\gamma_\lambda\underline{P}_1\gamma_4]. \tag{16b}$$

Now, (16*a*) is effectively equal to (16*b*), since the spur of a product of Dirac's matrices equals the spur of the same product, with reversed order of factors. The other terms follow from those written above by total or partial substitution of $\underline{p}'$, $\underline{p}''$, $\underline{p}'''$, $\underline{p}$, $\underline{P}_1$ and $\underline{P}_2$ with constant multiples of the unity matrix; it is clear that this property holds for these also, so that the coefficient of $f_1 g_1$ is:

$$2\,\mathrm{Sp}\,[\Lambda^{(+)}(p')\gamma_4(\underline{P}_1 + im)\gamma_\mu \Lambda^{(+)}(p)\gamma_\lambda(\underline{P}_2 + im)\gamma_4 \Lambda^{(+)}(p'')\gamma_\mu \Lambda^{(-)}(p''')\gamma_\lambda]\,.$$

In general, we may write:

$$S M_\lambda^{(1)} M_\mu^{(2)*} = S M_\lambda^{(1)*} M_\mu^{(2)}\,, \tag{17}$$

whence

$$\sum_{\lambda,\mu=1}^{4} f_\lambda g_\mu S M_\lambda^{(1)} M_\mu^{(2)*} + \sum_{\lambda,\mu=1}^{4} g_\lambda f_\mu S M_\lambda^{(2)} M_\mu^{(1)*} = 2 \sum_{\lambda,\mu=1}^{4} f_\lambda g_\mu S M_\lambda^{(1)} M_\mu^{(2)*}\,. \tag{18}$$

A careful investigation of the structure of the sixteen coefficients appearing in (18) shows that it is possible to express all of them in terms of three « typical forms », which are defined as follows:

$$S_1(p_1, \ldots, p_6) = \\ = \mathrm{Sp}\,[(\underline{p}_1 + im)\gamma_4(\underline{p}_2 + im)\gamma_\mu(\underline{p}_3 + im)\gamma_\lambda(\underline{p}_1 + im)\gamma_4(\underline{p}_5 + im)\gamma_\mu(\underline{p}_6 + im)\gamma_\lambda]\,,$$

$$S_2(p_1, \ldots, p_6) = \\ = \mathrm{Sp}\,[(\underline{p}_1 + im)(\underline{p}_2 + im)\gamma_\mu(\underline{p}_3 + im)\gamma_\lambda(\underline{p}_4 + im)\gamma_\mu(\underline{p}_5 + im)\gamma_\lambda(\underline{p}_6 + im)]\,,$$

$$S_3(p_1, \ldots, p_6) = \\ = \mathrm{Sp}\,[(\underline{p}_1 + im)\gamma_4(\underline{p}_2 + im)\gamma_\mu(\underline{p}_3 + im)\gamma_4(\underline{p}_4 + im)\gamma_\lambda(\underline{p}_5 + im)\gamma_\mu(\underline{p}_6 + im)\gamma_\lambda]\,.$$

The development of these three forms is elementary, and gives:

$$\begin{aligned} S_1(p_1, \ldots, p_6) = \\ = &- 4\,\mathrm{Sp}\,(\bar{\underline{p}}_2\bar{\underline{p}}_1\bar{\underline{p}}_4\underline{p}_5\underline{p}_3\underline{p}_6) - 8p_{2,1}\,\mathrm{Sp}\,(\underline{p}_4\gamma_4\underline{p}_5\underline{p}_3\underline{p}_6\underline{p}_1) - 4\,\mathrm{Sp}\,(\bar{\underline{p}}_2\bar{\underline{p}}_3\bar{\underline{p}}_4\underline{p}_5\underline{p}_6\underline{p}_1) - \\ &- 4\,\mathrm{Sp}\,(\underline{p}_5\underline{p}_4\underline{p}_6\bar{\underline{p}}_1\underline{p}_2\underline{p}_3) \quad 4\,\mathrm{Sp}\,(\bar{\underline{p}}_2\bar{\underline{p}}_3\underline{p}_4\underline{p}_6\underline{p}_5\underline{p}_1) + 8(p_4\cdot p_6)\,\mathrm{Sp}\,(\bar{\underline{p}}_5\bar{\underline{p}}_1\underline{p}_2\underline{p}_3) - \\ &- 16p_{5,4}(p_4\cdot p_6)\,\mathrm{Sp}\,(\underline{p}_3\underline{p}_2\gamma_4\underline{p}_1) - \\ &- m^2\{- 4\,\mathrm{Sp}\,(\underline{p}_3\underline{p}_4\bar{\underline{p}}_6\underline{p}_2) \quad - 8p_{4,4}\,\mathrm{Sp}\,(\underline{p}_3\underline{p}_6\gamma_4\underline{p}_2) + 8p_{2,4}\,\mathrm{Sp}\,(\underline{p}_4\gamma_4\underline{p}_3\underline{p}_6) - \\ &\quad - 4\,\mathrm{Sp}\,(\underline{p}_4\bar{\underline{p}}_5\bar{\underline{p}}_6\underline{p}_2) \quad + 64p_{2,4}p_{5,4}(p_4\cdot p_6) \quad - 8p_{2,4}\,\mathrm{Sp}\,(\gamma_4\underline{p}_5\underline{p}_4\underline{p}_6) + \\ &\quad + 4\,\mathrm{Sp}\,(\bar{\underline{p}}_4\underline{p}_5\underline{p}_6\underline{p}_1) \quad - 8p_{1,4}\,\mathrm{Sp}\,(\gamma_4\underline{p}_5\underline{p}_4\underline{p}_6) + 64p_{1,4}p_{5,4}(p_4\cdot p_6) + \\ &\quad + 8p_{1,4}\,\mathrm{Sp}\,(\underline{p}_4\gamma_4\underline{p}_3\underline{p}_6) + 4\,\mathrm{Sp}\,(\underline{p}_3\bar{\underline{p}}_4\underline{p}_6\underline{p}_1) \quad - 8p_{4,4}\,\mathrm{Sp}\,(\underline{p}_3\underline{p}_6\underline{p}_1\gamma_4) + \end{aligned} \tag{19}$$

$$
\begin{aligned}
&+4\,\mathrm{Sp}\,(\underline{p}_5\underline{p}_6\underline{p}_1\bar{\underline{p}}_2) \quad +8p_{5,4}\,\mathrm{Sp}\,(\underline{p}_6\underline{p}_1\underline{\gamma}_4\underline{p}_2) \quad +8p_{5,4}\,\mathrm{Sp}\,(\underline{p}_4\underline{p}_1\underline{\gamma}_4\underline{p}_2)+\\
&+32(p_5\cdot p_4)(\bar{p}_1\cdot p_2) \quad -4\,\mathrm{Sp}\,(\bar{\underline{p}}_4\underline{p}_1\bar{\underline{p}}_2\bar{\underline{p}}_5) \quad -4\,\mathrm{Sp}\,(\underline{p}_5\bar{\underline{p}}_3\bar{\underline{p}}_2\underline{p}_1)+\\
&+8p_{5,4}\,\mathrm{Sp}\,(\underline{p}_3\underline{p}_2\underline{\gamma}_4\underline{p}_1)-4\,\mathrm{Sp}\,(\bar{\underline{p}}_2\underline{p}_3\underline{p}_4\underline{p}_1) \quad -8p_{3,4}\,\mathrm{Sp}\,(\underline{p}_4\underline{p}_1\underline{\gamma}_4\underline{p}_2)+\\
&+8\,\mathrm{Sp}\,(\underline{p}_3\underline{p}_4\bar{\underline{p}}_1\underline{p}_2) \quad +16p_{4,4}\,\mathrm{Sp}\,(\underline{p}_3\underline{p}_1\underline{\gamma}_4\underline{p}_2)+4\,\mathrm{Sp}\,(\bar{\underline{p}}_5\bar{\underline{p}}_4\underline{p}_6\underline{p}_3)-\\
&-8p_{5,4}\,\mathrm{Sp}\,(\underline{p}_4\underline{\gamma}_4\underline{p}_6\underline{p}_3)+4\,\mathrm{Sp}\,(\bar{\underline{p}}_3\underline{p}_4\bar{\underline{p}}_5\bar{\underline{p}}_6) \quad +8p_{2,4}\,\mathrm{Sp}\,(\underline{\gamma}_4\underline{p}_5\underline{p}_3\underline{p}_6)+\\
&+4\,\mathrm{Sp}\,(\bar{\underline{p}}_2\bar{\underline{p}}_3\underline{p}_5\underline{p}_6) \quad -8p_{5,4}\,\mathrm{Sp}\,(\underline{p}_3\underline{p}_6\underline{\gamma}_4\underline{p}_2) \quad +4\,\mathrm{Sp}\,(\underline{p}_3\underline{p}_4\bar{\underline{p}}_5\underline{p}_2)+\\
&+8p_{2,4}\,\mathrm{Sp}\,(\underline{p}_3\underline{p}_4\underline{\gamma}_4\underline{p}_5)+8p_{1,4}\,\mathrm{Sp}\,(\underline{\gamma}_4\underline{p}_5\underline{p}_3\underline{p}_6) \quad -4\,\mathrm{Sp}\,(\bar{\underline{p}}_3\underline{p}_5\underline{p}_6\underline{p}_1)-\\
&-8p_{5,4}\,\mathrm{Sp}\,(\underline{p}_3\underline{p}_6\underline{p}_1\underline{\gamma}_4)-4\,\mathrm{Sp}\,(\underline{p}_3\underline{p}_4\bar{\underline{p}}_5\bar{\underline{p}}_1) \quad +8p_{1,4}\,\mathrm{Sp}\,(\underline{p}_3\underline{p}_4\underline{\gamma}_4\underline{p}_5)-\\
&-4\,\mathrm{Sp}\,(\underline{p}_6\underline{p}_1\bar{\underline{p}}_2\bar{\underline{p}}_4) \quad +8p_{4,4}\,\mathrm{Sp}\,(\underline{p}_6\underline{p}_1\underline{\gamma}_4\underline{p}_2) \quad +32(p_3\cdot p_6)(\bar{p}_1\cdot p_2)\big\}+\\
&+m^4\big\{-16(\bar{p}_1\cdot p_2) \quad +16(p_1\cdot p_3)-32(p_1\cdot p_4)+32(\bar{p}_1\cdot p_5)-16(\bar{p}_1\cdot p_6)-\\
&-16(\bar{p}_2\cdot p_3) \quad +32(\bar{p}_2\cdot p_4)-32(p_2\cdot p_5)+16(p_2\cdot p_6)-16(\bar{p}_3\cdot p_4)+\\
&+16(p_3\cdot p_5) \quad -32(p_3\cdot p_6)-16(\bar{p}_4\cdot p_5)+16(p_4\cdot p_6)-16(\bar{p}_5\cdot p_6)\big\}-16m^6;
\end{aligned}
$$

(20)
$$
\begin{aligned}
S_2(p_1,\ldots,p_6) &= -8(p_3\cdot p_5)\,\mathrm{Sp}\,(\underline{p}_4\underline{p}_6\underline{p}_1\underline{p}_2)-\\
&-m^2\big\{-32(p_4\cdot p_6)(p_3\cdot p_5)+4\,\mathrm{Sp}\,(\underline{p}_5\underline{p}_4\underline{p}_6\underline{p}_2)+4\,\mathrm{Sp}\,(\underline{p}_5\underline{p}_3\underline{p}_6\underline{p}_2)+\\
&+32(p_3\cdot p_4)(p_2\cdot p_6)-4\,\mathrm{Sp}\,(\underline{p}_2\underline{p}_3\underline{p}_4\underline{p}_6)-32(p_3\cdot p_5)(p_2\cdot p_4)+\\
&+4\,\mathrm{Sp}\,(\underline{p}_5\underline{p}_4\underline{p}_6\underline{p}_1)+4\,\mathrm{Sp}\,(\underline{p}_5\underline{p}_3\underline{p}_6\underline{p}_1)+4\,\mathrm{Sp}\,(\underline{p}_6\underline{p}_1\underline{p}_4\underline{p}_3)-\\
&-32(p_1\cdot p_4)(p_3\cdot p_5)+4\,\mathrm{Sp}\,(\underline{p}_6\underline{p}_1\underline{p}_2\underline{p}_5)+4\,\mathrm{Sp}\,(\underline{p}_6\underline{p}_1\underline{p}_2\underline{p}_4)+\\
&+4\,\mathrm{Sp}\,(\underline{p}_5\underline{p}_4\underline{p}_1\underline{p}_2)+4\,\mathrm{Sp}\,(\underline{p}_3\underline{p}_6\underline{p}_1\underline{p}_2)+4\,\mathrm{Sp}\,(\underline{p}_1\underline{p}_2\underline{p}_5\underline{p}_3)+4\,\mathrm{Sp}\,(\underline{p}_1\underline{p}_2\underline{p}_4\underline{p}_3)\big\}+\\
&+m^4\big\{-32(p_1\cdot p_2)+16(p_1\cdot p_3)+16(p_1\cdot p_4)+16(p_1\cdot p_5)-32(p_1\cdot p_6)+\\
&+16(p_2\cdot p_3)+16(p_2\cdot p_4)+16(p_2\cdot p_5)-32(p_2\cdot p_6)+16(p_3\cdot p_4)+\\
&+16(p_3\cdot p_5)+16(p_3\cdot p_6)+16(p_4\cdot p_5)+16(p_4\cdot p_6)+16(p_5\cdot p_6)\big\}+32m^6;
\end{aligned}
$$

(21)
$$
\begin{aligned}
S_3(p_1,\ldots,p_6) &=\\
&=-4\,\mathrm{Sp}\,(\underline{p}_5\underline{p}_6\underline{p}_4\bar{\underline{p}}_3\underline{p}_1\underline{p}_2)-8p_{1,3}\,\mathrm{Sp}\,(\underline{p}_5\underline{p}_6\underline{p}_1\underline{\gamma}_4\underline{p}_3\underline{p}_2)+4\,\mathrm{Sp}\,(\bar{\underline{p}}_1\bar{\underline{p}}_6\bar{\underline{p}}_4\underline{p}_3\underline{p}_5\underline{p}_2)-\\
&-m^2\big\{4\,\mathrm{Sp}\,(\underline{p}_5\underline{p}_6\underline{p}_4\bar{\underline{p}}_3)-4\,\mathrm{Sp}\,(\bar{\underline{p}}_6\bar{\underline{p}}_4\underline{p}_3\underline{p}_5)+8p_{2,4}\,\mathrm{Sp}\,(\underline{p}_5\underline{p}_6\underline{p}_4\underline{\gamma}_4)-\\
&-4\,\mathrm{Sp}\,(\underline{p}_6\underline{p}_4\bar{\underline{p}}_5\bar{\underline{p}}_2)+8p_{2,4}\,\mathrm{Sp}\,(\underline{p}_5\underline{p}_6\underline{\gamma}_4\underline{p}_3) \quad +4\,\mathrm{Sp}\,(\bar{\underline{p}}_6\underline{p}_3\underline{p}_5\underline{p}_2)-\\
&-4\,\mathrm{Sp}\,(\bar{\underline{p}}_4\underline{p}_3\underline{p}_6\underline{p}_2)-4\,\mathrm{Sp}\,(\bar{\underline{p}}_4\underline{p}_3\underline{p}_5\underline{p}_2) \quad +8p_{1,4}\,\mathrm{Sp}\,(\underline{p}_5\underline{p}_6\underline{p}_4\underline{\gamma}_4)+\\
&+4\,\mathrm{Sp}\,(\underline{p}_6\underline{p}_4\bar{\underline{p}}_5\underline{p}_1)+8p_{1,4}\,\mathrm{Sp}\,(\underline{p}_5\underline{p}_6\underline{\gamma}_4\underline{p}_3)-4\,\mathrm{Sp}\,(\underline{p}_6\bar{\underline{p}}_3\bar{\underline{p}}_5\underline{p}_1)+
\end{aligned}
$$

$$+ 4\,\mathrm{Sp}\,(\underline{p}_4\underline{\bar{p}}_3\underline{\bar{p}}_6\underline{p}_5) + 4\,\mathrm{Sp}\,(\underline{p}_4\underline{\bar{p}}_3\underline{\bar{p}}_5\underline{p}_1) \quad - 8p_{6,4}\,\mathrm{Sp}\,(\underline{p}_5\underline{p}_2\gamma_4\underline{p}_1) +$$
$$- 4\,\mathrm{Sp}\,(\underline{\bar{p}}_6\underline{p}_2\underline{p}_1\underline{p}_1) + 4\,\mathrm{Sp}\,(\underline{p}_4\underline{\bar{p}}_5\underline{p}_2\underline{p}_1) \quad - 4\,\mathrm{Sp}\,(\underline{\bar{p}}_1\underline{p}_3\underline{p}_6\underline{p}_2) -$$
$$- 4\,\mathrm{Sp}\,(\underline{\bar{p}}_1\underline{p}_3\underline{p}_5\underline{p}_2) + 4\,\mathrm{Sp}\,(\underline{\bar{p}}_1\underline{p}_3\underline{p}_1\underline{p}_2) \quad + 8p_{3,4}\,\mathrm{Sp}\,(\underline{p}_4\underline{p}_2\gamma_4\underline{p}_1)\} +$$
$$m^4\{-16(\bar{p}_1\cdot p_2) - 32p_{1,4}p_{3,4} - 32p_{1,4}p_{4,4} - 16(\bar{p}_1\cdot p_5) - 16(\bar{p}_1\cdot p_6) - 32p_{2,4}p_{3,4} -$$
$$- 32p_{2,4}p_{4,4} + 16(p_2\cdot p_5) + 16(p_2\cdot p_6) - 16(\bar{p}_3\cdot p_4) + 16(p_3\cdot p_5) +$$
$$+ 16(p_3\cdot p_6) - 16(\bar{p}_4\cdot p_5) - 16(\bar{p}_4\cdot p_6) - 32p_{5,4}p_{6,4}\} - 16m^6\,.$$

For the coefficients of the terms $f_\lambda g_\mu$ we may then write:

(22) f_1g_1: $\quad -(8m^4)^{-1}S_1(p', P_1, p, P_2, p'', -p''')$

(23) f_1g_2: $\quad -(8m^4)^{-1}S_2(-\bar{p}', P_1, p, p'', -p''', P_1)$

(24) f_1g_3: $\quad -(8m^4)^{-1}S_3(p', P_1, p, P_3, p'', -p''')$

(25) f_1g_4: $\quad -(8m^4)^{-1}S_3(-p''', P_4, p', P_1, p, p'')$

(23′) f_2g_1: $\quad$ from (23), with $p' \rightleftarrows p''$, $p \rightleftarrows -p'''$

(22′) f_2g_2: $\quad$ from (22), with $p' \rightleftarrows p''$, $p \rightleftarrows -p'''$

(25′) f_2g_3: $\quad$ from (25), with $p' \rightleftarrows p''$, $p \rightleftarrows -p'''$

(24′) f_2g_4: $\quad$ from (24), with $p' \rightleftarrows p''$, $p \rightleftarrows -p'''$

(26) f_3g_1: $\quad -(8m^4)^{-1}S_3(P_3, p, P_2, p'', -p''', p')$

(27) f_3g_2: $\quad -(8m^4)^{-1}S_3(P_1, p', P_3, p, p'', -p''')$

(28) f_3g_3: $\quad -(8m^4)^{-1}S_2(-\bar{p}, P_3, p'', -p''', p', P_3)$

(29) f_3g_4: $\quad -(8m^4)^{-1}S_1(P_3, p, p'', -p''', P_4, p')$

(27′) f_4g_1: $\quad$ from (27), with $p' \rightleftarrows p''$, $p \rightleftarrows -p'''$

(26′) f_4g_2: $\quad$ from (26), with $p' \rightleftarrows p''$, $p \rightleftarrows -p'''$

(29′) f_4g_3: $\quad$ from (29), with $p' \rightleftarrows p''$, $p \rightleftarrows -p'''$

(28′) f_4g_4: $\quad$ from (28), with $p' \rightleftarrows p''$, $p \rightleftarrows -p'''$

Finally, we must consider the coefficients of the terms $f_\lambda f_\mu$ and $g_\lambda g_\mu$ (with $\lambda \neq \mu$). Putting:

$$(30)\quad T_{\mu\lambda}(p_1, p_2, p_3) = \mathrm{Sp}\,[(\underline{p}_1 + im)\gamma_4(\underline{p}_2 + im)\gamma_\mu(\underline{p}_3 + im)\gamma_\lambda] =$$
$$= \mathrm{Sp}\,(\underline{p}_1\gamma_4\underline{p}_2\gamma_\mu\underline{p}_3\gamma_\lambda) - m^2\{\mathrm{Sp}\,(\gamma_4\gamma_\mu\underline{p}_3\gamma_\lambda) + \mathrm{Sp}(\gamma_4\underline{p}_2\gamma_\mu\gamma_\lambda) + \mathrm{Sp}\,(\underline{p}_1\gamma_4\gamma_\mu\gamma_\lambda)\},$$

it is easily seen that:

$$(31)\qquad f_1 f_2\text{:}\qquad (8m^4)^{-1}T_{\mu\lambda}(p', P_1, p)\,T_{\mu\lambda}(P_2, p'', -p''')$$

$$(32)\qquad f_1 f_4\text{:}\qquad (8m^4)^{-1}T_{\mu\lambda}(p', P_1, p)\,T_{\mu\lambda}(P_4, -p''', p'')\,.$$

For the coefficient of $f_1 f_3$, we have:

$$(33)\quad 2S M_1^{(1)} M_3^{(1)*} =$$
$$= 2m^{-2}\{\mathrm{Sp}\,[\Lambda^{(+)}(p')\gamma_4(P_1 + im)\underline{p}''\Lambda^{(+)}(p)\gamma_4(P_3 + im)\underline{p}'''] +$$
$$+ \mathrm{Sp}\,[\Lambda^{(+)}(p')\gamma_4(P_1 + im)\underline{p}'''\Lambda^{(+)}(p)\gamma_4(P_3 + im)\underline{p}''] -$$
$$- (p''\cdot p''' - m^2)\,\mathrm{Sp}\,[\Lambda^{(+)}(p')\gamma_4(P_1 + im)\gamma_\lambda\Lambda^{(+)}(p)\gamma_4(\underline{P}_3 + im)\gamma_\lambda]\}\,.$$

Introducing the notation:

$$(34)\quad T(p_1, \ldots, p_6) = \mathrm{Sp}[(\underline{p}_1 + im)(\underline{p}_2 + im)\underline{p}_3(\underline{p}_4 + im)(\underline{p}_5 + im)\underline{p}_6] =$$
$$= \mathrm{Sp}\,(\underline{p}_1\underline{p}_2\underline{p}_3\underline{p}_4\underline{p}_5\underline{p}_6) -$$
$$- m^2\{\mathrm{Sp}\,(\underline{p}_3\underline{p}_4\underline{p}_5\underline{p}_6) + \mathrm{Sp}\,(\underline{p}_2\underline{p}_3\underline{p}_5\underline{p}_6) + \mathrm{Sp}\,(\underline{p}_2\underline{p}_3\underline{p}_4\underline{p}_6) +$$
$$+ \mathrm{Sp}\,(\underline{p}_1\underline{p}_3\underline{p}_5\underline{p}_6) + \mathrm{Sp}\,(\underline{p}_1\underline{p}_3\underline{p}_4\underline{p}_6) + \mathrm{Sp}\,(\underline{p}_1\underline{p}_2\underline{p}_3\underline{p}_6)\} + m^4\,\mathrm{Sp}\,(\underline{p}_3\underline{p}_6)\,,$$

the first two terms in the right-hand side of (33) become:

$$(35)\qquad -(2m^4)^{-1}T(p', -\bar{P}_1, -\bar{p}'', -\bar{p}, P_3, p''')$$

and

$$(36)\qquad -(2m^4)^{-1}T(p', -P_1, -\bar{p}''', -\bar{p}, P_3, p'')$$

respectively, while the last one gives:

$$(37)\quad -(2m^4)^{-1}(p''\cdot p''' - m^2)\{2\,\mathrm{Sp}\,(\underline{P}_3\underline{p}\underline{p}'\underline{P}_1) + 4P_{3,4}\,\mathrm{Sp}\,(\underline{p}\underline{p}'\gamma_4\underline{P}_1) + 8m^2(\bar{p}\cdot P_3) +$$
$$+ 16m^2P_{1,4}P_{3,4} + 16m^2p_4P_{1,4} + 16m^2p_1'P_{3,4} + 16m^2p_4p_4' + 8m^2(\bar{p}'\cdot P_1) + 8m^4\}.$$

The remaining coefficients are deduced from these by the following substitutions:

(32′) $f_2 f_3$: from $f_1 f_4$, with $p' \rightleftarrows p''$, $p \rightleftarrows -p'''$

(33′) $f_2 f_4$: from $f_1 f_3$, with $p' \rightleftarrows p''$, $p \rightleftarrows -p'''$

(31′) $f_3 f_4$: from $f_1 f_2$, with $p \rightleftarrows p''$, $p' \rightleftarrows -p'''$.

Finally, the coefficients of the terms $g_\lambda g_\mu$ (with $\lambda \neq \mu$) may be written down immediately by interchanging p' and p'' in the above formulas.

3. – Deduction of the Cross-Section.

We are now able to obtain the differential cross-section. For this purpose, we follow the procedure given in Pauli's « Feldquantisierung ».

Denoting by $F(p, p', p'', p''')$ the expression (11), and putting:

$$\omega_1(|\boldsymbol{p}|) = \sqrt{|\boldsymbol{p}|^2 + m^2} \quad \text{(energy of the incoming electron)}$$

$$\omega_2(|\boldsymbol{p}'|, |\boldsymbol{p}''|, |\boldsymbol{p}'''|) = \sqrt{|\boldsymbol{p}'|^2 + m^2} + \sqrt{|\boldsymbol{p}''|^2 + m^2} + \sqrt{|\boldsymbol{p}'''|^2 + m^2}$$

(sum of the energies of the final particles)

the differential cross-section for the process in which only a single Fourier component of the external potential is taken into account is (l. c., eq. (135)).

$$(38)\quad \mathrm{d}\sigma(\boldsymbol{k}) = (2\pi)^2 \cdot |\boldsymbol{v}|^{-1} \cdot 2\pi^2 e^6 |g(\boldsymbol{k})|^2 \,\mathrm{d}\Omega\, \mathrm{d}^3\boldsymbol{p}''' \cdot \int |\boldsymbol{p}'|^2 F(p, p', p + k - p' - p''', p''') \cdot \delta[\omega_1(|\boldsymbol{p}|) - \omega_2(|\boldsymbol{p}'|, |\boldsymbol{p} + \boldsymbol{k} - \boldsymbol{p}' - \boldsymbol{p}'''|, |\boldsymbol{p}'''|)] \,\mathrm{d}|\boldsymbol{p}'|.$$

The effect of the whole potential is then obtained by integrating (38) over $\mathrm{d}^3\boldsymbol{k}$. Observing that we can write:

$$(38')\quad \mathrm{d}\sigma(\boldsymbol{k}) = (2\pi)^2 \cdot |\boldsymbol{v}|^{-1} \cdot 2\pi^2 e^6 |g(\boldsymbol{k})|^2 \,\mathrm{d}\Omega\, \mathrm{d}^3\boldsymbol{p}''' \int |\boldsymbol{p}'|^2 F(p, p', p'', p''') \cdot \delta[\omega_1(|\boldsymbol{p}|) - \omega_2(|\boldsymbol{p}'|, |\boldsymbol{p}''|, |\boldsymbol{p}'''|)] \delta^{(3)}(\boldsymbol{p} + \boldsymbol{k} - \boldsymbol{p}' - \boldsymbol{p}'' - \boldsymbol{p}''') \,\mathrm{d}|\boldsymbol{p}'| \,\mathrm{d}^3\boldsymbol{p}'',$$

we easily get:

$$(39)\quad \mathrm{d}\sigma = \int \mathrm{d}\sigma(\boldsymbol{k}) \,\mathrm{d}^3\boldsymbol{k} = 8\pi^4 e^6 |\boldsymbol{v}|^{-1} \,\mathrm{d}\Omega\, \mathrm{d}^3\boldsymbol{p}''\, \mathrm{d}^3\boldsymbol{p}''' \int |\boldsymbol{p}'|^2 \cdot g(\boldsymbol{p}' + \boldsymbol{p}'' + \boldsymbol{p}''' - \boldsymbol{p})|^2 \cdot F(p, p', p'', p''') \delta[\omega_1(|\boldsymbol{p}|) - \omega_2(|\boldsymbol{p}'|, |\boldsymbol{p}''|, |\boldsymbol{p}'''|)] \,\mathrm{d}|\boldsymbol{p}'| =$$

$$= 8\pi^4 e^6 |\boldsymbol{v}|^{-1} \,\mathrm{d}\Omega\, \mathrm{d}^3\boldsymbol{p}''\, \mathrm{d}^3\boldsymbol{p}''' \{|\boldsymbol{p}'| \cdot \sqrt{|\boldsymbol{p}'|^2 + m^2} \cdot |g(\boldsymbol{p}' + \boldsymbol{p}'' + \boldsymbol{p}''' - \boldsymbol{p})|^2 \cdot F(p, p', p'', p''')\}_{|\boldsymbol{p}'| = \sqrt{(\omega_1 - \sqrt{|\boldsymbol{p}''|^2 + m^2} - \sqrt{|\boldsymbol{p}'''|^2 + m^2})^2 - m^2}}$$

This equation gives the differential cross-section for the process in which the direction of one of the final particles lies into the solid angle element $\mathrm{d}\Omega$, the other two having moments lying into the elements $\mathrm{d}^3\boldsymbol{p}''$ and $\mathrm{d}^3\boldsymbol{p}'''$, respectively.

The total cross-section follows from (39) by integrating over $\mathrm{d}\Omega$, $\mathrm{d}^3\boldsymbol{p}''$ and $\mathrm{d}^3\boldsymbol{p}'''$. After some transformations, we obtain:

$$\sigma = 8\pi^4 e^6 |\boldsymbol{v}| \int_1^{\sqrt{(\omega_1 - 2m)^2 - m^2}} \mathrm{d}|\boldsymbol{p}''| \int_{\sqrt{(\omega_1 - m - \sqrt{|\boldsymbol{p}''|^2 + m^2})^2 - m^2}} \mathrm{d}|\boldsymbol{p}'''| \, G(p, |\boldsymbol{p}''|, |\boldsymbol{p}'''|), \tag{40}$$

where:

$$G(p, |\boldsymbol{p}''|, |\boldsymbol{p}'''|) = \int \mathrm{d}\Omega \, \mathrm{d}\Omega'' \, \mathrm{d}\Omega''' \{ |\boldsymbol{p}'| \cdot \sqrt{|\boldsymbol{p}'|^2 + m^2} \cdot |g(\boldsymbol{p}' + \boldsymbol{p}'' + \boldsymbol{p}''' - \boldsymbol{p})|^2 \cdot F(p, p', p'', p''') \}_{|\boldsymbol{p}'| = A},$$

and

$$A = \sqrt{(\omega_1 - \sqrt{|\boldsymbol{p}''|^2 + m^2} - \sqrt{|\boldsymbol{p}'''|^2 + m^2})^2 - m^2}. \tag{40a}$$

4. – Conclusions.

Our results are merely theoretical, but they could give, after numerical evaluation of the integrals (corresponding to different values of the energy of the incoming electron), informations on the phenomena of electron scattering and pair creation. It would then be possible to compare the theoretical previsions with the experimental results, and to see whether quantum electrodynamics is confirmed by experiment in high energies processes.

* * *

We wish to thank Prof. P. Caldirola for his kind interest, and to express our gratitude for helpful discussions to the friends Drs. P. Bocchieri and A. Loinger, of the University of Pavia.

Appendix

We collect here some formulas, which we have used in the calculation of the spurs arising from the sums over the spins (cfr. Sect. 2).

$$\sum_{i=1}^{2} u_\alpha^{(i)}(p) \bar{u}_\beta^{(i)}(p) = \begin{cases} (2im)^{-1}(\not{p} + im)_{\alpha\beta} = \Lambda_{\alpha\beta}^{(+)}(p) \text{ for electron states } u, \\ (2im)^{-1}(\not{p} - im)_{\alpha\beta} = \Lambda_{\alpha\beta}^{(-)}(p) \text{ for positron states } u, \end{cases} \tag{A.1}$$

$$\text{(A.2)} \qquad A^{(-)}(p) = -A^{(+)}(-p)\,, \qquad \gamma_4 A^{(+)}(p)\gamma_4 = A^{(+)}(-\bar{p})\,,$$

$$\text{(A.3)} \qquad \gamma_\mu \underline{A} \gamma_\mu = -2\underline{A}\,, \qquad \gamma_4 \underline{A} \gamma_4 = -\underline{A}\,,$$

$$\text{(A.4)} \qquad \gamma_\mu \gamma_\alpha \gamma_\beta \gamma_\mu = 4\delta_{\alpha\beta}\,, \qquad \gamma_\mu \gamma_\alpha \gamma_\beta \gamma_\lambda \gamma_\mu = 2\gamma_\lambda \gamma_\alpha \gamma_\beta - 4\delta_{\alpha\beta}\gamma_\lambda = -2\gamma_\lambda \gamma_\beta \gamma_\alpha\,,$$

$$\text{(A.5)} \qquad \mathrm{Sp}\,(\underline{A}\underline{B}\underline{C}\underline{D}) = 4\{(A\cdot B)(C\cdot D) - (A\cdot C)(B\cdot D) + (A\cdot D)(B\cdot C)\}\,,$$

$$\text{(A.6)} \qquad \mathrm{Sp}\,(\underline{A}\underline{B}\underline{C}\underline{D}\underline{E}\underline{F}) \quad (A\cdot B)\,\mathrm{Sp}\,(\underline{C}\underline{D}\underline{E}\underline{F}) - (A\cdot C)\,\mathrm{Sp}\,(\underline{B}\underline{D}\underline{E}\underline{F}) +$$
$$+ (A\cdot D)\,\mathrm{Sp}\,(\underline{B}\underline{C}\underline{E}\underline{F}) - (A\cdot E)\,\mathrm{Sp}\,(\underline{B}\underline{C}\underline{D}\underline{F}) + (A\cdot F)\,\mathrm{Sp}\,(\underline{C}\underline{D}\underline{E}\underline{B})\,.$$

BIBLIOGRAPHY

F. J. Dyson: *Lectures on Advanced Quantum Mechanics* (1951).
R. P. Feynman: *Phys. Rev.*, **76**, 769 (1949).
W. Heitler: *The Quantum Theory of Radiation*, 3-rd ed. (1954).
W. Pauli: *Ausgewählte Kapitel aus der Feldquantisierung*, p. 110-112.

RIASSUNTO

Col metodo dei grafici di Feynman, si calcola la sezione d'urto differenziale e si dà l'espressione di quella totale per il processo di scattering elettronico in un campo nucleare con creazione di coppie.

On the 7.7 MeV Level of Carbon 12.

A. Hossain (*) and D. J. Prowse

H. H. Wills Physical Laboratory - University of Bristol

(ricevuto l'11 Gennaio 1957)

Summary. — The analysis of the α-particle spectrum from the reaction $^{14}N(d, \alpha)^{12}C$ at a bombarding energy fo 20 MeV and of the inelastically scattered proton spectrum from carbon 12 at an energy of 9.5 MeV has revealed the presence of the 7.7 MeV level in carbon 12. Approximate values are given for the cross-sections leading to the formation of this level in both reactions.

In recent years a number of experiments have been performed investigating the energy level scheme of ^{12}C ([1-4]) but it was only in 1953 that Dunbar *et al.* ([5]) finally obtained evidence which was conclusive for the existence of a level at 7.7 MeV. These workers used the $^{14}N(d, \alpha)^{12}C$ reaction at a bombarding energy of 620 keV; by the use of magnetic analysis they were able to determine the energy of the level accurately as (7.68 ± .03) MeV. It is this level that was predicted from astronomical evidence on the relative abundance of ^{16}O, ^{12}C and ^{4}He in hot stars which have exhausted their hydrogen ([6]). The cross-section for the formation of this level seems to be very small and it was thought of interest to determine whether or not it would contribute to the reaction

(*) Now at University of Dacca, Pakistan.

([1]) M. G. Holloway and B. L. Moore: *Phys. Rev.*, **58**, 847 (1940).

([2]) W. M. Gibson: *Proc. Roy. Soc.* (*London*), A **62**, 586 (1949).

([3]) R. Malm and W. W. Buechner: *Phys. Rev.*, **81**, 519 (1951).

([4]) W. H. Guier, H. W. Bertini and J. H. Roberts: *Phys. Rev.*, **85**, 426 (1952).

([5]) D. N. F. Dunbar, R. E. Pixley, W. A. Wenzel and W. Whaling: *Phys. Rev.*, **92**, 649 (1953).

([6]) F. Hoyle: private communication to Dunbar *et al.*: quoted in ref. ([5]).

at a higher bombarding energy and whether or not it would appear in any other reaction.

During the course of a long series of experiments on the scattering of 19.0 MeV deuterons and 9.5 MeV protons from light gaseous elements [7-10] we have examined the energy levels of carbon participating in the reaction $^{14}N(d, \alpha)^{12}C$ and in the scattering reaction $^{12}C(p, p')^{12}C$.

The scattering camera used was that described by BURROWS *et al.* [11]. It was used in conjunction with the proton and deuteron beams from the University of Birmingham 60 in. Cyclotron. Ilford C2 emulsions were used to detect the particles resulting from the reaction or scattering processes. These could be scanned for the α-particle, deuteron or proton tracks under investigation at scattering angles from 15° to 165°.

1. – The $^{14}N(d, \alpha)^{12}C$ Reaction.

Typical histograms of the α-particles observed at different angles are shown in Fig. 1. In (*A*) groups at 253, 196, 157 and 136 μm are clearly visible, being well resolved from the background; these are due to the formation of ^{12}C in its ground state and in states at 4.4, 7.7 and 9.7 MeV. The background of α-particles appears to start at about 140 μm and rises rapidly at lower ranges; it is due to the reactions $^{14}N(d, 2\alpha)^{8}Be$ and $^{14}N(d, 4\alpha)$. In (B) the same groups are clearly resolved and it can be seen that the cross section for the formation of the 7.7 MeV state has increased with respect to that for the for-

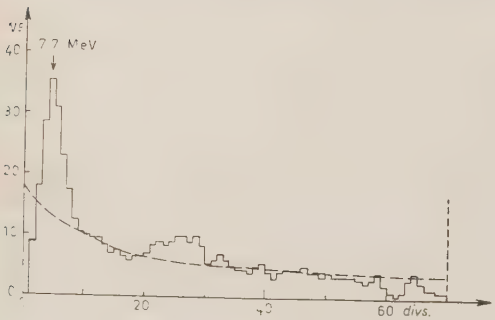

Fig. 1. – Histograms of the α-particles observed at (*A*) $\theta = 80°$ and (*B*) $\theta = 130°$. The distributions have been smoothed by adding to each ordinate the mean of its neighbours.

(7) W. E. BURCHAM, W. M. GIBSON, A. HOSSAIN and J. ROTBLAT: *Phys. Rev.*, **92**, 1266 (1953).

(8) R. G. FREEMANTLE, W. M. GIBSON, D. J. PROWSE and J. ROTBLAT: *Phys. Rev.*, **92**, 1268 (1953).

(9) R. G. FREEMANTLE, A. HOSSAIN, D. J. PROWSE and J. ROTBLAT: *Phys. Rev.*, **96**, 1270 (1954).

(10) R. G. FREEMANTLE, D. J. PROWSE and J. ROTBLAT: *Phys. Rev.* **96** 1268 (1954).

(11) H. B. BURROWS, C. F. POWELL and J. ROTBLAT: *Proc. Roy. Soc.*, A **209**, 461 (1951).

mation of the 4.4 MeV state. The presence of the background α-particles prevents an accurate measurement of the total cross-section for the 7.7 MeV state. An upper limit from measurements at various angles is .34 mb.

A beam energy of (19.40 $\pm$ .05) MeV was deduced from the range of the ground state α-particle group taking the Q-value as 13.570 MeV ([12]) and using a range-energy relation for α-particles deduced from that for protons ([13]) by the equation ([14]):

$$R_\alpha(E) = 0.9931\, R_p(E/3.973) + 1.5\,,$$

where R_p and R_α are the ranges in microns of proton and α-particle respectively and E is in MeV. The value obtained was confirmed by that determined from the ranges of the elastically scattered deuterons at various angles. The mean value of the energy of the state is (7.70 $\pm$ 0.02) MeV.

2. – The $^{12}C(p, p')^{12}C$ Reaction.

In a previous paper ([7]) on the scattering of 9.5 MeV protons by carbon the only level identified was that at 4.4 MeV. We have since made an intensive search for the 7.7 MeV level at angles where it would be expected to give rise to scattered protons of sufficient range to be measurable in the emulsion. The pressure of the acetylene which was used as a target was kept as low as reasonably possible but the particles still lost an appreciable amount of energy in traversing the gas. At forward angles the background of short tracks is quite large but they are due to the scattering of some of the protons in the main beam from the collimating tube before they reach the scattering gap. The number of such tracks falls with increasing angle and at 40°, the first distinct group appears at a range which corresponds to an energy of 7.6 MeV for the excited state. The energy lost in the gas was calculated from the data given by BROLLEY and RIBE ([15]) and from measurements at 40°, 95° and 100°, the energy of the state has been determined as (7.6 $\pm$ 0.1) MeV. The appearance of the group at 95° is shown in Fig. 2.

Because of uncertain numbers of background tracks an accurate measurement of the cross-section could not easily be made.

([12]) F. AJZENBERG and T. LAURITSEN: *Rev. Mod. Phys.*, **27**, 77 (1955).
([13]) W. M. GIBSON, D. J. PROWSE and J. ROTBLAT: *Nature*, **173**, 1180 (1954).
([14]) J. J. WILKINS: AERE Report G/R 664.
([15]) J. E. BROLLEY and F. L. RIBE: *Phys. Rev.*, **98**, 1112 (1955).

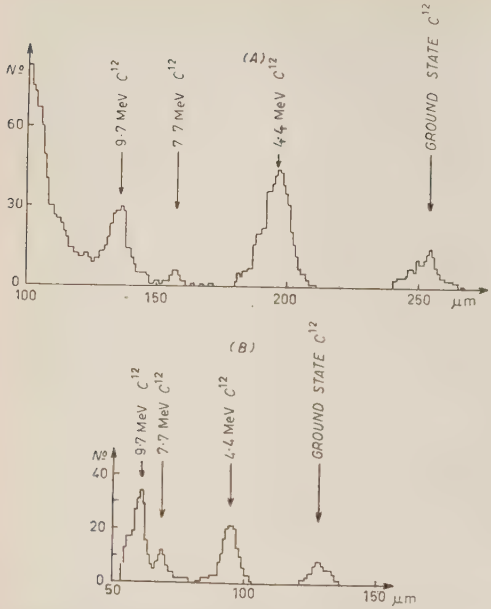

At 95°, the best value is (0.8 ± .2) mb/sr. Previous experiments on (p, p′) scattering have not definitely detected the level but a very tentative piece of evidence put forward by BRITTEN in 1952 [16] on the scattering of 31.5 MeV protons gave a cross-section of (.16 ± ± .10) mb/sr at 90°. Within the very large errors it therefore appears that the cross-section decreases with energy.

Fig. 2. – Histogram of proton tracks measured at 95°. Each division represents 0.8 μm. The distribution has been smoothed by adding to each ordinate the mean of its neighbours. The dotted line represents the number of background tracks.

* * *

We are greatly indebted to Prof. W. E. BURCHAM, Prof. J. ROTBLAT and Dr. W. M. GIBSON for many discussions and we thank Dr. R. G. FREEMANTLE for help with the exposure. We appreciate the help of Miss MARION PEARCE in the scanning.

We are grateful to Prof. C. F. POWELL for his continued interest and encouragement.

([16]) R. BRITTEN: *Phys. Rev.*, **88**, 283 (1952).

RIASSUNTO (*)

L'analisi dello spettro delle particelle α originate nella reazione $^{14}N(d, \alpha)^{12}C$ con un'energia di bombardamento di 20 MeV e dello spettro dello scattering anelastico dei protoni emessi da ^{12}C ad un'energia di 9.5 MeV ha rivelato la presenza del livello 7.7 MeV nel ^{12}C. Si danno valori approssimati per le sezioni d'urto che portano alla formazione di questo livello nelle due reazioni.

(*) *Traduzione a cura della Redazione.*

IL NUOVO CIMENTO Vol. V, N. 4 1° Aprile 1957

An Analysis of the Pairs Produced by ^{8}Be γ-Rays in Photographic Emulsions.

D. J. Prowse

H. H. Wills Physical Laboratory - University of Bristol (*)

(ricevuto l'11 Gennaio 1957)

Summary. — Electron-positron pairs produced in photographic emulsion by the γ-rays emitted from the proton bombardment of lithium have been analysed. The energy of the pair components has been measured by the multiple scattering technique and using the known values of 17.6 and 14.6 MeV for the γ-ray energies, scattering constants, applicable to the co-ordinate method, of $25.0^{+}_{-1.0}{}^{.3}$ and $22.7^{+}_{-1.0}{}^{.3}$ have been obtained for no cut off and for a $> 4\bar{\alpha}$ cut-off respectively. The projected angle of opening of the pairs has been measured and a correlation between angle of opening and disparity obtained which agrees fairly well with the theory of Stearns.

1. – Experimental Method.

Ilford G5 plates of size 1 in. × 3 in. with emulsions 400 μm thick were placed so that they received radiation, at a distance of about 30 cm, from the proton bombardment of a lithium hydroxide target by the resolved 500 keV beam from the larger of the Cockcroft-Walton accelerators at Cambridge. The plates were exposed in pairs with the emulsions facing each other, each pair being separately wrapped in black paper.

The plates were set in the microscope with the direction of the pairs parallel to the x-screw movement. The angles of opening of the pairs were measured by an angular scale on the eyepiece.

The angular method was used to measure the scattering on both pair components, when each exceeded 500 μm in length. A cell size of 50 μm was chosen

(*) Presented at the Turin Conference (11th-16th Sept. 1956) by Professor C. F. Powell, F.R.S.

because, although this relatively large cell size reduces the number of independent observations, the effect of noise is much reduced. Measurements on a cosmic-ray particle which happened to pass through the emulsion gave a value of $\alpha = .04°/100\ \mu m$. This is therefore the upper limit to the noise of the microscope stage used. No measurements were taken of the emulsion distortion but it is believed to be small as no systematic variations in the differences between successive readings were found.

2. – Results.

2·1. *Energy of the Pairs.* – The distribution of the total pair-energy is shown in Fig. 1 together with that obtained by WALKER and MCDANIEL [1] and VOYVODIC and PICKUP [2]. The histogram of Voyvodic and Pickup was used by them to determine the scattering constant; to bring the centre of gravity of the group to the correct value; a scattering constant of 21.3 was found necessary with a $> 4\alpha$ cut-off. The distribution obtained here, can be accounted for by the two lines at 14.6 and 17.6 MeV if a value of $25.0^{+}_{-1.0}{}^{.3}$ is used for the scattering constant applicable to the co-ordinate method without cut-off; if a $> 4\alpha$ cut-off is used a value of $22.7^{+}_{-0.1}{}^{.3}$ is required; these results are satisfactory since it is in agreement with the theory of Molière on which much recent work has been based. The relative proportions of 14.6 MeV and 17.6 MeV radiations obtained by different workers are seen to be different; there is evidence of angular asymmetry (VOYVODIC and PICKUP [2], DEVONS and HINE [3]) which can account for this.

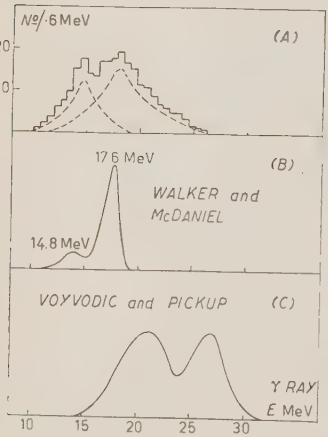

Fig. 1. – (*A*) Histogram of the total pair energy together with the distributions obtained by (*B*) WALKER and MC DANIEL and (*C*) VOYVODIC and PICKUP.

The energy of both components was determined in 255 cases, the pairs were then divided into groups according to the fraction F, of the total energy carried off by the less energetic particle; for equal division of energy, F is 0.5 while for large disparity, F approaches zero. The resultant distribution did

(1) R. L. WALKER and B. D. MC DANIEL: *Phys. Rev.*, **74**, 315 (1948).
(2) L. VOYVODIC and E. PICKUP: *Phys. Rev.*, **81**, 471 (1951).
(3) S. DEVONS and M. G. N. HINE: *Phys. Rev.*, **74**, 976 (1948).

not agree very well with that expected from theory. There was a deficiency of pairs for which the disparity lay between .1 and .3. This is the same as the deficiency found by BARONI, BORSELLINO, SCARSI and VANDERHAEGHE [1] in an analysis of pairs produced by cosmic radiation. It is difficult to see how the scattering method could introduce such a deficiency. Two independent observers scanned the plates and the variation in the numbers found was only 5%. The pairs constituting this 5% were found to have the same disparity distribution as was observed for the pairs found by both observers. It is therefore unlikely to be due to pairs with this disparity having been missed when scanning the emulsion.

2·2. *Angles of Opening of the Pairs.* – The projected angle of opening of the pair was measured for a total of 466 pairs, of which 255 had both the electron and positron tracks greater than 500 μm in length; their disparity could therefore be measured as described above from the scattering measurements. The angles were split up into three groups those with $F \geqslant .35$, $.25 < F < .35$ and $F \leqslant .25$; some of the resulting histograms are shown in Fig. 2. It can be quite easily seen that for a high disparity ($F \leqslant .25$) the angular distribution has a much longer tail in the high angle direction.

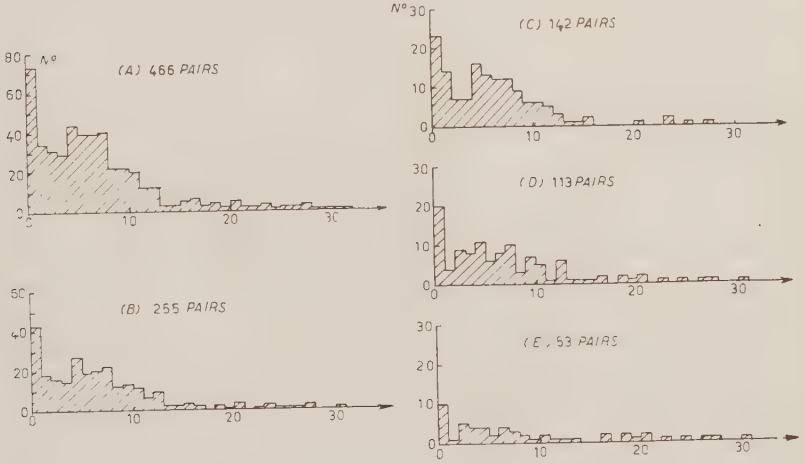

Fig. 2. – Histograms of the projected angle of opening of the pairs. (*A*) All pairs found (466); (*B*) All pairs on which scattering measurements were made ($F \leqslant .5$); (*C*) Pairs for which $F \geqslant .35$ (note change of vertical scale); (*D*) Pairs for which $F < .35$; (*E*) Pairs for which $F \leqslant .25$.

(1) G. BARONI, A. BORSELLINO, L. SCARSI and G. VANDERHAEGHE: *Nuovo Cimento*, **10**, 1653 (1953).

No significant difference was obtained between the distribution in angle for all pairs found (466) and that for all on which disparity measurements were possible (see Fig. 2). This confirms that the probability of losing pairs with high disparity, due to the electron of small energy being scattered out of the emulsion and thus having a track length < 500 μm, is small, and that the distribution obtained is unlikely to be deficient in such pairs.

3. – Comparison with Theory.

STEARNS [5] has calculated that the mean square angle between the electron and the incident γ-ray as a function of disparity, using the Bethe formula [6]. Assuming there is no correlation between θ^- and θ^+ the mean square value of the projected angle between the components of the pair will be $(2/\pi)(\theta^{-2} + \theta^{+2})^{\frac{1}{2}}$. The values of this expression obtained using the method of Stearns to calculate θ^- and θ^+ are shown in the table. Taking our disparity distribution we obtain 6.3°, 7.1° and 8.2° as the r.m.s. angles for the three intervals of disparity chosen in Fig. 2.

F	R.M.S. Projected Angle
.1	16.0
.2	9.1
.3	6.6
.4	5.5
.5	5.3

Because of the large high-angle tail to the distribution care has to be taken in interpreting the resultant r.m.s. values of θ and Stearns' calculations are for a value of $\theta_{\max} = 20°$. The experimental r.m.s. values employing the same cut-off are 6.6°, 7.8° and 8.1° agreeing well will those expected theoretically.

BORSELLINO [7] has calculated the distribution of opening angle expected. If we call this distribution $F(x)$, where x is the real angle in space, the number δN, with a projected angle between φ and $\varphi + \delta\varphi$ is equal to

$$\frac{2}{\pi}\,\delta\varphi \int_{x=\varphi}^{x_{\max}} \frac{F(x)\,\mathrm{d}x}{(1-(\varphi^2/x^2))^{\frac{1}{2}}}\,.$$

[5] M. STEARNS: *Phys. Rev.*, **76**, 836 (1949).
[6] H. A. BETHE: *Proc. Cam. Soc.*, **30**, 524 (1934).
[7] A. BORSELLINO: *Phys. Rev.*, **89**, 1023 (1953).

This has been integrated graphically for all x above $\varphi + \delta x$. The integrand goes to ∞ as $x \to \varphi$, so it is not possible to do a reliable graphical integration in this region. A mathematical integration assuming $F(x)$ constant over the interval, δx, gives in this region, the expression,

$$\frac{2}{\pi}(F(x))_{x=\varphi} \cdot \cosh^{-1} x\varphi \cdot \delta p \qquad \text{for } \delta N.$$

The result is shown in Fig. 3, $F(x)$ has been calculated for a γ-ray energy of 16 MeV and for a disparity of .5. Taking into account other disparities we obtain the following values of the most probable angles:

For $F < 0.5$; 3.9°, $F \geqslant 0.35$; 3.3°, $F < 0.35$; 4.1° and for $F \leqslant 0.25$; 5.0°. These angles appear to be smaller than those given by the small peaks in Fig. 2. In the case of $F < 0.35$ agreement is good but in the other cases the experimental angles are about 1° too low. The rise in the cross-section at $\varphi = 0$ is not expected from Fig. 3. It would appear that the experimental minima are caused by small errors in the measurement of angle tending to increase the numbers with $\varphi = 0$ at the expense of those with $\varphi = 0 \div 2°$.

Fig. 3. – Result of the integration giving the number of pairs, δN, with a projected angle between φ and $\varphi + \delta\varphi$ from the theory of Borsellino.

In conclusion we may say that agreement with theory is fair, the correlation between high disparity and high angle being very good. Further accurate experiments are however needed to provide a more complete check.

* * *

The author wishes to express his thanks to Drs. G. O. Jones and D. H. Wilkinson for the use of the accelerator. Thanks are due to Mrs. B. M. Herman, and Mrs. J. F. Juritz for much of the microscope work and to Dr. E. J. Burge for some calculations. I am grateful for the help and guidance of Dr. W. M. Gibson who suggested the problem. I am deeply indebted to Professor C. F. Powell, F. R. S., for his continued interest and encouragement. The receipt of a maintenance grant from the Department of Scientific and Industrial Research is gratefully acknowledged.

RIASSUNTO (*)

Si sono analizzate coppie di elettroni-positroni prodotte in emulsioni fotografiche dai raggi γ emessi dal bombardamento protonico del litio. L'energia delle particelle componenti la coppia è stata misurata con la tecnica dello scattering doppio e usando i noti valori di 17.6 e 14.6 MeV per le energie dei raggi γ: si sono ottenute costanti di scattering, applicabili al metodo delle coordinate, di $25.0^{+}_{-1.0}{}^{.3}$ e $22.7^{+}_{-1.0}{}^{.3}$ in assenza di taglio e, rispettivamente, per un taglio $> 4\bar{\alpha}$. La proiezione dell'angolo di apertura delle coppie è stato misurato e si è ottenuta una correlazione tra angolo di apertura e disparità che si accorda abbastanza bene colla teoria di Stearn.

(*) *Traduzione a cura della Redazione.*

IL NUOVO CIMENTO Vol. V, N. 4 1° Aprile 1957

A System of General Relativistic Equations of Low Type.

R. Omnes (*)

CERN - Geneva

(ricevuto il 22 Gennaio 1957)

Summary. — Using Bogoliubov's methods (3), we give here a new demonstration of the Low equation, thus displaying its general character. The method has been extended to give a set of equations of Low type for the productions of mesons by mesons and one nucleon.

1. – Introduction.

It has been known for some time that the Low equation (1) is a general property of quantized systems. In particular, Lehmann, Symanzik and Zimmermann (2) were able to derive it by general methods not involving the concept of renormalization. Recently, a new formulation of quantum theory of fields by N. N. Bogoliubov and his collaborators (3), formulated in terms of a few mathematical and physical postulates, allowed to establish in a rigorous way the dispersion relations for scattering.

In this work we have used these new methods to derive the Low equation thus exhibiting its general character. The method is quite easily extended to derive a complete system of Low equations for the processes of creation of any number of mesons by a nucleon and some incident mesons. It is still

(*) On leave of absence from C.E.A. Saclay.

(1) F. E. Low: *Phys. Rev.*, **97**, 1392 (1955).

(2) H. Lehmann, K. Symanzick and W. Zimmermann: *Nuovo Cimento*, **1**, 205 (1955).

(3) N. N. Bogoliubov (*Phys. Rev.* to be published). Reported at the International Conference for Theoretical Physics in Seattle, September 1956.

not evident, however, how one might extend the Low equation to include nucleon-nucleon scattering and production of particles.

2. – Summary of Bogoliubov's Hypothesis.

Let us recall some important features of Bogoliubov's methods.

2·1. *General features.*

1) There exist asymptotic states $\rangle$ without mutual interaction.

2) There exists a group G of some transformations L (including Lorentz transformations) unitarily represented by operators U_L over the states .

3) If $|p\rangle$ is an eigenstate of energy-momentum with eigenvalue p

$$U_{L_a}|p\rangle = \exp[-ipa]|p\rangle\,, \tag{1}$$

for the translation $x \to x + a$. There exists in particular a unique vacuum $|0\rangle$ such that

$$U_{L_a}|0\rangle = |0\rangle\,. \tag{2}$$

A result of conditions 1), 2), 3) is the additivity of momentum and energy of asymptotic states.

4) There exists a complete set of eigenstates of energy and momentum with *positive* eigenvalues of energy. Thus one may write

$$\langle\alpha|AB|\beta\rangle = \langle\alpha|A|0\rangle\langle 0|B|\beta\rangle + \sum_n \frac{1}{(2\pi)^3}\int \mathrm{d}\bar{k}\langle\alpha|A|n\bar{k}\rangle\langle n\bar{k}|B|\beta\rangle\,. \tag{3}$$

5) There exists a unitary matrix S characterizing transition probabilities.

6) One may group asymptotic states into three classes:

a) one particle states,

b) bound states,

c) direct product of some states from classes *a*) and *b*).

One assumes stability of one-particle and bound states (and, of course, of the vacuum) i.e. for these states

$$S|\alpha\rangle = |\alpha\rangle\,. \tag{4}$$

2·2. *Physical properties.*

1) Elementary particles are characterized by creation operators $a_\varrho^{(-)}(\bar{q})$ and annihilation operators $a_\varrho^{(-)}(\bar{q})$ which can act on asymptotic states and verify the known commutation relations

$$(5)\qquad \begin{cases} [a_\alpha^{(-)}(\bar{q}'),\ a_{\alpha'}^{(+)}(\bar{q}')] = \delta_{\alpha\alpha'}\delta(\bar{q}-\bar{q}')\,, \\ [a_\alpha^{(-)}(\bar{q}),\ a_{\alpha'}^{(-)}(\bar{q}')] = [a_\alpha^{(+)}(\bar{q}),\ a_{\alpha'}^{(+)}(\bar{q}')] = 0\,. \end{cases}$$

(We have considered the case of bosons which is the only one to have interesting consequences for us.)

One may define operators $\varphi_\varrho(x)$ in space-time configuration by

$$(6)\qquad \varphi_\varrho(x) = \frac{1}{(2\pi)^{\frac{3}{2}}}\int \frac{\mathrm{d}k}{\sqrt{2k^0}}\left\{\exp[ikx]a_p^{(+)}(\bar{k}) + \exp[-ikx]a_\varrho^{(-)}(\bar{k})\right\}.$$

Note that these operators verify the Klein-Gordon equation where enters the real mass of mesons.

2) One may define S-matrix as

$$(7)\qquad S = \sum_{l,m=0}^{\infty}\int \mathrm{d}\bar{k}_1' \ldots \mathrm{d}\bar{k}_l'\,\mathrm{d}\bar{k}_1 \ldots \mathrm{d}\bar{k}_m f^{lm}(k_1' \ldots k_m')a_{(\bar{k}_1')}^{(-)} \ldots a_{(\bar{k}_l')}^{(-)}a_{(\bar{k}_1)}^{(\pm)} \ldots a_{(\bar{k}_m)}^{(\pm)}\,,$$

or, from (5) and (6), by introducing Wick's normal product,

$$(8)\qquad S = \sum_{n=0}^{\infty}\int \mathrm{d}x_1 \ldots \mathrm{d}x_n f^n(x_1 \ldots x_n) : \varphi(x_1) \ldots \varphi(x_n) : .$$

The functional derivative $\delta S/\delta\varphi(x)$ will be defined from (8) by subtracting an operator $\varphi(x_i)$ in every possible manner and replacing it by a $\delta(x - x_i)$. So for the S matrix element between a state α with one nucleon p and r mesons $q_1 \ldots q_r$, and a state ω with one nucleon p' and s mesons $q_1' \ldots q_s'$, it is possible to write,

$$(9)\qquad S(\alpha\omega) = \langle p'q_1' \ldots q_s'|S|pq_1 \ldots q_r\rangle = \\ = \langle p'|a_{\varrho_1'}^{(-)}(\bar{q}_1') \ldots a_{\varrho_s'}^{(-)}(\bar{q}_s')Sa_{\varrho_1}^{(+)}(\bar{q}_1) \ldots a_{\varrho_r}^{(+)}(\bar{q}_r)|p\rangle\,.$$

From (5) and (6) result the commutation relations

$$(10)\qquad \begin{cases} [a_\varrho^{(+)}(\bar{p}),\ \varphi_{\varrho'}(x)] = \dfrac{\delta_{\varrho\varrho'}}{(2\pi)^{\frac{3}{2}}}\dfrac{\exp[-ipx]}{\sqrt{2p^0}}\,, \\ [a_\varrho^{(-)}(\bar{p}),\ \varphi_{\varrho'}(x)] = \dfrac{\delta_{\varrho\varrho'}}{(2\pi)^{\frac{3}{2}}}\dfrac{\exp[ipx]}{\sqrt{2p^0}}\,, \end{cases}$$

from which follows

$$[a_\varrho^{(+)}(\overline{p}), S] = \frac{1}{(2\pi)^{\frac{3}{2}}}\int \mathrm{d}x \frac{\delta S}{\delta\varphi(x)} \frac{1}{\sqrt{2p^0}} \exp[-ipx], \tag{11.1}$$

$$[a_\varrho^{(-)}(\overline{p}), S] = \frac{1}{(2\pi)^{\frac{3}{2}}}\int \mathrm{d}x \frac{\delta S}{\delta\varphi(x)} \frac{1}{\sqrt{2p^0}} \exp[ipx]. \tag{11.2}$$

After introduction in (9), (11) gives

$$S(\alpha\omega) = \frac{(-1)^s}{(2\pi)^{3((r+s)/2)}} \cdot \int \mathrm{d}x_1' \ldots \mathrm{d}x_s' \mathrm{d}x_1 \ldots \mathrm{d}x_s \frac{\exp[i\sum q_i' x_i' - i\sum q_i x_i]}{2^{(r+s)/2}(q_1'^0 \ldots q_s'^0 q_1^0 \ldots q_r^0)^{\frac{1}{2}}} \left\langle p' \left| \frac{\delta^{r+s} S}{\delta\varphi(x_1') \ldots \delta\varphi(x_r)} \right| p \right\rangle. \tag{12}$$

3) One has the causality condition in the form (*)

$$\frac{\delta}{\delta\varphi(x)}\left[\frac{\delta S}{\delta\varphi(y)} S^+\right] = 0 \qquad \text{for } x \lesssim y. \tag{13}$$

(the notation meaning: x anterior to y, or $x - y$ space-like, the coincidence $x = y$ being excluded) With the aid of these assumptions which have been used by Bogoliubov, Medvedev and Polivanov to give a rigorous demonstration of the dispersion relations, we shall establish a complete set of integral equations of the type of Low.

3. – Derivation of the Low Equation.

First, let us derive the classical Low equation.

For the matrix element of S between an initial state α with a nucleon of momentum p and a meson of momentum q to a final state ω, p', q', (12) becomes

$$S(\alpha pq, \omega p'q') = \frac{-1}{(2\pi)^3}\int \mathrm{d}x\,\mathrm{d}y \frac{\exp[iq'x - iqy]}{\sqrt{4q^0 q'^0}} \left\langle p' \left| \frac{\delta^2 S}{\delta\varphi_{\varrho'}(x)\delta\varphi_\varrho(y)} S^+ \right| p \right\rangle, \tag{14}$$

or, from the causality condition (13)

$$\frac{1}{(2\pi)^3}\int \mathrm{d}x\,\mathrm{d}y \frac{\exp[iq'x - iqy]}{\sqrt{4q^0 q'^0}} \langle p' | T(j_{\varrho'}(x), j_\varrho(y)) | p \rangle, \tag{15}$$

(*) One may show that a hamiltonian theory always verifies (13).

with

$$j_\varrho(x) = i\frac{\delta S}{\delta q_\varrho(x)}\,S^+\,. \tag{16}$$

One may write

$$T(j_{\varrho'}(x')j_\varrho(y)) = \theta(x-y)j_{\varrho'}(x)j_\varrho(y) + \theta(y-x)j_\varrho(y)j_{\varrho'}(x)$$

and, for instance, using the complete set of states $|n\bar{k}\rangle$

$$\langle p'|j_{\varrho'}(x)j_\varrho(y)|p\rangle = \langle p'|j_{\varrho'}(x)|0\rangle\langle 0|j_\varrho(y)|p\rangle + \tag{17}$$
$$+\frac{1}{(2\pi)^3}\sum_n\int \mathrm{d}\bar{k}\langle p'|j_{\varrho'}(x)|n\bar{k}\rangle\langle n\bar{k}|j_\varrho(y)|p\rangle\,.$$

Noting that

$$\langle\alpha|j(x)|\beta\rangle = \exp[i(p_\alpha - p_\beta)x]\langle\alpha|j(0)|\beta\rangle\,, \tag{18}$$

one may group (15), (16), (17), (18) to obtain, after performing the integrations

$$S(\alpha pq,\,\omega p'q') = \frac{(2\pi)^4}{(2\pi)^3}\,\frac{\delta(q'+p'-q-p)}{\sqrt{4q^0q'^0}}\cdot \tag{19}$$
$$\cdot\sum_n\left[\frac{\langle p'|j_{\varrho'}(0)|n\bar{k}_-\rangle\langle n\bar{k}_-|j_\varrho(0)|p\rangle_{\bar{k}=\bar{p}-\bar{q}}}{E-E_n+i\varepsilon} + \frac{\langle p'|j_\varrho(0)|n\bar{k}\rangle\langle n\bar{k}|j_{\varrho'}(0)|p\rangle_{\bar{k}=\bar{p}'-\bar{q}}}{-E+p'^0-p^0-E_n+i\varepsilon}\right].$$

The last point in the demonstration of Low's equation is to interpret the quantities $\langle p'|j(0)|n\rangle$ in terms of S matrix-elements, when n is on the energy-shell.

In this case one has

$$S(\alpha pq,\,n) = \langle n|S|\alpha pq\rangle$$
$$= \langle n|Sa_\varrho^{(+)}(q)|p\rangle,$$

but

$$Sa_\varrho^{(+)}(\bar{q}) = [S,\,a_\varrho^{(+)}(\bar{q})] + a_\varrho^{(+)}(\bar{q})S\,. \tag{20}$$

For the second term of (20) one may write

$$a_\varrho^{(+)}(\bar{q})S|p\rangle = a_\varrho^{(+)}(q)|p\rangle = |pq\alpha\rangle\,,$$

where the first equality follows from (4) and the second one is self-evident.

From (11), the first term of (20) reads

$$\frac{1}{(2\pi)^{\frac{3}{2}}}\int \mathrm{d}x \frac{\delta S}{\delta \varphi_\varrho(x)} \frac{1}{\sqrt{2q^0}} \exp[-iqx],$$

from which follows

$$S(\alpha pq, n) = \delta n, \alpha pq - \frac{1}{(2\pi)^{\frac{3}{2}}}\int \frac{\mathrm{d}x}{\sqrt{2q^0}} \exp[-iqx]\left\langle n \left| \frac{\delta S}{\delta q_\varrho(x)} S^+ \right| p\alpha \right\rangle,$$

where we have used $|p\rangle = S|p\rangle$ and $S^+S = 1$ to write

$$|p\rangle = S^+|p\rangle .$$

We have thus obtained

$$S(\alpha pq, n) = \delta qp\alpha, n - \frac{1}{(2\pi)^{\frac{3}{2}}}\int \frac{\mathrm{d}x}{\sqrt{2q^0}} \exp[-iqx]\langle n|j_\varrho(x)|p\rangle . \tag{21}$$

Using (14), (11) and putting

$$S(if) = \delta if + i\,\delta(p^i - p^f)Tif ,$$

one thus has

$$T_{qp\alpha, n} = \frac{i}{(2\pi)^{\frac{3}{2}}} \frac{\langle n|j_\varrho(0)|p\rangle}{\sqrt{2q^0}} , \tag{22}$$

and this equation may be used as a definition of the T matrix element out of the energy-shell. We have thus obtained the Low equation without explicit appearence of the renormalization local term (λ term) which appeared in the first formulation of Low, (*) and which contains only matrix elements of scattering (note that as ever these elements are not on the energy-shell).

One may note that there is a flaw in the demonstration given here: one has multiplied a distribution $\theta(x - y)$ by a T-product which is strongly singular for $x = y$ (note that the causality condition (13) leads to a commutability of $j_\varrho(x)$ and $j_\varrho(y)$ when $x - y$ is space-like so that the only difficulty is for $x = y$). Thus, strictly speaking, one has demonstrated nothing at all (just as in the current derivations). However, it is very easy, by using Bogoliubov's techniques, to pass from the causal form of T to its retarded form and justify (14) rigorously.

(*) This term is potentially included in $j(x)$ and would appear by explicit calculation of the one-nucleon term of (19).

4. - Extension to the Transition from One to Two Mesons. General Case.

We wish now to derive, by the same methods as above, a Low equation for the transition from a state containing one nucleon of momentum p and one meson of momentum q_1 to a state with one nucleon of momentum p' and and two mesons of momenta q_2 and q_3. The total energy of these two states will be designed by E.

From (12), one has

$$S(pq_1 \cdot p'q_2q_3) = -\frac{1}{(2\pi)^{\frac{3}{2}}}\int \mathrm{d}x_1\,\mathrm{d}x_2\,\mathrm{d}x_3\,\frac{\exp\left[i(q_2x_2 + q_3x_3 - q_1x_1)\right]}{\sqrt{8q_1^0q_2^0q_3^0}}\cdot \tag{23}$$

$$\cdot\left\langle p' \left| \frac{\delta^3 S}{\delta q_{\varrho_1}(x_1)\delta q_{\varrho_2}(x_2)\delta q_{\varrho_3}(x_3)} S^+ \right| p \right\rangle .$$

Let us study

$$\frac{\delta^3 S}{\delta q(x_1)\delta q(x_2)\delta q(x_3)} S^+ ,$$

in the case where

$$x_1 \lesssim x_2 , \qquad x_2 \lesssim x_3 . \tag{24}$$

One may write

$$\frac{\delta^3 S}{\delta q(x_1)\delta q(x_2)\delta q(x_3)} S^+ = \frac{\delta}{\delta q(x_2)}\frac{\delta}{\delta q(x_1)}\left(\frac{\delta S}{\delta q(x_3)} S^+\right) - \tag{25}$$

$$-\left[\frac{\delta}{\delta q(x_1)}\left(\frac{\delta S}{\delta q(x_3)} S^-\right)\right] S\,\frac{\delta S^-}{\delta q(x_2)} -$$

$$\cdot\left(\frac{\delta S}{\delta q(x_3)} S^+\right)\frac{\delta}{\delta q(x_1)}\left(S\,\frac{\delta S^-}{\delta q(x_2)}\right) - \frac{\delta^2 S}{\delta q(x_2)\delta q(x_3)}\frac{\delta S^-}{\delta q(x_1)} .$$

Remembering the causality condition (6), one sees that the three first terms of (18) are zero. Thus one can write

$$\frac{\delta^3 S}{\delta q(x_1)\delta q(x_2)\delta q(x_3)} S^+ = -\theta(x_2 - x_1)\,\theta(x_3 - x_1)\,\frac{\delta^2 S}{\delta q(x_2)\delta q(x_3)}\frac{\delta S^+}{\delta q(x_1)} - \tag{26}$$

$$-\theta(x_3 - x_2)\,\theta(x_2 - x_2)\,\frac{\delta^2 S}{\delta q(x_3)\delta q(x_1)}\frac{\delta S^+}{\delta q(x_2)} -$$

$$-\theta(x_1 - x_3)\,\theta(x_2 - x_3)\,\frac{\delta^2 S}{\delta q(x_1)\delta q(x_2)}\frac{\delta S^+}{\delta q(x_3)} .$$

Introducing (26) in (23) and putting, for instance

$$(27)\quad \left\langle p' \left| \frac{\delta^2 S}{\delta q(x_1)\delta q(x_2)} \frac{\delta S^-}{\delta q(x_3)} \right| p \right\rangle \equiv \left\langle p' \left| \frac{\delta^2 S}{\delta q(x_1)\delta q(x_2)} \right| 0 \right\rangle \left\langle 0 \left| \frac{\delta S^+}{\delta q(x_3)} \right| p \right\rangle + \\ + \sum_n \frac{1}{(2\pi)^3} \int d\bar{k} \left\langle p' \left| \frac{\delta^2 S}{\delta\varphi(x_1)\delta\varphi(x_2)} \right| n\bar{k} \right\rangle \left\langle n\bar{k} \left| \frac{\delta S^+}{\delta\varphi(x_3)} \right| p \right\rangle ,$$

defining

$$(28)\quad \left\langle p \left| \frac{\delta^2 S}{\delta q(x_1)\delta q(x_2)} \right| n\bar{k} \right\rangle = (2\pi)^3 \exp\left[i \frac{p-k}{2}(x+y) \right] F_{p\varrho_1\varrho_2, nk}(x-y) ,$$

$$(29)\quad \left\langle p \left| \frac{\delta S}{\delta\varphi(x)} \right| n\bar{k} \right\rangle = \frac{i}{(2\pi)^4} T_{p\varrho, nk} \exp[i(p-k)x] ,$$

and introducing the Fourier transform

$$(30)\quad F_{p\varrho_1\varrho_2, nk}(x) = \frac{1}{(2\pi)^8} \int dk' \exp[-ik'x] T_{p\varrho_1\varrho_2, nk}(k') .$$

One obtains the equation

$$(31)\quad \langle p'q_2q_3|S|pq_1\rangle = 2\pi \frac{\delta(q_2+q_3+p'-p-q_1)}{\sqrt{8q_1^0q_2^0q_3^0}} (A_1 + A_2 + A_3) ,$$

where

$$(32.1)\quad A_1 = \sum_n \int \frac{T_{p\varrho_2\varrho_3, nk}(k') T^*_{p\varrho_1, nk} \Big| \begin{matrix} k = \bar{p}' + \bar{q}_2 + \bar{q}_3 \\ k' = (\bar{q}_2 - \bar{q}_3)/2 \end{matrix}}{\left(q_2^0 + \frac{p'^0 - E_n(k)}{2} - k'^0 + i\varepsilon \right) \left(q_3^0 + \frac{p'^0 - E_n(k)}{2} + k'^0 + i\varepsilon \right)} dk'^0 .$$

$$(32.2)\quad A_2 = \sum_n \int \frac{T_{p\varrho_3\varrho_1, nk}(k') T^*_{p\varrho_2, nk} \Big| \begin{matrix} k = \bar{p}' - \bar{q}_3 - \bar{q}_1 \\ k' = (\bar{q}_1 + \bar{q}_3)/2 \end{matrix}}{\left(-q_1^0 + \frac{p'^0 - E_n(k)}{2} + k'^0 + i\varepsilon \right) \left(q_3^0 + \frac{p'^0 - E_n(k)}{2} - k'^0 + i\varepsilon \right)} dk'^0$$

And A_3 is deduced from A_2 by exchange of q_2 and q_3.

One may note that, as in the first Low equation, the different coefficients of the θ-functions are identical when the arguments are space-like, the only singularity being for $x_1 = x_2$ or $x_1 = x_3$, etc., which could result in the addition of polynomials in equation (32).

The remaining task is to interpret the T coefficient by means of elements of the scattering matrix, i.e. to relate the first members of (28) and (29) directly to S matrix when the intermediate states are on the energy-shell.

Let us study the S matrix element between an arbitrary state n and a state consisting of one nucleon p and one meson q. One has, from (11)

$$\langle pq|S|n\bar{k}\rangle = \langle p|a_{\varrho}^{(-)}(\bar{q})S|n\bar{k}\rangle = \\ = \delta pq, n\bar{k} + \frac{1}{(2\pi)^{\frac{3}{2}}}\int \mathrm{d}x \frac{\exp[iqx]}{\sqrt{2q^0}}\left\langle p\left|\frac{\delta S}{\delta\varphi(x)}\right|n\bar{k}\right\rangle,$$

so

$$\langle pq|S|n\bar{k}\rangle = \delta pq, n\bar{k} + \frac{i}{(2\pi)^{\frac{3}{2}}}\frac{\delta(p+q-k)}{\sqrt{2q^0}}T_{pq,n\bar{k}}. \tag{33}$$

For the S matrix element between a state n and a state with one nucleon p and two mesons q_1q_2 one has

$$pq_1q_2|S|n\bar{k}\rangle = \langle p|a_{\varrho_1}^{(-)}(\bar{q}_1)a_{\varrho_2}^{(-)}(\bar{q}_2)S|n\bar{k}$$

by using equations (4) and (11), one obtains

$$pq_1q_2\ S\ n\bar{k} = \frac{1}{(2\pi)^3}\int\left\langle p\left|\frac{\delta^2 S}{\delta\varphi_{\varrho_1}(x)\delta\varphi_{\varrho_2}(y)}\right|n\bar{k}\right\rangle\frac{\exp[i(q_1x+q_2y)]}{\sqrt{4q_1^0q_2^0}}\,\mathrm{d}x\,\mathrm{d}y - \tag{34}$$

$$+\left[\frac{1}{(2\pi)^{\frac{3}{2}}}\sum_{\lambda=1}^{n}\int\left\langle p\left|\frac{\delta S}{\delta\varphi(x_2)}\right|n\lambda\right\rangle\delta_{q_2p_\lambda}\frac{\exp[iq_2x_2]}{\sqrt{2q_2^0}}\,\mathrm{d}x + \text{Permuted term } (+2)\right] + \delta_{pq_1q_2,n\bar{k}}.$$

This equation has been obtained by commuting the operators $a^{(-)}$ with S. The term $\delta_{q_1p_\lambda}|n_\lambda$ is provided by action of an operator $a_{\varrho_1}^{(-)}(q_1)$ over the state n when there exists in n one meson (p_λ) identical to q_1. In this case $|n_\lambda$ represents the incident state composed of the same particles as n with the exception of the meson p_λ.

Retaining the principal part of $pq_1q_2|S|n\bar{k}$ which consists of the first term of (34) (it is the only one which appears in the general case where n does not contain q_1 nor q_2) one has

$$\langle pq_1q_2|S|n\bar{k}\rangle = \frac{1}{(2\pi)^3}\int\left\langle p\left|\frac{\delta^2 S}{\delta\varphi_{\varrho_1}(x)\delta\varphi_{\varrho_2}(y)}\right|n\bar{k}\right\rangle\frac{\exp[i(q_1x+q_2y)]}{\sqrt{4q_1^0q_2^0}}\,\mathrm{d}x\,\mathrm{d}y,$$

which, following (28) and (30) is identical with

$$\frac{i}{(2\pi)^3}\delta(p+q_1+q_2-k)\frac{T_{pq_1q_2,n\bar{k}}((q_1-q_2)/2)}{\sqrt{4q_1^0q_2^0}}. \tag{35}$$

Again we shall use (30) and (29) as the definition of the T matrix-elements

out of the energy-shell so that the only matrix-elements appearing in eq. (31) are those of the reaction matrix T.

It is now clear how one can derive a complete set of relativistic Low equations. Every transition matrix element between a state with one nucleon and r mesons and another one with one nucleon and s mesons will be expressible in a form analogous to (16) where the variational derivative of order $r+s$ will be expressible as the ordered product of two variational derivatives of order $(r+s-1)$ and 1. By the same process as outlined will be obtained an expression for this element consisting in a sum of terms, each one having the form of the inverse product of $(r+s-1)$ terms of the form $(E'-En+i\varepsilon)$ multiplied by the product of two matrix elements of T. One of these matrix elements will be between the arbitrary state n and the initial nucleon plus one meson from the set of the ingoing and outgoing ones, the other element being between n and the final nucleon plus all the other mesons.

There are no analogous formulae for transition between states containing nucleon-antinucleon pairs, or hyperons, if any, although all these states must appear in the sums $\sum_n$. So the system is not quite complete in this resepct.

A delicate feature of these equations is that they contain matrix elements from an arbitrary state n to a known state in which we are interested and not, as it can be done in the classical Low equation, between the studied state and an arbitrary one. On the whole this does not eliminate the possibility of doing effective calculations and approximations.

Finally, let us signal that the crossing relations

$$T_{q_2\varrho_2,\, q_3\varrho_3;\, q_1\varrho_1} = T_{-q_1\varrho_1;\, -q_2\varrho_2,\, -q_3\varrho_3} = T_{q_2\varrho_2,\, -q_1\varrho_1;\, -q_3\varrho_3} - T_{-q_1\varrho_1,\, q_3\varrho_3;\, -q_2\varrho_2} \tag{36}$$

are fairly evident on equation (24).

One could use (32) to study numerically the production of mesons by one meson bypassing to the non-relativistic limit, but this work has already been done directly in the Chew and Low model [4].

Finally let us note that (31) (32) is not the only possible form of Low equations obtainable by this method.

* * *

The author would like to thank Professor C. J. BAKKER, Director-General of CERN, for the hospitality extended to him at this Organization. He is

[4] R. OMNES: To be published.

very grateful to Professor B. FERRETTI, Director of the Theoretical Study Division (Geneva), as well as to the other members of the division for valuable comments and interesting discussions, and he particularly thanks Professor F. VILLARS who kindly read and corrected the manuscript of this article.

The author gratefully acknowledges financial support from the French Commissariat à l'Énergie Atomique.

RIASSUNTO (*)

Servendoci dei metodi di Bogoliubov diamo qui una nuova dimostrazione dell'equazione di Low, mettendo così in evidenza il suo carattere generale. Il metodo è stato esteso per ottenere una serie di equazioni del tipo di quella di Low per la produzione di mesoni da parte di mesoni interagenti con un nucleone.

(*) *Traduzione a cura della Redazione.*

IL NUOVO CIMENTO Vol. V, N. 4 1° Aprile 1957

The Lifetime of Positive Heavy Mesons.

B. Bhowmik (+), D. Evans, S. Nilsson (*) and D. J. Prowse

H. H. Wills Physical Laboratory - University of Bristol

F. Anderson, D. Keefe and A. Kennan

University College - Dublin

N. N. Biswas, M. Ceccarelli and P. Waloschek

Max-Planck-Institut für Physik - Göttingen

J. E. Hooper

Universitetets Institut for Teoretisk Fysik - København

M. Grilli and L. Guerriero

Istituto di Fisica dell'Università - Padova
Istituto Nazionale di Fisica Nucleare - Sezione di Padova

(ricevuto il 25 Gennaio 1957)

Summary. — Over two hundred examples of the decay in flight of positive heavy mesons produced at the Bevatron have been observed in the photographic emulsions, and from these the lifetime of the particles has been estimated. The lifetime averaged over all modes of decay is found to be $1.35^{+0.16}_{-0.13}$ s. The effect of experimental biases is discussed, and the final result is compared with that of other authors.

1. – Introduction.

Recently the results of several experiments on the lifetime of positive heavy mesons, carried out under a variety of conditions and with different exper-

(+) On leave of absence from the University of Delhi.
(*) On leave of absence from the University of Uppsala.

imental techniques ([1-8]), have been reported. One of the major difficulties involved in the interpretation of the values obtained from these different experiments is that the lifetime may not be identical for the various decay modes especially if the heavy mesons consist of more than one kind of particle. An early indication that such differences were likely to be small was provided by the fact that the relative frequencies of the decay modes in stacks exposed under very different conditions to the cosmic radiation, to artificially accelerated protons and to the K^+ beam at the Bevatron ([9]), are very similar.

More recently, comparative measurements of the lifetime for the τ-mode of decay ([3,6]) and other distinctive modes ([7,8]) have suggested that if such differences exist, they are probably less than 20%. However, while the statistical uncertainties are rather large, there appear to be some discrepancies among the absolute values obtained for the mean K-meson lifetime by the different methods.

The values found from counter measurements of K-mesons produced by cosmic rays and on the attenuation of the K-meson beam at the Bevatron appear to be smaller ($0.7 \div 1.0 \cdot 10^{-8}$ s) (*) than those obtained from counter measurements on stopped heavy mesons produced at the Cosmotron and the Bevatron ($1.2 \div 1.4 \cdot 10^{-8}$ s).

Results based on a different method, in which individual decays in flight are observed in emulsion have been reported by Iloff *et al.* ([5]) who used emulsions exposed to the K^+ beam at the Bevatron. They scanned 31.6 m of heavy meson track and found 19 decays in flight which corresponds to a mean lifetime of $1.01^{+.33}_{-.21} \cdot 10^{-8}$ s.

([1]) L. Mezzetti and J. Keuffel: *Phys. Rev.*, **95**, 859 (1954); *Nuovo Cimento*, **4**, 1096 (1956).

([2]) P. R. Barker, D. M. Binnie, B. D. Hyams, R. J. Rout and J. Shepherd: *Phil. Mag.*, **46**, 307 (1955).

([3]) W. Alvarez and S. Goldhaber: *Nuovo Cimento*, **2**, 344 (1955).

([4]) K. Robinson: *Phys. Rev.*, **99**, 1606 (1955).

([5]) E. L. Iloff, W. W. Chupp, G. Goldhaber, S. Goldhaber, J. E. Lannutti, A. Pevsner and D. Ritson: *Phys. Rev.*, **99**, 1617 (1955).

([6]) G. Harris, J. Orear and S. Taylor: *Phys. Rev.*, **100**, 932 (1955).

([7]) V. Fitch and R. Motley: *Phys. Rev.*, **101**, 496 (1956).

([8]) L. Alvarez, F. S. Crawford, M. L. Good and M. L. Stevenson: *Phys. Rev.*, **101**, 503 (1956).

([9]) Table V of R. W. Birge, D. H. Perkins, J. R. Peterson, D. H. Stork and M. N. Whitehead: *Nuovo Cimento*, **4**, 834 (1956).

(*) *Note added in proof.* In recent measurements, done with the attenuation method the following values have been obtained:

$$1.11^{+0.18}_{-0.11} \cdot 10^{-8} \text{ for } K_L \quad \text{and} \quad 1.04^{+0.42}_{-0.23} \cdot 10^{-8} \text{ for } \tau$$

(J. Orear, G. Harris and S. Taylor: *Phys. Rev.*, **104**, 1463 (1956)). These last values are in good agreement with the data of the other authors shown in Table III and Fig. 2.

In the course of experiments carried out during the last year in several European laboratories [10] on the nuclear interactions of K particles in emulsion it has been possible to increase considerably the statistical precision of the lifetime obtained by this method. In the present work we describe these new measurements and discuss how they lead to a reliable estimate of the mean lifetime.

2. – Experimental Details.

Two stacks of stripped emulsions were exposed to the magnetically analyzed and focussed beam of K^- mesons produced at an angle of 90° with respect to the proton beam at the Bevatron [11]. The proper time of flight of the K^+ particles from production in the target to entry into the stacks lay between 1.0 and $1.7 \cdot 10^{-8}$ s; the momentum at entry varied between 280 and 460 MeV c. The tracks of the heavy mesons were observed a few centimetres from the edge of the stacks and, if they conformed to certain conditions, were followed through the stack to their ends. Details of the scanning procedure, the criteria for track selection and the methods for evaluating the percentage contamination of proton and light meson tracks among those followed are fully described in the papers of reference [10].

In the course of these experiments, in which 466 m of K^+ meson track have been scanned (see Table I) 220 events have been observed which were interpreted as being due to decays in flight.

TABLE I.

Lab.	Metres	T (10^{-8} s)	D. F.	Stops
Br + Du	151.3	93.2	46	24 (15 + 9)
Gö (*)	110.6	80.0	55	17 (12 + 5)
Ko	78.6	57.5	29	11 (7 + 4)
Pd	125.5	76.1	46	16 (10 + 6)
Total	466.0	309.8	176	68 (44 + 24)

(*) The Göttingen data refer only to K-tracks which have been completely followed to the end. They should therefore not be compared with other published data on the total K length followed.

[10] *Reports of the Bristol, Dublin, Göttingen and Padua groups.* International Congress, Turin, September 1956 (*Nuovo Cimento*, in press).

[11] L. T. KERTH, D. H. STORK, R. W. BIRGE, R. P. MADDOCK and M. N. WHITEHEAD: *Bull. Am. Phys. Soc.*, **30**, n. 3 (1955).

The relatively large number of events observed has considerably reduced the statistical errors with respect to other experiments; this has made it necessary to consider carefully the small systematic sources of bias which cannot under these circumstances be ignored.

The following ways in which it might have been possible to overlook decays in flight have been considered:

a) Loss of an event for technical reasons.

b) Incorrect classification as a decay at rest, if the residual range is small.

c) Incorrect classification of a decay event as a zero-prong charge exchange interaction.

a) The likelihood of an observer failing to notice an event during the track scanning is considered to be negligible unless the event occurred very near the air or the glass surfaces of the emulsion. In these cases, in fact, the difficulty of distinguishing between tracks which leave a plate and which cannot be found in the next, and those representing decays in flight or charge exchanges, has necessarily led to the classification of all of them as « abandoned ». From the experimental distribution of the depth in the emulsion at which our decays in flight have been found, it is evident that such a loss (if it really exists), can only occur within about 10 μm from the upper and lower surfaces of the unprocessed emulsion. To be completely sure that this loss cannot influence our results, we have excluded all those events lying within 30 μm from the air or glass surfaces. This has led to rejection of about 10% of the total number of available events and also to a corresponding reduction of the total track length followed.

b) If a heavy meson decays in flight when close to the end of its range, the particle may be erroneously classified as having decayed at rest. This source of loss can be eliminated by excluding from consideration the time spent by the heavy mesons in the last part of their ranges and, naturally, any decays found in this distance.

The effect of excluding various residual ranges (determined by means of ionization measurements) can be seen in Table II); cut-offs at residual ranges of 0.9, 3.0, and 6.0 mm have been used.

c) The plateau grain density in the emulsion stacks used was low ($g_p \simeq$ 15-17 grains per 100 μm) and it was sometime difficult to see tracks of low specific ionization.

In a considerable fraction of all cases (15 ÷ 30%) (*) a heavy meson was

(*) Each laboratory has determined its own visibility factor; no commun factor has been applied to correct the data reported in Table II.

observed to come to rest without any associated visible secondary track starting from the end point. These particles were thought to be due largely to the $K_{\mu 2}$ mode and also, but less probably, to the $K_{\pi 2}$ mode. Corresponding to

TABLE II.

Cutoff (mm)	T (10^{-8} s)	D. F.	Stops (*)	n	N	Lifetime (10^{-8} s)	
						K^+	K_L
> 0	309.8	176	68 (44 + 24)	220	203	$1.37^{+0.16}_{-0.13}$	$1.32^{+0.15}_{-0.13}$
> 0.9	293.6	172	65 (41 + 24)	213	196	$1.35^{+0.16}_{-0.13}$	$1.27^{+0.14}_{-0.12}$
> 3.0	270.3	167	58 (34 + 24)	201	184	$1.33^{+0.15}_{-0.13}$	$1.27^{+0.14}_{-0.12}$
> 6.0	246.1	155	53 (29 + 24)	184	170	$1.30^{+0.15}_{-0.13}$	$1.23^{+0.14}_{-0.12}$

T = Total time of flight, including the 10 % glass and surface regions.
D.F. = no. of observed decays in flight.
n = Total number of decays in flight including cases without visible decay secondary.
N = Number of decays in flight, including cases without visible decay secondary, when we exclude two layers of 5 % emulsion at surface and at glass.
(*) In brackets are reported the « stops » assumed to be decays in flight + « stops » assumed to be real charge exchanges.

these K^- mesons decaying at rest without visible secondaries, one would expect to find a certain number of decays in flight, also without secondaries. The fraction of decays thus lost will be larger for the particles decaying in fligth rather than at rest, because in these lighter tracks the point at which the particle decays is not so well defined by the final grain, thus making it more difficult to locate an associated track of light ionization.

On the other hand, one can expect events of the type [10]:

$$K^+ + \text{bound neutron} = K^0 + \text{bound proton}\,.$$

Those examples of charge exchange scattering in which excitation of the nucleus is so small that it does not lead to an evaporation of charged particles will also be recorded as « stops », and are not distinguishable from those decays in flight where the secondary particle escapes detection.

Fig. 1 shows the depth distribution of the stops, and the relative frequency of events can be seen to be greater in the regions near the upper and lower surfaces of the emulsion where it is more difficult to recognize the thin track of a lightly ionizing secondary particle.

There are two ways in which one can estimate the number of genuine decay

events which have been called stops. Firstly, one may use the known efficiency factor for detecting the decay tracks associated with decays at rest in order to correct the number of observed decays in flight (*). This method, for reasons mentioned earlier, is likely to lead to a slight underestimate. Alternatively one can try to use the number of charge-exchange stars with prongs for estimating the number without prongs; in doing this it has been assumed that the ratio of the number of stars without prongs to those with prongs is the same of K particles suffering charge-exchange and non charge-exchange scattering. This assumption may not be valid if the inelasticity in charge-exchange scattering differs appreciably from that in ordinary scattering; however, the number of charge exchange events involved is so small that this difference must be very large before it can affect significantly the estimated number of decays in flight.

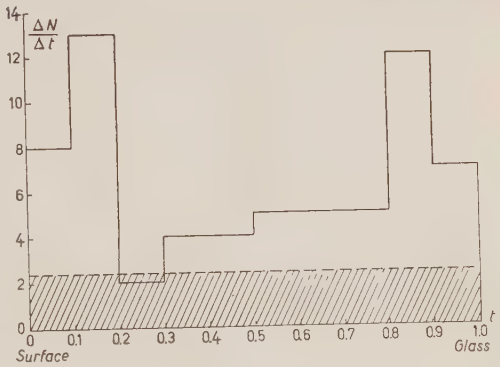

Fig. 1. - Depth distribution of the « stops ». ▨ Estimated charge exchanges.

3. – Results.

In all, 176 decay events were observed in which the tracks of the secondary particle could be unambiguously identified, and where it was certain that the heavy meson had decayed in flight. The total number of stops found was 68, of which it was estimated that 44 were decay events (see footnote on page 997) where the light track had escaped notice: the remaining 24 events were then due to charge exchange scattering. The estimates by the two independent methods discussed earlier agreed very well and the number of decays in flight is very unlikely to be in error by more than ± 7.

The total number of decays in flight thus becomes 220. The error, including the statistical uncertainty, is then ± 15. From these 220 events we have eliminated 17 which lay within 30 μm of the air and glass surfaces. This is 8% of the total number of events, instead of the estimated 10 $\pm$ 3%, and has therefore been interpreted as indicating that our loss cannot have been very great.

(*) See footnote on page 997.

Next we have eliminated those which decayed with residual ranges less than 0.9, 3.0, and 6.0 mm. From Table II it can be seen that the number of events rejected by each of these range cut-offs is proportional to the total time of flight rejected by the same means. This shows that the cut-off of 0.9 mm is already effective and sufficient, and consequently this has been adopted. The number of events then becomes 196 ± 14.

The corresponding total time of flight remaining has been calculated by means of the curves of BARONI *et al.* [12] and the error which we give takes account of the possible mixture of spurious tracks [10]; it value is: $T = (264 \pm 10) \cdot 10^{-8}$ s.

While in principle it is possible to identify the various modes of decay of the K's, the number of events in which this would have been possible is small, and the only distinction easily made is that between K_L and τ's.

The mean lifetime has been calculated and is given on Table I, respectively for all events, including τ's (column K_L).

The final results are:

$$\text{Mean lifetime for K (all modes)} = (1.35^{+0.16}_{-0.13}) \cdot 10^{-8} \text{ s}$$

$$\text{Mean lifetime for K (without } \tau \text{ mode)} = (1.27^{+0.14}_{-0.12}) \cdot 10^{-8} \text{ s}$$

where the errors are the total errors.

We have found only 6 τ's which decayed in flight instead of 12 which are to be expected, if one assumes a single common lifetime for all K^+ modes

The mean lifetime for τ's on the basis of these few events is then $(2.8^{+2.4}_{1.0}) \cdot 10^{-8}$ s. The difference between this value and that quoted for K is not significant, owing to the small statistics for the τ's.

4. – Discussion.

In order to compare our results with other measurements on lifetime, we have collected in Table III all the data at present available. In this Table are indicated for each measurement the delay time (Δt) between the production in the target and the beginning of observation, the angle of emission (θ) of the heavy meson, and also the different primary energies (cosmic rays, Bevatron).

We note that the closest agreement with our results is given by those of some recent counter measurements by FITCH and MOTLEY [7] and ALVAREZ

[12] G. BARONI, C. CASTAGNOLI, G. CORTINI, C. FRANZINETTI and A. MANFREDINI: CERN 88/9 (1954).

TABLE III.

Mode of decay (*)	Lifetime (10^{-8} s)	Δt (10^{-8} s) (flight + strumental)	E_K		Primary	Method	Reference
K_L (+)	0.96 ± 0.08 1.40 ± 0.15	$1.6 - 0.3 + 1.3$ $4.3 - 0.3 + 4.0$	80 MeV	Forward	Cosmic rays	Counters (Decay Curve)	(1)
K_L	$1.10^{+0.41}_{0.24}$	0.45 0.05 + 0.4		Forward	Cosmic rays	Counters + Wilson Ch. (Decay Curve)	(2)
K_L (−)	0.81 + 0.07	1.5 0.3 − 1.2	80 MeV	Forward	Cosmic rays	Counters (Decay curve)	(4)
$K_{\pi 2}$ $K_{\pi 2}$	$1.17^{+0.08}_{0.07}$ $1.21^{+0.11}_{0.10}$	2.9 2.2 + 0.7	190 MeV	60°	(3 GeV p)	Counters (Decay Curve)	(7)
$K_{\mu 2}$ $K_{\mu 2}$ K	1.4 0.2 1.3 + 0.2 1.3 + 0.1	2.0 1.8 + 0.2 (?)	100 ÷ 140	90	(6.2 GeV p)	Counters (Decay Curve)	(8)
τ^+	$1.0^{0.7}_{0.3}$	0.18 (I exp.) 1.8 (II exp.)	110 (+)	90	(6.2 GeV p)	Emulsion (Attenuation Method)	(5)
τ K_L	$0.8^{+0.5}_{0.2}$ $0.7^{+0.15}_{0.10}$	1.3 (I exp.) 2.1 (II exp.)	110	90	(6.2 GeV p)	Emulsion (Attenuation Method)	(6)
K_L	$1.01^{+0.33}_{-0.21}$	1.3	100 ÷ 170	90	(6.2 GeV p)	Emulsion (Decay in flight)	(3)
K_L K	$1.27^{+0.11}_{-0.12}$ $1.35^{+0.16}_{-0.13}$	1.35	115	90	(6.2 GeV p)	Emulsion (Decay in flight)	Present work

(*) K_L means all K-mesons excluding only the τ's.
(+) In the second exposure the energy of K is 110 MeV, in the first there is no magnetic resolution.
(−) In these experiments the Čerenkov efficiency for detecting the charged π from the $K_{\pi 2}$ decay is lower than for the μ from $K_{\mu 2}$ decay.
(†) See note added in proof on page 995.

et al. (5) (delay time between 1.3 and $3.0 \cdot 10^{-8}$ s), whereas there is some disagreement with some cosmic ray measurements (1,4) and with those from the attenuation method (3,6) (see Fig. 2).

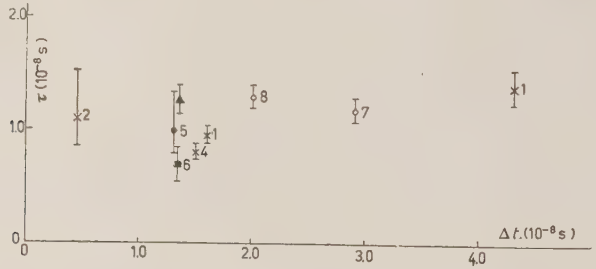

Fig. 2. – Lifetime measurements for K_L versus delay time Δt (The numbers indicate the reference). — x Counters (decay curve): cosmic rays; ○ Counters (decay curve): 6.2 GeV or 3 GeV P; ● Emulsion (decay in flight): 6.2 GeV P; ■ Emulsion (attenuation): 6.2 GeV P; ▲ Present work.

It is difficult to decide if these differences are significant or not, since the experiments have been carried out under a wide variety of conditions: in fact the selection systems were different, the background varied from experiment to experiment, and the losses and biases depended on the nature of the measurements (see also the discussion by MEZZETTI *et al.* (1)).

From the data so far published there is no evidence for any clear difference between the mean lifetimes for the various decay modes. In particular there is no appreciable increase of the mean lifetime with increasing delay time. This result is in agreement with the fact that direct measurements under identical conditions of the mean lifetimes for the two most frequent decay modes, $K_{\mu 2}$ and $K_{\pi 2}$, are almost the same (7.8) and their occurrence frequencies remain the same under different experimental conditions (9).

Owing to the basic difference between the methods which have been used so far in attacking this problem, it is difficult to obtain definite conclusions about the connection between the delay time and the lifetime. It is therefore evident that more experimental material is necessary and that these new data should all be obtained with the same experimental method.

* * *

We are very grateful to Dr. E. J. LOFGREN and Dr. R. W. BIRGE for arranging and making the exposures to the Berkeley Bevatron, and to Prof. C. F. POWELL, F.R.S. for arranging the collaboration.

On behalf of U.C. Dublin, thanks are also due to Mr. J. LOSTY, and to

the Misses B. MAHER, D. O'BRIEN and M. SMITH for their help with the measurements.

J.E.H. M.G., and L.G. wish to thank the other members of their emulsion groups for the friendly interest and help in the course of the work. M.G. and L.G. would like to thank Profs. N. DALLAPORTA and L. MEZZETTI for interesting discussions.

D.E. is grateful to the University of Bristol for a graduate scholarship and S.N. and B.B. would like to thank respectively the Swedish Atomic Energy Commission and the Colombo plan authorities for financial support.

J.E.H. takes this opportunity of expressing his gratitude to the Rask-Ørsted and Ford foundations for financial support.

N.M. thanks the Government of India, M.C. the Max-Planck Gesellschaft and P.W. the Argentine Comisión Nacional de la Energía Atómica for maintenance grants.

RIASSUNTO

Sono stati osservati, in lastre nucleari, oltre 200 decadimenti in volo di K^+, prodotti al bevatrone. A partire da questi eventi si è valutata la vita media per i K^+ (media per tutti i modi di decadimento) e per i soli K_L. La vita media è risultata, rispettivamente $1.35^{+0.16}_{-0.13} \cdot 10^{-8}$ s e $1.27^{+0.11}_{-0.12} \cdot 10^{-8}$ s. Nel presente lavoro si discutono gli effetti di eventuali errori sistematici e viene confrontato il presente risultato con quello di altri Autori.

LETTERE ALLA REDAZIONE

«La responsabilità scientifica degli scritti inseriti in questa rubrica è completamente lasciata dalla Direzione del periodico ai singoli autori»

A Reply to a Criticism by Mr. A. Gamba.

K. M. Case and C. N. Yang

The Institute for Advanced Study - Princeton, New Jersey

R. Karplus

Physics Department, University of California - Berkeley, California

(ricevuto il 27 Novembre 1956)

In a recent article in this Journal [1] Mr. A. Gamba has criticized a note published by the present authors on «*Strange Particles and the Conservation of Isotopic Spin*» [2]. This seems to have resulted from a mis-understanding of the question that we were investigating.

Our *starting point* was the fact that for the low dimensional representations invariance under only a finite group of isotopic spin transformations implies precisely the same consequences as invariance under the continuous full group. Apparently a misunderstanding of the text led Mr. Gamba to think that we missed this obvious fact. He gave a proof of it for a special system involving a single meson and a single nucleon. His proof is certainly correct. The main point of our note was, however, to raise the *further* question whether assuming isotopic space *in general* to have only finite symmetries leads to a theory consistent with experimental information.

[1] A. Gamba: *Nuovo Cimento*, **3**, 1486 (1956).

[2] K. M. Case, R. Karplus and C. N. Yang: *Phys. Rev.*, **101**, 874 (1956).

IL NUOVO CIMENTO Vol. V, N. 4 1° Aprile 1957

On Some Aspects of Processing Thick Nuclear Emulsions.

E. J. Burge (*), J. H. Davies, I. J. van Heerden (**) and D. J. Prowse
H. H. Wills Physical Laboratory - University of Bristol

(ricevuto l'11 Gennaio 1957)

The use of stripped emulsions for the study of high energy nuclear events is now well established. One of the technical difficulties encountered has been the prevention of « blistering » during the processing of remounted emulsions [Powell (1)]. Various precautions have been taken at different times, such as using boiled water in the solution for sticking the emulsion onto the glass during the « rolling-on » process. It was also believed that a higher temperature during the « hot stage » reduced blistering although it was recognised that this would increase the distortion. We now believe that neither of these precautions is necessary. During tests made with samples from the same batch of emulsion no significant diminution was noted in the number of blisters or bubbles when these precautions were taken. Communications from other laboratories (2) have suggested that other measures such as the avoidance of rapid changes of temperature and concentration tend to reduce the number of bubbles. Fluctuations of concentration are certainly important and rapid changes of temperature are undesirable on other grounds and are normally avoided in all development procedures except perhaps during the transfer from the hot-plate stage to the cold stop bath. The omission of this sudden change in this laboratory has been found to make no difference. Even so, unaccountable increases still occur and they are often attributed to variations in manufacture. We have now reduced the incidence of bubbles to very small proportions by adherence to a standard technique.

The appearance of the bubbles is always the same. They are remarkably uniform in maximum size (ca. 7 mm diameter) except when they link up, or break through the edge of the emulsion. The distribution in any one plate is roughly uniform, with a tendency for more to form near the edge. They first become apparent during the fixing process, and they have never been observed prior to this stage despite the most vigorous treatment. The first signs are observed as early as 12 h after transfer to the fixer and they can then be observed to form at any time until near the end of the dilution stage. Too rapid

(*) Now at Wheatstone Laboratory, King's College, London.

(**) Now at National Physical Lab. Pretoria, S. A.

(1) C. F. Powell: *Phil. Mag.*, **44**, 219 (1953).

(2) M. Teucher: private communication for example.

dilution increases the tendency to form bubbles. They usually commence as very tiny irregularities in the emulsion and then steadily grow until they have reached the uniform size. The treatment in the fixing bath is also of great importance. We have noticed a tendency for more to form if the silver concentration rises to a figure above 10 g/l. However, the concentration is maintained above 2 g/l which prevents etching under oor processing conditions in a cupboard under a slow stream of air at room temperature. No fading of the latent image has ever been observed for times of this order of magnitude, and for the temperatures and humidities ordinarily encountered.

The rate of fixing has also been recently examined. The normal practice is to use acid fixing solution at a temperature of 8 °C in a bath of 30 litres capacity containing 10 plates in a rack. After 1 h a flow of fresh fixing solution

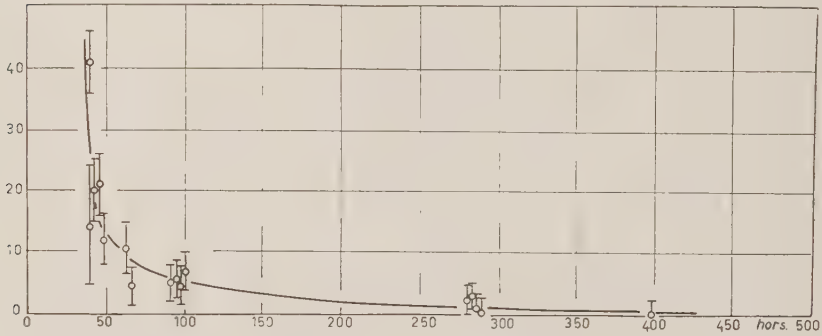

Fig. 1. – Number of bubbles per plate plotted against the drying time after « rolling-on » (in hours).

The hypo-solution is normally diluted at a rate of not more than 5% per hour.

During the processing of some recent stacks (Bristol 4.5 GeV Berkeley π^- stack and the K_1^+ European collaboration stack) it has been confirmed that the incidence of blistering is critically dependent on the interval which is allowed to elapse between the « rolling-on » stage and the first stage of the development — the drying time. The results are shown in Fig. 1, where the number of bubbles on a plate 16 in. × 10 in. averaged over each processing batch of some 8 or 9 plates, is plotted against drying time in hours. The present practice is to use a drying time of 100 h and the average number of bubbles is now less than 1 per plate. The plates are dried is started and is kept constant at a rate of 5 litres per hour. The silver concentration of the solution in grams per litre is plotted as a function of time in Fig. 2. The maximum concentration is reached after a period of 6÷8 h and the flow of 5 litres per hour suffices to keep it below 8 g/l. From this graph we have calculated the rate at which the silver is removed from the emulsion as a function of time and this curve appears in Fig. 3. The expected form of this curve is exponential, in fact, it appears to be composed of three exponentials each with a different exponent. This seems to us to indicate that the fixing process is inhibited by two distinct factors: *a*) the concentration of silver in the fixing bath which begins to retard fixation after about 3 h (6 g/l) and

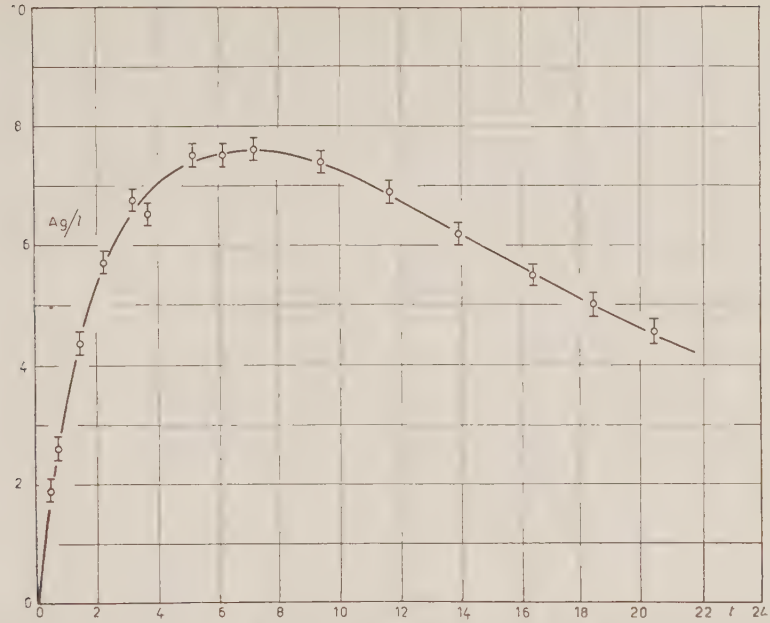

Fig. 2. Concentration in g l of silver in the fixing solution plotted against time in hours.

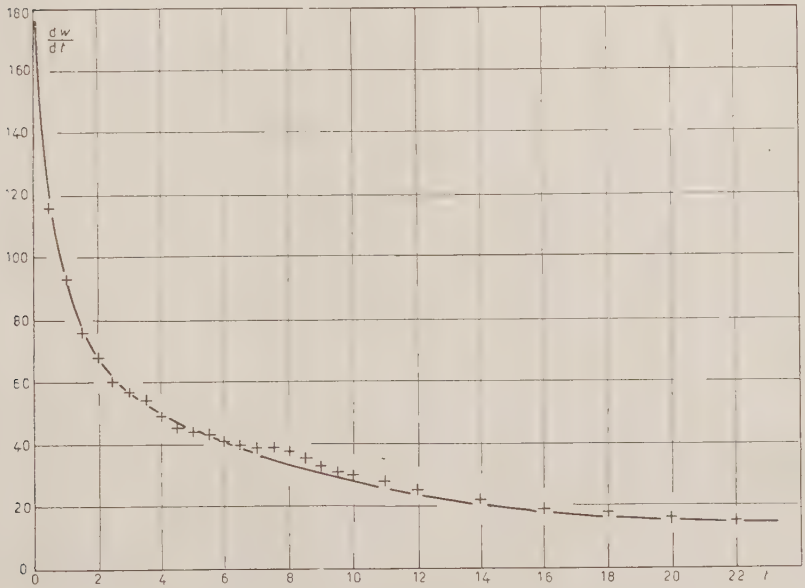

Fig. 3. – Rate of removing the silver from the emulsions in g/h plotted against time in hours. The fixing bath contained 8 emulsions 16 in. × 10 in. × 600 μm.

b) after about 20 h when fixing is again retarded by the formation of silver-hypo complexes which are only removed with difficulty from the emulsion. These complexes are known to exist and are thought to be responsible for the fact that the final fixing of an incompletely fixed plate is much easier to accomplish if it is first thoroughly washed. Laboratory tests on small nuclear emulsions have shown that the fixing time does follow the expected variation with silver concentration. The variation with temperature is also as expected ([3]).

([3]) MEES: *Theory of the Photographic Method*, (London, 1954), pp. 709 ff.

There is very little literature on the processing of stripped emulsions and reports from different laboratories ([4-7]) indicate that a variety of techniques is employed based on principles which are not always compatible. It is hoped that this communication will stimulate interest in the obtaining of consistently good results based on methods which are better understood.

([4]) B. STILLER, M. M. SHAPIRO and F. W. O'DELL: *Rev. Sci. Inst*, **25**, 4, 340 (1954).

([5]) A. H. ROSENFELD *et al.*: *How to Develop Emulsion*. Privately circulated manual from the Institute of Nuclear Studies, Chicago.

([6]) D. LAL, YASH PAL and B. PETERS: *Proc. Ind. Acad. Sci.*, A **38**, 277 (1953).

([7]) R. W. BIRGE *et al.*: UCRL 2690.

A Classical Calculation of the Nucleon-Meson Coupling Costant.

G. Stephenson

Department of Mathematics, Imperial College - London

(ricevuto il 14 Gennaio 1957)

Although a complete mathematical description of elementary particles and their interactions will almost certainly be based on quantum field theory, the following simple classical calculation of the nucleon-meson coupling constant does not seem to have been noticed before and may be of some interest.

In electromagnetic theory, the static spherically symmetric potential of a point electron with electric charge e is given by $\varphi = e/r$. Similarly, the corresponding potential of a point nucleon described by a scalar meson field is $V = g \exp[-\mu r/r]$, where μ is the meson rest-mass in certain units and g is the nuclear charge. We shall now suppose that the rest-mass ratio of the nucleon and electron, M/m, is given by the ratio of the total energies of the fields associated with the point particles. As is well known, these energies (obtained by integrating the four-four component of the energy-momentum tensors of the meson and electromagnetic field, $T_{\mu\nu}$ and $E_{\mu\nu}$ respectively, over all space with $r = 0 \to \infty$) are infinite. However, we may obtain a finite energy ratio by introducing a non-zero lower limit $r = a$ in each integral and evaluating their ratio, and then proceeding to the limit $a \to 0$. This gives

$$\frac{M}{m} = \lim_{a\to 0}\left\{\frac{\int_a^\infty T_{44}\cdot 4\pi r^2\,\mathrm{d}r}{\int_a^\infty E_{44}\cdot 4\pi r^2\,\mathrm{d}r}\right\} =$$

$$= \lim_{a\to 0}\left\{\frac{\int_a^\infty [(\mathrm{d}V/\mathrm{d}r)^2 + \mu^2 V^2]\, r^2\,\mathrm{d}r}{\int_a^\infty (\mathrm{d}\varphi/\mathrm{d}r)^2\, r^2\,\mathrm{d}r}\right\} =$$

$$= \frac{g^2}{e^2}\cdot\lim_{a\to 0}\{(\mu a + 1)\exp[-2\mu a]\} = \frac{g^2}{e^2}\,.$$

Taking the observed value $M/m = 1836$ and $e^2/\hbar c = 1/137$, we find the nucleon-meson coupling constant $g^2/\hbar c = 13.4$, which is in good agreement with the value of about 14 adopted in meson field calculations.

We see from this simple theory that the rest-masses of the nucleon and electron in units of 137 electron masses are numerically equal to the coupling constants $g^2/\hbar c$ and $e^2/\hbar c$ respectively. If x is a measure of rest-mass in these units, we have then

$$(x - 1/137)(x - 13.4) = 0\,.$$

This quadratic equation, whose roots have a ratio 1836, may be written as

$$10x^2 - 134.07x + 0.98 = 0 ,$$

which is almost identical with the equation

$$10x^2 - 136x + 1 = 0 ,$$

for the proton-electron rest-mass ratio derived by EDDINGTON [1] in a highly obscure manner. The ratio of the roots of Eddington's equation, however, gives 1849, which is larger than the observed mass ratio.

[1] A. S. EDDINGTON: *Relativity Theory of Protons and Electrons* (Cambridge, 1936), Chapter 12.

IL NUOVO CIMENTO Vol. V, N. 4 1° Aprile 1957

Photographic Evidence for the Existence of the Neutrino.

J. Csikai

Nuclear Research Institute of the Hungarian Academy of Sciences - Debrecen, Hungary

(ricevuto il 24 Gennaio 1957)

Prof. A. Szalay suggested to me the investigation of the β-decay of ^{6}He by means of a cloud chamber, filled with hydrogen. This decay process seemed to be exceptionally advantageous for the observation of the recoil effect i.e. the missing impulse carried away by the neutrino.

$$^6\mathrm{He} \rightarrow {}^6\mathrm{Li} + \beta^- + 3.6\ \mathrm{MeV} + \nu\,.$$

This process has a large transmutation energy and (with the exception of ^{3}H) the possible smallest residual mass (^{6}Li). No γ-radiation is emitted in the process and the ^{6}He atom is not bounded in a molecule. In this process the residual nucleus gains a high recoil energy and the detection of its track in a cloud chamber filled with hydrogen under low pressure could be hoped.

Our expectations were justified as represented by the stereo-photos of Fig. 1 here. The photos show clearly that the recoil track of the residual nucleus encloses generally an oblique angle with the emitted β-particle. It is clearly demonstrated that impulse is missing, because the direction of the impulse of the recoil nucleus is not opposite (180°) to the electron. Further it seems in principle possible to measure the impulse of the particles and to determine the impulse of the neutrino in individual atomic events.

We are aiming at the determination of the angle-correlation between the particles. We hope that we may gain important information upon the type of interaction between nucleons and leptons.

* * *

I wish to express my gratitude to Prof. A. Szalay director of this Institute for this problem and for his steady guidance in planning the equipment and measurements.

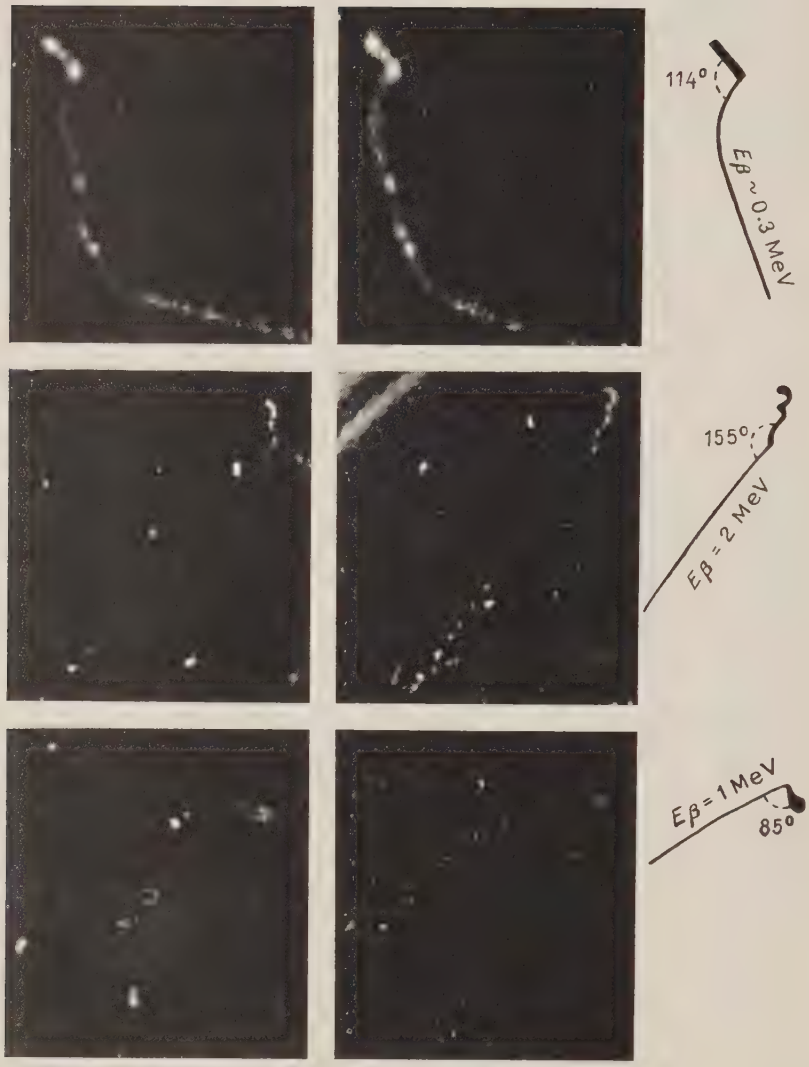

Fig. 1. – Stereoscopic (24° angle) cloud chamber photos of the β-decay of ^{6}He. The oblique angles between the tracks of the electrons and recoiled ^{6}Li nuclei clearly demonstrate the missing impulse carried away by the neutrino. Right: scheme of the event in its own plane.

IL NUOVO CIMENTO Vol. V, N. 4 1° Aprile 1957

Further Evidence for a Longlived Neutral K-Particle.

S. v. Friesen and K. Kristiansson

Department of Physics, University of Lund - Lund, Sweden

(ricevuto il 19 Febbraio 1957)

Fry *et al.* [1] have recently given an account of four unusual events found by them in a pellicle stack exposed to negative particles from the Berkeley Bevatron, where unstable particles originated in the emulsion from a small star produced by a neutral particle. They point out that the events can be explained by assuming that longlived neutral K-mesons were produced at the target with about the same frequency as the K^+-mesons. In some of the events, at least, one cannot exclude the possibility that a K^--meson has suffered charge exchange and produced a short-lived neutral K-particle (θ^0).

A similar event has been found at Lund in an emulsion exposed to K^--particles produced by 6.2 GeV protons in a copper target. The K-particles emerge at 90° and the channel defines a momentum of 445 MeV/c.

1. – The Event.

Fig. 1 shows a drawing of the event. From a small star of the type 4 + 0n comes a hyperfragment which stops in the emulsion and emits 2 singly charged particles. A small blob can also be seen. Gap counts on the tracks AB, AC and AD seem to show that they were produced by a proton and two deuterons.

There are 33 δ rays of four or more grains in the 1166 μm of the fragment AE. This indicates the charge 3. The disintegration tracks confirm this identification. The mean track width (MTW) has also been measured photometrically [2]. The profile of the track was determined by moving a slit (length 10 μm, width 0.8 μm when projected in the emulsion) at right angles across the track. Details of the method will be published shortly by T. Johansson. The MTW-value is 31% higher than the corresponding value for a singly charged particle some hundred microns from the end of the track. Measurements in emulsions of the same development give a 30% difference between particles with the charges 3 and 1. The track is therefore definitely identified as that of a Lithium fragment. See Fig. 2.

That the fragment has stopped before the disintegration or is very close to the

[1] W. F. Fry, J. Schneps and M. S. Swami: *Phys. Rev.* **103**, 1904 (1956); see also: W. B. Fowler, G. Maenchen, W. M. Powell, G. Saphir and R. W. Wright: *Phys. Rev.* **103**, 208 (1956).

[2] See e.g. K. Kristiansson: *Ark. f. Fys.* **10**, 447 (1956).

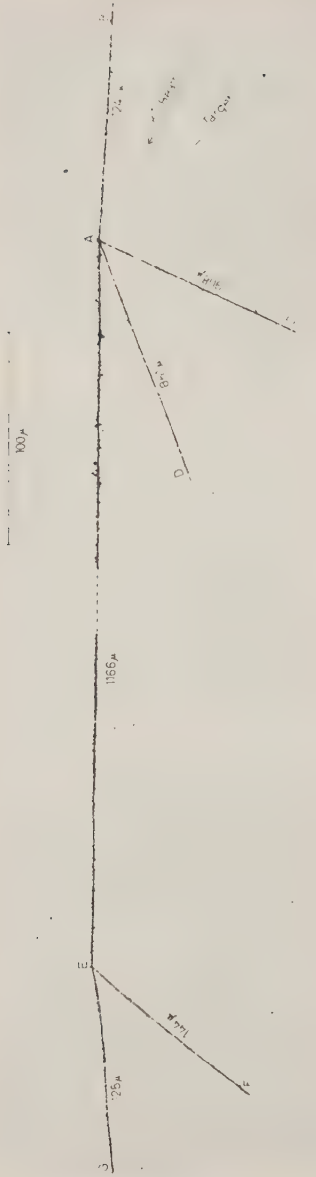

Fig. 1.

end of its range is shown by two circumstances:

1) The decrease of the MTW value towards the end of the track.

2) The sudden decrease of the scatter of the individual MTW values due to the absence of one-grain δ-rays close to the end.

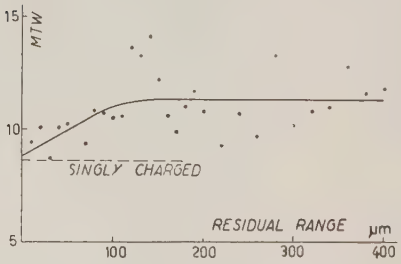

Fig. 2.

The MTW value at $R = 0$ of particles with $Z > 1$ lies higher than that of singly charged particles. The position of the intersection with the MTW-axis and our experience of measurements on Li fragments puts an extreme upper limit to the range of the fragment of $15 \div 20$ μm at the intersection, with the most probable value equal to 0. This makes the kinetic energy less than ~ 8 MeV, an energy too small to overcome the potential barrier of any of the nuclei in the emulsion. This proves that the track AE is that of a Lithium hyperfragment.

If we assume that the built-in hyperon is a Λ^0 the total visible energy of the star A is ~ 345 MeV for ${}^{6}_{\Lambda}\mathrm{Li}$ and ~ 355 for ${}^{7}_{\Lambda}\mathrm{Li}$. A heavy recoil track which is present at A is sufficient to account for the momentum balance if its kinetic energy is ~ 10 MeV.

2. – The Incoming Particle.

The nature of the incoming neutral particle is unknown. The following

possibilities will be discussed: Neutron, neutral hyperon (Ξ^0, Σ^0), and neutral K-particle (K_1^0 and K_2^0).

Neutrons are to be expected from the target, from other parts of the Bevatron and from Cosmic Radiation. The required energy of the neutron is ~ 1 GeV. Geometrical considerations practically exclude neutrons of this energy coming from the target. Systematic scanning for neutron stars with an energy ~ 1 GeV, shows that they are rare. This fact combined with the very low percentage of stars with hyperfragments and the prong distribution of such stars makes it highly improbable that the incoming particle is a neutron. Life time and energy considerations exclude a neutral hyperon.

It is likely therefore, that the hyperfragment was produced by a neutral K-particle. In the Gell-Mann scheme Λ^0 has the strangeness -1 and this must have been preserved in a fast process. This implies that the incoming particle should have the strangeness -1 and the charge 0. Since the K^+-particles, which pass through the emulsion have strangenesses $+1$ charge exchange would produce the well known shortlived θ^0. Our particle cannot, therefore, have been produced in this manner. It is likely to be a K_2^0 with a time of flight of $\sim 10^{-8}$ s produced at the target in confirmation of Fry *et al.*'s assumption of a longlived neutral particle and excluding production by charge exchange in a more definite manner.

An alternate explanation would be in terms of hyperons with the strangeness $+1$.

* * *

We are indebted to Dr. Fry for the loan of the emulsion.

Gravitational Forces and Quantum Theory.

P. Bocchieri (*) and P. Gulmanelli (**)

Istituto Nazionale di Fisica Nucleare - Sezione di Milano
(*) *Istituto di Fisica dell'Università - Pavia*
(**) *Istituto di Scienze Fisiche dell'Università - Milano*

(ricevuto il 22 Febbraio 1957)

Attempts to derive gravitational forces on the basis of elementary processes of quantum field theory have been made by some authors. Gamow and Teller [1] suggested that the exchange of a neutrino pair between two nucleons could be responsible for gravitational forces.

More recently Corben [2] has proposed an explanation of gravity based on the usual β-theories. He considers a suitable fourth order process (with two nucleons in the initial and final states) in which the effect of the interaction amounts to an exchange of two neutrinos. It is generally considered that such an exchange of zero mass particles gives rise, in the static approximation, to an interaction potential that goes as $1/r$ at large distances. However the actual calculation of the matrix element turns out to be impossible owing to convergence difficulties and final results are not obtainable in an unambiguous way because of the non renormalizability of β-theories.

Calculations [3] have been made using non-local theories, but the results depend in an essential way on the choice of the form factor, and therefore are not reliable.

The need has therefore been felt of constructing a theory in which Corben's and Gamow and Teller's guesses could in principle be verified.

The most direct way of tackling the problem is to modify the β-theory so as to avoid the aforementioned convergence difficulties.

Let us suppose that an X-meson exists, which interacts with the neutron according to the scheme: $N \rightleftarrows X + \nu$ and with the proton according to $X \rightleftarrows P + e$. The corresponding interaction Lagrangian density can be written as follows, where the bar stands for antiparticle:

$$g_1(\bar{\psi}_\nu \Gamma \psi_N \varphi_X + \text{h.c.}) + g_2(\psi_P \bar{\Gamma}' \psi_e \varphi_X + \text{h.c.}).$$

(With this interaction the β-decay is obviously a second order process).

(1) G. Gamow and E. Teller: *Phys. Rev.*, **51**, 289 (1937); G. Gamow: *Phys. Rev.*, **71**, 550 (1947).

(2) H. C. Corben: *Nuovo Cimento*, **10**, 1485 (1953).

(3) P. Budini: *Nuovo Cimento*, **10**, 1486 (1953).

In order to prevent the neutron decay into an X-meson it is enough to suppose the meson mass greater than the neutron mass. Furthermore it can be easily shown that with the meson mass a little greater than the nucleon mass the decay spectra in this theory coincide with those of the corresponding β-theories:

$$g\bar{\psi}_\nu \Gamma \psi_N \bar{\psi}_P \Gamma' \psi_e ,$$

provided that the product $g_1 g_2$ of the coupling constants (not equal in principle) of the two elementary processes is correctly normalized. In this scheme the interaction of two nucleons through the exchange of two neutrinos is still a fourth order effect. But at variance with β-theory we do not have any longer the electron closed loops that make the matrix element divergent, so that this model has the advantage that, apart from practical difficulties of computation, the interaction potential is finite and in principle evaluable.

It would therefore be possible to see if the Gamow-Teller and Corben conjectures are correct. The $1/r$ dependence should be checked in the static approximation. If the guess will turn out to be wrong, one will be compelled to conclude that it is impossible in the frame of the existing theories to derive gravitational forces from the exchange of virtual neutrinos.

* * *

It is a pleasure for us to thank our friend A. LOINGER for useful discussions.

Electrochemistry of Metallic Single Crystals.

I - Exchange Overvoltages on Silver and Copper (*).

R. Piontelli, G. Poli and L. Paganini

Laboratorio di Elettrochimica, Fisica Chimica e Metallurgia del Politecnico - Milano

(ricevuto il 28 Febbraio 1957)

Researches are carried out in this Laboratory on the anodic and cathodic behavior of single crystal surfaces, having a well defined orientation, in order to get direct and quantitative information on the anisotropy of the overvoltage effects. Single crystals, prepared by a somewhat modified Bridgman method, starting from very pure metals, after control by X-rays and electron diffraction, have been cut by chemical and electrochemical methods [1] (thus avoiding the intervening of stresses), electrolytically polished, and treated by different methods of superficial finish.

Very pure chemicals, and solutions carefully freed from oxygen and other organic and inorganic impurities have been used.

The polarization cell was of the type here realized [2] ensuring the uniformity of the current distribution on the electrode surface and avoiding the systematic errors by shielding or by ohmic drop involved by the usual techniques. Stirring of solution has been performed by liquid flow entering tangentially to the electrode surface. The concentration overvoltage is thus reduced to a minimum.

The electrode voltage in respect to a reference electrode of the same metal in the same solution has been recorded by a cathodic oscilloscope: before, during and after the passage of rectangular current pulses, having duration up to 1 s. For longer current pulses, a Leeds and Northrup recording apparatus has been used.

Figs. 1 and 2 presents results concerning typically oriented lattice planes of silver and copper single crystals.

The behavior of polycrystalline electrodes, prepared by identical finish methods, is also reported for comparison. The surface structure of the electrodes has been investigated before and after the electrolysis, to define the changes which may have occurred.

For silver single crystals, in $AgClO_4$ 1 M solution, at 25 °C, the behavior, both anodic and cathodic, of the (100) and (111) lattice planes cannot be distinguished from that of polycrystalline

(*) The researches reported in this paper have been sponsored in part by the ARDC USAF under Contract AF 61(514)-733C through the European Office ARDC.

(1) R. Piontelli, B. Rivolta and G. Sternheim: *Rev. Scient. Instr.*, **26**, 1206 (1955).

(2) R. Piontelli, G. Bianchi, U. Bertocci, C. Guerci and B. Rivolta: *Zeits. Elektrochemie*, **58**, 54 (1954); R. Piontelli, U. Bertocci, G. Bianchi, C. Guerci and G. Poli: *Zeits. Elektrochemie*, **58**, 86 (1954).

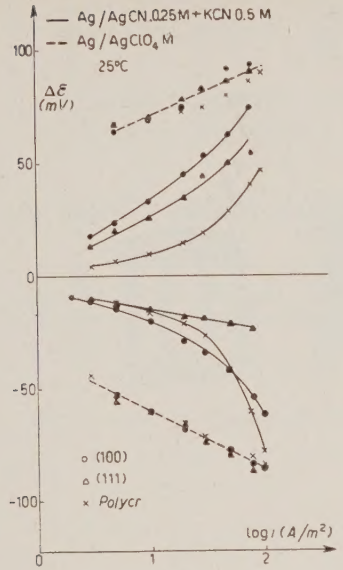

Fig. 1.

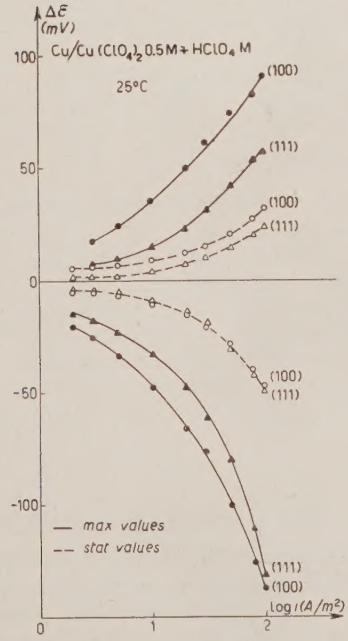

Fig. 2.

silver. The deposition does not follow, as a rule, the orientation of the basis metal; the anodic attack being, on the other hand, practically uniform. Tafel law holds true.

In a solution of AgCN 0.25 M + + KCN 0.5 M, the cathode overvoltages are lower for (111) than for (100) (for which initial maxima are met with), and intermedium for the polycrystalline electrode. On (111) and (100), the metal deposition occurs following the basis metal. On the (111) surface some tendential formation of twins is however met with.

The anode overvoltage is slightly lower for (111) than for (100), both presenting maxima, not encountered, however, with the polycrystalline electrode, on which overvoltages are clearly lower.

In a bath: AgCNS 0.25 M + KCNS 2.25 M, both (111) and (100) present maxima, either on the anodic or on the cathodic side. The overvoltage differences are, however, very small. Metal deposition does not follow, as a rule, the basis metal orientation in any regular way.

The anodic overvoltages of copper in a bath: $CuSO_4$ 0.5 M + H_2SO_4 1 M at 25 °C, are distinctly lower for (111) than for (100), either in very short or propolonged experiments.

On the cathodic side, this holds true only in very short experiments, whereas the stationary values of the overvoltages become lower for (100), when c.d. is higher than 10 A/m². The anodic attack respects the basis orientation although it be not entirely uniform. The cathodic deposition follows closely the orientation of the basis metal.

In a bath: $Cu(ClO_4)_2$ 0.5 M + $HClO_4$ M, the results are similar.

For prolonged current pulses, the cathodic overvoltages are, however, practically coincident for (111) and (100). Tafel law is not followed as a rule. Technical details, further results and discussion are given in successive papers.

EMENDATION

A. KIND and L. JESS – **On the Real Part of the Complex Potential Well of the Nucleus,** *Il Nuovo Cimento*, **4**, 595 (1956).

The normalization condition (2) is wrong. To fit correctly the experimental low energy behaviour of the two nucleon systems, condition (2) has to be replaced by

(2′) $$W(1+\alpha) = 48.4 \text{ MeV } (^1).$$

Consequently, the results of Fig. 1 have to be replaced by those of Fig. 1′.

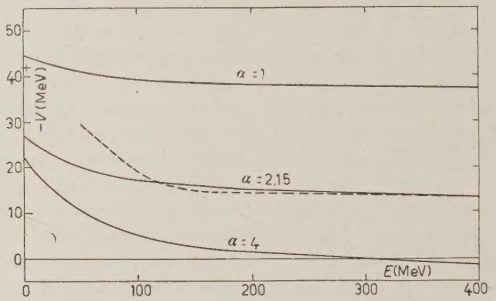

Fig. 1′.

The values of α for which accord between theory and experiment is reached at $E = 400$ MeV is 2,15 instead of 2.3.

(1) W. WILD and K. WILDERMUTH: *Zeits. f. Naturf.*, **9***a*, 799 (1954).

Direttore responsabile: G. POLVANI Tipografia Compositori - Bologna

Questo fascicolo è stato licenziato dai torchi il 27-III-1957